NASA TECHNICAL
TRANSLATION

NASA TT F-691
c. 1

TECH LIBRARY KAFB, NM
0069179

LOAN COPY: RETU
AFWL (DOU
KIRTLAND AFB

NASA TT F-691

THE TURBULENT BOUNDARY LAYER IN SUPERSONIC GAS FLOWS

by Yu. V. Lapin

"Nauka" Press, Moscow, 1970

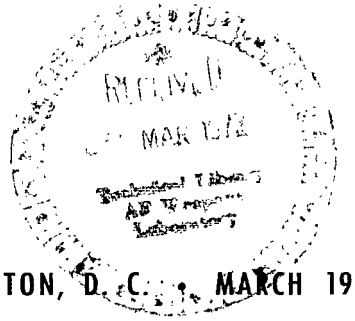

NATIONAL AERONAUTICS AND SPACE ADMINISTRATION • WASHINGTON, D. C. • MARCH 1972

TECH LIBRARY KAFB, NM
0069179

THE TURBULENT BOUNDARY LAYER IN SUPERSONIC GAS FLOWS

By Yu. V. Lapin

Translation of "Turbulentnyy pogranichnyy sloy v sverkhzvukovykh potokakh gaza"
"Nauka" Press, Moscow, 1970

NATIONAL AERONAUTICS AND SPACE ADMINISTRATION

For sale by the National Technical Information Service, Springfield, Virginia 22151
$3.00

THE TURBULENT BOUNDARY LAYER IN SUPERSONIC GAS FLOWS

Yu. V. Lapin

"Nauka" Press
Main Publishing House for Physico-Mathematical Literature
Moscow, 1970.

* * * * * *

"Turbulentnyy Pogranichnyy Sloy v Sverkhzvukovykh Potokakh Gaza", Yu. V. Lapin, Glavnaya Redaktsiya Fiziko-Matematicheskoy Literatury Izdatel'stva "Nauka", Moscow, 1970, 344 pages.

This book presents the theoretical and experimental results of studies of pressure drop, heat and mass transfer in turbulent boundary layers at supersonic gas velocities. In addition, the book contains a presentation of the fundamentals of the molecular theory of gas flows, derivations of the equations of turbulent motion and of the boundary layer equations, in particular for the case of multicomponent reacting gases. Information is given on the kinetics of chemical reactions, including the kinetics of dissociation reactions in air. Problems of heat and mass transfer on permeable surfaces are considered.

TABLE OF CONTENTS

	Page
FOREWORD	vii
CHAPTER I - THE GAS DYNAMIC EQUATIONS	1
1. Introduction	1
2. Elements of the molecular theory of gas flows	2
3. The gas-dynamic transport equations expressed in terms of the flux density vectors	7
4. The rate of diffusion, flux density vectors and transport coefficients	14
5. Equations for the dynamics of multicomponent reacting gases	26
CHAPTER II - TURBULENCE IN GAS-DYNAMIC FLOWS	31
6. The equations of turbulent motion	31
7. The turbulent boundary layer equations in a multicomponent reacting gas	43
8. The semiempirical theory of turbulence. Reynolds' analogy	49
9. The integral momentum and energy relationships	51
CHAPTER III - THE TURBULENT BOUNDARY LAYER IN A HOMOGENEOUS GAS STREAM AT SUPERSONIC VELOCITIES	57
10. Introduction	57
11. Experimental investigations of turbulent boundary layers in supersonic streams (friction and velocity profiles)	63
12. Semiempirical methods of calculating friction on flat plates	81
13. The effects of compressibility and heat transfer on the laminar sublayer	104
14. Empirical methods of calculating drag on a flat plate	109
15. Relationship between friction and heat transfer on a flat plate (Reynolds' analogy). Recovery coefficient	118
16. The turbulent boundary layer on a cone at zero angle of attack	132
17. The turbulent boundary layer in the presence of a longitudinal pressure drop	134
18. The turbulent layer on a sphere	146

TABLE OF CONTENTS (Cont'd) Page

CHAPTER IV - THE TURBULENT BOUNDARY LAYER IN DISSOCIATING GASES 156
19. Some remarks on the thermodynamic properties of air at high temperature 156
20. Some information on the kinetics of chemical reactions 159
21. The properties of partially excited dissociating and ideally dissociating gases 180
22. Formulation of the problem of the turbulent boundary layer in a dissociating gas 185
23. Velocity profiles, integral thicknesses, and friction on a flat plate 191
24. Flow along a flat plate at Schmidt and Prandtl numbers equal to unity 193
25. Heat and mass transfer in a boundary layer on a flat plate at Prandtl and Schmidt numbers different from unity 201
26. Conclusions 222

CHAPTER V - TURBULENT BOUNDARY LAYERS IN THE PRESENCE OF MASS TRANSFER BETWEEN THE GAS AND A SOLID SURFACE 224
27. Introduction 224
28. The main directions in the study of turbulent boundary layers in the presence of mass transfer between the gas and a surface 226
29. Experimental studies of turbulent boundary layers in the presence of mass transfer 231
30. The boundary conditions at the wall and at the outer edge of the boundary layer in the presence of mass transfer between a surface and the gas. The heat flux at the wall 242
31. Velocity profiles and drag on a flat plate during injection of material into the boundary layer 246
32. The boundary layer on a flat plate in the presence of blowing at Prandtl and Schmidt numbers equal to unity 251
33. Heat and mass transfer in the boundary layer on a flat plate in the presence of blowing at Prandtl and Schmidt numbers other than unity 257

REFERENCES 267

NOTATION 276

AUTHOR INDEX 281

FOREWORD

Problems of turbulence in general and of turbulent boundary layers in particular continue to be very real at present, in spite of the ever-increasing importance of their applications.

In connection with the rapid developments in the fields of aviation, space flight, construction of equipment for energy conversion and other areas of technology of particular interest to investigators and engineers, problems have frequently arisen involving the motion of gases at supersonic velocities in boundary layers which may be homogeneous or nonhomogeneous as regards the gas composition. In many cases, motion at supersonic velocities leads to very large increases in the temperature of the gas, which then begins to take part in thermochemical processes leading to the breakdown of the gas molecules into atoms, and of the atoms into ions and electrons, and the formation of oxides and other compounds. When flows at supersonic velocities are being considered it is necessary in some cases to allow for processes occurring at the surfaces of bounding bodies, such as melting, ablation (evaporation), chemical reactions, etc. Many of these phenomena have been and remain the subjects of detailed investigations of a theoretical and experimental nature. In the present book an attempt is made to present a systematic discussion of some of the results of these investigations; as usual, on the theoretical level preference is given to results obtained on the basis of the semi-empirical theory of turbulence.

The semi-empirical theory of turbulence, as a branch of the statistical theory of turbulence, continues to be very important at present, and in many cases provides the only instrument available for solving the great majority of practical problems. Originally set up on the basis of investigations of the flow of incompressible fluids in pipes, channels, boundary layers, jets and wakes, and used mainly for predicting the properties of incompressible fluid flows, the semi-empirical theory of turbulence also possesses wide possibilities for the study of much more complex flows such as the flow of compressible and heat-conducting gases, the flow of multicomponent reacting gas mixtures, etc. This is shown conclusively by the results of numerous experimental and theoretical investigations carried out in recent years.

The book does not pretend to give an exhaustive treatment of all the problems which arise in investigations of the movement of gases in boundary layers in supersonic flows. This is partly due to the fact that some of these problems

have received insufficient attention; this is particularly true of turbulent boundary layers on decomposing surfaces, the motion of ionized and radiating gases, etc. A part is also played by the personal interests of the author. In particular, in the special chapters of the book (III to V) only those branches of the theory of turbulent boundary layer are included in which the author has to some extent played a part in their development.

Chapter I contains a discussion of the fundamentals of the molecular theory of gas flows and a derivation of the dynamic equations of a multicomponent reacting gas based on the fundamental equation of the kinetic theory of gases — Boltzmann's equation.

A derivation of the system of equations for the turbulent motion of a multicomponent reacting gas is given in Chapter II. The turbulent boundary layer equations are then obtained from this system of equations. The integral momentum and energy relationships, which play an important role in the semi-empirical theory of turbulence, are also introduced at this point.

The theoretical and experimental results obtained during investigations of the characteristics of turbulent boundary layers on impermeable surfaces in supersonic gas streams which are homogeneous in composition are discussed in Chapter III. Both semi-empirical and empirical methods are used for calculating the boundary layer on a flat plate. The effects of compressibility and heat transfer on the laminar sublayer are analyzed. Experimental and theoretical data on the parameters characterizing heat transfer between the gas and a wall are presented (including the parameters of Reynolds' analogy, which establishes a relationship between friction and heat transfer, and the recovery coefficient). A generalized semi-empirical method of calculation is given for the cases of flow around a cone at zero angle of attack, around spheres, and also for flow around nondetached bodies of arbitrary shapes.

Chapter IV considers the motion of a dissociating gas in a turbulent boundary layer. Detailed information is provided on the kinetics of chemical reactions occurring in the gas and at the surface of the body, and in particular, data are provided on the kinetics of the dissociation reactions of oxygen and nitrogen. Various models of dissociating gases are described, including ideally dissociating and partly excited dissociating gases. A semi-empirical method is proposed for calculating friction and heat transfer on a flat plate for equilibrium, frozen and nonequilibrium states of the gas.

Chapter V gives the results of experimental and theoretical investigations of turbulent boundary layers in the case of mass transfer between the gas and the surface along which flow occurs. Methods are proposed for calculating the friction and heat transfer on a porous plate during the blowing of gases of various types into the boundary layer.

The author expresses his deep thanks to his teacher Lev Gerasimovich Loytsyanskiy for his assistance and support in writing the book, and in particular for his very valuable discussions of many of the problems considered in the book.

The author expresses his appreciation to V. P. Mugalev who read through the manuscript of the book for a number of important comments.

CHAPTER I.

THE GAS DYNAMIC EQUATIONS

1. Introduction

The development of the aviation and astronautical industries in the last /8
decade has led to considerable interest in the problems of gas flow at supersonic and hypersonic velocities. The study of these problems has shown that these flows cannot be described in terms of classical gas dynamics alone, in which flows with relatively small velocities are considered. In addition to gas dynamics, it becomes necessary to consider many other fields of physics and chemistry.

Any motion of a viscous gas is accompanied by dissipation of mechanical energy, which is converted into heat, but at small velocities the viscous dissipation does not lead to the appearance of any noticeable temperature nonhomogeneities (temperature gradients). Under these conditions, the density and viscosity of the gas can be regarded as constant physical properties which do not depend on the nature of the motion.

As the velocity of a gas flow is increased from small subsonic to moderate supersonic velocities appreciable temperature nonhomogeneities arise during passage of the gas through density discontinuities and in flow in boundary layers, and these make it necessary to take into account the temperature dependences of density, viscosity and heat capacity, even when the moving gas can be regarded as homogeneous.

The transition to hypersonic velocities causes such large increases in the gas temperature in density discontinuities and boundary layers that thermal processes begin to occur in the gas, which lead to splitting of the gas molecules into atoms (dissociation) and break-up of the atoms into ions and electrons (ionization), /9
and to the formation of oxides and other chemical compounds. Furthermore, in some cases it is necessary to make allowance for processes which occur on the surfaces of the bodies around which flow takes place, such as melting and sublimation of the surface layers of the solid body, chemical reactions with it, etc. Under these conditions the flowing medium has to be regarded as a mixture of several components differing in their physico-chemical properties. The study of such complicated processes by the usual methods of classical (phenomenological)

gas dynamics is very difficult in many cases, particularly if the thermodynamics of the process proceed in a nonequilibrium manner.

It should be noted that the thermodynamic route to the study of various gas-dynamic phenomena is based on the postulate that there exist definite relationships between the velocity gradient and the shear stress (Newton's law), between the temperature gradient and the heat flux (Fourier's law), and between the concentration gradient and the diffusion flux (Fick's law), and that equations can be used which are derived from the fundamental laws of thermodynamics and classical mechanics. The transport coefficients, i.e., the proportionality coefficients in Newton's, Fourier's and Fick's laws, reflect definite properties of the gas molecules, and which are therefore determined by the gas microstructure. These coefficients appear in the phenomenological theory as constants or state functions which are known beforehand; they cannot be calculated theoretically, but must be determined from experiments. It is entirely to be expected that the phenomenological theory, which is based on an approximate macro-model of the gas, will not be capable of describing many of the complex phenomena in the study of which it is necessary to take into account various types of microprocesses (disturbances of the internal degrees of freedom of molecules, dissociation, ionization, etc.). The method of the kinetic theory of gases provides a means for describing such processes.

The kinetic theory of gases makes it possible to determine the transport /10
coefficients as functions of the temperature of the gas mixture, the molecular weights of the constituents of the mixture, and various parameters describing the field of intermolecular forces, as well as to set up macroscopic equations of motion for the gas being studied. The kinetic theory of gases is valid only at quite small gas densities when the effects of collisions of more than two molecules can be neglected. If the mean free flight path of the molecules in the gas is small compared with characteristic macroscopic dimensions of a body, the gas behaves as a continuum. In this case it is possible to obtain the gas dynamic transport equations and expressions for the transport coefficients from the basic equation of the kinetic theory of gases (Boltzmann's equation). Since it is intended to follow this path later, some of the elements of the kinetic theory of gases are discussed here briefly. Some knowledge of the fundamentals of the kinetic theory of gases is necessary in order to understand the interrelationships between micro- and macro-procedures which occur in gases, and is also useful from a practical point of view in studying flows of multicomponent reacting gas mixtures. Only the parts of the kinetic theory of gases which are important in the subsequent derivations are given below. A much deeper and more detailed presentation of this theory is contained in the monographs by Hirschfelder, Curtiss and Bird [1] and Chapman and Cowling [2].

2. Elements of the molecular theory of gas flows

The dynamic state of a system of particles is completely defined if the positions and velocities (momenta) of all the particles are specified. From a known dynamic state of the system at the initial moment of time, the laws of classical mechanics make it possible to predict its state at any subsequent moment of time.

At any given moment of time each of the particles has some velocity, and so each of the particles can be given a definite position in the velocity space characterized by the vector v_i. The position of the particles in physical space is determined by the vector r. /11

In order to make a complete description of the dynamic state of a system of particles, the concept of a distribution function is introduced in the kinetic theory of gases. If a mixture of gases (strictly speaking, of monatomic gases) is considered, for the case when the mixture is in a nonequilibrium state, the properties of each component of the mixture can be expressed in terms of distribution function $f_i(r_i, v_i, t)$, which is defined as the number of particles of the i^{th} sort which at the moment of time t are in an elementary unit volume of physical space around the point r and which possess velocities within the elementary unit volume of velocity space close to the point v_i.

The space (x, y, z, v_{ix}, v_{iy}, v_{iz}) is a multiphase type, since the position coordinates and the velocity coordinates are independent variables.

The total number of particles in an elementary unit volume of physical space at the moment of time t is obtained by integrating the distribution function over all possible values of the velocities v_{ix}, v_{iy} and v_{iz}:

$$n_i(r, t) = \int_{-\infty}^{+\infty}\int_{-\infty}^{+\infty}\int_{-\infty}^{+\infty} f_i\, dv_{ix}\, dv_{iy}\, dv_{iz}. \tag{1.1}$$

The quantity n_i has the significance of a number density of particles of the i^{th} sort. For convenience, the triple integral

$$\int_{-\infty}^{+\infty}\int_{-\infty}^{+\infty}\int_{-\infty}^{+\infty}(\ldots)\, dv_{ix}\, dv_{iy}\, dv_{iz}$$

will subsequently be denoted by

$$\int(\ldots)\, dv_i.$$

When the distribution function is known, it is possible to calculate the mean value of any quantity ψ_i connected with the particles of the i^{th} sort and which is a function of the velocity components only. The formula for evaluating the mean value of ψ_i will obviously have the form /12

$$\bar{\psi}_i(r, t) = \frac{1}{n_i}\int f_i(r, v_i, t)\psi_i(v_i)\,dv_i = \frac{\int f_i\psi_i dv_i}{\int f_i dv_i}. \qquad (1.2)$$

The bar above ψ_i is the symbol for averaging. Thus, the mean velocity $\bar{v}_i$ of the particles of the i^{th} component, which have a number density n_i, is defined as follows:

$$\bar{v}_i(r, t) = \frac{1}{n_i}\int v_i f_i(r, v_i, t)\,dv_i. \qquad (1.3)$$

The mass average velocity, which is a weighted mean quantity, since each particle makes a contribution to this velocity proportional to its mass m_i, is defined according to the formula

$$v(r, t) = \frac{\sum_i m_i n_i \bar{v}_i}{\sum_i m_i n_i}, \qquad (1.4)$$

where $\sum_i m_i n_i = \rho(r, t)$ is the density of the medium at some point.

The mass average velocity is usually termed the stream velocity or flow velocity and has the property that the momentum of unit volume of the gas is the same as it would be if all the gas particles in this volume moved with this velocity.

The thermal velocity of the particles of the i^{th} sort is defined as the velocity of the particles relative to a system of coordinates moving with the mass-average velocity v:

$$V_i(v_i, r, t) \quad v_i - v. \qquad (1.5)$$

The diffusion velocity of the i^{th} component is defined as the velocity of the particles of this component relative to a system of coordinates moving with the mass average velocity of the gas. In other words, the diffusion velocity is the average of the thermal velocities: /13

$$\bar{V}_i(r, t) = \frac{1}{n_i}\int (v_i - v) f_i(r, v_i, t)\,dv_i = \bar{v}_i - v. \qquad (1.6)$$

In the kinetic theory, the temperature is defined in terms of the kinetic energy of the thermal motions averaged over all the particles:

$$\frac{3}{2}kT = \frac{1}{n}\sum_i \frac{1}{2} m_i n_i \overline{V_i^2}, \qquad (1.7)$$

where $n = \sum_i n_i$, and k is Boltzmann's constant.

If all the expressions for the macroscopic quantities are given in terms of the distribution function, we find that

$$\left.\begin{aligned} \rho(r, t) &= \sum_i m_i n_i = \sum_i m_i \int f_i \, dv_i, \\ T(r, t) &= \frac{1}{3nk} \sum_i m_i \int V_i^2 f_i \, dv_i, \\ v(r, t) &= \frac{1}{\rho} \sum_i m_i \int v_i f_i \, dv_i, \\ p_i &= \rho_i \frac{k}{m_i} T, \quad \rho_i = n_i m_i, \quad p = \sum_i p_i. \end{aligned}\right\} \tag{1.8}$$

In the case of gases in a nonequilibrium state, the fields of one or more of the quantities characterizing the macroscopic properties of the system must be nonuniform. The nonuniformity of the fields, i.e., the existence of gradients of the macroscopic quantities (the mass average velocity v, the temperature T, the mass concentration $c_i = \rho_i/\rho$, etc.) is the cause of a molecular transfer of momentum $m_i V_i$, kinetic energy $1/2\,(m_i V_i^2)$ and of mass m_i in the gas.

As a characteristic of the molecular transfer of one or other substance the concept of a vector flux density of the quantity ψ_i(*) /14

$$\Psi_i = \int \psi_i f_i V_i \, dV_i. \tag{1.9}$$

is introduced in the kinetic theory. The physical significance of the flux density vector is that its component in any direction represents the flux density of the corresponding physical quantity through a surface normal to this direction.

If $\psi_i = m_i$, equation (1.9) leads to the mass flux density vector

$$j_i = m_i \int f_i V_i \, dV_i = m_i n_i \overline{V}_i. \tag{1.10}$$

---

*It should be noted that in evaluating the average of a quantity, integration with respect to V_i is equivalent to integration with respect to v_i, since these velocities differ by a constant quantity, and the integration is carried out over all values of the velocity.

If $\psi_i = m_i V_i$, then

$$P_i = m_i \int f_i V_i V_i dV_i = m_i n_i \overline{V_i V_i} \tag{1.11}$$

represents a symmetrical tensor of rank 2, characterizing the partial pressure of the i^{th} component in the gas (*). The sum of the partial pressure tensor over all the components in the gas leads to the pressure tensor of the mixture

$$P = \sum_i P_i = \sum_i m_i n_i \overline{V_i V_i}. \tag{1.12}$$

The diagonal components of the pressure tensor, P_{xx}, P_{yy}, P_{zz} are equal to the normal stresses, while the nondiagonal components represent shear or tangential stresses. For example, the quantity P_{yx} is equal to the force acting on a unit cross-sectional area perpendicular to the y direction in the x direction.

If $\psi_i = m_i V_i^2/2$, then /15

$$q_i = \frac{1}{2} m_i \int f_i V_i^2 V_i dV_i = \frac{1}{2} m_i n_i \overline{V_i^2 V_i} \tag{1.13}$$

is the flux vector characterizing the transport of kinetic energy by particles of the i^{th} sort. The sum of these vectors over all the components of the gas mixture gives the heat flux density vector:

$$q = \sum_i q_i = \sum_i \frac{1}{2} m_i n_i \overline{V_i^2 V_i}. \tag{1.14}$$

The components q_x, q_y, q_z of the heat flux density vector represent the flux densities of kinetic energy in the x, y and z directions respectively.

---

* In equation (1.11) the tensor P_i is regarded as the result of the dyadic multiplication of two vectors $V_i V_i$, where in contrast to the scalar $V_i \cdot V_i$ and vector $V_i \times V_i$ products of these vectors, there is no multiplication sign in the dyadic product.

It follows from equations (1.8) and (1.10) to (1.14) that if the distribution function f_i is known, the problem of determining the flow field and the transport characteristics can be solved completely.

The way in which the distribution function f_i varies is described by Boltzmann's integro-differential equation, which assumes the form

$$\frac{\partial f_i}{\partial t} + v_i \cdot \frac{\partial f_i}{\partial r} = \sum_j I_{ij}. \tag{1.15}$$

when no external force field is present. Here

$$I_{ij} = 2\pi \iint (f_i' f_j' - f_i f_j) g_{ij} b \, db \, dv_j \tag{1.16}$$

is the collision integral, which takes into account the change in the number of particles of the group being considered as a result of collisions; $g_{ij} = | v_i - v_j |$ is the absolute value of the relative velocity of the particles of the i^{th} and j^{th} sorts before impact; b is the minimum distance to which colliding particles can approach each other without the occurrence of an interaction (the sighting distance); f_i' and f_j' are the distribution functions of the colliding particles of the i^{th} and j^{th} sorts after impact; f_i and f_j are the distribution functions of the colliding particles before impact.

Equations analogous to equation (1.15) can be written for all the components of a gas mixture. In each of these equations the distribution functions for all the components of the mixture appear within the integral sign on the right hand side of the equation. These integrals depend implicitly on the type of intermolecular interaction. The distribution functions f_i' and f_j' are functions of the velocities v_i' and v_j' which can be derived on the basis of the laws of mechanics for known values of v_i, v_j, b and the intermolecular interaction potential. /16

3. The gas-dynamic transport equations expressed in terms of the flux density vectors.

The fundamental gas-dynamic transport equations (the equations for the conservation of mass, momentum and energy) can be obtained directly from the Boltzmann equation without determining the form of the distribution function. By multiplying the Boltzmann equation (1.15) by ψ_i and integrating the result over all values of the velocity v_i, it is found that

$$\int \psi_i \left(\frac{\partial f_i}{\partial t} + v_i \cdot \frac{\partial f_i}{\partial r} - \sum_j I_{ij} \right) dv_{ij} = 0. \tag{1.17}$$

The first two terms on the left side of this equation can be converted to the form

$$\int \psi_i \frac{\partial f_i}{\partial t} dv_i = \frac{\partial}{\partial t} \int \psi_i f_i \, dv_i - \int f_i \frac{\partial \psi_i}{\partial t} dv_i =$$
$$\frac{\partial}{\partial t} (n_i \overline{\psi_i}) - n_i \overline{\frac{\partial \psi_i}{\partial t}},$$
$$\int \psi_i v_i \cdot \frac{\partial f_i}{\partial r} dv_i = \frac{\partial}{\partial r} \cdot \int f_i \psi_i v_i \, dv_i - \int f_i \left(v_i \cdot \frac{\partial \psi_i}{\partial r} \right) dv_i =$$
$$\frac{\partial}{\partial r} \cdot (n_i \overline{\psi_i v_i}) - n_i \overline{\left(v_i \cdot \frac{\partial \psi_i}{\partial r} \right)}.$$

By substituting these equations into the left side of equation (1.17) it is seen that

$$\frac{\partial}{\partial t} (n_i \overline{\psi_i}) + \frac{\partial}{\partial r} \cdot (n_i \overline{\psi_i v_i}) - n_i \left(\overline{\frac{\partial \psi_i}{\partial t}} + \overline{v_i \cdot \frac{\partial \psi_i}{\partial r}} \right) =$$
$$\sum_j \int \psi_i I_{ij} \, dv_i. \tag{1.18}$$

This equation is known as the generalized Enskog transport equation for the quantity ψ_i due to particles of the i^{th} sort. /17

By summing equation (1.18) over all the components the transport equation for the mixture is obtained:

$$\frac{\partial}{\partial t} \sum_i n_i \overline{\psi_i} + \frac{\partial}{\partial r} \cdot \sum_i n_i \overline{\psi_i v_i} - \sum_i n_i \left(\overline{\frac{\partial \psi_i}{\partial t}} + \overline{v_i \cdot \frac{\partial \psi_i}{\partial r}} \right) =$$
$$\sum_{j,i} \int \psi_i I_{ij} \, dv_i. \tag{1.19}$$

The use of equation (1.19) for an arbitrary quantity ψ_i is made very difficult by the appearance of a very complex integral on the right-hand side of the equation. However, if ψ_i is the mass m_i, the momentum $m_i V_i$, or the kinetic energy of a molecule $m_i V_i^2/2$ (in the case of multi-atomic molecules it is necessary to take the internal energy into account in the kinetic energy term), it can be shown that the right-hand part of equation (1.19) is equal to zero, and the equation is greatly simplified. Actually, it is assumed that the interacting system consists of two particles: one is a particle of sort i with mass m_i, and the other is a particle of sort j and mass m_j. Suppose that the velocities of the particles before collision are V_i and V_j respectively, while the corresponding velocities after collision are denoted by V_i' and V_j'. If the system of colliding particles as a whole is not subjected to the action of an external force, and if the collision is adiabatic, then

on the basis of the laws of conservation of mass, momentum and energy it is possible to write

$$\left.\begin{aligned} &m_i + m_j = m_i' + m_j', \\ &m_i V_i + m_j V_j = m_i' V_i' + m_j' V_j', \\ &\frac{1}{2} m_i V_i^2 + \frac{1}{2} m_j V_j^2 = \frac{1}{2} m_i' V_i'^2 + \frac{1}{2} m_j' V_j'^2. \end{aligned}\right\} \qquad (1.20)$$

In the absence of chemical reactions, $m_i = m_i'$, $m_j = m_j'$.

The expressions for the conservation relationships, (1.20), can be represented in the following generalized form for a system of colliding particles: /18

$$\psi_i + \psi_j = \psi_i' + \psi_j', \qquad (1.21)$$

where ψ_i represents any of the quantities m_i, $m_i V_i$ and $m_i V_i^2/2$. It can be shown that any function of the velocity which satisfies the relationship (1.21) is a linear combination of these quantities. The quantities ψ_i which satisfy equation (1.21) are usually termed summatory invariants.

Now let us turn to a consideration of the integral appearing in the summation on the right-hand part of equation (1.19). This integral

$$\frac{1}{2\pi} \int \psi_i I_{ij}\, dv_i = \iiint \psi_i (f_i' f_j' - f_i f_j)\, g_{ij}\, b\, db\, dv_j\, dv_i \qquad (1.22)$$

is equal to the integral

$$\iiint \psi_i' (f_i f_j - f_i' f_j')\, g_{ij}' b'\, db'\, dv_j'\, dv_i', \qquad (1.23)$$

written for the reverse collision.

It can be shown that $g_{ij} = g_{ij}'$, $b = b'$ and $dv_j \cdot dv_i' = dv_j' \cdot dv_i'$; the integral (1.23) can therefore be written in the form

$$-\iiint \psi_i' (f_i' f_j' - f_i f_j)\, g_{ij} b\, db\, dv_j dv_i. \qquad (1.24)$$

Since the integrals (1.22) and (1.24) are equal, each of them is equal to half the sum of both integrals, i.e.,

$$\frac{1}{2\pi}\int \psi_i I_{ij}\, dv_i = \frac{1}{2}\iiint (\psi_i - \psi_i')(f_i' f_j' - f_i f_j)\, g_{ij} b\, db\, dv_j\, dv_i.$$

By summing these integrals with respect to i and j, and noting that i and j are interchangeable, it is found that /19

$$\frac{1}{2\pi}\sum_{i,j}'\int \psi_i I_{ij}\, dv_i = \frac{1}{4}\sum_{i,j}'\iiint (\psi_i + \psi_j - \psi_i' - \psi_j') \times (f_i' f_j' - f_i f_j)\, g_{ij} b\, db\, dv_j\, dv_i. \tag{1.25}$$

For summatory invariants the quantity $\psi_i + \psi_j - \psi_i' - \psi_j'$ is equal to zero, and so the right-hand part of the generalized Enskog transport equation (1.19) becomes equal to zero if ψ_i is equal to m_i, $m_i V_i$ or $m_i V_i^2/2$.

Thus, the transport of mass, momentum or energy in a gas mixture is described by the following equation:

$$\frac{\partial}{\partial t}\sum_i n_i \overline{\psi_i} + \frac{\partial}{\partial r}\cdot\sum_i n_i \overline{\psi_i v_i} - \sum_i n_i\left(\overline{\frac{\partial \psi_i}{\partial t}} + \overline{v_i \cdot \frac{\partial \psi_i}{\partial r}}\right) = 0. \tag{1.26}$$

Now let us pass on to the derivation of the transport equations for concrete molecular quantities. Assume that $\psi_i = m_i$. In this case, equation (1.18) takes the form

$$\frac{\partial n_i}{\partial t} + \frac{\partial}{\partial r}\cdot(n_i \bar{v}_i) = \sum_j'\int I_{ij}\, dv_i = K_i. \tag{1.27}$$

The integral $\int I_{ij} dv_i$ is equal to the rate of increase of the number of particles of the i^{th} sort due to collisions with particles of the j^{th} sort per unit volume (this integral is equal to zero in the absence of chemical reactions). The quantity

$$\sum_j'\int I_{ij}\, dv_i = K_i$$

expresses the overall increase in the number of particles of the i^{th} sort per unit volume due to collisions with all sorts of particles, including the i^{th} sort (as a result of chemical reactions). By substituting v_i according to equation (1.6) in equation (1.27), the continuity equation for the i^{th} component of the gas is obtained:

$$\frac{\partial n_i}{\partial t} + \frac{\partial}{\partial r}\cdot[n_i(v + \overline{V}_i)] = K_i. \tag{1.28}$$

When a change is made in equation (1.28) from n_i to the mass concentration /20

$$c_i = \frac{n_i m_i}{\sum_i n_i m_i} = \frac{n_i m_i}{nm} = \frac{\rho_i}{\rho}, \qquad m = \left(\sum_i \frac{c_i}{m_i}\right)^{-1}, \tag{1.29}$$

it is found that

$$\frac{\partial}{\partial t}(\rho c_i) + \frac{\partial}{\partial r}\cdot[\rho c_i(v + \overline{V}_i)] = w_i, \tag{1.30}$$

where $w_i = m_i K_i$ is the mass rate of formation of the i^{th} component per unit volume.

By summing equation (1.30) over all values of i, the continuity equation for the gas mixture is obtained in the form

$$\frac{\partial \rho}{\partial t} + \frac{\partial}{\partial r}\cdot(\rho v) = 0, \tag{1.31}$$

since $\sum_i \rho_i V_i = 0$ from the definition of the diffusion velocity, while $\sum_i w_i = 0$ according to equations (1.21) and (1.25). The condition

$$\sum_i w_i = 0 \tag{1.32}$$

expresses the law of conservation of mass of the gas mixture in the presence of chemical reactions.

By using the continuity equation for the gas mixture (1.31), the continuity equation for the i^{th} component can be rearranged into the form

$$\rho \frac{\partial c_i}{\partial t} + \rho v \cdot \frac{\partial c_i}{\partial r} = w_i - \frac{\partial}{\partial r}\cdot(\rho c_i \overline{V}_i). \tag{1.33}$$

It should be noted that within the differentiation sign on the right side of equation (1.33) a quantity appears which was defined earlier (see equation (1.10)) as the mass flux density vector.

In order to obtain the equation for the transport of momentum, the quantity /21 $\psi_i = m_i V_i$ is substituted into equation (1.26), giving

$$\sum_i m_i\left[\frac{\partial(n_i\overline{V_i})}{\partial t}+\frac{\partial}{\partial r}\cdot(n_i\overline{v_iV_i})-n_i\frac{\overline{\partial V_i}}{\partial t}-n_i\overline{\left(v_i\cdot\frac{\partial}{\partial r}\right)V_i}\right]=0. \tag{1.34}$$

This equation can be simplified by using the relationships among the velocities (1.5) and (1.6) and the definition of the pressure tensor (1.12). During differentiation, however, it must be remembered that r, v_i and t are independent quantities. After some simple rearrangements, the equations of motion for a gas mixture can be reduced to the following form:

$$\frac{\partial v}{\partial t}+\left(v\cdot\frac{\partial}{\partial r}\right)v=-\frac{1}{\rho}\left(\frac{\partial}{\partial r}\cdot P\right). \tag{1.35}$$

The equation for the transport of energy is obtained by substituting the quantity $\psi_i = m_iV_i^2/2$ in equation (1.26):

$$\sum_i\frac{1}{2}m_i\left[\frac{\partial(n_i\overline{V_i^2})}{\partial t}+\frac{\partial}{\partial r}\cdot n_i\overline{v_iV_i^2}-n_i\frac{\overline{\partial V_i^2}}{\partial t}-n_i\overline{\left(v_i\cdot\frac{\partial V_i^2}{\partial r}\right)}\right]=0. \tag{1.36}$$

By using the relationships among the velocities (1.5), (1.6) and the definition of the pressure tensor (1.12), and by introducing the energy flux density vector q defined by equation (1.14), the energy balance equation is obtained:

$$\frac{\partial}{\partial t}(\rho E)+\frac{\partial}{\partial r}\cdot\rho vE+\frac{\partial}{\partial r}\cdot q+\left(P\cdot\frac{\partial}{\partial r}\right)\cdot v=0. \tag{1.37}$$

Here

$$E=\frac{1}{\rho}\sum_i m_in_iV_i^2 \tag{1.38}$$

is the internal energy of the gas per unit mass, which is equal to the energy of the translational motion of the molecules (the kinetic energy of the translational motion of the gas stream as a whole does not appear in this energy). In the last term on the left-hand side of equation (1.37) the symbol $P\cdot\frac{\partial}{\partial r}$ expresses the operation of multiplying the tensor P by the vector $\partial/\partial r$. It will be recalled that this operation, which can be represented in the general case as T.A, is defined as a vector with the projections /22

$$(T\cdot A)_x=T_{xx}A_x+T_{xy}A_y+T_{xz}A_z \quad \text{etc.}$$

Equation (1.37) can be simplified by using the continuity equation for the mixture, equation (1.31). As a result of this, it is found that

$$\rho \cdot \frac{\partial E}{\partial t} + \rho v \cdot \frac{\partial E}{\partial r} = -\frac{\partial}{\partial r} \cdot q - \left(P \cdot \frac{\partial}{\partial r}\right) \cdot v. \tag{1.39}$$

Equation (1.39) is valid for gases consisting of multiatomic molecules which possess internal degrees of freedom. In this case the quantity E is taken to mean the sum of the energies of the translational and internal degrees of freedom of the molecules:

$$E = \frac{1}{\rho} \sum_i \frac{1}{2} m_i n_i \overline{V_i^2} + \frac{1}{\rho} \sum_i n_i e_i, \tag{1.40}$$

while the expression for the energy flux density vector (1.14) must be replaced by the expression

$$q = \frac{1}{2} \sum_i m_i n_i \overline{V_i^2 V_i} + \sum_i n_i e_i \overline{V_i}, \tag{1.41}$$

where e_i is the energy of the internal degrees of freedom for particles of the i^{th} sort.

The energy balance equation (1.39) can also be written in terms of the temperature. In this case, using the continuity equation for the i^{th} component, equation (1.30), it is found that

$$\rho c_v \left(\frac{\partial T}{\partial t} + v \cdot \frac{\partial T}{\partial r}\right) = -\frac{\partial}{\partial r} \cdot q - \left(P \cdot \frac{\partial}{\partial r}\right) \cdot v - \sum_i w_i E_i + \sum_i E_i \left(\frac{\partial}{\partial r} \cdot \rho c_i \overline{V}_i\right). \tag{1.42}$$

Here

$$c_v = \sum_i c_i \left(\frac{\partial E_i}{\partial T}\right)_v = \sum_i c_i c_{vi} \tag{1.43}$$

is the mean heat capacity at constant volume per unit weight of the mixture.

4. The rate of diffusion, flux density vectors and transport coefficients.

/23

The fundamental gas-dynamic equations of continuity (1.33), motion (1.35), and energy (1.39) or (1.42) have been obtained from the Boltzmann equation without defining the form of the distribution function. However, it will be clear from a consideration of these equations that in order to make use of them in practice it is necessary to have expressions for the rates of diffusion and the flux density vectors for mass, momentum and energy in terms of derivatives of macroscopic quantities with respect to the coordinates and the transport coefficients.

In order to determine these quantities it is necessary to solve Boltzmann's equation. An extensive literature exists on the problem of obtaining approximate solutions of the Boltzmann equation (*). It is not possible to deal in detail with this problem within the confines of the present book, and so we will confine ourselves to only a brief discussion of the concepts behind the most widely used method (the perturbation method of Enskog and Chapman) for solving the Boltzmann equation.

As is well known, a gas which is adiabatically isolated and which does not experience any external perturbing effects over a sufficiently long period of time ultimately reaches some equilibrium (steady) state. For systems which are in the steady state the distribution function f_i does not depend on time, as a result of which the right-hand part of the Boltzmann equation (1.15) becomes equal to zero. The equality to zero of the right-hand part of this equation expresses an equilibrium state in the collision processes which consists of the fact that the number of particles of the i^{th} sort lost due to collisions over a certain range of velocities is exactly compensated by the number of particles arising as a result of collisions during this time period. The conditions sufficient for equilibrium to exist can be obtained if it is assumed that the integrand in the right-hand part of the Boltzmann equation is equal to zero, i.e., /24

$$f_i' f_j' = f_i f_j. \tag{1.44}$$

However, it is not clear if this is the necessary condition, since for the right-hand part of the Boltzmann equation to be equal to zero it is necessary only that the integrand should assume positive and negative values in the region of integration so that the integral is found to be zero. The fact that condition (1.44) is necessary is proved by the H-theorem of Boltzmann, the proof of which can be found in the monograph by Hirschfelder, Curtiss and Bird [1].

The equation (1.44) can be written in the form

---

*See, for instance, the monographs by Hirschfelder, Curtiss and Bird and by Chapman and Cowling [1, 2], which contain the results of the earlier work. A discussion of the results of more recent work can be found in the monograph by Kogan [3].

$$\ln f_i + \ln f_j = \ln f_i + \ln f_j. \tag{1.45}$$

As a result, the logarithms of the distribution functions are summatory invariants of the molecular collisions. However, according to the conservation equations (1.20), the only quantities which can be summatory invariants during collisions are the mass m_i, the momentum $m_i v_i$, and the kinetic energy $m_i v_i^2/2$. In the general case, therefore, $\ln f_i$ must be a linear combination of these quantities, i.e.,

$$\ln f_i = a_i m_i + b \cdot (m_i v_i) + c\left(\frac{1}{2} m_i v_i^2\right), \tag{1.46}$$

where a_i, b and c are constants which depend (through the initial distribution function) on the total number of molecules of the i^{th} sort, the total momentum and the total energy of the system. By determining these constants from the conditions

$$\left.\begin{aligned} \int f_i \, dv_i &= n_i, \\ \sum_i m_i \int v_i f_i \cdot dv_i &= \rho v, \\ \frac{1}{2} \sum_i m_i \int (v_i - v)^2 f_i \, dv_i &= \frac{3}{2} nkT, \end{aligned}\right\} \tag{1.47}$$

the well-known Maxwell law is obtained for the distribution functions of systems which are at equilibrium /25

$$f_i = n_i \left(\frac{m_i}{2\pi kT}\right)^{3/2} \exp\left[-\frac{m_i}{2kT}(v_i - v)^2\right], \tag{1.48}$$

where $v_i - v = V_i$ is the thermal velocity.

If the gas mixture is in a nonequilibrium state, the distribution function can be derived by the Enskog-Chapman method by introducing into the Boltzmann equation a perturbation parameter ε ($1/\varepsilon$ is a measure of the frequency of collisions). At small values of ε the collisions occur very frequently, as a result of which the gas can be regarded as a continuum, at each point of which local equilibrium is attained. In this case the distribution function can be expanded in a series with respect to the parameter ε:

$$f_i = f_i^{(0)} + \varepsilon f_i^{(1)} + \varepsilon^2 f_i^{(2)} + \ldots \tag{1.49}$$

By substituting this series into the transformed Boltzmann equation

$$\frac{\partial f_i}{\partial t} + v_i \cdot \frac{\partial f_i}{\partial r} = \frac{1}{\varepsilon} \sum_j I_{ij} \tag{1.50}$$

and equating the coefficients for equal powers of ε, a system of equations is obtained for the functions $f_i^{(0)}$, $f_i^{(1)}$, etc.:

$$\left.\begin{aligned} 0 &= \sum_j I_{ij}(f_i^{(0)}, f_j^{(0)}), \\ \frac{\partial f_i^{(0)}}{\partial t} &+ v_i \cdot \frac{\partial f_i^{(0)}}{\partial r} = \\ &\sum_j [I_{ij}(f_i^{(0)}, f_j^{(1)}) + I_{ij}(f_i^{(1)}, f_j^{(0)})] \text{ etc.} \end{aligned}\right\} \tag{1.51}$$

It is not difficult to see that the solution of the first equation of the system (1.51) is the Maxwellian distribution (1.48).

The quantities /26

$$n_i = n_i(r, t), \quad v = v(r, t) \text{ and } T = T(r, t),$$

which appear in the expression (1.48) are arbitrary functions of the coordinates and time. In order for these quantities to correspond to their local values, it is necessary that the solutions of the remaining equation of the system (1.51) satisfy the condition (1.47). In other words, the following conditions must be fulfilled for the distribution functions for approximations higher than the zeroth approximation, $f_i^{(k)}$, $k = 1, 2, 3, \ldots$:

$$\left.\begin{aligned} \int f_i^{(k)} dv_i &= 0, \\ \sum_i m_i \int v_i f_i^{(k)} dv_i &= 0, \\ \frac{1}{2} \sum_i m_i \int (v_i - v)^2 f_i^{(k)} dv_i &= 0 \\ \text{where } k &= 1, 2, 3, \ldots \end{aligned}\right\} \tag{1.52}$$

By using the conditions (1.52) it is possible to obtain a solution for the second equation of the system (1.51), etc. The Enskog-Chapman method is, essentially, a successive approximation method, which can be extended, in principle, to systems with large gradients of the thermodynamic and gas-dynamic variables. However, for solving the majority of gas-dynamic problems it appears to be sufficient in practice to solve the Boltzmann equation to the first approximation. In this case, the manner in which the distribution function varies differs little

from the Maxwellian law (1.48), while the gradients of the quantities characterizing the macroscopic properties of the gas are small in the sense that these quantities do not vary appreciably in a distance equal to the mean free path of the molecules.

Readers who are interested in the details of the mathematical solution of the system (1.51) are referred to the monograph by Hirschfelder et al. [1], which also gives some of the results obtained by solving the Boltzmann equations to the first approximation.

The expression for the rate of diffusion is of the form /27

$$\overline{V}_i = -\frac{n^2}{\rho n_i}\sum_{j=1}^{N} m_j D_{ij}\left[\frac{\partial}{\partial r}\left(\frac{n_j}{n}\right) + \left(\frac{n_j}{n} - \frac{n_j m_j}{\rho}\right)\frac{\partial \ln p}{\partial r}\right] - \frac{1}{n_i m_i}\mathscr{D}_i^T \frac{\partial \ln T}{\partial r}, \qquad i = 1, 2, \ldots, N, \tag{1.53}$$

where D_{ij} and $\mathscr{D}_i^T$ are the diffusivity and the thermodiffusion coefficient, respectively, in the multicomponent mixture; p is the pressure. It can be seen from equation (1.53) that in the absence of bulk forces, diffusion can arise for three reasons: 1) due to the action of a concentration gradient (mass diffusion); 2) due to the action of a pressure gradient (barodiffusion), and 3) due to the action of a temperature gradient (thermodiffusion).

It should be noted that in the zeroth approximation (with a Maxwellian distribution of the particles with respect to the velocity, (1.48), the diffusion velocity V_i and as a result, the mass flux density vector for the ith component, j_i, are equal to zero.

The expression for the diffusion velocity of the ith component of the mixture (1.53) is usually difficult to use in practical calculations, since the diffusion coefficients D_{ij} of the multicomponent mixture which appear in this expression can be given to a first approximation in the form of a determination of the Nth order (N is the number of components of the mixture) in terms of the diffusion coefficients $\mathscr{D}_{ij}$ of the binary mixtures, and also the concentrations and molecular weights of the components.

Instead of N formulas of the type (1.53), it is much more convenient to use the N-1 independent relationships

$$\sum_{\substack{j=1\\ j\neq i}}^{N} \frac{n_i n_j}{n^2 \mathscr{D}_{ij}}(\overline{V}_j - \overline{V}_i) = \frac{\partial}{\partial r}\left(\frac{n_i}{n}\right) + \left(\frac{n_i}{n} - \frac{n_i m_i}{\rho}\right)\frac{\partial \ln p}{\partial r} - \frac{\partial \ln T}{\partial r}\sum_{\substack{j=1\\ j\neq i}}^{N} \frac{n_i n_j}{n^2 \mathscr{D}_{ij}}\left(\frac{\mathscr{D}_j^T}{n_j m_j} - \frac{\mathscr{D}_i^T}{n_i m_i}\right). \tag{1.54}$$

The derivation of these relationships, which are sometimes termed the Stefan-Maxwell relationships, can be found in the monograph by Hirschfelder, Curtiss and Bird [1].

If thermodiffusion and barodiffusion can be neglected compared with mass diffusion, equation (1.54) can be simplified and assumes the form /28

$$\sum_{\substack{j=1\\ j\neq i}}^{N} \frac{n_i n_j}{n^2 \mathcal{D}_{ij}} (\bar{V}_j - \bar{V}_i) = \frac{\partial}{\partial r}\left(\frac{n_i}{n}\right). \tag{1.55}$$

By using equation (1.29) for the mass concentration, (1.55) can be transformed into the following form [4]

$$\frac{\partial c_i}{\partial r} = \sum_{\substack{j=1\\ j\neq i}}^{N} \frac{c_i c_j m}{m_j \mathcal{D}_{ij}} (\bar{V}_j - \bar{V}_i) = \sum_{k=1}^{N} c_k \sum_{\substack{j=1\\ j\neq i}}^{N} \frac{c_i c_j m}{m_j \mathcal{D}_{kj}} (\bar{V}_j - \bar{V}_k). \tag{1.56}$$

By making use of equation (1.56) it is possible to introduce the idea of the so-called effective diffusivity $\mathcal{D}_i$ (*):

$$j_i = -\rho \mathcal{D}_i \frac{\partial c_i}{\partial r}, \tag{1.57}$$

where $\mathcal{D}_i$ can be determined from one of the following formulas:

$$\frac{1}{\mathcal{D}_i} = \sum_{j=1}^{N} \frac{m}{m_j} \frac{c_j}{\mathcal{D}_{ij}} \left(1 - \frac{\bar{V}_j}{\bar{V}_i}\right) + \sum_{k=1}^{N} c_k \sum_{j=1}^{N} \frac{m}{m_j} \frac{c_j}{\mathcal{D}_{kj}} \frac{\bar{V}_i - \bar{V}_k}{\bar{V}_i} =$$
$$\sum_{j=1}^{N} \frac{m}{m_j} \frac{c_j}{\mathcal{D}_{ij}} \left(1 - \frac{c_i j_i}{c_j j_i}\right) + \sum_{k=1}^{N} c_k \sum_{j=1}^{N} \frac{m}{m_j} \left(\frac{c_i j_i}{c_j j_i} - \frac{c_i j_k}{c_k j_i}\right). \tag{1.58}$$

From the definition of the effective diffusivity in (1.58) it is clear that in the general case this coefficient depends not only on the composition of the gas mixture but also on the ratio of diffusion fluxes of the components, i.e., essentially /29

*The concept of an effective diffusivity was introduced into practical boundary layer calculations by G. A. Tirskiĭ. See, for instance, [5] and also the paper by this author mentioned above [4].

on the quantities being determined in an actual problem. This fact, which in some cases can lead to certain inconveniences in the calculation process, is not important in calculating turbulent boundary layers in multicomponent gas mixtures (*), since in most cases the method of successive approximations is the most convenient one.

The value of the binary diffusivity $\mathcal{D}_{ij}$ is determined from the expression

$$\mathcal{D}_{ij} = 0{,}0026280 \sqrt{\frac{1}{2}\left(\frac{1}{M_i} + \frac{1}{M_j}\right)} \frac{T^{3/2}}{p\sigma_{ij}^2 \Omega_{ij}^{(1,1)*}(T_{ij}^*)} \frac{\text{cm}^2}{\text{sec}}. \qquad (1.59)$$

where p is the pressure, atm.; M_i is the molecular weight of the i^{th} component; $\Omega_{ij}^{(1,1)*}(T_{ij}^*)$ is the collision integral for mass transfer, which is a measure of the deviation from the model in which the gas molecules are regarded as solid spheres, for which $\Omega_{ij}^{(1,1)*} = 1$; T is the temperature, °K; $T_{ij}^* = kT/\varepsilon_{ij}$ is a characteristic temperature, °K; ε_{ij}/k is the potential energy parameter of the molecule characterizing interactions of molecules of the i^{th} and j^{th} sorts, °K; σ_{ij} is the effective collision diameter of the molecules (Ångstrom units).

Values of the function $\Omega_{ij}^{(1,1)*}(T_{ij}^*)$ for $0.3 \leq T_{ij}^* \leq 400$ are given in [1].

It can be seen from equation (1.59) that the binary mixture diffusivities $\mathcal{D}_{ij}$ are relatively insensitive to moderate changes in the molecular weights of the components. Thus, if any gas mixture consists of two groups of components, each of which has an approximately uniform atomic or molecular weight and an approximately constant transverse cross-sectional area of collision, then this mixture can be regarded as an "effective" binary mixture in which each of the groups behaves as one component, However, it must be remembered that in computing energy transport it is necessary to take into account strictly the enthalpies of the individual components. /30

For a binary mixture it is not difficult to obtain from equation (1.53) the following expression for the diffusion flux of the i^{th} component:

---

*Detailed information on molecular diffusion, just as information on molecular thermal conduction and viscosity, is an essential requirement for studying turbulent boundary layers in hypersonic streams as a result of the important part which is played by the laminar sublayer in processes involving the transport of heat and mass.

$$j_i = m_i n_i \bar{V}_i = -\frac{n^2}{\rho} m_i m_j \mathscr{D}_{ij} \left[\frac{\partial}{\partial r} \left(\frac{n_i}{n} \right) + \left(\frac{n_i}{n} - \frac{n_i m_i}{\rho} \right) \frac{\partial \ln p}{\partial r} - k_T \frac{\partial \ln T}{\partial r} \right]. \quad (1.60)$$

Here

$$k_T = \frac{\rho}{n^2 m_i m_j} \frac{\mathscr{Z}_i^T}{\mathscr{Z}_{ij}} \quad (1.61)$$

is the ratio of the thermodiffusion coefficient to the binary diffusivity, which is known as the thermodiffusion ratio. This ratio characterizes the relative importance of thermodiffusion and mass diffusion.

By using equation (1.29) it is possible to rewrite equation (1.60) in terms of the mass concentration, giving

$$j_i = -\rho c_i \mathscr{D}_{ij} \left[\frac{\partial \ln c_i}{\partial r} + \frac{m_j - m_i}{m} c_j \frac{\partial \ln p}{\partial r} + \frac{m_i m_j}{m^2 c_i} k_T \frac{\partial \ln T}{\partial r} \right]. \quad (1.62)$$

In flows of the boundary layer type the contribution of barodiffusion to the total mass transfer is always negligibly small compared with the contribution of mass diffusion, since to an accuracy to terms of the order of 1/Re, the pressure is constant across the boundary layer. The term characterizing thermodiffusion is also usually small compared with that describing mass diffusion. In a turbulent boundary layer, where it is only necessary to take molecular diffusion into account in the laminar sublayer which usually occupies a small part of the total boundary layer (although in some cases the sublayer thickness may be more than 50% of the thickness of the total boundary layer), it is possible to confine our attention to mass diffusion only (*). In this case, equation (1.62) assumes the form known as Fick's law: /31

$$j_i = -\rho \mathscr{D}_{ij} \frac{\partial c_i}{\partial r}. \quad (1.63)$$

Continuing the consideration of the results obtained by solving the Boltzmann equation to the first approximation, the expression for the pressure tensor can be written as

$$P = p\dot{\mathscr{E}} - 2\mu\dot{S}, \quad (1.64)$$

*Exceptions must be made for flows of multicomponent gas mixtures containing components which differ very widely in molecular weight, such as, for example, hydrogen and air, helium and air.

where

$$p = nkT \tag{1.65}$$

is the equilibrium static pressure at the local temperature and density of the particles;

$$\dot{\mathscr{E}} = \begin{pmatrix} 1 & 0 & 0 \\ 0 & 1 & 0 \\ 0 & 0 & 1 \end{pmatrix} \tag{1.66}$$

is the unit tensor; $\dot{S}$ is the rate of deformation (shear rate) tensor, defined by

$$\dot{S}_{\alpha\alpha} = \frac{\partial v_\alpha}{\partial x} - \frac{1}{3}\left(\frac{\partial}{\partial r}\cdot v\right), \quad \dot{S}_{\alpha\beta} = \frac{1}{2}\left(\frac{\partial v_\beta}{\partial x} + \frac{\partial v_\alpha}{\partial \beta}\right), \quad \alpha,\beta = 1,2,3, \tag{1.67}$$

μ is the dynamic viscosity.

The diagonal and nondiagonal elements of the pressure tensor are equal to

$$\left.\begin{aligned} P_{\alpha\alpha} &= p + \frac{2}{3}\mu\left(\frac{\partial}{\partial r}\cdot v\right) - 2\mu\frac{\partial v_\alpha}{\partial x}, \\ P_{\alpha\beta} &= -\mu\left(\frac{\partial v_\beta}{\partial x} + \frac{\partial v_\alpha}{\partial \beta}\right), \quad \alpha, \beta = 1, 2, 3. \end{aligned}\right\} \tag{1.68}$$

It can be seen from equation (1.68) that the pressure tensor differs from the one usually considered in continuum mechanics [6] and termed the stress tensor only in the sign. /32

In the case of an N-component gas mixture, the dynamic viscosity introduced above is determined from the expression [1]:

$$\mu = \frac{\begin{vmatrix} H_{11} & H_{12} & H_{13} & \dots & H_{1N} & x_1 \\ H_{12} & H_{22} & H_{23} & \dots & H_{2N} & x_2 \\ H_{13} & H_{23} & H_{33} & \dots & H_{3N} & x_3 \\ \dots & \dots & \dots & \dots & \dots & \dots \\ H_{1N} & H_{2N} & H_{3N} & \dots & H_{NN} & x_N \\ x_1 & x_2 & x_3 & \dots & x_N & 0 \end{vmatrix}}{\begin{vmatrix} H_{11} & H_{12} & H_{13} & \dots & H_{1N} \\ H_{12} & H_{22} & H_{23} & \dots & H_{2N} \\ H_{13} & H_{23} & H_{33} & \dots & H_{3N} \\ \dots & \dots & \dots & \dots & \dots \\ H_{1N} & H_{2N} & H_{3N} & \dots & H_{NN} \end{vmatrix}}, \tag{1.69}$$

where

$$\left.\begin{aligned} H_{ii} &= \frac{x_i^2}{\mu_i} + \sum_{\substack{k=1 \\ k\neq i}}^{N} \frac{2x_i x_k}{\mu_{ik}} \frac{M_i M_k}{(M_i + M_k)^2}\left[\frac{5}{3A_{ik}^*} + \frac{M_k}{M_i}\right], \\ H_{ij} &= -\frac{2x_i x_j}{\mu_{ij}} \frac{M_i M_j}{(M_i + M_j)^2}\left[\frac{5}{3A_{ij}^*} - 1\right], \quad i \neq j, \end{aligned}\right\} \tag{1.70}$$

$x_i = n_i/n$ is the molal concentration of the i^{th} component; μ_i is the viscosity of the i^{th} component, equal to

$$\mu_i = 266.93 \cdot 10^{-7} \frac{\sqrt{M_i T}}{\sigma_i^2 \Omega_i^{(2,2)^*}(T_i^*)} \frac{g}{cm \cdot sec}; \tag{1.71}$$

σ_i is the collision diameter; $T_i^* = kT/\varepsilon_i$ is a characteristic temperature; ε_i/k is the potential function parameter for intermolecular interactions; $\Omega_i^{(2,2)^*}$ is the collision integral for momentum transfer, which is a measure of the deviation from the model in which the gas molecules are regarded as solid spheres, for which $\Omega_i^{(2,2)^*} = 1$. Values of the function $\Omega_i^{(2,2)^*}(T_i^*)$ are given for a wide range of values of T_i^* in the monograph by Hirschfelder et al. [1]; μ_{ij} is a coefficient given by

/33

$$\mu_{ij} = 266.93 \cdot 10^{-7} \frac{\sqrt{\frac{2M_i M_j}{M_i + M_j} T}}{\sigma_{ij}^2 \Omega_{ij}^{(2,2)^*}(T_{ij}^*)} \frac{g}{cm \cdot sec}, \tag{1.72}$$

where $\Omega_{ij}^{(2,2)^*}$ is the collision integral for momentum transfer of the i^{th} and j^{th} components. These values are also given in [1]. The quantity A_{ij}^* appearing in (1.70) is equal to $A_{ij}^* = \Omega_{ij}^{(2,2)^*}/\Omega_{ij}^{(1,1)^*}$.

In equation (1.69) the nondiagonal elements H_{ij} are usually small compared with the diagonal elements H_{ii}. For the nondiagonal elements to be exactly equal to zero, it is necessary that $A_{ij}^* = 5/3$. If this assumption is used for the diagonal elements, equation (1.69) assumes the form

$$\mu = \sum_{i=1}^{N} \frac{x_i^2}{\Pi_{ii}} = \sum_{i=1}^{N} \frac{x_i^2}{\frac{x_i^2}{\mu_i} + 2\sum\limits_{\substack{k=1 \\ k \neq i}}^{N} \frac{x_i x_k}{\mu_{ik}} \frac{M_k}{M_i + M_k}}. \tag{1.73}$$

However, equation (1.73) is not very well confirmed by experiments. In order to bring this formula into agreement with the experimental data it is necessary only to replace the factor 2 in the denominator by the empirical coefficient 1.385, i.e.,

$$\mu = \sum_{i=1}^{N} \frac{x_i^2}{\frac{x_i^2}{\mu_i} + 1{,}385\sum\limits_{\substack{k=1 \\ k \neq i}}^{N} \frac{x_i x_k}{\mu_{ik}} \frac{M_k}{M_i + M_k}}. \tag{1.74}$$

Calculation of mixture viscosities according to this formula is quite time-consuming, so that in many cases it is more convenient to use the admittedly less accurate relationships of a simpler nature. In particular, the dynamic viscosity of a pure gas can be calculated from the well-known Sutherland formula: /34

$$\mu_i = K' \frac{T^{3/2}}{T + C'}. \tag{1.75}$$

Values of the coefficients K' and C' for several gases and also generalized data on the viscosities of pure gases and mixtures are contained in the monographs [7, 8].

The energy flux density vector q for a multicomponent mixture of monatomic gases which is obtained by solving the Boltzmann equation to the first approximation has the form

$$q = -\lambda \frac{\partial T}{\partial r} + \sum_{i}^{N} \rho c_i \overline{V}_i h_i + \frac{kT}{n} \sum_{i}^{N} \sum_{\substack{j \\ j \neq i}}^{N} \frac{n_j \mathcal{D}_i^T}{m_i \mathcal{D}_{ij}} (\overline{V}_i - \overline{V}_j). \tag{1.76}$$

where λ is the thermal conductivity and h_i is the enthalpy of the i^{th} component per unit weight, given by

$$h_i = \frac{5}{2} \frac{kT}{m_i}. \tag{1.77}$$

It is clear from equation (1.76) that in a multicomponent mixture the transfer of energy is accomplished by three mechanisms. The first term in the right-hand part of equation (1.76) describes the transfer of energy as a result of thermal conduction, the second the transfer of energy as a result of mass transfer by means of all forms of diffusion (mass diffusion, barodiffusion and thermodiffusion), and the third term describes the additional energy flux caused by the diffusion thermoeffect (the Dufour effect).

For gas mixtures consisting of polyatomic molecules, the energy flux density vector has the same form as for monoatomic gases, (1.76), except that in the enthalpy h_i it is necessary to include all of the quantities given in the sum /35

$$h_i = \left(\frac{5}{2} kT + e_i\right) \frac{1}{m_i}, \tag{1.78}$$

where e_i is the energy of the internal degrees of freedom of the molecules.

In flows of the boundary layer type the contribution of the diffusion thermoeffect to the total transfer of energy is usually not large, so that with a sufficient degree of accuracy for practical purposes it can be assumed that the energy flux density vector for a multicomponent mixture is given by the expression

$$q = -\lambda \frac{\partial T}{\partial r} + \sum_i^N \rho c_i \overline{V}_i h_i. \tag{1.79}$$

If equation (1.53) is used for the mass flux density vector of the i^{th} component, and if it is assumed that thermodiffusion and barodiffusion can be neglected, then equation (1.79) can be rewritten in the form

$$q = -\left(\lambda - \sum_i \sum_j \frac{n^2}{\rho} m_i m_j D_{ij} h_i \frac{\partial x_i}{\partial T}\right) \frac{\partial T}{\partial r} \tag{1.80}$$

The quantity in brackets can be regarded as an effective thermal conductivity, consisting of two parts: λ is the thermal conductivity of the gas mixture caused by molecular collisions, and

$$\lambda_R = -\sum_i \sum_j \frac{n^2}{\rho} m_i m_j D_{ij} h_i \frac{\partial x_i}{\partial T} \tag{1.81}$$

is the conduction of heat due to mass transfer, i.e.,

$$\lambda_{eff} = \lambda + \lambda_R. \tag{1.82}$$

If the transfer of mass is as a result of the occurrence of some chemical reaction (dissociation, ionization, etc.), the thermal conductivity λ is termed the thermal conductivity of the gas in the "frozen" state, i.e., in the absence of chemical reactions, and λ_R is the thermal conductivity as a result of the chemical reaction. For gases which consist of molecules of one sort which do not possess internal degrees of freedom (the internal degrees of freedom are "frozen"), the thermal conductivity is expressed as follows ($\lambda_R = 0$): /36

$$\lambda = \frac{5}{2}\mu c_v, \tag{1.83}$$

where c_v is the heat capacity per unit weight at constant volume.

Gases consisting of molecules of one sort which possess internal degrees of freedom and which are in various excited quantum states can be regarded as gases represented by a chemically reacting mixture with a large number of components, each of which possesses no internal degrees of freedom. If it is assumed that the transfer of energy from the translational to the internal degrees of freedom is large, or, in other words, that the distribution of molecules with respect to the various states is an equilibrium distribution corresponding to the local temperature, then for monoatomic molecules (of one sort) it is possible to obtain the following expression for the effective thermal conductivity [1]:

$$\lambda_{\text{eff}} = \frac{1}{4}\left[\left(15 - 6\frac{\rho\mathcal{D}}{\mu}\right)\gamma - \left(15 - 10\frac{\rho\mathcal{D}}{\mu}\right)\right]c_v\mu, \tag{1.84}$$

where $\gamma = c_p/c_v$, $\mathcal{D}$ is the self-diffusivity, which is defined as the limiting form of the diffusivity of a binary mixture. An expression for the self-diffusivity can be obtained from equation (1.59) by substituting i = j in it. The dimensionless quantity $\rho\mathcal{D}/\mu$ is a function of temperature, and has a value of the order of unity. If this quantity is assumed to be equal to unity, the following formula is obtained for the thermal conductivity of the monoatomic gas:

$$\lambda_{\text{eff}} = \frac{1}{4}(9\gamma - 5)c_v\mu. \tag{1.85}$$

The factor $(9\gamma - 5)/4$ is termed the Eucken correction. Equations (1.84) and (1.85) do not agree very well with experimental data at ordinary temperatures, since the transfer of energy from the translational to the internal degrees of freedom is difficult at these temperatures; however, at high temperatures, equation (1.84) appears to be quite accurate. /37

At present the thermal conductivities of mixtures of monoatomic gases can be calculated to a high degree of accuracy on the basis of the Chapman and Enskog theory. The existing methods of calculation are extensions of the Chapman-Enskog method, and make it possible in principle to calculate the thermal

conductivities of mixtures of monoatomic gases at high temperatures. To carry out calculations with these methods it is necessary to know the interaction potentials among the particles. However, in many cases of practical importance, these potentials are still not sufficiently well known. Information is particularly limited on the interaction potentials of electrons with atoms, ions and molecules. Collisions in which electrons participate can be neglected in calculating the viscosity, since the electrons transport only an insignificant part of the total momentum as a result of their very small mass. However, it is impossible to neglect collisions of electrons with other particles in calculating the thermal conductivity, since with their high velocities the electrons transport a significant part of the total kinetic energy. A detailed consideration of the problems of determining the transport properties in air at high temperatures can be found in the paper by Hansen [9]. Practical methods of calculating thermal conductivities in pure gases amd mixtures are contained in the monograph by Bretsznajder [8].

5. Equations for the dynamics of multicomponent reacting gases.

The expressions obtained in the preceding section for the flux density vector for mass (the diffusion velocity) of the i^{th} component, (1.53), the pressure tensor, (1.64), and the energy flux density vector, (1.76), make it possible to write the gas-dynamic transport equations (section 3) in macroscopic form. However, /38
before doing this, let us collect all the transport equations, retaining the vector-tensor notation. The continuity equation for a gas mixture is

$$\frac{\partial \rho}{\partial t} + \frac{\partial}{\partial \vec{r}} \cdot (\rho v) = 0, \tag{1.31}$$

the continuity equation for the i^{th} component is

$$\rho \frac{\partial c_i}{\partial t} + \rho v \cdot \frac{\partial c_i}{\partial \vec{r}} = w_i - \frac{\partial}{\partial \vec{r}} \cdot \boldsymbol{j}_i, \tag{1.33}$$

the equation of motion is

$$\frac{\partial v}{\partial t} + \left(v \cdot \frac{\partial}{\partial \vec{r}}\right) v = -\frac{1}{\rho}\left(\frac{\partial}{\partial \vec{r}} \cdot P\right), \tag{1.35}$$

and the energy equation is

$$\rho \frac{\partial E}{\partial t} + \rho v \cdot \frac{\partial E}{\partial \vec{r}} = -\frac{\partial}{\partial \vec{r}} \cdot q - \left(P \cdot \frac{\partial}{\partial \vec{r}}\right) \cdot v. \tag{1.39}$$

In order to close the system of equations (1.31), (1.33), (1.35) and (1.39), which involve the five variables v, ρ, p, c_i and E (or T), it is necessary to add to this system the equation of state for the gas mixture

$$p = \rho RT \sum_{i}^{N} \frac{c_i}{M_i}. \tag{1.86}$$

By substituting into equation (1.35) in place of the pressure tensor its expression (1.64), the following form of this equation is obtained:

$$\rho \frac{dv}{dt} = -\frac{\partial p}{\partial r} + 2\frac{\partial}{\partial r} \cdot \mu S. \tag{1.87}$$

Both here and subsequently,

$$\frac{d}{dt} = \frac{\partial}{\partial t} + v \cdot \frac{\partial}{\partial r}. \tag{1.88}$$

The energy equation (1.39) can be converted from the internal energy E to the enthalpy h, which are interrelated by the formula

$$h = E + \frac{p}{\rho}, \tag{1.89}$$

with simultaneous replacement of the pressure tensor by equation (1.64), giving /39

$$\rho \frac{dh}{dt} = \frac{dp}{dt} - \frac{\partial}{\partial r} \cdot q + 2\mu\left(\dot{S} \cdot \frac{\partial}{\partial r}\right) \cdot v. \tag{1.90}$$

Bearing in mind the equation

$$\left(\dot{S} \cdot \frac{\partial}{\partial r}\right) \cdot v = \dot{S}^2, \tag{1.91}$$

equation (1.90) can be transformed into

$$\rho \frac{dh}{dt} = \frac{dp}{dt} - \frac{\partial}{\partial r} \cdot q + 2\mu\dot{S}^2. \tag{1.92}$$

There is still another form of the energy equation, which can be obtained readily from equation (1.39) by using equations (1.35), (1.64), (1.88) and (1.89):

$$\rho \frac{d}{dt}\left(h + \frac{v^2}{2}\right) = \frac{\partial p}{\partial t} - \frac{\partial}{\partial r} \cdot q + 2\frac{\partial}{\partial r} \cdot (\mu\dot{S} \cdot v). \tag{1.93}$$

In what follows, the quantity

$$h + \frac{v^2}{2} = H \tag{1.94}$$

will be termed the total enthalpy of the gas.

If the expression for the mass flux density vector (1.10) is substituted into the equation of continuity for the i^{th} component, and use is made of relationship (1.53) for the diffusion velocity and the molal concentration x_i is replaced by the mass concentration c_i by means of equation (1.29), it is found that

$$\rho \frac{\partial c_i}{\partial t} + \rho v \cdot \frac{\partial c_i}{\partial r} = w_i - \frac{\partial}{\partial r}\left\{\frac{\rho m_i}{m^2}\sum_j D_{ij}\left[\frac{\partial}{\partial r}(c_j m) + c_j(m - m_j)\frac{\partial \ln p}{\partial r}\right] - \mathcal{D}_i^T \frac{\partial \ln T}{\partial r}\right\}. \tag{1.95}$$

If barodiffusion and thermodiffusion are neglected in comparison with mass diffusion, and if the effective diffusivity $\mathcal{D}_i$ defined by equation (1.58) is used in place of the diffusivity of the multicomponent mixture $\mathcal{D}_{ij}$, equation (1.95) assumes the form /40

$$\rho \frac{\partial c_i}{\partial t} + \rho v \cdot \frac{\partial c_i}{\partial r} = w_i + \frac{\partial}{\partial r} \cdot \left(\rho \mathcal{I}_i \frac{\partial c_i}{\partial r}\right). \tag{1.96}$$

In the case of a binary mixture, $\mathcal{I}_i$ is equal to the diffusivity of the binary mixture $\mathcal{I}_{ij}$, and equation (1.96) can then be written in the form

$$\rho \frac{\partial c_i}{\partial t} + \rho v \cdot \frac{\partial c_i}{\partial r} = w_i + \frac{\partial}{\partial r} \cdot \left(\rho \mathcal{I}_{ij} \frac{\partial c_i}{\partial r}\right). \tag{1.97}$$

Let us now consider the energy equation in the form (1.93). By substituting the expressions for the energy flux density vector (1.76) and the mass flux density vector (1.10), (1.53) into this equation it is found that

$$\rho \frac{dH}{dt} = \frac{\partial p}{\partial t} + 2\frac{\partial}{\partial r}\cdot(\mu\dot{S}\cdot v) + \frac{\partial}{\partial r}\cdot\left(\lambda\frac{\partial T}{\partial r}\right) - \frac{\partial}{\partial r}\left\{\frac{\rho^2}{m}\sum_{i=1}^{N}\left[\sum_{j=1}^{N} m_i D_{ij}\left(\frac{\partial}{\partial r}(c_j m) + c_j(m - m_j)\frac{\partial \ln p}{\partial r}\right) - \mathscr{D}_i^T\frac{\partial \ln T}{\partial r}\right] h_i\right\} + \frac{\partial}{\partial r}\cdot\left\{kT\sum_{i=1}^{N}\frac{\mathscr{D}_i^T}{c_i m}\left[\frac{\partial}{\partial r}(c_i m) + c_i(m - m_i)\frac{\partial \ln p}{\partial r} - \frac{\partial \ln T}{\partial r}\sum_{\substack{j=1\\ j\neq i}}^{N}\frac{m^2}{m_j D_{ij}\rho}(c_i\mathscr{D}_j^T - c_j\mathscr{D}_i^T)\right]\right\}. \quad (1.98)$$

As mentioned above, the contributions of barodiffusion to the transport of mass and energy are very insignificant in flows of the boundary layer type. In many cases, the contributions of thermodiffusion in the transport of mass and energy (the diffusion thermoeffect) are also very small. If these effects are neglected and the effective diffusivity is used instead of the diffusivity in the multicomponent mixture the following form of the energy equation is obtained:

$$\rho \frac{dH}{dt} = \frac{\partial p}{\partial t} + 2\frac{\partial}{\partial r}\cdot(\mu\dot{S}\cdot v) + \frac{\partial}{\partial r}\cdot\left(\lambda\frac{\partial T}{\partial r} + \sum_{i=1}^{N}\rho\mathscr{D}_i h_i\frac{\partial c_i}{\partial r}\right). \quad (1.99)$$

However, bearing in mind that /41

$$h = \sum_{i}^{N} c_i h_i, \qquad h_i = \int_0^T c_{pi}\,dT + h_i^0 \quad (1.100)$$

and that consequently,

$$\frac{\partial T}{\partial r} = \frac{1}{c_p}\left(\frac{\partial h}{\partial r} - \sum_{i=1}^{N} h_i\frac{\partial c_i}{\partial r}\right), \qquad c_p = \sum_{i=1}^{N} c_i c_{pi}, \quad (1.101)$$

equation (1.99) can be transformed to

$$\rho \frac{dH}{dt} = \frac{\partial p}{\partial t} + 2\frac{\partial}{\partial r}\cdot(\mu\dot{S}\cdot v) + \frac{\partial}{\partial r}\left\{\frac{\mu}{\mathrm{Pr}}\left[\frac{\partial h}{\partial r} + \sum_{i=1}^{N}(\mathrm{Le}_i - 1)\,h_i\frac{\partial c_i}{\partial r}\right]\right\}. \quad (1.102)$$

Here h_i° is the heat of formation of the i^{th} component under standard conditions.

Two new parameters, the Lewis number and the Prandtl number, have been introduced in equation (1.102); these are defined as

$$Le_i = \frac{\rho \mathcal{D}_i c_p}{\lambda}, \qquad Pr = \frac{\mu c_p}{\lambda}. \tag{1.103}$$

The effective Schmidt number is dependent on these parameters; it is defined as the ratio of the Prandtl and Lewis numbers:

$$Sc_i = \frac{Pr}{Le_i} = \frac{\mu}{\rho \mathcal{D}_i}. \tag{1.104}$$

In the general case the effective Lewis and Schmidt numbers introduced in this way cannot be regarded as similarity parameters like the Prandtl number, since the effective diffusivity depends by definition on the diffusion fluxes of the individual components, and hence on the parameters to be determined in most problems. However, in the special case of a binary mixture the coefficient $\mathcal{D}_i$ becomes equal to the binary mixture diffusivity $\mathcal{D}_{ij}$, which, as equation (1.59) shows, is independent of the unknown flow parameters. In this case the Lewis and Schmidt numbers formed from the binary mixture diffusivities

/42

$$Le = \frac{\rho \mathcal{D}_{ij} c_p}{\lambda}, \qquad Sc = \frac{\mu}{\rho \mathcal{D}_{ij}}, \tag{1.105}$$

can be regarded as similarity parameters.

By considering equation (1.102) it can be seen that if the Lewis number is equal to unity ($Le_i = 1$) the energy equation has the same form as the usual energy equation for a gas of uniform composition.

CHAPTER II.

TURBULENCE IN GAS-DYNAMIC FLOWS

6. The equations of turbulent motion

/43

In turbulent flow the fields of velocity, pressure, temperature, concentration and other gas-dynamic properties have very complex structures. The complexity of these fields is caused by the extremely irregular and random nature of the changes in these parameters in both space and time. If the space-time scales of the turbulence (i.e., the minimum spatial dimension of the turbulent nonuniformities and the characteristic period of the turbulent pulsations) are much larger than the space-time scales of the molecular motion (i.e., the mean free path of the molecules and the mean time between two molecular collisions, respectively), the equations obtained in the preceding section can be used in principle for describing the turbulent motion.

Experiments have shown that the space-time scales of turbulence are always several orders of magnitude greater than the space-time scales of molecular motion, and, as a result, the description of the turbulent motion by means of the differential transport equations is quite valid. However, it is impossible to apply these equations directly in practice, since the fields of the gas-dynamic quantities in turbulent flows are always in the unsteady-state and are strongly influenced by the initial conditions, which are usually far from completely known. This means that a complete, detailed description of turbulent motion is impossible. However, in practice this detailed information on the fields of the gas-dynamic quantities is not required in most cases, since interest centers only on the averaged (statistical) characteristics of these fields. The fact that turbulent motion can be described by the differential transport equations is very important, since as a result of this it appears possible to establish (though not completely) relationships among the averaged characteristics of the fields of the gas-dynamic quantities.

/44

The procedure which makes it possible to establish this type of relationship for the case of flow of an incompressible isothermal fluid was first indicated by Reynolds [10]. This procedure has not been described in quite sufficient detail in the literature [11, 6], and so we will only note very briefly its essential points. Reynolds proposed to represent the values of all the gas-dynamic properties in a turbulent stream in the form of sums of averaged and pulsating components, and to study only the averaged parts, which vary relatively smoothly in time and space.

In order to determine the mean value of any particular quantity, Reynolds proposed the use of ordinary averaging over a suitable time period (time averaging). It should be noted that other forms of averaging are also possible, for example, averaging over a given region at a particular moment of time (spatial averaging), or averaging for a large number of fields which vary both from point to point and also from one moment of time to another (statistical ensemble averaging). Without going into details of the advantages and disadvantages of the various forms of averaging, it should only be noted that the instruments usually used make it possible to measure the average values of quantities with respect to time, so that time averaging appears to be the most important type*.

Following Reynolds, the instantaneous value of each of the unknown quantities or their combinations is expressed in the form of the sum of an averaged (f) and the pulsating components (f'): /45

$$f = \bar{f} + f'. \tag{2.1}$$

Time averaging, as described by the equation

$$\bar{f} = \frac{1}{\Delta t} \int_{t}^{t+\Delta t} f\,dt, \tag{2.2}$$

is understood by the term "averaging", in which the averaging interval Δt is assumed to be quite large in comparison with the characteristic pulsation period of the field and sufficiently small compared with the period of averaging of the field. If the averaged field is steady, i.e., if its period is infinitely large, the mean value of the quantity f can be expressed by the relationship

$$\bar{f} = \lim_{\Delta t \to \infty} \left[\frac{1}{\Delta t} \int_{t}^{t+\Delta t} f\,dt \right]. \tag{2.3}$$

As Reynolds showed, in any averaging process (not only time-averaging) a necessary requirement is that the following relationships (which have become known as the Reynolds conditions) must be satisfied

$$\begin{aligned} &1)\ \overline{\bar{f} + \bar{g}} = \bar{f} + \bar{g}; \\ &2)\ \overline{a\bar{f}} = a\bar{f}, \quad \text{if } a = \text{const}; \\ &3)\ \bar{a} = a, \quad \text{if } a = \text{const}; \end{aligned} \tag{2.4}$$

*A detailed discussion of the problems of evaluating averages of quantities in the theory of turbulence can be found in the monograph by A. S. Monin and A. M. Yaglom [11] to which reference was made above.

4) $\frac{\overline{\partial f}}{\partial s} = \frac{\partial \bar{f}}{\partial s}$, where s is x, y, z or t;

5) $\overline{\bar{f}\bar{g}} = \bar{f}\bar{g}$. (2.4 cont'd)

By substituting successively in (2.4) g = 1, g = $\bar{h}$, and g = h' = h - $\bar{h}$ (where the prime denotes the pulsating component of the quantity) the following important results are obtained from the Reynolds conditions: /46

$$\bar{\bar{f}} = \bar{f}, \quad \overline{f'} = \bar{f} - \bar{\bar{f}} = 0, \quad \overline{\bar{f}\bar{h}} = \bar{f}\bar{h}, \quad \overline{\bar{f}h'} = \bar{f}\overline{h'} = 0. \tag{2.5}$$

By using these results, it is possible to establish the following important further rules for the averaging of products of two or three variable quantities:

$$\overline{fg} = \overline{(\bar{f} + f')(\bar{g} + g')} = \bar{f}\bar{g} + \overline{f'g'}, \tag{2.6}$$

$$\overline{fgh} = \bar{f}\bar{g}\bar{h} + \bar{f}\overline{g'h'} + \bar{g}\overline{f'h'} + \bar{h}\overline{f'g'} + \overline{f'g'h'}. \tag{2.7}$$

The pulsating components of products of two variables are obviously given by

$$\begin{aligned}(fg)' = fg - \overline{fg} &= (\bar{f} + f')(\bar{g} + g') - \overline{fg} = \\ &\bar{f}\bar{g} + f'\bar{g} + \bar{f}g' + f'g' - \bar{f}\bar{g} - \overline{f'g'} = \\ &f'\bar{g} + \bar{f}g' + f'g' - \overline{f'g'}.\end{aligned} \tag{2.8}$$

Passing now to the derivation of the averaged equations of turbulent motion for multicomponent reacting gas mixtures * it is convenient to write the continuity equations for the mixture and for the i^{th} component and the equations for momentum and energy transport in tensor notation: double repeated subscripts are taken to mean summation with respect to the values 1, 2, 3, corresponding to the components of the vectors or tensors in the x, y, and z directions respectively (this rule is not extended to the subscript i).

In this notation, the continuity equation for a gas mixture (1.31) assumes the form

$$\frac{\partial \rho}{\partial t} + \frac{\partial}{\partial s_j}(\rho v_j) = 0. \tag{2.9}$$

The continuity equation for the i^{th} component, (1.33), can be rearranged by using equation (2.9) to the form /47

---

*The derivation of the equations of turbulent motion of a compressible homogeneous gas was first given by Van Driest [12].

$$\frac{\partial}{\partial t}(\rho c_i) + \frac{\partial}{\partial s_j}(\rho v_j c_i) = w_i - \frac{\partial}{\partial s_j}(\rho c_i \overline{V}_{ij}). \tag{2.10}$$

For writing the momentum transport equation use is made of equation (2.9) and the expression for the pressure tensor, (1.64), as a result of which

$$\frac{\partial}{\partial t}(\rho v_k) + \frac{\partial}{\partial s_j}(\rho v_j v_k) = -\frac{\partial p}{\partial s_k} + \frac{\partial}{\partial s_j}(2\mu \dot{S}_{jk}). \tag{2.11}$$

The energy transport equation is taken in the form (1.93). By using the expression for the heat flux (1.79) and equation (2.9), it is found that

$$\frac{\partial}{\partial t}\left(\rho h + \frac{\rho v_k^2}{2}\right) + \frac{\partial}{\partial s_j}\left(\rho v_j h + \frac{1}{2}\rho v_j v_k^2\right) = \frac{\partial p}{\partial t} + \frac{\partial}{\partial s_j}\left(\lambda \frac{\partial T}{\partial s_j} - \sum_i \rho_i \overline{V}_{ij} h_i + 2\mu \overline{\dot{S}}_{jk} v_k\right). \tag{2.12}$$

In these equations the subscript i denotes the number of the component, while the subscripts j and k assume the values of 1, 2, 3.

By combining with the continuity equation (2.9) the averaging operation (2.2), and assuming that it is possible to represent this operation with differentials with respect to the spatial coordinates and time (the fourth of Reynolds' conditions in 2.4), it is found that

$$\frac{\partial \bar{\rho}}{\partial t} + \frac{\partial}{\partial s_j}(\overline{\rho v_j}) = 0. \tag{2.13}$$

On expanding the term $\overline{\rho v_j}$ according to equation (2.6), it is found that

$$\overline{\rho v_j} = \bar{\rho}\bar{v}_j + \overline{\rho' v_j}. \tag{2.14}$$

Thus, in the flow of a turbulent incompressible gas, the continuity equation for the compressible gas will have the form

$$\frac{\partial \bar{\rho}}{\partial t} + \frac{\partial}{\partial s}(\bar{\rho}\bar{v}_j) + \frac{\partial}{\partial s_j}(\overline{\rho' v_j'}) = 0. \tag{2.15}$$

In contrast to the continuity equation for incompressible fluids, equation (2.15) contains derivatives with respect to the coordinates of the averaged flow rate of the pulsating momentum. The deficiencies of our knowledge of the general nature of turbulence make it impossible at present to make a quantitative evaluation of the contribution of the term $\frac{\partial}{\partial s_j}(\rho' v'_j)$ in the continuity equation. From physical

/48

reasoning it is clear that

$$\overline{\rho' v_j} < \bar{\rho}\bar{v}_j,$$

but the conditions under which it is possible to neglect the quantity $\overline{\rho' v'_j}$ in comparison with $\overline{\rho v_j}$ remain an open problem. This fact makes the derivation of the equation for the averaged turbulent motion of a compressible gas (if density pulsations are not neglected) an essentially formal procedure.

If the continuity equation for the i^{th} component, equation (2.10), is now averaged it is found that

$$\frac{\partial}{\partial t}\overline{\rho c_i} + \frac{\partial}{\partial s_j}\overline{(\rho v_j) c_i} = \bar{w}_i - \frac{\partial}{\partial s_j}\overline{(\rho \bar{V}_{ij})\, c_i}. \tag{2.16}$$

By applying the relationship (2.6) to this equation and carrying out the differentiation indicated in the left part of the equation, it is found that

$$\begin{aligned} \bar{c}_i \frac{\partial \bar{\rho}}{\partial t} + \bar{\rho}\frac{\partial \bar{c}_i}{\partial t} + \frac{\partial}{\partial t}\overline{\rho' c'_i} + \bar{\rho}\bar{v}_j \frac{\partial \bar{c}_i}{\partial s_j} + \overline{\rho' v_i}\frac{\partial c_i}{\partial s_j} + \\ \bar{c}_i \frac{\partial}{\partial s_j}(\bar{\rho}\bar{v}_j + \overline{\rho' v'_j}) + \frac{\partial}{\partial s_j}\overline{(\rho v_j)' c_i} = \\ \bar{w}_i - \frac{\partial}{\partial s_j}\overline{(\rho \bar{V}_{ij})}\,\bar{c}_i - \frac{\partial}{\partial s_j}\overline{(\rho \bar{V}_{ij})' c'_i}. \end{aligned} \tag{2.17}$$

It can be noted that the sum of the first and sixth terms of the left-hand part of equation (2.17) is equal to zero as a result of the equation of continuity (2.15), and that the last term on the right-hand side of the equation can be discarded because of its smallness compared with the second term on the same side of the equation: /49

$$\left|\overline{(\rho \bar{V}_{ij})' c'_i}\right| \ll \left|(\rho \bar{V}_{ij})\,\bar{c}_i\right|. \tag{2.18}$$

It is then seen that*

$$\begin{aligned} \bar{\rho}\frac{\partial \bar{c}_i}{\partial t} + \bar{\rho}\bar{v}_j \frac{\partial \bar{c}_i}{\partial s_j} = \\ \bar{w}_i - \frac{\partial}{\partial s_j}\left[(\rho \bar{V}_{ij})\,\bar{c}_i + \overline{(\rho v_j)' c'_i}\right] - \frac{\partial}{\partial t}\overline{\rho' c'_i} - \bar{\rho}\bar{v}_j \frac{\partial \bar{c}_i}{\partial s_j} \end{aligned} \tag{2.19}$$

*It should be noted that the operation of averaging the mass rate of formation of the i^{th} component w_i is not indicated here, since at the present time in using the averaged continuity equation for the i^{th} component in a turbulent stream the approximation is generally accepted according to which $\bar{w}_i$ is taken to mean the expression (w_i) in which all the variables are averaged with respect to time. Attempts to take into account pulsating terms in the expression $\bar{w}_i$ lead to difficulties which are presently insurmountable.

The validity of the inequality (2.18) is based on the circumstance that, as is well known, the molecular properties of the medium play an important part in turbulent streams only in the region adjacent to the walls (the laminar sublayer), where the turbulence is damped. Since $\bar{V}_{ij}$ is the rate of molecular diffusion it is clear that the pulsating component of the diffusion flux in this zone will be small compared with the averaged component.

It can be seen from equation (2.19) that in addition to the transport of material caused by molecular diffusion, in turbulent flows there is also a transport of material caused by the mixing set up by the pulsations of density, velocity and concentration $\overline{(\rho v_j)' c_i'}$. By analogy with molecular diffusion, the process of mass transfer in a turbulent stream caused by pulsations of the density, velocity and concentration is termed turbulent diffusion.

The derivation of the averaged equations of motion (based on equation (2.11)) does not contain any further difficulties beyond those in the derivation of the averaged continuity equation (2.19), and is completely analogous to the latter. Thus, omitting details of the derivation, these equations can be written in final form

/50

$$\bar{\rho}\frac{\partial \bar{v}_k}{\partial t} + \bar{\rho}\bar{v}_j\frac{\partial \bar{v}_k}{\partial s_j} = -\frac{\partial \bar{p}}{\partial s_k} + \frac{\partial}{\partial s_j}[2\bar{\mu}\bar{S}_{jk} - \overline{(\rho v_j)' v_k'}] - \frac{\partial}{\partial t}\overline{\rho' v_k'} - \overline{\rho' v_j}\frac{\partial \bar{v}_k}{\partial s_j}. \qquad (2.20)$$

It should be noted that in deriving these equations the terms involving viscosity pulsations were neglected compared with the terms containing the averaged values of the viscosity, for the reasons indicated in the note to equation (2.18). Equation (2.20) is known as the Reynolds equation for a compressible gas. The quantities $\overline{(\rho v_j)' v_k}$ appearing in (2.20) have the significance of components of an additional stress tensor which arises as a result of the presence of the turbulent pulsations of the mass flow rate and velocity. These additional stresses are usually termed the Reynolds stresses.

In setting up the equations for energy transport in the averaged turbulent motion of a multicomponent reacting mixture, the pulsations of viscosity, thermal conductivity, diffusivity and specific heat capacity are compared with their average values.

By averaging equation (2.12), and using as before the interchangeability of the operations of averaging and differentiation with respect to the coordinates and time, it is found that

$$\frac{\partial}{\partial t}\overline{\rho h} + \frac{1}{2}\frac{\partial}{\partial t}\overline{\rho v_k v_k} + \frac{\partial}{\partial s_j}\overline{\rho v_j h} + \frac{1}{2}\frac{\partial}{\partial s_j}\overline{\rho v_j v_k^2} = \frac{\partial \bar{p}}{\partial t} + \frac{\partial}{\partial s_j}\left[\bar{\lambda}\frac{\partial \bar{T}}{\partial s_j} - \sum_i \overline{\rho_i \bar{V}_{ij} h_i} + 2\overline{\bar{\mu} S_{jk} v_k}\right]. \qquad (2.21)$$

Each of the four terms on the left-hand side of this equation can be rearranged individually, making use of relationships (2.6) - (2.8); this gives

$$\frac{\partial}{\partial t}\overline{\rho h} = \frac{\partial}{\partial t}(\overline{\rho}\bar{h} + \overline{\rho' h'}) = \bar{\rho}\frac{\partial \bar{h}}{\partial t} + \bar{h}\frac{\partial \bar{\rho}}{\partial t} + \frac{\partial}{\partial t}\overline{\rho' h'},$$

$$\frac{1}{2}\frac{\partial}{\partial t}\overline{\rho v_k v_k} = \frac{1}{2}\frac{\partial}{\partial t}[\bar{\rho}\overline{v_k^2} + \bar{\rho}\bar{v}_k^2 + 2\bar{v}_k\overline{\rho' v_k'} + \overline{\rho' v_k'^2}] =$$

$$\frac{\overline{v_k^2}}{2}\frac{\partial \bar{\rho}}{\partial t} + \bar{\rho}\bar{v}_k\frac{\partial \bar{v}_k}{\partial t} + \frac{1}{2}\frac{\partial}{\partial t}\bar{\rho}\overline{v_k'^2} + \frac{\partial}{\partial t}\bar{v}_k\overline{\rho' v_k'} + \frac{1}{2}\frac{\partial}{\partial t}\overline{\rho' v_k'^2},$$

$$\frac{\partial}{\partial s_j}\overline{\rho v_j h} = \frac{\partial}{\partial s_j}\overline{(\rho v_j)h} = \frac{\partial}{\partial s_j}[\overline{(\rho v_j)}\bar{h} + \overline{(\rho v_j)' h'}] = \qquad \underline{51}$$

$$\overline{\rho v_j}\frac{\partial \bar{h}}{\partial s_j} + \bar{h}\frac{\partial}{\partial s_j}\overline{\rho v_j} + \frac{\partial}{\partial s_j}\sum_i \overline{(\rho v_j)'(c_i h_i)'} =$$

$$\overline{\rho v_j}\frac{\partial \bar{h}}{\partial s_j} + \overline{\rho' v_j'}\frac{\partial \bar{h}}{\partial s_j} + \bar{h}\frac{\partial}{\partial s_j}(\bar{\rho}\bar{v}_j + \overline{\rho' v_j'}) +$$

$$+ \frac{\partial}{\partial s_j}\sum_i \bar{c}_i\overline{(\rho v_j)' h_i'} + \frac{\partial}{\partial s_j}\sum_i \bar{h}_i\overline{(\rho v_j)' c_i'} + \frac{\partial}{\partial s_j}\sum_i \overline{(\rho v_j)' c_i' h_i'},$$

$$\frac{1}{2}\frac{\partial}{\partial s_j}\overline{\rho v_j v_k^2} = \frac{1}{2}\frac{\partial}{\partial s_j}\overline{(\rho v_j)v_k^2} =$$

$$= \frac{1}{2}\frac{\partial}{\partial s_j}[\bar{\rho}\bar{v}_j\overline{v_k^2} + \overline{(\rho v_j)' v_k'^2}] =$$

$$\frac{1}{2}\frac{\partial}{\partial s_j}[\bar{\rho}\bar{v}_j(\bar{v}_k^2 + \overline{v_k'^2}) + 2\bar{v}_k\overline{(\rho v_j)' v_k'} + \overline{(\rho v_j)' v_k'^2}] =$$

$$\frac{\bar{v}_k^2}{2}\frac{\partial}{\partial s_j}(\bar{\rho}\bar{v}_j + \overline{\rho' v_j'}) + \bar{\rho}\bar{v}_j\bar{v}_k\frac{\partial \bar{v}_k}{\partial s_j} + \overline{\rho' v_j'}\bar{v}_k\frac{\partial \bar{v}_k}{\partial s_j} +$$

$$+ \frac{1}{2}\frac{\partial}{\partial s_j}\overline{\rho v_j v_k^2} + \frac{\partial}{\partial s_j}\bar{v}_k\overline{(\rho v_j)' v_k'} + \frac{\partial}{\partial s_j}\overline{(\rho v_j)' v_k'^2}.$$

When these expressions are substituted into the initial equation (2.21) the result is

$$\underset{(1)}{\bar{\rho}\frac{\partial \bar{h}}{\partial t}} + \underset{(2)}{\bar{h}\frac{\partial \bar{\rho}}{\partial t}} + \underset{(3)}{\frac{\partial}{\partial t}\overline{\rho' h'}} + \underset{(4)}{\frac{\bar{v}_k^2}{2}\frac{\partial \bar{\rho}}{\partial t}} + \underset{(5)}{\bar{\rho}\bar{v}_k\frac{\partial \bar{v}_k}{\partial t}} +$$

$$\underset{(6)}{\frac{1}{2}\frac{\partial}{\partial t}\bar{\rho}\overline{v_k^2}} + \underset{(7)}{\bar{v}_k\frac{\partial}{\partial t}\overline{\rho' v_k'}} + \underset{(8)}{\frac{1}{2}\frac{\partial}{\partial t}\overline{\rho' v_k'^2}} + \underset{(9)}{\overline{\rho v_j}\frac{\partial \bar{v}_k}{\partial s_j}} +$$

$$\underset{(10)}{\overline{\rho' v_j'}\frac{\partial \bar{h}}{\partial s_j}} + \underset{(11)}{\bar{h}\frac{\partial}{\partial s_j}(\bar{\rho}\bar{v}_j + \overline{\rho' v_j'})} + \underset{(12)}{\frac{\partial}{\partial s_j}\sum_i \bar{c}_i\overline{(\rho v_j)' h_i'}} +$$

$$\underset{(13)}{\frac{\partial}{\partial s_j}\sum_i \bar{h}_i\overline{(\rho v_j)' c_i'}} + \underset{(14)}{\frac{\partial}{\partial s_j}\sum_i \overline{(\rho v_j)' c_i' h_i'}} +$$

$$\underset{(15)}{\frac{\bar{v}_k^2}{2}\frac{\partial}{\partial s_j}(\bar{\rho}\bar{v}_j + \overline{\rho' v_j'})} + \underset{(16)}{\bar{\rho}\bar{v}_j\bar{v}_k\frac{\partial \bar{v}_k}{\partial s_j}} + \underset{(17)}{\overline{\rho' v_j' v_k}\frac{\partial \bar{v}_k}{\partial s_j}} + \qquad (2.22)$$

$$+\underset{(18)}{\frac{1}{2}\frac{\partial}{\partial s_j}\overline{\rho v_j v_k^2}}+\underset{(19)}{\frac{\partial}{\partial s_j}\bar{v}_k\overline{(\rho v_j)'v_k'}}+\underset{(20)}{\frac{\partial}{\partial s_j}\overline{(\rho v_j)'v_k'^2}}+\underset{(21)}{\overline{\rho' v_k'}\frac{\partial \bar{v}_k}{\partial t}}=$$

$$\underset{(1)}{\frac{\partial \bar{p}}{\partial t}}+\underset{(2)}{\frac{\partial}{\partial s_j}\bar{\lambda}\frac{\partial \bar{T}}{\partial s_j}}-\underset{(3)}{\frac{\partial}{\partial s_j}\sum_i \overline{\rho_i \bar{V}_{ij}}\bar{h}_i}-$$

$$\underset{(4)}{\frac{\partial}{\partial s_j}\sum_i \overline{(\rho_i \bar{V}_{ij})'h_i'}}+\underset{(5)}{2\frac{\partial}{\partial s_j}\bar{\mu}\bar{S}_{jk}\bar{v}_k}+\underset{(6)}{2\frac{\partial}{\partial s_j}\overline{\mu S_{jk}v_k}}. \qquad (2.22 \text{ Cont'd})$$

In this equation, the sum of the second, fourth, eleventh and fifteenth terms of the left-hand part is equal to zero as a result of the continuity equation (2.15); the eight, fourteenth and twentieth of the left side can be discarded as a result of their smallness, since they contain triple products of pulsating quantities. It is not difficult to see that the sixth and eighteenth terms on the left side can also be neglected, since $\overline{v_k'^2} \ll \overline{v_k^2}$. For the same reasons for which the last term in equation (2.17) was omitted, it is possible to omit the fourth and sixth terms of the right side of the equation. In order to simplify equation (2.22) further, the fifth, seventh, sixteenth and seventeenth terms of the left side are grouped together, giving

$$\bar{v}_k\left[\bar{\rho}\frac{\partial \bar{v}_k}{\partial t}+\bar{\rho}\bar{v}_j\frac{\partial \bar{v}_k}{\partial s_j}+\overline{\rho' v_j'}\frac{\partial \bar{v}_k}{\partial s_j}+\frac{\partial}{\partial t}\overline{\rho' v_k'}\right],$$

and it is not difficult to see from equation (2.20) that this is equivalent to the expression

$$\bar{v}_k\left[-\frac{\partial \bar{p}}{\partial s_k}+\frac{\partial}{\partial s_j}(2\bar{\mu}\bar{S}_{jk})-\frac{\partial}{\partial s_j}\overline{(\rho v_j)'v_k'}\right].$$

Bearing this in mind, and carrying out some simple rearrangements, the energy equation is reduced to the following form

$$\bar{\rho}\frac{\partial \bar{h}}{\partial t}+\bar{\rho}\bar{v}_j\frac{\partial \bar{h}}{\partial s_j}=\frac{\partial \bar{p}}{\partial t}+\bar{v}_k\frac{\partial \bar{p}}{\partial s_k}+$$

$$[2\bar{\mu}\bar{S}_{jk}-\overline{(\rho v_j)'v_k'}]\frac{\partial \bar{v}_k}{\partial s_j}+\frac{\partial}{\partial s_j}\left[\bar{\lambda}\frac{\partial \bar{T}}{\partial s_j}-\sum_i \bar{c}_i\overline{(\rho v_j)'h_i'}\right]- \qquad /53$$

$$\frac{\partial}{\partial s_j}\left[\sum_i \bar{\rho}_i\bar{V}_{ij}\bar{h}_i+\sum_i \bar{h}_i\overline{(\rho v_j)'c_i'}\right]-$$

$$-\frac{\partial}{\partial t}\overline{\rho' h'}-\overline{\rho' v_j'}\frac{\partial \bar{h}}{\partial s_j}-\overline{\rho' v_k'}\frac{\partial \bar{v}_k}{\partial t}. \qquad (2.23)$$

In equation (2.23) the term $\overline{(\rho v_j)'h_i'}$ expresses the transfer of energy of

the i^{th} component caused by turbulent pulsations. The term $\sum_i \overline{(\rho v_j)' c_i' h_i'}$ expresses the transfer of energy as a result of turbulent mass transfer (turbulent diffusion). The term $\overline{(\rho v_j)' v_k'} \frac{\partial \bar{v}_k}{\partial s_j}$ defines the rate of conversion of energy of the averaged motion into turbulent energy as a result of the action of the Reynolds stresses. The term $\sum_i \bar{c}_i \overline{(\rho v_j)' h_i'}$ expresses the total quantity of energy transferred by all the components of the mixture as a result of the turbulent pulsations.

By analogy with molecular heat conduction, the process of energy transport in a turbulent stream caused by the pulsations of density, velocity and enthalpy is termed turbulent heat conduction.

Let us now consider the averaging of the equation of state (1.86). By using the rule (2.7) and neglecting triple products of pulsating quantities, it is found that

$$\bar{p} = \bar{\rho} R \bar{T} \sum_i \frac{\bar{c}_i}{M_i} \left[1 + \frac{\overline{c_i' T'}}{\bar{c}_i \bar{T}} + \frac{\overline{c_i' \rho'}}{\bar{c}_i \bar{\rho}} + \frac{\overline{\rho' T'}}{\bar{\rho} \bar{T}} \right] \tag{2.24}$$

Equations (2.15), (2.19), (2.20), (2.23) and (2.24) represent the system of equations for the averaged turbulent motion of a multicomponent reacting gas mixture. It must be mentioned at once that at present it is impossible to utilize this system of equations even within the limits of the semiempirical boundary layer theory without making a whole series of assumptions, the validity of which in many cases is far from obvious. As mentioned already above, our information on the nature of turbulence does not permit the evaluation of the contributions to the transport processes of the terms in the equations which involve density pulsations. In all existing theories which use these equations or modifications of them, therefore, the terms containing the density pulsations are neglected. Of course, this does not mean that the density is regarded as constant. Where necessary, the averaged density $\bar{\rho}$ is regarded as a variable quantity. /54

If the terms containing the pulsations of density are neglected in the equations for the averaged turbulent motion of a multicomponent reacting gas mixture, and if all the pulsating terms are neglected in the equation of state*, so that only "steady-state" turbulent flow is considered in what follows in which the averaged values of the velocity, enthalpy, density, etc., are independent of time, the following system of equations is obtained:

$$\frac{\partial}{\partial s_j} (\bar{\rho} \bar{v}_j) = 0, \tag{2.25}$$

* For the equation of state the same assumption is made as for the mass rate of formation of the i^{th} component w_i (see note on p. 48).

$$\bar{\rho}\bar{v}_j\frac{\partial\bar{c}_i}{\partial s_j}=\bar{w}_i-\frac{\partial}{\partial s_j}(\bar{\rho}\overline{V}_{ij}\bar{c}_i+\bar{\rho}\overline{v_j'c_i'}),\tag{2.26}$$

$$\bar{\rho}\bar{v}_j\frac{\partial\bar{v}_k}{\partial s_j}=-\frac{\partial\bar{p}}{\partial s_k}+\frac{\partial}{\partial s_j}(2\bar{\mu}\overline{S}_{jk}-\bar{\rho}\overline{v_j'v_k'}),\tag{2.27}$$

$$\begin{aligned}\bar{\rho}\bar{v}_j\frac{\partial\bar{h}}{\partial s_j}=\bar{v}_k\frac{\partial\bar{p}}{\partial s_k}+(2\bar{\mu}\overline{S}_{jk}-\bar{\rho}\overline{v_j'v_k'})\frac{\partial\bar{v}_k}{\partial s_j}+\\ \frac{\partial}{\partial s_j}\left(\bar{\lambda}\frac{\partial\bar{T}}{\partial s_j}-\sum_i\bar{c}_i\bar{\rho}\,\overline{v_j'h_i'}\right)-\frac{\partial}{\partial s_j}\left(\sum_i\bar{\rho}_i\overline{V}_{ij}\bar{h}_i+\sum_i\bar{h}_i\bar{\rho}\,\overline{v_j'c_i'}\right),\end{aligned}\tag{2.28}$$

$$\bar{p}=\bar{\rho}R\bar{T}\sum_i\frac{\bar{c}_i}{\bar{M}_i}.\tag{2.29}$$

It will also be assumed in formal terms that

$$-\bar{\rho}\overline{v_j'v_k'}=\varepsilon\frac{\partial\bar{v}_k}{\partial s_j},\tag{2.30}$$

$$-\bar{\rho}\,\overline{v_j'c_i'}=\bar{\rho}\mathcal{D}_T\frac{\partial\bar{c}_i}{\partial s_j},\tag{2.31}$$

$$-\bar{\rho}\overline{v_j'h_i'}=\lambda_T\frac{\partial\bar{T}}{\partial s_j},\tag{2.32}$$

where ε, $\mathcal{D}_T$ and λ_T are respectively the turbulent viscosity, turbulent diffusivity and turbulent thermal conductivity. In contrast to the molecular viscosity, diffusivity and thermal conductivity, the turbulent viscosity, diffusivity and thermal conductivity do not represent physical properties of the gas, but are statistical properties of the pulsating motion. These coefficients are therefore functions of position and time. It is important to note that far from a solid surface the turbulent transport coefficients greatly exceed the values of the corresponding coefficients of molecular transport. /55

By analogy with the molecular Prandtl, Lewis and Schmidt numbers, equations (1.103) - (1.105), their turbulent analogs can be introduced here:

$$\mathrm{Pr}_T=\frac{\varepsilon\bar{c}_p}{\lambda_T},\tag{2.33}$$

$$\mathrm{Le}_T = \frac{\bar{\rho}\bar{\mathcal{D}}_T\bar{c}_p}{\lambda_T}. \tag{2.34}$$

$$\mathrm{Sc}_T = \frac{\varepsilon}{\bar{\rho}\bar{\mathcal{D}}_T} = \frac{\mathrm{Pr}_T}{\mathrm{Le}_T}. \tag{2.35}$$

Although the turbulent transport coefficients ε, $\mathcal{D}_T$ and λ_T are in general functions of position and time, their dimensionless combinations Pr_T, Le_T and Sc_T are usually regarded as quantities which vary very little, and in many cases of practical importance it is possible to regard them as constants. Numerical values of Pr_T, Le_T and Sc_T have not been accurately established up to the present time. The few available experiments data on the magnitudes of these numbers are rather contradictory; nevertheless it can be said that in boundary-layer type flows close to solid surfaces Pr_T and Sc_T are close to unity; in turbulent jet flows they are close to 0.5 - 0.7*.

By using relationships (2.30) - (2.32), and omitting the averaging symbol for simplicity in what follows, the system of equations (2.25) - (2.29) is reduced to the form /56

$$\frac{\partial}{\partial s_j}(\rho v_j) = 0, \tag{2.36}$$

$$\rho v_j \frac{\partial c_i}{\partial s_j} = w_i - \frac{\partial}{\partial s_j}\left(\rho \overline{V}_{ij} c_i - \rho \mathcal{D}_T \frac{\partial c_i}{\partial s_j}\right), \tag{2.37}$$

$$\rho v_j \frac{\partial v_k}{\partial s_j} = -\frac{\partial p}{\partial s_k} + \frac{\partial}{\partial s_j}\left(2\mu \dot{S}_{jk} + \varepsilon \frac{\partial v_k}{\partial s_j}\right), \tag{2.38}$$

$$\rho v_j \frac{\partial h}{\partial s_j} = v_k \frac{\partial p}{\partial s_k} + \left(2\mu \dot{S}_{jk} + \varepsilon \frac{\partial v_k}{\partial s_j}\right)\frac{\partial v_k}{\partial s_j} + \frac{\partial}{\partial s_j}\left[(\lambda + \lambda_T)\frac{\partial T}{\partial s_j}\right] - \frac{\partial}{\partial s_j}\left(\sum_i \rho c_i \overline{V}_{ij} h_i - \sum_i \rho \mathcal{D}_T h_i \frac{\partial c_i}{\partial s_j}\right), \tag{2.39}$$

$$p = \rho R T \sum_i \frac{c_i}{M_i}. \tag{2.40}$$

By using equation (1.101), which in tensor notation has the form

* See Section 15 for a discussion of the turbulent Prandtl number.

$$\frac{\partial T}{\partial s_j} = \frac{1}{c_p}\left(\frac{\partial h}{\partial s_j} - \sum_i h_i \frac{\partial c_i}{\partial s_j}\right), \tag{2.41}$$

and bearing in mind equations (2.33) - (2.35), the energy equation (2.39) can be rearranged to the form

$$\rho v_j \frac{\partial h}{\partial s_j} = v_k \frac{\partial p}{\partial s_k} + \left(2\mu \dot{S}_{jk} + \varepsilon \frac{\partial v_k}{\partial s_j}\right)\frac{\partial v_k}{\partial s_j} + \frac{\partial}{\partial s_j}\left[\left(\frac{\mu}{\mathrm{Pr}} + \frac{\varepsilon}{\mathrm{Pr}_T}\right)\frac{\partial h}{\partial s_j} - \sum_i \left(\rho c_i \overline{V}_{ij} h_i - \frac{\mu}{\mathrm{Pr}} h_i \frac{\partial c_i}{\partial s_j}\right) + \frac{\varepsilon}{\mathrm{Pr}_T}(\mathrm{Le}_T - 1)\sum_i h_i \frac{\partial c_i}{\partial s_j}\right]. \tag{2.42}$$

If equation (2.42) is written in terms of the total enthalpy H, defined by equation (1.94) instead of the enthalpy h the following equation is obtained by using (2.38):

$$\rho v_j \frac{\partial H}{\partial s_j} = \frac{\partial}{\partial s_j}\left[\left(\frac{\mu}{\mathrm{Pr}} + \frac{\varepsilon}{\mathrm{Pr}_T}\right)\frac{\partial H}{\partial s_j} - \sum_i \left(\rho c_i \overline{V}_{ij} h_i - \frac{\mu}{\mathrm{Pr}} h_i \frac{\partial c_i}{\partial s_j}\right) + \frac{\varepsilon}{\mathrm{Pr}_T}(\mathrm{Le}_T - 1)\sum_i h_i \frac{\partial c_i}{\partial s_j} + \varepsilon\left(1 - \frac{1}{\mathrm{Pr}_T}\right)\frac{\partial}{\partial s_j}\left(\frac{v_k^2}{2}\right) + 2\mu v_k \dot{S}_{jk} - \frac{\mu}{\mathrm{Pr}}\frac{\partial}{\partial s_j}\left(\frac{v_k^2}{2}\right)\right]. \tag{2.43}$$

The system (2.36) - (2.40) contains 5 + N + j equations (of the N equations for the concentrations only N - 1 are independent, since $\sum_i c_i = 1$), and does not, generally speaking, define the turbulent flow completely, since it contains the 5 + N + j unknown functions v_j, p, ρ, h, c_i (i = 1, 2, ..., N) and the undefined coefficients of turbulent viscosity ε, diffusivity $\mathcal{D}_T$ and thermal conductivity λ_T. In other words, the system of equations (2.36) - (2.40) is not a closed system. This unclosed nature of the system of equations describing the processes of turbulent transport makes it impossible at present to set up theories of the type which would make it possible to calculate turbulent motions by purely theoretical means even in the very simple case of the flow of a homogeneous, incompressible isothermal fluid. All the existing theories of turbulence in incompressible homogeneous fluids are semiempirical, since they are based both on certain rational arguments and on a number of empirical results. The solution of problems of turbulent motion in the more complicated cases of flows of compressible heat-conducting reacting gases is usually based on generalizing to these cases the semiempirical theories developed for incompressible fluids. However, even in such a semiempirical approach the use of the system of equations (2.36) - (2.40) obtained above is very difficult as a result of its great mathematical complexity. As a result, in many cases of practical importance it is very desirable to make simplifications to this system which are based on the boundary-layer theory.

/57

7. The turbulent boundary layer equations in a multicomponent reacting gas.

The application of the system of equations (2.36) - (2.40) to the flows in the thin boundary layers which are formed on the walls of channels or on the surfaces of bodies during their motion through gaseous media makes it possible to simplify the system appreciably. The series of assumptions involved (first formulated by L. Prandtl) and which form the basis of modern boundary-layer theory are well known.

Let us consider a fully developed two-dimensional averaged flow with averaged velocities $v_1 = u$ and $v_2 = v$ in the directions $s_1 = x$ along the surface of the body and $s_2 = y$ along the normal to the surface of the body, respectively (Fig. 1). /58

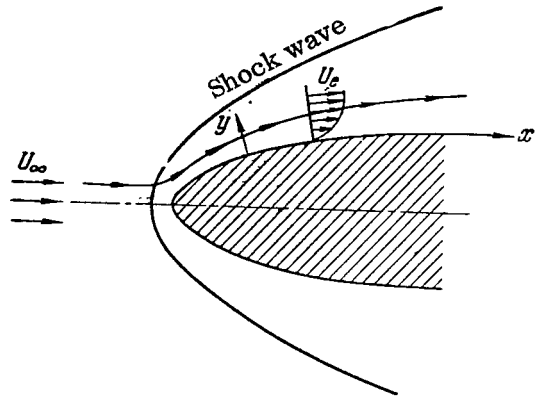

Figure 1.

Following Prandtl's fundamental idea, the entire flow field is divided into two regions: a thin region of eddying flow adjacent to the surface of the solid in which the flow parameters vary rapidly from the wall values to the values in the outer stream (the boundary layer), and a zone of irrotational (potential) flow (the external flow). The thickness of the boundary layer δ is regarded as small compared with the distance x. The quantities x and u are taken to be of the order of unity, i.e.,

$$x \sim O(1) \text{ and } u \sim O(1);$$

then

$$y \sim O(\delta) \text{ and } v \sim O(\delta)$$

and so

$$\frac{\partial}{\partial x} \sim O(1) \text{ and } \frac{\partial}{\partial y} \sim O\left(\frac{1}{\delta}\right),$$
$$\frac{\partial^2}{\partial x^2} \sim O(1) \text{ and } \frac{\partial^2}{\partial y^2} \sim O\left(\frac{1}{\delta^2}\right).$$

The orders of magnitude of the pressure, density, concentration and enthalpy are taken to be unity: /59

$$p \sim O(1),\ \rho \sim O(1),\ c_i \sim O(1),\ h \sim O(1).$$

If it is assumed that the terms in the equations of the system (2.36) - (2.39) which contain μ, λ, ε, $\mathcal{D}_T$, λ_T and $\overline{V}_i$ do not exceed in their order of magnitude the remaining terms, it is not difficult to conclude that μ, λ, ε, $\mathcal{D}_T$, and λ_T must have orders of magnitude not exceeding $-\delta^2$ and that $\overline{V}_i$ has an order of magnitude not greater than δ.

On the basis of these evaluations and by retaining in the equations of the system (2.36) - (2.39) only the terms of the same order of magnitude, this system is reduced to the following form

$$\frac{\partial}{\partial x}(\rho u) + \frac{\partial}{\partial y}(\rho v) = 0, \tag{2.44}$$

$$\rho u \frac{\partial c_i}{\partial x} + \rho v \frac{\partial c_i}{\partial y} = w_i - \frac{\partial}{\partial y}\left(\rho c_i \overline{V}_{iy} - \rho \mathcal{D}_T \frac{\partial c_i}{\partial y}\right), \tag{2.45}$$

$$\rho u \frac{\partial u}{\partial x} + \rho v \frac{\partial u}{\partial y} = -\frac{\partial p}{\partial x} + \frac{\partial}{\partial y}\left[(\mu + \varepsilon)\frac{\partial u}{\partial y}\right], \tag{2.46}$$

$$0 = -\frac{\partial p}{\partial y}, \tag{2.47}$$

$$\rho u \frac{\partial h}{\partial x} + \rho v \frac{\partial h}{\partial y} = u \frac{\partial p}{\partial x} + (\mu + \varepsilon)\left(\frac{\partial u}{\partial y}\right)^2 + \frac{\partial}{\partial y}\left[(\lambda + \lambda_T)\frac{\partial T}{\partial y} - \sum_i \rho c_i \overline{V}_{iy} h_i - \rho \mathcal{D}_T \sum_i h_i \frac{\partial c_i}{\partial y}\right]. \tag{2.48}$$

Equations (2.42) and (2.43) respectively assume the forms

$$\rho u \frac{\partial h}{\partial x} + \rho v \frac{\partial h}{\partial y} = u \frac{\partial p}{\partial x} + (\mu + \varepsilon)\left(\frac{\partial u}{\partial y}\right)^2 + \frac{\partial}{\partial y}\left[\left(\frac{\mu}{\mathrm{Pr}} + \frac{\varepsilon}{\mathrm{Pr}_T}\right)\frac{\partial h}{\partial y} - \sum_i \rho c_i \overline{V}_{iy} h_i - \frac{\mu}{\mathrm{Pr}} \sum_i h_i \frac{\partial c_i}{\partial y} + \frac{\varepsilon}{\mathrm{Pr}_T}(\mathrm{Le}_i - 1)\sum_i h_i \frac{\partial c_i}{\partial y}\right] \tag{2.49}$$

and

$$\rho u\frac{\partial H}{\partial x}+\rho v\frac{\partial H}{\partial y}=\frac{\partial}{\partial y}\left\{\left(\frac{\mu}{\mathrm{Pr}}+\frac{\varepsilon}{\mathrm{Pr}_{\tau}}\right)\frac{\partial H}{\partial y}+\left[\mu\left(1-\frac{1}{\mathrm{Pr}}\right)+\varepsilon\left(1-\frac{1}{\mathrm{Pr}_{\tau}}\right)\right]\frac{\partial}{\partial y}\left(\frac{u^2}{2}\right)-\sum_i \rho c_i \overline{V}_{iy}h_i-\frac{\mu}{\mathrm{Pr}}\sum_i h_i\frac{\partial c_i}{\partial y}+\frac{\varepsilon}{\mathrm{Pr}_{\tau}}(\mathrm{Le}_{\tau}-1)\sum_i h_i\frac{\partial c_i}{\partial y}\right\}. \qquad (2.50)$$

/60

In equations (2.45) and (2.48) - (2.50) the diffusion rate is determined in general from the expression (1.53). However, as noted in section 3, the effects of baro- and thermo-diffusion are usually small in boundary layers. This is particularly true of turbulent boundary layers where the region in which the molecular transport processes have an effect occupies only a part (and often a very insignificant part) of the total boundary layer. If the effects of baro- and thermo-diffusion on mass transfer are neglected compared with mass diffusion, an expression arising from (1.57) is obtained for the rate of diffusion. The projection onto the y axis is

$$\overline{V}_{iy}=-\frac{\mathscr{D}_i}{c_i}\frac{\partial c_i}{\partial y}. \qquad (2.51)$$

Here $\mathscr{D}_i$ is the effective diffusivity, defined by equation (1.58). In the case of a binary mixture, $\mathscr{D}_i$ becomes the binary diffusivity $\mathscr{D}_{ij}$ for the mixture.

By substituting equation (2.51) into the continuity equation for the i^{th} component, (2.45), and the energy equation (2.48), and dropping the relationship (2.47), the system of equations for the turbulent boundary layer in a multicomponent reacting gas mixture is reduced to the folling form:

$$\frac{\partial}{\partial x}(\rho u)+\frac{\partial}{\partial y}(\rho v)=0, \qquad (2.44)$$

$$\rho u\frac{\partial u}{\partial x}+\rho v\frac{\partial u}{\partial y}=-\frac{dp}{dx}+\frac{\partial}{\partial y}\left[(\mu+\varepsilon)\frac{\partial u}{\partial y}\right], \qquad (2.52)$$

$$\rho u\frac{\partial c_i}{\partial x}+\rho v\frac{\partial c_i}{\partial y}=w_i+\frac{\partial}{\partial y}\left[\rho(\mathscr{D}_i+\mathscr{D}_{\tau})\frac{\partial c_i}{\partial y}\right], \qquad (2.53)$$

$$\rho u\frac{\partial h}{\partial x}+\rho v\frac{\partial h}{\partial y}=u\frac{dp}{dx}+(\mu+\varepsilon)\left(\frac{\partial u}{\partial y}\right)^2+\frac{\partial}{\partial y}\left\{\left(\frac{\mu}{\mathrm{Pr}}+\frac{\varepsilon}{\mathrm{Pr}_{\tau}}\right)\frac{\partial h}{\partial y}+\sum_i\left[\frac{\mu}{\mathrm{Pr}}(\mathrm{Le}_i-1)+\frac{\varepsilon}{\mathrm{Pr}_{\tau}}(\mathrm{Le}_{\tau}-1)\right]h_i\frac{\partial c_i}{\partial y}\right\}. \qquad (2.54)$$

The energy equation in the form (2.50) can be transformed to the following form by substituting equation (2.51) in it:

$$\rho u \frac{\partial H}{\partial x} + \rho v \frac{\partial H}{\partial y} = \frac{\partial}{\partial y}\left\{\left(\frac{\mu}{\mathrm{Pr}} + \frac{\varepsilon}{\mathrm{Pr}_T}\right)\frac{\partial H}{\partial y} + \sum_i\left[\frac{\mu}{\mathrm{Pr}}(\mathrm{Le}_i - 1) + \frac{\varepsilon}{\mathrm{Pr}_T}(\mathrm{Le}_T - 1)\right]h_i\frac{\partial c_i}{\partial y} + \left[\mu\left(1 - \frac{1}{\mathrm{Pr}}\right) + \varepsilon\left(1 - \frac{1}{\mathrm{Pr}_T}\right)\right]\frac{\partial}{\partial y}\left(\frac{u^2}{2}\right)\right\}. \quad (2.55)$$

It should be noted that in a turbulent boundary layer there is a transitional (buffer) zone at some distance from the wall; in this zone the molecular and turbulent transport coefficients have the same order of magnitude. In this zone also, the boundary layer equations derived above are inexact, since certain quantities (pulsations of the molecular terms) which play an important part in the transition zone were neglected in deriving the general equations of turbulent motion, from which in turn the boundary layer equations were obtained. As a result, the equations of motion (2.52), energy (2.54), (2.55), and continuity for the i^{th} component (2.53) in the form in which they are written assume that the boundary layer is divided into two zones, with different flow conditions: the turbulent core, in which $\mu \ll \varepsilon$, $\lambda \ll \lambda_T$, $\mathcal{D}_i \ll \mathcal{D}_T$, and the laminar sublayer, in which $\mu \gg \varepsilon$, $\lambda \gg \lambda_T$, and $\mathcal{D}_i \gg \mathcal{D}_T$.

The continuity equation for the i^{th} component, equation (2.53) is written for mass concentrations of the individual components of the mixture, and is nonhomogeneous in the presence of homogeneous chemical reactions in the stream ($w_i \neq 0$). In some cases it is more convenient to write these equations not for the mass concentrations of the components but for the mass concentrations of the individual chemical elements regardless of the fact that these elements are combined into chemical compounds. In this case, the diffusion equation becomes homogeneous in the absence of nuclear reactions. Actually, if we use the notation /62

$$c_{ki} = \frac{m_k N_k}{m_i} \quad (2.56)$$

for the concentration of the k^{th} element in the i^{th} component of the mixture, where N_k is the number of atoms of the k^{th} element in the i^{th} component, then the quantity $w_i c_{ki}$ represents the mass rate of transfer of element k in component i. Since the mass of the element is conserved during a chemical reaction,

$$\sum_i c_{ki} w_i \equiv w_k = 0. \quad (2.57)$$

The concentration of the element k in the mixture will obviously be equal to $c_k = \sum_i c_{ki} c_i$. Consequently, by multiplying the diffusion equation (2.53) by c_{ki} and summing over all the components of the mixture, an expression is obtained for the continuity equation of the k^{th} element in the form

$$\rho u \frac{\partial c_k}{\partial x} + \rho v \frac{\partial c_k}{\partial y} = \frac{\partial}{\partial y}\left[\rho(\mathcal{D}_k + \mathcal{D}_\tau)\frac{\partial c_k}{\partial y}\right],$$
$$\mathcal{D}_k = \sum_i \mathcal{D}_i c_{ki} \frac{\partial c_i/\partial y}{\partial c_k/\partial y}. \qquad (2.58)$$

Sometimes it is convenient to write the turbulent boundary layer equations in terms of the variables derived by L. Crocco. As one of the variables, Crocco proposed the use of the longitudinal velocity component u. The formulas for converting from the variables x, y to the Crocco variables $\xi = x$, u are of the form *:

$$\left.\begin{aligned}\frac{\partial}{\partial y} &= \frac{\partial u}{\partial y}\frac{\partial}{\partial u} = \frac{\tau}{\mu+\varepsilon}\frac{\partial}{\partial u},\\ \frac{\partial}{\partial x} &= \frac{\partial}{\partial \xi} - \frac{\partial y}{\partial \xi}\frac{\tau}{\mu+\varepsilon}\frac{\partial}{\partial u}.\end{aligned}\right\} \qquad (2.59)$$

When this conversion is carried out for the continuity equation (2.44) and the result is multiplied by $(\mu + \varepsilon)/\tau$, it is found that /63

$$\frac{\mu+\varepsilon}{\tau}\frac{\partial}{\partial \xi}(\rho u) - \frac{\partial y}{\partial \xi}\frac{\partial}{\partial u}(\rho u) + \frac{\partial}{\partial u}(\rho v) = 0. \qquad (2.60)$$

After converting to the variables ξ, u and reducing both parts by the same factor $\tau/(\mu + \varepsilon)$, the equation of motion (2.52) assumes the form

$$-\rho u \frac{\partial y}{\partial \xi} + \rho v = -\frac{dp}{d\xi}\frac{\mu+\varepsilon}{\tau} + \frac{\partial \tau}{\partial u}. \qquad (2.61)$$

By differentiating both parts of (2.61) with respect to u, it is found that

$$-\rho u \frac{\partial}{\partial \xi}\left(\frac{\partial y}{\partial u}\right) - \frac{\partial y}{\partial \xi}\frac{\partial}{\partial u}(\rho u) + \frac{\partial}{\partial u}(\rho v) = -\frac{dp}{d\xi}\frac{\partial}{\partial u}\left(\frac{\mu+\varepsilon}{\tau}\right) + \frac{\partial^2 \tau}{\partial u^2}.$$

By subtracting both parts of this equation term by term from (2.60) and using the

*The derivation of these conversion formulas is given in [13], p. 335.

relationship $\partial y/\partial u = (\mu + \varepsilon)/\tau$, v can be eliminated to leave

$$u\frac{\partial}{\partial\xi}\left[\frac{(\mu+\varepsilon)\rho}{\tau}\right]+\frac{\partial^2\tau}{\partial u^2}-\frac{dp}{d\xi}\frac{\partial}{\partial u}\left(\frac{\mu+\varepsilon}{\tau}\right)=0. \tag{2.62}$$

Similar rearrangements can be carried out for the continuity equation of the i^{th} component (2.53). This is first rewritten in terms of the new variables

$$\rho u\frac{\partial c_i}{\partial\xi}+\left(-\rho u\frac{\partial y}{\partial\xi}+\rho v\right)\frac{\tau}{\mu+\varepsilon}\frac{\partial c_i}{\partial u}= w_i+\frac{\tau}{\mu+\varepsilon}\frac{\partial}{\partial u}\left[\frac{\rho(\mathscr{D}_i+\mathscr{D}_\tau)}{\mu+\varepsilon}\tau\frac{\partial c_i}{\partial u}\right]$$

and then by means of (2.61) the expression within the round brackets on the left can be eliminated; bearing in mind equations (1.104) and (2.35), it is possible to obtain after simple rearrangements

$$\rho u\frac{\mu+\varepsilon}{\tau}\frac{\partial c_i}{\partial\xi}+\left(\frac{\partial\tau}{\partial u}-\frac{dp}{d\xi}\frac{\mu+\varepsilon}{\tau}\right)\frac{\partial c_i}{\partial u}= \frac{\mu+\varepsilon}{\tau}w_i+\frac{\partial}{\partial u}\left[\left(\frac{1}{Sc_i}+\frac{1}{Sc_\tau}\right)\tau\frac{\partial c_i}{\partial u}\right). \tag{2.63}$$

By applying the transformation (2.69) to the energy equation (2.55), and carrying out certain obvious simplifications as before, it is found that /64

$$\rho u\frac{\mu+\varepsilon}{\tau}\frac{\partial H}{\partial\xi}+\left(\frac{\partial\tau}{\partial u}-\frac{dp}{d\xi}\frac{\mu+\varepsilon}{\tau}\right)\frac{\partial H}{\partial u}= \frac{\partial}{\partial u}\left\{\tau\left[\left(\frac{1}{Pr}+\frac{1}{Pr_\tau}\right)\frac{\partial H}{\partial u}+\sum_i\left(\frac{1}{Pr}(Le_i-1)+\frac{1}{Pr_\tau}(Le_\tau-1)\right)h_i\frac{\partial c_i}{\partial u}+\left(1-\frac{1}{Pr}-\frac{1}{Pr_\tau}\right)u\right]\right\}. \tag{2.64}$$

The energy equation in Crocco variables in terms of the enthalpy h can be easily obtained from equation (2.64) by substituting equation (1.94) for H and bearing in mind that $\partial u/\partial\xi = 0$; the result is

$$\rho u(\mu+\varepsilon)\frac{\partial h}{\partial\xi}-(\mu+\varepsilon)\left(u+\frac{\partial h}{\partial u}\right)\frac{dp}{d\xi}+\tau\frac{\partial\tau}{\partial u}\frac{\partial h}{\partial u}\times \left(1-\frac{1}{Pr}-\frac{1}{Pr_\tau}\right)-\tau^2\left[1+\frac{\partial}{\partial u}\left(\frac{1}{Pr}+\frac{1}{Pr_\tau}\right)\frac{\partial h}{\partial u}\right]- \sum_i\left[\frac{1}{Pr}(Le_i-1)+\frac{1}{Pr_\tau}(Le_\tau-1)\right]h_i\frac{\partial c_i}{\partial u}=0. \tag{2.65}$$

The equations (2.62), (2.63), (2.64) (or (2.65)), together with the equation of state (2.40) represent the system of turbulent boundary layer equations in Crocco variables. This system, like the system of equations (2.44), (2.52), (2.54) (or 2.55)) assumes that the boundary layer is divided into two zones, the turbulent core and the laminar sublayer. In using these equations within the laminar sublayer it is necessary to omit the terms containing the turbulent transport coefficients and their dimensionless combinations (ε, λ_T, $\mathcal{D}_T$, Pr_T, Le_T, Sc_T); similarly, in the turbulent core it is necessary to omit the terms containing the molecular transport coefficients and their dimensionless combinations (μ, λ, $\mathcal{D}_i$, Pr, Le_i, Sc_i).

When flow in the boundary layer on an axisymmetric body of revolution is considered, the continuity equation can be written in the form

$$\frac{\partial}{\partial x}(r_w \rho u) + \frac{\partial}{\partial y}(r_w \rho v) = 0, \tag{2.66}$$

and the term $\frac{\rho u(\mu + \varepsilon)}{\tau} \frac{1}{r_w} \frac{dr_w}{d\xi}$ must be added to the left hand part of the equation of motion in Crocco variables (2.62), as a result of which it assumes the form /65

$$u \frac{\partial}{\partial \xi}\left[\frac{(\mu+\varepsilon)\rho}{\tau}\right] + \frac{\partial^2 \tau}{\partial u^2} - \frac{dp}{d\xi}\frac{\partial}{\partial u}\left(\frac{\mu+\varepsilon}{\tau}\right) + \frac{\rho u(\mu+\varepsilon)}{\tau}\frac{1}{r_w}\frac{dr_w}{d\xi} = 0. \tag{2.67}$$

Here $r_w = r_w(x) = r_w(\xi)$ is the radius of transverse curvature of the body. These equations (2.66) and (2.67) are valid only if the boundary layer thickness δ is considerably smaller than r_w, i.e., if $\delta \ll r_w$. This condition is not satisfied in the downstream part of a long axisymmetric body or in a long channel. All the other turbulent boundary layer equations for the case of an axisymmetric body are the same as those for a flat boundary layer.

8. The semiempirical theory of turbulence. Reynolds' analogy.

The system of turbulent boundary layer equations obtained in the preceding section is not a closed system, just like the initial system (2.36) - (2.40), since the number of unknown exceeds the number of equations. It is known that in investigations of the turbulent motion of incompressible, homogeneous and isothermal liquids, the semiempirical theory of turbulence is used to close the system. All modern semiempirical theories of turbulence in incompressible fluids are based on a series of assumptions which are contained in the hypothesis which is usually given the name "the hypothesis of the localness of the mechanism

of turbulent transport" [14]. The most important of these assumptions is the assumption that the mechanism of turbulent momentum transport is completely specified if the local values of the derivative of the averaged velocity with respect to the coordinate perpendicular to the direction of flow and the physical properties of the fluid are given. The hypothesis of localness does not take into account the effects of processes occurring far from the point being considered. On the basis of the hypothesis of localness and dimensional considerations it is possible to obtain the equations of the semiempirical theory of Prandtl and von Kármán [15]. /66

In Prandtl's theory it is assumed that the local change of the averaged velocity depends only on the first derivative of the velocity du/dy; dimensional considerations therefore lead to the need for introducing the additional concept of a "mixing length", without which it is impossible to set up a relationship for the shear stress. By using dimensional arguments it can be shown that the only possible combination of the quantities ρ (the fluid density), 1 (the mixing length) and du/dy (the velocity gradient) which expresses the shear stress τ is

$$\tau = \rho l^2 \left(\frac{du}{dy}\right)^2. \tag{2.68}$$

The quantitative expression for the relationship $l(y)$ must be determined from other considerations.

In von Kármán's theory the change in the averaged velocity is given in terms of the first two derivatives of the velocity, du/dy and d^2u/dy^2. Similar dimensional considerations lead to the conclusion that the only equation for von Kármán's shear stress is

$$\tau = \rho \varkappa^2 \frac{\left(\frac{du}{dy}\right)^4}{\left(\frac{d^2u}{dy^2}\right)^2}. \tag{2.69}$$

The application of the semiempirical theories to processes and turbulent heat and mass transfer is based on the so-called "Reynolds analogy". According to this analogy it is assumed that the turbulent transport coefficients for momentum, heat and mass have the same values. This assumes that there is no effect of changes in heat content and concentration in the stream on the mechanism of turbulent mixing and is probably valid for not too large changes in heat content and concentration. The assumption that the coefficients of turbulent transport for momentum, heat and mass are the same is obviously equivalent to assuming that the turbulent analogs of the Prandtl and Schmidt numbers are equal to unity: /67

$$\mathrm{Pr}_T = \mathrm{Sc}_T = 1. \tag{2.70}$$

The Reynolds analogy can be represented quantitatively in the form

$$\tau = \varepsilon \frac{du}{dy}, \quad q = \varepsilon \frac{dh}{dy}, \quad j_{i\tau} = \varepsilon \frac{dc_i}{dy} \tag{2.71}$$

or

$$\frac{q}{\tau} = \frac{dh}{du}, \quad \frac{j_{i\tau}}{\tau} = \frac{dc_i}{du}. \tag{2.72}$$

In studying turbulent flows in which it is necessary to take into account the effects of compressibility, heat and mass transfer, chemical reactions, etc., (all together or only some), the only possible procedure available up to now is the method of generalizing the semiempirical theories of turbulence for incompressible fluids to deal with these more complicated cases; usually the generalization is reduced to the direct utilization of the semiempirical formulas of Prandtl (2.68) and von Kármán (2.69). The forms of the Prandtl and von Kármán equations are retained entirely except that the quantity ρ (the density) is regarded as a variable. As regards the value of the turbulence constant $\varkappa$ (it will be recalled that the expression $l = \varkappa y$ is often used for the mixing length) it may be noted that although there are certain experimental data indicating that the compressibility factor and heat transfer affect its value, these data do not permit us to draw any quantitative conclusions as to these effects*. For the constant $\varkappa$ it is therefore usual to take the value for incompressible fluids ($\varkappa = 0.39 - 0.41$). /68

9. The integral momentum and energy relationships

The integral conditions for the conservation of momentum and energy are used in boundary layer theory for setting up approximate methods (or so-called integral methods) for calculating friction and heat transfer. In order to obtain these, boundary conditions are set up on the surface of the solid body and the outer edge of the boundary layer for the velocity, total enthalpy and concentration of the components; in order to be as general as possible, the surface of the solid body will be regarded as being permeable. These conditions have the form

$$\left.\begin{array}{llll} u = 0, & v = v_w, & H = h_w, \; c_i = c_{iw} & \text{at } y = 0; \\ u \to U_e, & H \to H_e, & c_i \to c_{ie} & \text{at } y \to \infty; \\ \dfrac{\partial u}{\partial y} \to 0, & \dfrac{\partial H}{\partial y} \to 0, & \dfrac{\partial c_i}{\partial y} \to 0 & \text{at } y \to \infty. \end{array}\right\} \tag{2.73}$$

The second condition on the wall, $v = v_w$, is the condition expressing the permeability of the wall; if the wall is impermeable, $v_w = 0$. The last three conditions

*This problem is discussed in detail in Chapter III.

characterize a smooth junction of the profiles for the velocity, total enthalpy and concentration at the boundary between the boundary layer and the external stream.

The external stream will be regarded as isentropic, and consequently the velocity at the outer boundary U_e will be related to the pressure on the surface of the body by means of Bernoulli's equation:

$$-\frac{dp}{dx} = \rho_e U_e \frac{dU_e}{dx}. \tag{2.74}$$

The boundary layer equations in terms of the variables x and y are used in deriving the integral relationships. The continuity equation (2.66) is rewritten in the form /69

$$\frac{\partial}{\partial x}(\rho u) + \frac{\partial}{\partial y}(\rho v) + \rho u \frac{1}{r_w^\nu}\frac{dr_w^\nu}{dx} = 0, \tag{2.75}$$

where $\nu = 0$ for plane flow and $\nu = 1$ for axisymmetric flow in the boundary layer.

The integral momentum relationship. By using equations (2.74) and (2.75), the equation of motion (2.52) is rewritten in the form

$$\frac{\partial}{\partial x}(\rho u^2) + \frac{\partial}{\partial y}(\rho uv) + \rho u^2 \frac{1}{r_w^\nu}\frac{dr_w^\nu}{dx} = \rho_e U_e \frac{dU_e}{dx} + \frac{\partial}{\partial y}\left[(\mu + \varepsilon)\frac{\partial u}{\partial y}\right].$$

By multiplying both sides of equation (2.75) by U_e, it is found that

$$\frac{\partial}{\partial x}(\rho u U_e) + \frac{\partial}{\partial y}(\rho v U_e) + \rho u U_e \frac{1}{r_w^\nu}\frac{dr_w^\nu}{dx} = \rho u \frac{dU_e}{dx}.$$

By subtracting from this equation both parts of the previous equation, it is possible to arrive at the expression

$$\frac{\partial}{\partial x}\rho u(U_e - u) + \frac{\partial}{\partial y}\rho v(U_e - u) + (\rho_e U_e - \rho u)\frac{dU_e}{dx} + \rho u(U_e - u)\frac{1}{r_w^\nu}\frac{dr_w^\nu}{dx} = -\frac{\partial}{\partial y}\left[(\mu + \varepsilon)\frac{\partial u}{\partial y}\right].$$

By integrating this expression across the boundary layer with respect to y from zero to infinity, and introducing into the discussion the integral thicknesses:

$$\delta^{**} = \int_0^\infty \frac{\rho u}{\rho_e U_e}\left(1 - \frac{u}{U_e}\right) dy \tag{2.76}$$

which is the momentum loss thickness, and

$$\delta^{*} = \int_0^\infty \left(1 - \frac{\rho u}{\rho_e U_e}\right) dy \tag{2.77}$$

which is the displacement thickness, and by using the boundary condition (2.73) for the velocity, it is found that /70

$$\frac{d}{dx}(\rho_e U_e^2 \delta^{**}) + \delta^{*}\rho_e U_e \frac{dU_e}{dx} + \\ + \rho_e U_e^2 \delta^{**} \frac{1}{r_w^v}\frac{dr_w^v}{dx} = \tau_w + \rho_w v_w U_e, \tag{2.78}$$

where

$$\tau_w = \left(\mu \frac{\partial u}{\partial y}\right)_w$$

is the wall shear stress.

By carrying out the differentiation in (2.78) and noting that

$$\frac{\rho_e'}{\rho_e} = -M_e^2 \frac{U_e'}{U_e}, \tag{2.79}$$

the following integral momentum relationship is obtained after dividing both sides of equation (2.78) by $\rho_e U_e^2$:

$$\frac{d\delta^{**}}{dx} + \frac{U_e'}{U_e}(2 + H^{*} - M_e^2)\delta^{**} + \frac{\delta^{**}}{r_w^v}\frac{dr_w^v}{dx} = \frac{\tau_w}{\rho_e U_e^2} + \frac{\rho_w v_w}{\rho_e U_e}. \tag{2.80}$$

Here

$$H^{*} = \frac{\delta^{*}}{\delta^{**}} \tag{2.81}$$

is the boundary layer form parameter; $M_e = U_e/a_e$ is the Mach number; a_e is the velocity of sound at the outer edge of the boundary layer. The primes denote

derivatives with respect to the coordinate x. It should be noted that equation (2.79) is not difficult to obtain from Bernoulli's equation (2.74) if the latter is written in the form

$$-\left(\frac{dp}{d\rho}\right)_e \frac{d\rho_e}{dx} = \rho_e U_e \frac{dU_e}{dx}.$$

If the definition of the velocity of sound

$$a_e^2 = \left(\frac{dp}{d\rho}\right)_e, \tag{2.82}$$

is recalled, equation (2.79) follows directly.

The integral momentum relationship can be written in several other forms, /71
bearing in mind that

$$a_e^2 = \gamma R T_e, \qquad T_e\left(1 + \frac{\gamma - 1}{2} M_e^2\right) = \text{const}$$

and so

$$\frac{U_e'}{U_e} = \frac{(M_e a_e)'}{M_e a_e} = \frac{M_e'}{M_e} + \frac{a_e'}{a_e} = \frac{M_e'}{M_e} + \frac{1}{2}\frac{T_e'}{T_e} = \frac{M_e'}{M_e} - \frac{(\gamma - 1) M_e^2}{1 + \frac{\gamma - 1}{2} M_e^2} \cdot \frac{M_e'}{M_e} = \frac{1}{1 + \frac{\gamma - 1}{2} M_e^2} \cdot \frac{M_e'}{M_e}. \tag{2.83}$$

As a result, it is found that

$$\frac{d\delta^{**}}{dx} + \frac{M_e'}{M_e} \frac{2 + H^* - M_e^2}{1 + \frac{\gamma - 1}{2} M_e^2} \delta^{**} + \frac{\delta^{**}}{r_w^v} \frac{dr_w^v}{dx} = \frac{c_f}{2} + c_m. \tag{2.84}$$

Here

$$c_f = \frac{2\tau_w}{\rho_e U_e^2} \tag{2.85}$$

is the local coefficient of friction, and

$$c_m = \frac{\rho_w v_w}{\rho_e U_e} \tag{2.86}$$

is the relative mass rate of supply of material through the wall surface.

The integral energy relationship. By means of equation (2.75) the energy equation (2.56) can be transformed to the form:

$$\frac{\partial}{\partial x}(\rho u H)+\frac{\partial}{\partial y}(\rho v H)+\rho u H\frac{1}{r_w^{\nu}}\frac{dr_w^{\nu}}{dx}=\frac{\partial}{\partial y}\left[\left(\frac{\mu}{\mathrm{Pr}}+\frac{\varepsilon}{\mathrm{Pr}_T}\right)\frac{\partial H}{\partial y}+\right.$$
$$\sum_i\left[\frac{\mu}{\mathrm{Pr}}(\mathrm{Le}_i-1)+\frac{\varepsilon}{\mathrm{Pr}_T}(\mathrm{Le}_T-1)\right]h_i\frac{\partial c_i}{\partial y}+$$
$$\left.\left[\mu\left(1-\frac{1}{\mathrm{Pr}}\right)+\varepsilon\left(1-\frac{1}{\mathrm{Pr}_T}\right)\right]\frac{\partial}{\partial y}\left(\frac{u^2}{2}\right)\right].$$

By noting that H_e = const, the continuity equation can be written in the form /72

$$\frac{\partial}{\partial x}(\rho u H_e)+\frac{\partial}{\partial y}(\rho v H_e)+\rho u H_e\frac{1}{r_w^{\nu}}\frac{dr_w^{\nu}}{dx}=0.$$

By subtracting the previous equation from this one and carrying out the integration across the boundary layer from y = 0 to y = ∞, using boundary condition (2.73), it is found that

$$\frac{d}{dx}\int_0^{\infty}\rho u(H_e-H)\,dy-\rho_w v_w(H_e-H_w)+$$
$$\frac{1}{r_w^{\nu}}\frac{dr_w^{\nu}}{dx}\int_0^{\infty}\rho u(H_e-H)\,dy=q_w. \qquad (2.87)$$

where

$$q_w=\left(\frac{\mu}{\mathrm{Pr}}\frac{\partial H}{\partial y}+\frac{\lambda}{c_p}\sum_i(\mathrm{Le}_i-1)h_i\frac{\partial c_i}{\partial y}\right)_w \qquad (2.88)$$

is the heat flux from the gas to the wall.

By introducing the integral energy loss thickness

$$\delta_H^{**}=\int_0^{\infty}\frac{\rho u}{\rho_e U_e}\left(1-\frac{H}{H_e}\right)dy \qquad (2.89)$$

and making use of equation (2.79), the integral energy relationship is obtained in the following form

$$\frac{d\delta_{\text{н}}^{**}}{dx} + \frac{U_e'}{U_e}(1 - M_e^2)\delta_{\text{н}}^{**} + \frac{(r_w^{\nu})'}{r_w^{\nu}}\delta_{\text{н}}^{**} = \frac{q_w + \rho_w v_w (H_e - h_w)}{\rho_e U_e H_e}. \qquad (2.90)$$

By now introducing the dimensionless heat transfer coefficient (or Stanton number)

$$c_h = \frac{q_w}{\rho_e U_e (H_r - h_w)}, \qquad (2.91)$$

where

/73

$$H_r = h_e + r\frac{U_e^2}{2} \qquad (2.92)$$

is the equilibrium enthalpy of the surface along which flow occurs without transfer of heat, and r is a recovery coefficient characterizing the nonadiabatic nature of the flow in the boundary layer, and by making use of equations (2.83) and (2.86), the integral energy relationship (2.90) can be converted to the following form

$$\frac{d\delta_{\text{н}}^{**}}{dx} + \frac{M_e'}{M_e} \cdot \frac{1 - M_e^2}{1 + \frac{\gamma - 1}{2} M_e^2}\delta_{\text{н}}^{**} + \frac{(r_w^{\nu})'}{r_w^{\nu}}\delta_{\text{н}}^{**} = c_h \frac{H_r - h_w}{H_e} + c_m\left(1 - \frac{h_w}{H_e}\right). \qquad (2.93)$$

CHAPTER III.

THE TURBULENT BOUNDARY LAYER IN A HOMOGENEOUS GAS STREAM AT SUPERSONIC VELOCITIES

10. Introduction /74

The present chapter will deal with the theoretical and experimental results obtained from studies of the behavior of turbulent boundary layers on impermeable surfaces in homogeneous gas streams moving at supersonic velocities. The fact that the gas stream is homogeneous implies, essentially, that there are no chemical reactions in the stream. Most of the results presented refer to flows in which the specific heat capacity of the gas can be regarded as a constant quantity.

The problem of calculating the turbulent boundary layer on bodies of arbitrary shape at supersonic velocities is still far from being completely solved at present. It is well known that the problems which arise in studying flows with large positive pressure gradients in calculating the separation of the turbulent boundary layer have not yet been satisfactorily solved even in the case of incompressible fluid flow. The existing procedures for calculating turbulent boundary layers at supersonic velocities make it possible to determine friction factors and heat transfer coefficients only for bodies of relatively simple shape (plate, cone, in the neighborhood of the stagnation point of a blunt body, etc.). The most detailed results (experimental and theoretical) have been obtained for studies of flow along flat plates in the stream.

The literature on the calculation of friction factors for smooth flat plates is quite extensive, with several dozen references. Depending on the various /75 assumptions made by the various workers, it is possible to divide the work into three historical routes leading to the present.

The first route is based on generalizing the formulas of the semi-empirical theory of turbulence developed by Prandtl and von Kármán (equations (2.68) and (2.69)), which were obtained originally for incompressible fluids, to the case of gas flows with large velocities. The methods in this group can be characterized as those making use of logarithmic velocity profiles.

The use of power-law velocity is characteristic of the methods in the second group. The first and second groups of methods are natural developments of the traditional methods of the theory of turbulent boundary layers in incompressible fluids.

Finally, the third group can be termed empirical methods. The main feature of the methods in this group is the use of formulas which in form are the same as the formulas for incompressible fluids, but with the parameters evaluated at some specially selected "defining" temperature.

There are also other methods which occupy positions intermediate between these groups.

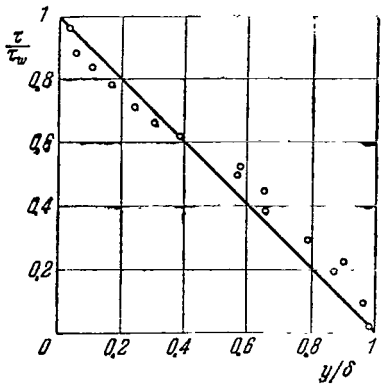

Figure 2.

In most of the papers in the first group the assumption is made that the frictional shear stress τ is constant across the boundary layer and is equal to the value at the wall:

$$\tau = \text{const} = \tau_w. \tag{3.1}$$

Actually, experiments carried out by Klebanoff [16] in the incompressible turbulent boundary layer on a flat plate (the circles in Fig. 2 represent the experimental points obtained by Klebanoff) showed that the dependence of the turbulent shear stress on the transverse coordinate was approximately linear (the straight line in Fig. 2) and could be approximated by the expression /76

$$\frac{\tau}{\tau_w} = 1 - \frac{y}{\delta}, \tag{3.2}$$

where δ is the thickness of the boundary layer.

Nevertheless, the approximation (3.1) does not introduce an appreciable error compared with (3.2) in calculating the integral characteristics of the boundary layer (friction, displacement thickness, momentum loss thickness, etc.). This fact becomes intelligible if the momentum loss thickness δ^{**} given by equation (2.76). By rearranging this equation to the form

$$\delta^{**} = \int_0^\infty \frac{\rho u}{\rho_e U_e}\left(1 - \frac{u}{U_e}\right)\left(\frac{du}{dy}\right)^{-1} du, \tag{3.3}$$

it can be seen that in this expression the quantity which depends on the shear stress distribution across the boundary layer is the derivative du/dy, (this is clear from the equations of Prandtl (2.68) and von Kármán (2.69). The greatest error caused by introducing into it the approximation (3.1) will obviously occur close to the outer edge of the boundary layer, where according to (3.1) $\tau = \tau_w$, while actually $\tau \to 0$ as $y \to \infty$. However, in this case, the derivative $(du/dy)^{-1}$ is multiplied by the small quantity $(1 - u/U_e)$, which is small because $u \to U_e$ as $y \to \infty$, and which leads in the final analysis to a small error in the value of δ^{**}. At the same time, as will be shown below, the friction coefficient at the wall is given by $c_f \sim (\ln \delta^{**})^2$. This fact also makes the error introduced into the calculation by the approximation (3.1) quite small.

The following simple arguments can also be presented as a basis for the assumption (3.1). By using the usual logarithmic velocity profile [17] /77

$$\frac{u}{v_*} = 2.5 \ln\left(\frac{yv_*}{\nu}\right) + 5.5, \quad v_* = \left(\frac{\tau_w}{\rho}\right)^{1/2}, \tag{3.4}$$

it is not difficult to obtain from equation (3.2) the following relationship between the shear stress in the boundary layer and the velocity:

$$\frac{\tau}{\tau_w} = 1 - e^{-0.4\zeta_0(1-\bar{u})}$$
$$\zeta_0 = \frac{U_e}{v_*} = \sqrt{\frac{2}{c_{f0}}},$$
$$\bar{u} = \frac{u}{U_e}. \tag{3.5}$$

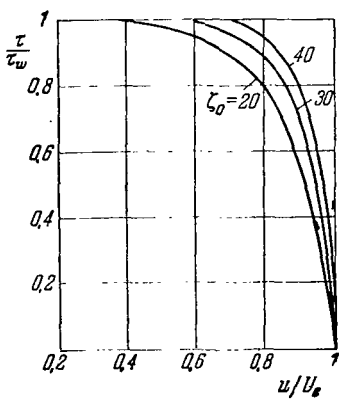

Figure 3.

The results of calculations by equation (3.5) for three values of the friction parameter $\zeta_0 = 20, 30, 40$ are shown in Fig. 3. For example, it can be seen from Fig. 3 that for a value of the parameter $\zeta_0 = 30$ (which corresponds to a Reynolds number of $\sim 10^7$), the shear stress fall in the range $0.9 \leq \tau/\tau_w \leq 1$ over the range of velocities $0 \leq \bar{u} \leq 0.8$, which confirms that it is valid to use (3.1) in practical calculations.

When (3.1) is used, the following expressions are obtained from the Prandtl formula (2.68) and the von Kármán formula for the velocity profiles

$$\eta = \frac{1}{C_1}\exp \varkappa\zeta \int \left(\frac{\rho}{\rho_w}\right)^{1/2} d\bar{u}, \tag{3.6}$$

$$\eta = C_3 + C_2\zeta \int \exp\left[\varkappa\zeta \int \left(\frac{\rho}{\rho_w}\right)^{1/2} d\bar{u}\right] d\bar{u}. \tag{3.7}$$

Here /78

$$\left.\begin{aligned} &\eta = \frac{yv_*}{\nu_w}; \quad \varphi = \frac{u}{v_*}; \quad v_* = \left(\frac{\tau_w}{\rho_w}\right)^{1/2}; \\ &\zeta = \frac{U_e}{v_*} = \left(\frac{2}{c_f}\frac{\rho_w}{\rho_e}\right)^{1/2}; \quad \frac{\varphi}{\zeta} = \bar{u}; \quad c_f = \frac{2\tau_w}{\rho_e U_e^2}; \end{aligned}\right\} \tag{3.8}$$

C_1, C_2, C_3 are integration constants; $\varkappa$ is an empirical turbulence constant, the value of which is usually assumed to be the same as the value in an incompressible fluid, i.e., $\varkappa = 0.39 - 0.41$.

The relationships (3.6) and (3.7) lead to the following equations, respectively, for the momentum loss thickness (2.76):

$$\delta^{**} = \frac{\varkappa\zeta^2\mu_w}{\rho_e U_e C_1}\int_0^1 \left(\frac{\rho}{\rho_w}\right)^{1/2} \bar{u}(1-\bar{u}) \exp\left[\varkappa\zeta \int \left(\frac{\rho}{\rho_w}\right)^{1/2} d\bar{u}\right] d\bar{u}, \tag{3.9}$$

$$\delta^{**} = \frac{\zeta^2\mu_w C_2}{\rho_e U_e}\int_0^1 \frac{\rho}{\rho_w}\bar{u}(1-\bar{u}) \exp\left[\varkappa\zeta \int \left(\frac{\rho}{\rho_w}\right)^{1/2} d\bar{u}\right] d\bar{u}. \tag{3.10}$$

The differences among the papers in the first group of approaches is usually found in the assumptions made relative to the integration constants C_1, C_2, or in the expression for ρ/ρ_w, or in the methods of evaluating the integrals in the expressions (3.9) and (3.10) for the momentum loss thickness*.

One of the papers which contributed originally to the wide use of the semi-empirical approach in the first group of approaches is the paper by F. I. Frankl and V. V. Voĭshel [19]. In this paper the authors use the approach of directly generalizing the von Kármán method [20]. Unfortunately, the power approximations used by Frankl and Voĭshel made it possible to carry out evaluations /79

*A detailed analysis of the various methods for calculating turbulent boundary layers on flat plates is contained in [18].

only up to Mach numbers lightly greater than one.

Going to larger Mach numbers would obviously require either even more complicated computational procedures than the already complicated procedure used by the authors or the direct use of numerical procedures.

After almost 25 years, this same method of generalizing von Kármán's equation (2.69) to the case of supersonic velocities was used by Wilson [21], who considered flow along a thermally insulated plate.

Almost simultaneously with Wilson, van Driest [12] considered the more general problem of the drag of a plate in a gas stream in the presence of heat transfer, but in this case Prandtl's formula (2.68) was used. Later, van Driest [22] obtained a friction formula on the basis of von Kármán's formula (2.69).

The method developed by V. M. Ievlev [23] has also been widely used in practice.

Further developments in the semiempirical method were made in the papers by I. P. Ginzburg and A. A. Shemets [24], L. E. Kalikhman [25], S. S. Kutateladze and A. I. Leont'ev [26], L. G. Loĭtsyanskii and Yu. V. Lapin [27], L. M. Zÿsina-Molozhen and I. N. Soskova [28] and other authors. /80

On turning briefly to the methods of calculating turbulent boundary layers in the second group, it will be recalled that the methods for calculating isothermal turbulent boundary layers in incompressible fluids using a power-law velocity profile are based on the experimental fact, which was first observed by Blasius, that during turbulent flow in a straight circular tube the change in velocity across the tube as a function of the distance from the wall and the shear stress at the wall (as a function of the Reynolds number calculated from the axial velocity U_a and the tube radius r_0) obeys the following power relationship:

$$\frac{u}{U_a} = \left(\frac{r}{r_0}\right)^{1/n}, \qquad c_f = \frac{A}{\left(\frac{U_a r_0}{\nu}\right)^m}. \tag{3.11}$$

The use of a power-law velocity profile for the conditions of the external flow of an incompressible fluid makes it possible to obtain a power relationship between the friction factor and the Reynolds number evaluated from the velocity of the approaching stream and the length of the plate. The value of the exponent for the velocity profile expression

$$\frac{u}{U_e} = \left(\frac{y}{\delta}\right)^{1/n}, \tag{3.12}$$

where δ is the boundary layer thickness, is usually selected to ensure agreement with the experimental data. It is therefore to be expected that the exponent will vary with the Reynolds number over quite a wide range: $6 < n < 13$. However, this fact is not particularly important, since in the absence of effects of the other parameters on the exponent, it is always possible to select the most satisfactory value of the exponent over any required range of Reynolds numbers. /81

It is quite otherwise in the flow of a compressible gas. In this case, the Mach number and the temperature factor affect the value of the exponent as well as the Reynolds number, which greatly complicates the selection of the correct value of the exponent. This leads to the fact that some methods of calculating boundary layers in compressible gases which are based on power-law velocity profiles [29] appear to be satisfactory only over relatively short ranges of the various parameters (Re_x, M_e, T_w/T_e).

A noteworthy example of the methods in the second group is the "effective length" method of V. S. Avduevskii [30]. Power-law distributions of the velocity and enthalpy in the boundary layer form the basis of this method; these distributions are described in therms of Dorodnitsyn variables as well as by experimentally determined relationships for skin friction and heat transfer on a flat plate. The calculation of friction and heat transfer in a turbulent boundary layer of a compressible gas with moderate longitudinal pressure drops can ultimately be reduced to calculations by the flat plate formula, except that in place of the actual coordinates giving the position of a point on the surface of the body, it is necessary to use some "effective length" determined from the integral conditions.

The essence of the third, or so-called empirical, approach to the problem of turbulent boundary layers in a compressible gas consists of attempts to generalize known relationships previously obtained for the flow of incompressible fluids for the case of flowing compressible gases by referring the physical properties of the gas to some characteristic temperature selected in some specified way. Thus, as early as at the 1935 Volta congress in Rome, von Kármán [31] proposed a formula for the friction drag on a thermally insulated plate in a compressible gas which was without theoretical basis, but which was obtained from simplifying assumptions that it would be possible to use at large velocities the same formulas as at small velocities as long as the physical properties were determined at the temperature of the wall. This formula for the average friction factor is /82

$$\frac{0{,}242}{\sqrt{c_F}}\left(1+\frac{\varkappa-1}{2}M_e^2\right)^{-1/2}=\lg\left(c_F\,\mathrm{Re}_L\right)-n\lg\left(1+\frac{\varkappa-1}{2}M_e^2\right). \qquad (3.13)$$

Comparison of von Kármán's formula with experimental results showed that the use of the wall temperature as the defining temperature in the boundary layer leads to an overestimate of the effects of compressibility.

Up to the present various authors have proposed a large number of empirical formulas for the "defining" temperature. Some of these are

$$\frac{T_{det}}{T_e} = 1 + \frac{1}{2}\left(\frac{T_r}{T_e} - 1\right) \quad \left[T_r = T_e\left(1 + r\frac{\gamma-1}{2}M_e^2\right)\right]^2);$$

$$\frac{T_{det}}{T_e} = 0{,}42 + 0{,}032\,M_e^2 + 0{,}58\,\frac{T_w}{T_e} \qquad \text{for } M_e < 5{,}5\ ^3);$$

$$\frac{T_{det}}{T_e} = 0{,}70 + 0{,}023\,M_e^2 + 0{,}58\,\frac{T_w}{T_e} \qquad \text{for } M_e > 5{,}5\ ^4).$$

It should be noted that the last two formulas for the defining temperature were obtained as a result of analyzing numerical solutions of the laminar boundary layer equations. Although these expressions are used for calculating friction in turbulent boundary layers, this fact must nevertheless be always remembered. Calculations using these formulas give lowered friction coefficients. /83

A method of calculation which differs from the others, but which is essentially an empirical method, has been developed by Spalding and Chi [18]. A comparison of the various methods of calculating friction in the turbulent boundary layer with experimental data then in existence was carried out by Spalding and Chi, and showed that the most exact methods of calculation are the method of Wilson and van Driest [12, 21, 22] (based on von Kármán's formula), the method of Kutateladze and Leont'ev [26], and the method of Spalding and Chi.

Based on this, a discussion is given in section 12 of the semiempirical methods of calculation for thermally insulated plates with reference to the results of Wilson, and for flow with heat transfer with reference to the results of van Driest. In addition, the method of Spalding and Chi is discussed briefly in section 13. The results of the semiempirical methods are used in the latter section. The simplicity and high degree of accuracy of this method make it convenient for carrying out engineering calculations.

11. Experimental investigations of turbulent boundary layers in supersonic streams (friction and velocity profiles).

Of the many problems of experimental aerodynamics, one of the most important and widely investigated over many years is the problem of determining the turbulent skin friction. Without going into the results of experimental investigations of the characteristics of turbulent boundary layers in incompressible fluids, we will consider here the most important and interesting experimental results from studies of velocity profiles and skin friction in turbulent boundary layers in compressible gases both on thermally insulated surfaces and on surface which exchange heat with the gas stream. Most of the results discussed below have been obtained since 1950. It should be noted that the experimental data existing at present are far from complete, particularly as regards measured information on velocity profiles in the boundary layer. /84

Of the papers dealing with investigations of the characteristics of boundary layers on heat insulated surfaces, the work of Wilson, Chapman and Kester, Cowles, Korkegi, Matting et al., and Moore and Harkness will be considered. In the case of investigations on surfaces with heat transfer, the work of Lobb et al., Hill, Sommer and Short, Winkler, and Kozlov will be considered. The results of other investigators will be introduced in the various graphs.

Experimental investigations on thermally insulated surfaces.

The experiments of Wilson [21]. Velocity profiles were measured with a Pitot tube at several cross sections in the boundary layer on a thermally insulated flat plate. The Mach and Reynolds numbers in the experiments varied over the following ranges

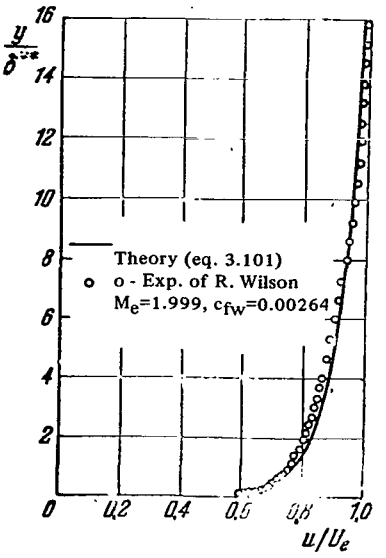

Figure 4.

$$1.579 \leqslant M_e \leqslant 2.186; \qquad 2.2 \leqslant Re_x \cdot 10^{-6} \leqslant 19.$$ /85

By way of an example, Fig. 4 shows the results for the velocity profiles at $M_e = 1.999$ (the circles denote the experimental points; the solid lines will be discussed later in section 12). From the velocity profiles the momentum loss thicknesses δ^{**} were evaluated, and then the mean friction coefficients were evaluated (see equations (2.76) and (3.64)). The values of the mean friction coefficients determined in this way are shown in Fig. 5.

The experiments of Chapman and Kester [35]. Measurements of the mean friction coefficient c_F were carried out on the surface of a long cylindrical body of rotation at subsonic and supersonic velocities of the stream for the following ranges of the Mach and Reynolds numbers: $4 \leq Re_x \cdot 10^{-6} \leq 32$, $0.51 \leq M_e \leq 3.60$. The surface friction forces were determined directly by tests on two models (shown diagrammatically in Fig. 6). In the experiments measurements were made of the difference between the total drag and the base resistance for each cone-cylinder and cone model: $(Q_1 - Q_{D1})$ and $(Q_2 - Q_{D2})$. The difference between these quantities gives the value of the frictional force acting on the cylindrical surface: /86

$$F = (Q_1 - Q_{D1}) - (Q_2 - Q_{D2}).$$

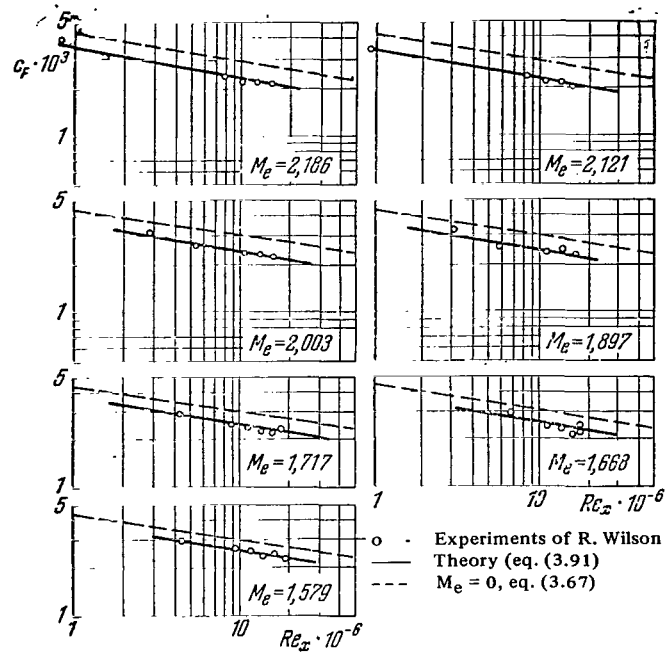

Figure 5.

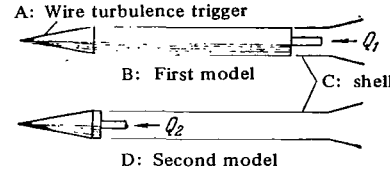

Figure 6.

The results are shown in Table 1. The value of the mean friction coefficient for the incompressible fluid $(c_{F0})_{exp}$, to which the friction coefficients measured at various Mach numbers are referred, was determined experimentally. In the lower line of the table the same coefficients are referred to the mean friction coefficient c_{F_0} calculated by von Kármán's formula, equation (3.59).

TABLE 1

M_e	0.51	0.81	1.99	2.49	2.95	3.36	3.60
$c_F/(c_{F_0})_{exp}$	0.985	0.929	0.746	0.671	0.623	0.578	0.551
c_F/c_{F_0}	0.994	0.924	0.757	0.672	0.630	0.571	0.552

The dependence of the experimental values of the friction coefficient c_F /87
on the Reynolds number Re_x at various values of the Mach number M_e is given in Fig. 7. The values of the friction coefficient c_{F_0} at $M_e = 0$ were obtained from von Kármán's formula, equation (3.59). As can be seen from Fig. 7, the curves corresponding to various values of the Mach number M_e are equidistant from the curve for $M_e = 0$, which indicates that the ratio c_F/c_{F_0} does not depend on the Reynolds number Re_x over the range of Re_x investigated. The slight degree of scatter of the experimental data at a given value of M_e was caused by the use of cylinders of various lengths (cylinders with ratios of length to diameter of $l/d = 8$, 13 and 23 were used in the experiments).

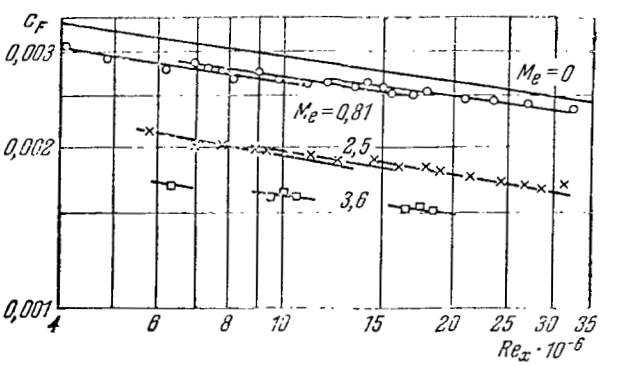

Figure 7.

Coles' experiments [36]. The values of the local and mean skin friction were determined in these experiments. The local friction was measured experimentally in a direct manner using a "floating" element set in the surface of the plate which was used in the working section of a supersonic wind tunnel. The mean friction was determined from the momentum loss thickness δ^{**} (equation 2.76). In these experiments the Mach number varied from $M_e = 2$ to $M_e = 4.5$, while the Reynolds number varied from $3 \cdot 10^6$ to $9 \cdot 10^6$. The experimental re- /88
sults are collected in Table 2.

TABLE 2

M_e	2.57	2.58	3.70	3.70	4.51	4.55	4.50	4.54
$\frac{U_e x}{\nu_e} \cdot 10^{-6}$	4.84	8.32	3.54	7.25	3.52	6.83	3.37	6.91
$c_f \cdot 10^3$	1.81	1.66	1.62	1.38	1.48	1.22	1.55	1.26
c_f/c_{f_0}	0.705	0.700	0.595	0.570	0.530	0.500	0.535	0.495
c_F/c_{F_0}	0.715	0.710	0.635	0.610	0.590	0.560	0.600	0.560

Korkegi's experiments [37]. As in the work of Coles, the local friction on a flat plate was measured by means of a "floating" element. Throughout the experiments the Mach number was held constant ($M_e = 5.8$), while the Reynolds number formed from the parameters at the outer edge of the boundary layer and the distance from the "floating" element to the leading edge of the plate varied from 10^6 to $4 \cdot 10^6$. Velocity and temperature profiles were measured in addition to the friction; from these the integral boundary layer thicknesses δ^* and δ^{**} were calculated, as well as the parameter $H^* = \delta^*/\delta^{**}$. The results of the experiments are shown in Table 3.

TABLE 3

M_e	Re**	δ^{**}/δ	δ^*/δ	H^*	$c_f \cdot 10^3$	c_f/c_{f_0} Re**	c_f/c_{f_0}
5.787	2477	0.0375	0.529	14.10	1.316	0.403	0.467
5.770	2780	0.0361	0.519	14.38	1.275	0.400	0.463
5.792	3429	0.0357	0.561	15.68	1.223	0.400	0.463
5.805	404	0.0385	0.561	15.79	1.179	0.397	0.462

In the last column but one of Table 3 the ratio c_f/c_{f_0} is evaluated for a constant value of Re**, i.e., c_{f_0} was evaluated at the same value of Re** at which c_f was determined. The ratio c_f/c_{f_0} in the last column of the table was evaluated for /89

$$\mathrm{Re}_x = \text{const} \qquad (5 \leqslant \mathrm{Re}_x \cdot 10^6 \leqslant 6).$$

The experiments of Matting, Chapman, Nyholm and Thomas [38]. The work by these four authors is an extensive and detailed experimental investigation of the turbulent boundary layer on a thermally insulated surface in the absence of a longitudinal pressure gradient. As a result of the experiments, data were obtained on the local friction and velocity profiles over a range of Mach numbers from 0.2 to 9.9 and of Reynolds numbers from 2.10^6 to 100.10^6. Air

was used as the working medium for $0.2 \leq M_e \leq 4.2$, while helium was used for $4.2 \leq M_e \leq 9.9$. Since the adiabatic exponent (the ratio of the specific heat capacities at constant pressure and at constant volume) $\gamma = c_p/c_v$ is appreciably different in the cases of air and helium ($\gamma_{air} = 1.4$, $\gamma_{He} = 1.66$) the parameter $(\gamma - 1)M_e^2$ was used as a similarity parameter. In this case the experimental results obtained in a helium stream at some Mach number $(M_e)_{He}$ will be equivalent to results obtained in an air stream at

$$(M_e)_{air} = (M_e)_{He} \sqrt{\frac{\gamma_{He} - 1}{\gamma_{air} - 1}} \approx 1{,}29\,(M_e)_{He}.$$

The validity of this relationship was confirmed experimentally. In particular, Fig. 8 shows velocity profiles in air ($M_e = 4.2$) and in helium ($M_e = 3.25$) for the same value of the Reynolds number ($Re_x = 6.2 \cdot 10^6$) on the upper figure and $Re_x = 35 \cdot 10^6$ on the lower figure. The agreement of the velocity profiles measured in the different gases appears to the very good.

/90

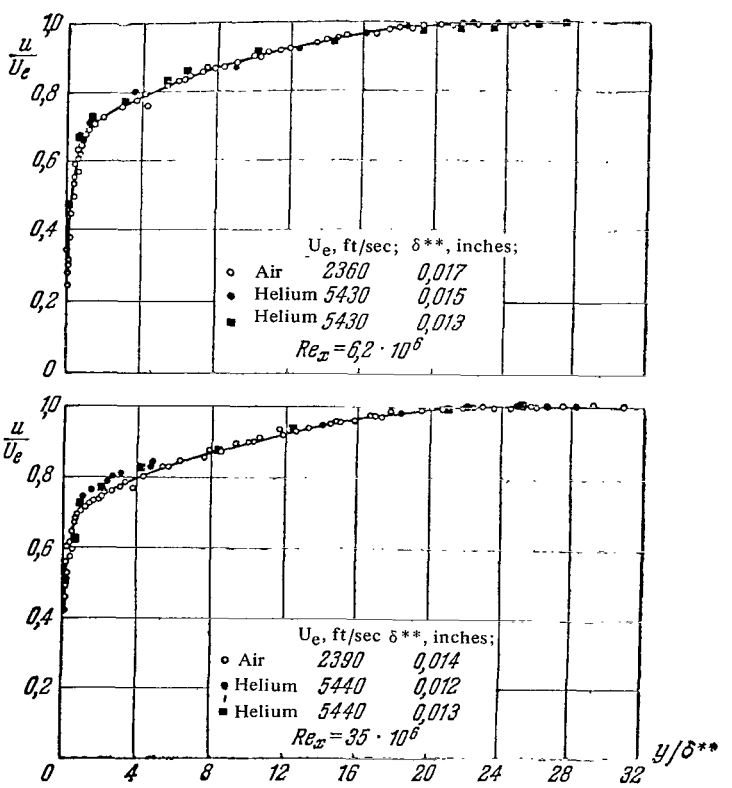

Figure 8.

The results of velocity measurements in the boundary layer at various Mach numbers $(M_e)_{air}$ are shown in Fig. 9. This graph is plotted in terms of the universal parameters φ and η (see equation (3.8)). Figure 9 shows that in the turbulent core the Mach number has an insignificant effect on the shape of the universal profile, which as usual is well described by a logarithmic formula. As the wall is approached (in the laminar sublayer) there is a large scatter of the experimental points, which fall above the curve $\varphi = \eta$. It is the author's opinion that the measurements near the wall are unreliable. An evaluation of the laminar sublayer thickness from the experimental data showed that this thickness increases with increase of the Mach number M_e, and for $(M_e)_{air} = 9.9$ it reaches 10% of the total boundary layer thickness.

/91

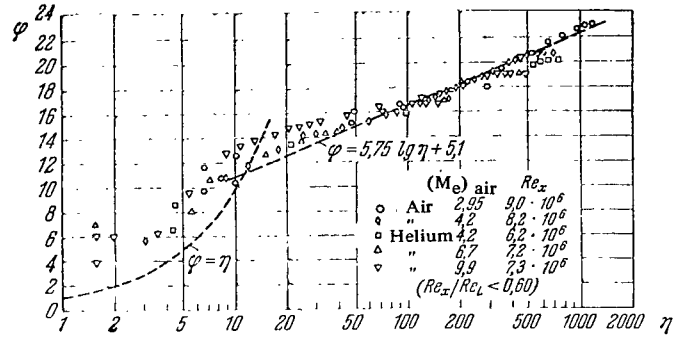

/90

Figure 9.

The local surface friction was also measured in the experiments using a floating element as well as the velocity profiles. The results of these measurements are shown in Figs. 10 and 11. As can be seen in Fig. 11 the Reynolds number has no effect on the ratio c_f/c_{f0} over the investigated range of this number. In Figs. 10 and 11 the "flags" denote the points obtained experimentally at small Reynolds numbers $(Re_x/Re_L) < 0.61$), where L is the length of the plate. There are difficulties involved in obtaining sufficiently accurate friction determinations at these points, due to the incomplete development of the turbulent flow at $(Re_x/Re_L) < 0.6$.

The experiments of Moore and Harkness [39]. This work contains the results of local friction and velocity profile measurements on a thermally insulated surface at a Mach number $M_e = 2.8$. The distinguishing feature of this investigation is that it includes the zone of very high Reynolds numbers up to $Re_x = 1.41 \cdot 10^9$. The local friction was measured by means of a floating element. The results of friction measurements on the wall of a supersonic diffuser of a wind tunnel are shown in Table 4.

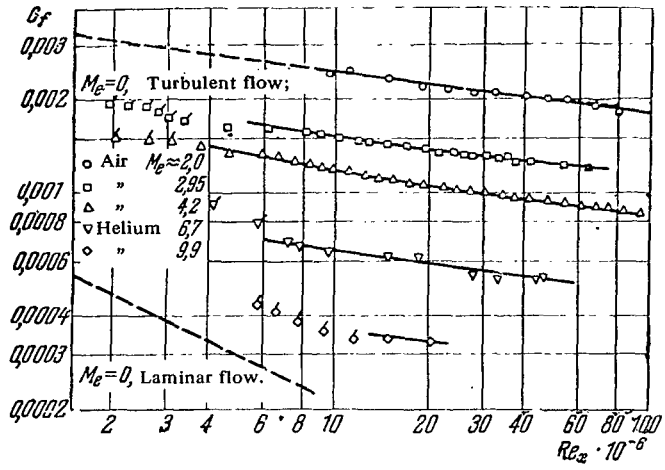

Figure 10.

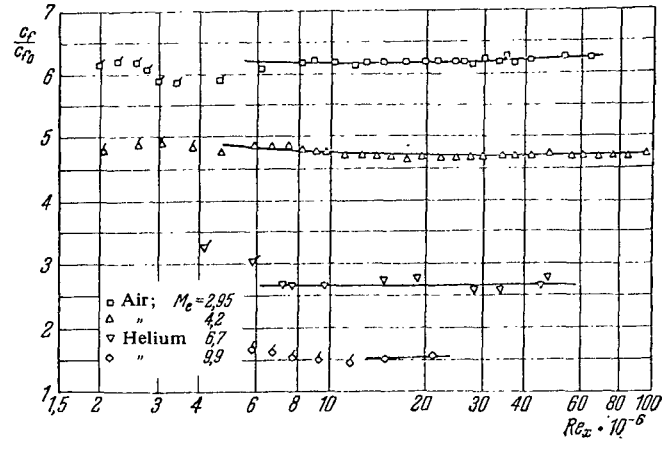

Figure 11.

TABLE 4 /93

M_e	T_e*, °K	δ**, mm	δ*, mm	δ, mm	Re** · 10^{-5}	Re_x · 10^{-3}	c_f
2.831	298	4.86	22.7	104.0	4.24	8.27	0.000900
2.843	292	4.61	21.4	116.9	3.26	6.11	0.000953
2.865	295	5.01	24.0	108.9	2.12	3.76	0.000958
2.897	289	5.82	28.1	114.6	1.82	3.18	0.001020
2.787	316	6.79	30.8	139.2	5.57	11.2	0.000849
2.809	317	6.76	31.1	144.2	4.46	8.73	0.000874
2.828	314	7.04	32.6	140.5	2.79	5.12	0.000946
2.699	305	8.11	34.7	153.5	7.02	14.1	0.000862
2.693	300	8.31	36.0	159.5	5.95	11.8	0.000891

Experimental investigations in the presence of heat transfer between the gas and solid surface.

The experiments of Lobb, Winkler and Persch [40]: The work considered in the previous section was concerned mainly with investigations of skin friction on thermally insulated surfaces, and gave relatively little information on the characteristics of the turbulent boundary layer such as the velocity and temperature profiles, thickness of the laminar sublayer, etc.

The paper by the three authors being considered here falls among the few papers in which all the characteristics of the turbulent boundary layer listed above were determined in addition to friction measurements. The investigations of the boundary layer were carried out on the walls of a two-dimensional nozzle of a supersonic wind tunnel; only a small pressure gradient existed at the cross section investigated. The local friction was determined from the velocity gradient close to the wall, and also from the measured heat flux in the investigated /94
cross section, using Reynolds' analogy.

The results of the local friction measurements and determinations of the flow characteristics for which the measurements were carried out are shown in Table 5.

TABLE 5

M_e	4.93	5.01	5.03	5.06	6.83	6.78	6.83	6.78	7.67
$(T_r-T_w)/T_e$	0	1.23	2.07	2.36	3.05	4.05	4.16	4.63	5.65
Re **	5350	6480	7950	7370	8550	8400	12640	7960	8130
$(c_f/c_{f0})_{Re**}$	0.372	0.3825	0.3416	0.3317	0.252	0.242	0.233	0.250	--
$c_f \cdot 10^3$	1.11	1.10	0.907	0.930	0.646	0.656	0.590	0.690	--

The quantity c_{f_0} was determined for the same values of Re** for which c_f was measured, using von Kármán's formula

$$c_{f_0} = \frac{0{,}02932}{\log(2\,\mathrm{Re}^{**})\left[\frac{1}{2}\log(2\,\mathrm{Re}^{**}) + 0{,}4343\right]}. \qquad (3.14)$$

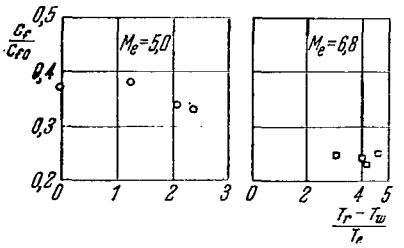

Figure 12.

The Reynolds number Re**, formed using the momentum loss thickness, was selected as the characteristic Reynolds number as a result of the difficulties arising in defining the origin of the boundary layer on the wind tunnel wall, which made it impossible to use the Reynolds number Re_x formed using the length. The dependence of $(c_f/c_{f_0})_{\mathrm{Re}^{**}}$ on the temperature factor $(T_r-T_w)/T_e$ is shown in Figure 12. Here T_r is the stagnation temperature. As can be seen from the figure, the ratio $(c_f/c_{f_0})_{\mathrm{Re}^{**}}$ depends only slightly on heat transfer.

In this paper, particular interest was attached to measurements of the velocity profiles in boundary layers. /95

Figure 13 shows the velocity profile for $M_e = 6.8$ and two values of the heat transfer factor (the greatest and smallest values for the given value of M_e).

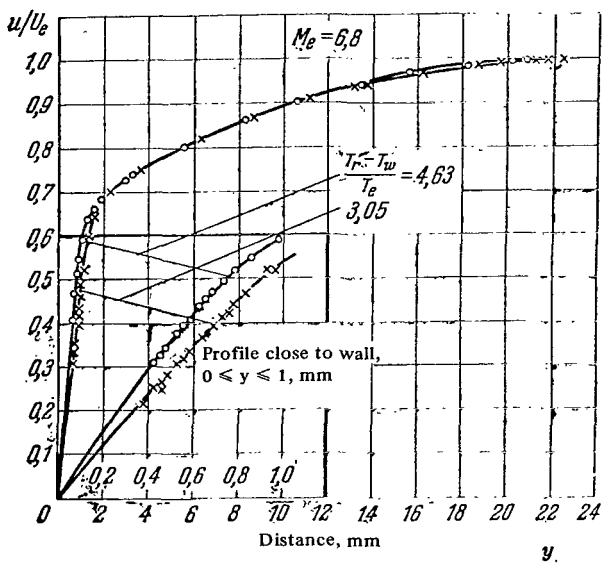

Figure 13.

In order to show the difference between the velocity profiles, the distance in mm is shown in two ranges on the abscissa. As can be seen in Fig. 13, the velocity profiles in the turbulent core differ very little as the heat transfer factor changes, while in the laminar sublayer the steepness of the curve increases as heat transfer increases.

The same velocity profiles, as well as the profiles for $M_e = 5$ are given in Figs. 14 and 15 in terms of the universal variables φ and η; these show a considerable displacement upwards of the curves in the turbulent core zone as the heat transfer factor increases. /97

/96

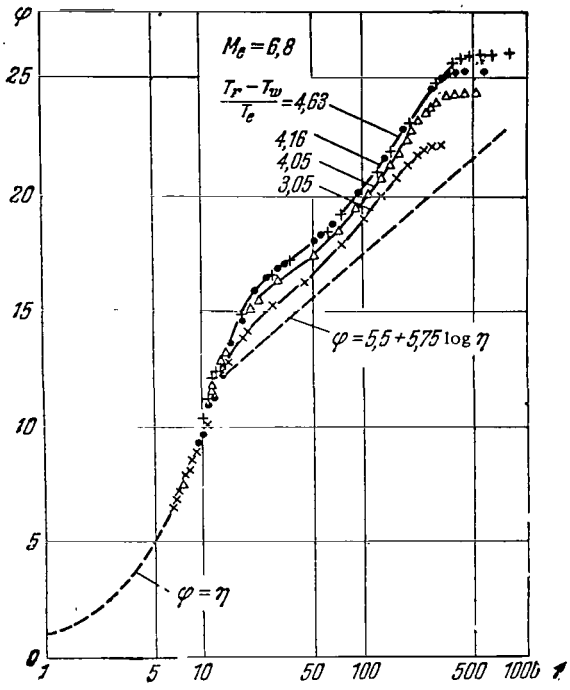

Figure 14.

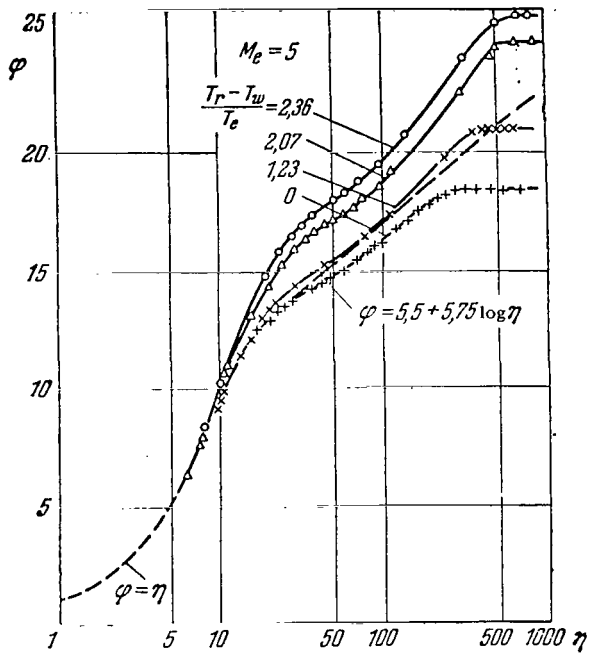

Figure 15.

For all values of the heat transfer factor the velocity profiles in the laminar sublayer are described well by the equation $\varphi = \eta$, but the thickness of the sublayer, as shown by Figs. 14 and 15, increases as the heat transfer factor increases. The value of the parameter η_L, which represents the thickness of the laminar sublayer and plays an important part in the theory of turbulent boundary layers, appears to be the same as the value for an incompressible fluid ($\eta_L = 11.9 = \alpha$) only in the absence of heat transfer (see the curve for $M_e = 5$, $(T_r - T_w)/T_e = 0$ in Fig. 15).

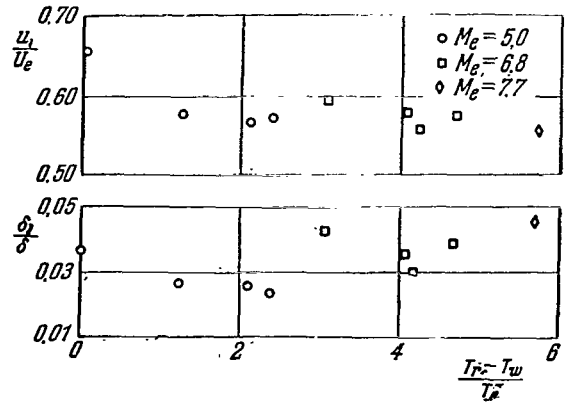

Figure 16.

The results of measurements of the laminar sublayer thickness and of the velocity at its edge are shown in Fig. 16. Although the scatter of points appears to be quite considerable (this is partly caused by the differences in Reynolds numbers) it is nevertheless possible to conclude that as the heat transfer intensity increases, the relative velocity at the edge of the laminar sublayer and the thickness of the sublayer both increase. From the same figure it can be seen that as the Mach number increases from 5 to 6.8, the thickness of the laminar sublayer within the boundary layer increases by a factor of approximately 2.

Hill's experiments [41] *. These experiments were carried out in a conical nozzle at a Mach number of 9.1 at the outlet. Velocity and temperature profiles in the boundary layers at various cross sections of the nozzle, using Pitot tubes and thermocouples. The conditions in the nozzle differed somewhat from the flow conditions on a flat plate since the walls of the nozzle were inclined with respect to its axis at an angle of 6°, and there was a small negative longitudinal pressure gradient. /98

Values of the local friction were calculated from the slopes of the velocity profiles close to the wall, using the formula $\tau_w = (\mu \partial u/\partial y)_w$. The data on the skin friction measurements are summarized in Table 6 (where c_f is the friction coefficient based on the parameters of the approaching stream).

*A more detailed paper by the same author [42], which is not considered in the present paragraph, is also recommended to the reader.

TABLE 6

M_e	T_w/T_e	Re **	$c_f \cdot 10^4$	(c_f/c_{f_0})Re **
8.99	7.68	1245	7.899	0.197
9.04	7.97	1607	8.910	0.235
9.07	8.28	1908	8.505	0.234
9.10	8.69	2287	8,000	0.227
8.22	7.17	2081	9.240	0.257
8.25	7.26	2498	9.102	0.265
8.27	7.34	2885	8.695	0.259
8.29	7.37	3202	8.202	0.247
8.29	7.41	3451	7.709	0.239

In the last column of Table 6 the friction coefficient c_f is referred to the friction factor c_{f_0} calculated by von Kármán's formula (3.14) for the values of the Reynolds number Re** given in the table.

In comparing the experimental data on friction with the theoretical calculations, it must be remembered that according to the evaluation carried out by Hill, the measured values of the friction coefficient may be 20% larger than the value of the friction coefficient on a flat plate as a result of the effects of the negative pressure gradient. /99

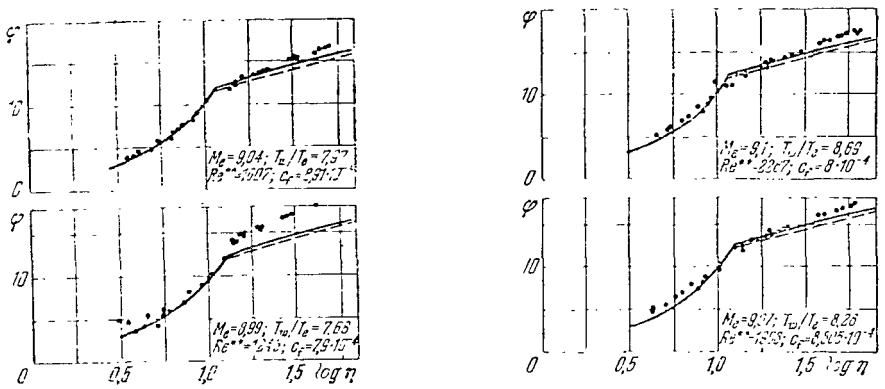

Figure 17.

The results of velocity profile measurements at various cross sections of the boundary layer in the nozzle are shown in Fig. 17, which is plotted in terms of the universal coordinates φ and η. The figure shows that in the laminar sublayer ($\lg \eta < 1.1$) the experimental points fall around the curve $\varphi = \eta$ (solid curve). In the turbulent core, the experimental points fall practically along straight lines which are displaced upwards from the dashed lines, which are drawn according to equation (3.4) for the velocity profiles in incompressible fluids (an explanation of the solid lines in the turbulent core region will be given in Section 12). Of these velocity profiles, the profile at $M_e = 8.99$ differs appreciably from the profiles for the other Mach numbers. The reason for this, as noted by Hill, is that this cross section occurred in a region of insufficiently developed turbulence. Of the other features in the velocity profiles, it is necessary to point out the thickening of the laminar sublayer. According to Hill's data, at $M_e = 9$ the laminar sublayer occupies about 15% of the total boundary layer thickness. /100

The experiments of Sommer and Short [43]. Drag was determined on an aero-ballistic apparatus from measurements of the head resistance of hollow cylindrical models which were fired through a supersonic wind tunnel. Mach numbers of $M_e = 2.8$ and 3.9 were obtained by firing through stationary air, while $M_e = 7.2$ was reached by firing against an air stream moving at $M_e = 2$. $M_e = 5.6$ was obtained on models with profiled leading edges, which reduced the Mach number from $M_e = 7$ to $M_e = 5.6$ at the outer edge of the boundary layer. The head resistance was computed from the retardation of the model, which was determined on the basis of taking chronographs and shadow photographs.

Turbulence generators in the form of threads cut into the outer and inner surfaces of the model were used to set up the turbulent boundary layer. In order to take into account the thickening of the boundary layer and the additional drag caused by the turbulence-generating threads, the so-called "effective" Reynolds number (Re_{eff} in Table 7) was calculated, and the coefficient of friction c_{f_0} corresponding to this for an incompressible fluid was found. Without going into the details of calculating Re_{eff}, it need only be said that this Reynolds number is formed from the length of the turbulent boundary layer required for the formation of a momentum loss thickness which would have occurred if the additional resistance caused by the turbulence generators had been due only to friction in the boundary layer.

The results of friction coefficient measurements are shown in Table 7. The values of the friction coefficients in the incompressible fluid were determined from von Kármán's formula, equation (3.59).

TABLE 7 * /101

M_e	T_w/T_e	$Re_{eff} \cdot 10^{-6}$	$Re_c \cdot 10^{-6}$	c_f	c_f/c_{f_0}
2.81	1.03	62.3	3.00	0.00284	0.867
3.82	1.05	84.0	4.07	0.00287	0.730
5.63	1.29	72.0	4.71	0.00170	0.562
6.90	1.60	82.0	4.06-6.09	0.00125	0.401-0.451
7.00	1.75	123.5	6.06-9.92	0.00115	0.395-0.446
3.78	1.05	84.0	4.92	0.00204	0.694
3.67	1.05	78.5	3.78	0.00240	0.724

*In this table, Re_c is the Reynolds number formed with respect to the parameters of the approaching stream and the length measured from the point of formation of the turbulent boundary layer.

Winkler's experiments [44]. In this work, studies were made of the turbulent boundary layer characteristics on a cooled flat plate at $M_e = 5.2$ and three values of the temperature factor. Measurements in the boundary layer were made with a total pressure probe (Pitot tube) and a thermocouple. The wall shear stress was determined by two parallel methods: from the slope of the velocity profile at the wall, $\tau_w = \mu_w (\partial u/\partial y)_w$, and from measurements of the value of the heat flux grom the gas to the wall, using Colburn's proposed relationship between friction and heat transfer, $c_f = 2c_h Pr^{2/3}$, where c_h is the heat transfer coefficient (the so-called generalized Reynolds analogy).

The results of friction measurements by the two methods are shown in Table 8 (here T_e^* is the stagnation temperature; c_f is the friction coefficient formed from the parameters of the approaching stream; Re_x is the Reynolds number formed from the parameters of the approaching stream). As can be seen from this table, the values obtained by the two different methods agree in most /102
cases to within ± 4%. At the same time, it must be noted that Winkler's data on how the temperature factor affects friction contradict the calculated results and experimental data of other authors.

The results of velocity profile measurements in the logarithmic layer at $M_e = 5.2$ and three values of the temperature factor are shown in Fig. 18. An approximate evaluation of the laminar sublayer thickness from the data of this figure shows that the laminar sublayer occupies about 9% of the total boundary layer.

The experiments of L. V. Kozlov [45]. Using a floating element technique, measurements were made of the local friction on a flat plate around which a supersonic stream flow in the presence of intensive heat transfer between the stream and the wall. In the experiments, the Mach number of the approaching /103
stream was 2.9, while the Reynolds number varied over the range

TABLE 8 /102

c_f/c_{f_0} (1)	c_f/c_{f_0} (2)	M_e	T_w/T_e *	$Re_x \cdot 10^{-6}$	Re**	δ**, mm	δ*, mm	$c_f \cdot 10^4$ (1)	$c_f \cdot 10^4$ (2)
0.487	0.494	5.20	0.801	2.72	2090	0.166	1.66	14.65	14.87
0.484	-	5.14	0.875	3.36	2936	0.189	1.57	13.89	-
0.508	0.478	5.20	0.840	4.07	3173	0.228	2.46	14.32	13.48
0.493	0.492	5.26	0.845	5.04	3880	0.284	2.86	13.46	13.43
0.492	0.480	5.29	0.845	5.94	4300	0.332	4.00	13.08	12.76
0.432	0.436	4.98	0.757	2.29	1900	0.179	1.96	13.35	13.48
0.530	-	5.18	0.744	2.58	1782	0.149	1.55	16.06	-
0.437	0.407	5.20	0.753	3.81	2960	0.227	2.51	12.48	11.65
0.414	0.421	5.24	0.773	4.55	3455	0.280	3.22	11.51	11.70
-	0.389	5.24	0.765	5.11	3790	0.330	3.88	-	10.63
0.447	0.381	5.17	0.613	2.01	1055	0.114	1.22	14.07	15.47
0.434	0.379	5.16	0.586	2.57	1652	0.188	2.05	13.23	13.35
0.442	-	5.10	0.578	2.73	1735	0.186	1.93	13.35	-
0.422	0.436	5.11	0.565	3.27	2488	0.281	2.84	12.36	12.79
0.420	-	5.20	0.589	3.57	2482	0.256	2.78	12.03	-
0.375	0.383	5.12	0.605	4.22	3256	0.343	3.74	10.54	10.75

$1.5 \leq Re_x \cdot 10^{-7} \leq 2.5$. After an analysis of the data, the author recommended the use of the following empirical formulas for the friction coefficients:

$$c_{fw} = \frac{2\tau_w}{\rho_w U_e^2} = 0{,}085\, Re_{xw}^{-0{,}29 - 0{,}01 \lg Re_{xw}} \left(\frac{T_w}{T_r}\right)^{0{,}39} \left(\frac{T_r}{T_e}\right)^{0{,}2}, \qquad (3.15)$$

where

$$Re_{xw} = \frac{\rho_w U_e x}{\mu_w}, \quad T_r = T_e\left(1 + r\frac{\gamma - 1}{2} M_e^2\right), \; r = 0{,}89.$$

The author noted that the mean square deviation of the experimental points from the curve given by equation (3.15) was ±5% over the investigated ranges of the Reynolds number and temperature factor.

Some remarks on the results of experimental investigations of turbulent boundary layers at supersonic velocities. /104 The results of measurements of the velocity profiles at various values of the Mach number of the approaching stream and of the temperature factor which have been presented in this section in Figs. 8, 13-15 and 17 show that the velocity profiles in the laminar sublayer are described satisfactorily by the linear equation $\varphi = \eta$.

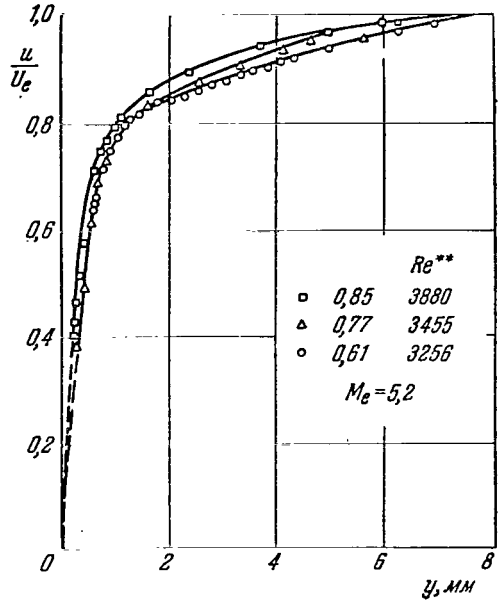

Figure 18.

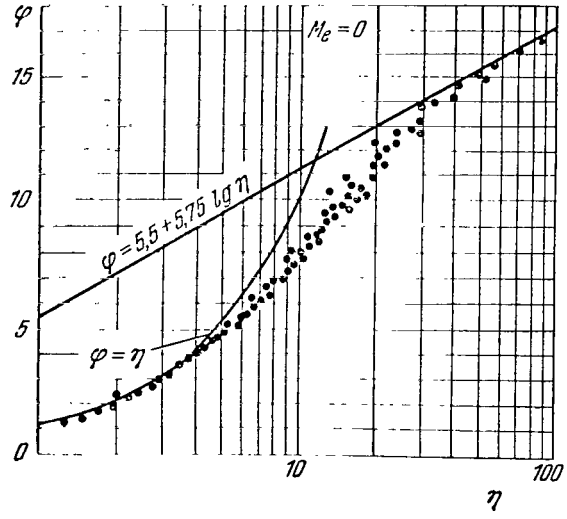

Figure 19.

In the turbulent core the velocity profiles are logarithmic (Figs. 9, 17). In the case of thermally insulated surfaces, the slope of the profile (Fig. 9) is the same as for incompressible fluids. In the presence of heat transfer, the slope of the velocity profiles in this zone is larger than for the incompressible fluid (Fig. 17); however, it should be noted that in Hill's experiments in Fig. 17, the increase in the slope of the profile can be partly explained by the effect of the negative pressure gradient.). As can be seen from Figs. 14 and 15, an increase in the intensity of heat transfer between the gas and the wall can lead to a change in slope of the velocity profile (the deformation of the profile at the junction of the laminar sublayer and the turbulent core can be explained by the presence of the pressure gradient, since the experiments were carried out on the surface of a two-dimensional nozzle.). /105

A comparison of the velocity profiles at large Mach numbers (Fig. 17) and those in incompressible fluids (Fig. 19, in which the points represent the experimental data of Nikuradse [46]) shows that at large Mach numbers the transitional (buffer) zone between the laminar sublayer and the turbulent core is considerably reduced in size. In incompressible fluids, the transition zone begins at $\eta = 5$ and ends at $\eta = 30 - 50$, while at large Mach numbers (for instance, in the experiments of Hill), the buffer zone disappears almost completely, and the transition from the laminar sublayer to the turbulent core becomes quite sharp. This fact justifies the application of the two-zone Prandtl scheme to the theory of turbulent boundary layers at large supersonic velocities. /106

Another important feature of the velocity profiles in supersonic streams is the increase in the thickness of the laminar sublayer as the Mach number increases. Figure 20 illustrates the nature of the change of the relative thickness of the laminar sublayer as the Mach number increases at various values of the Reynolds number (the experimental data of Hill, Lobb, Winkler and Persch, and of E. U. Repik are shown on this figure). As can be seen from the figure, in incompressible fluids the thickness of the laminar sublayer is no more than 3% of the total layer thickness δ. At Mach = 9, δ_L may become 30% or more of the total boundary layer thickness, and the rate of increase of the relative thickness of the laminar sublayer with increase of the Mach number also increases. A decrease of the Reynolds number Re** also leads to an increase in δ_L/δ.

Figure 21 shows the data of Lobb et al., Hill, and Monaghan [47] for the value of the universal coordinate η at the edge of the laminar sublayer, which is denoted by η_L. As can be seen from Fig. 21, the experimental data existing at present are insufficient to quantitatively determine the effects of the various parameters. This circumstance largely explains why in most existing theories of turbulent boundary layers in compressible gases η_L is assumed to have the same value as in an incompressible fluid, i.e., $\eta_L = \alpha = 10.8 - 12.5$*. /107

*This problem will be considered in more detail in Section 13.

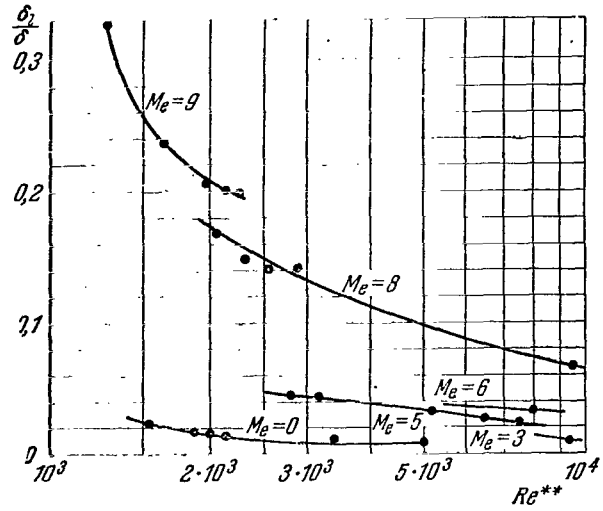

Figure 20.

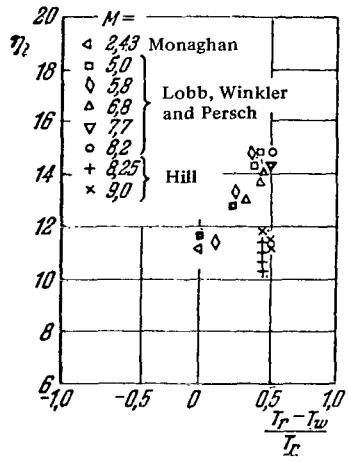

Figure 21.

12. Semiempirical methods of calculating friction on flat plates [48]. /107

Let us consider the flow of a supersonic gas stream around a smooth impermeable plate (Fig. 22). If the plate is placed at zero angle of attack (Fig. 22a) the velocity at the outer edge of the boundary layer will be constant

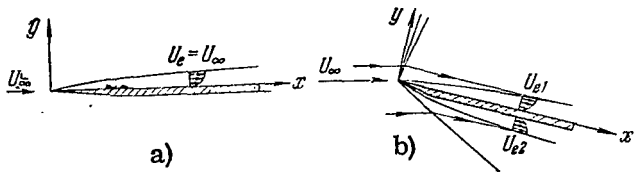

Figure 22.

and equal to the velocity of the approaching stream at infinity: $U_e = U_\infty$**. In the flow along a plate at some angle of attack (or along a wedge) there is an attached discontinuity on the lower surface and a radiating rarefaction wave on the top surface (Fig. 22b). In this case, the velocity at the outer edge of the boundary layer will also be constant and equal to the velocity behind the discontinuity or radiating rarefaction, respectively. The values of the velocities after an attached oblique shock wave and a radiating (normal) rarefaction wave can be determined from well known gas-dynamic relationships [50]. /108

In the case of two-dimensional flow with a constant velocity (U_e = const., $dU_e/d_x = 0$) on an impermeable wall, which is being considered here, so that $v_w = 0$, the integral momentum relationship (2.80) assumes the form

$$\frac{d\delta^{**}}{dx} = \frac{\tau_w}{\rho_e U_e^2}. \qquad (3.16)$$

Here δ^{**} is the momentum loss thickness given by equation (2.76). As before, the parameters at the outer edge of the boundary layer will be indicated by a subscript $_e$, bearing in mind that it is only in the special case of flow along a flat plate at zero angle of attack that these parameters are equal to the parameters of the approaching stream at infinity.

By introducing a Reynolds number formed from the momentum loss thickness,

---

**At large supersonic velocities it may become necessary to take into account the interaction between the boundary layer and the external inviscid flow. As a result of such interaction, the value of the pressure, and consequently, the velocity also, at the outer edge of the boundary layer may differ considerably from the values of these quantities at infinity. For further details of this problem, see, for instance, Kheĭz and Probstin [49]. In the present chapter, which deals with investigations of flows at relatively small supersonic velocities, it is not necessary to take into account these viscous interactions.

$$\mathrm{Re}^{**} = \frac{U_e \rho_e \delta^{**}}{\mu_e}. \tag{3.17}$$

and a Reynolds number formed from the value of the coordinate at the particular point on the plate

$$\mathrm{Re}_x = \frac{U_e \rho_e x}{\mu_e}, \tag{3.18}$$

it becomes possible to write (3.16) in the form

$$d\,\mathrm{Re}_x = \left(\frac{\rho_e}{\rho_w}\right) \zeta^2\, d\,\mathrm{Re}^{**}, \tag{3.19}$$

where ζ is a friction parameter, expressed by equation (3.8). When equation (3.19) is rewritten in integral form, it is found that

$$\mathrm{Re}_x = \frac{\rho_e}{\rho_w} \int_0^{\mathrm{Re}^{**}} \zeta^2\, d\,\mathrm{Re}^{**}. \tag{3.20}$$

As can be seen from equation (3.20), in order to solve this problem it is necessary to have a relationship between ζ and Re^{**}, i.e., it is necessary to establish a "resistance law". In order to establish this law, it is necessary to revert to the expression for the momentum loss thickness (equation (2.76)), and to rearrange this by introducing the universal parameters η and φ by equation (3.8), to give

/109

$$\delta^{**} = \frac{\nu_w \zeta^2}{U_e} \int_0^1 \frac{\rho}{\rho_e} \frac{\varphi}{\zeta} \left(1 - \frac{\varphi}{\zeta}\right) \frac{d\eta}{d\varphi}\, d\left(\frac{\varphi}{\zeta}\right). \tag{3.21}$$

By making use of equations (3.17) and (3.8), (3.21) is transformed to the form

$$\mathrm{Re}^{**} = \zeta^2 \frac{\mu_w}{\mu_e} \int_0^1 \frac{\rho}{\rho_w} \bar{u}(1 - \bar{u}) \frac{d\eta}{d\varphi}\, d\bar{u}. \tag{3.22}$$

The two-layer concept (laminar sublayer and turbulent core) will be used for the turbulent boundary layer (the basis for this simplification for supersonic streams is given in Section 11).

In order to determine the relationship $\frac{d\eta}{d\varphi}(\bar{u})$ in the turbulent core, the formula from the semiempirical theory of von Kármán is used (equation 2.69)). As regards the turbulence constant $\varkappa$ in this equation, it is assumed that it is independent of compressibility (i.e., of the Mach number) and of heat transfer (i.e., of the temperature factor T_w/T_e), and has the same numerical value as in an incompressible fluid, $\varkappa = 0.4$. When von Kármán's formula (2.69) is converted to the universal coordinates, it becomes

$$\frac{\varphi''^2}{\varphi'^4} = \varkappa^2 \frac{\frac{\rho}{\rho_w}}{\frac{\tau}{\tau_w}}, \tag{3.23}$$

where the primes denote differentiation with respect to η.

By taking the square root of both sides of this equation, it is found that

$$\frac{\varphi''}{\varphi'^2} = -\varkappa\Psi, \tag{3.24}$$

where /110

$$\Psi = \sqrt{\frac{\frac{\rho}{\rho_w}}{\frac{\tau}{\tau_w}}}. \tag{3.25}$$

The minus sign in the right-hand part of equation (3.24) is chosen because of the fact that on the plate $\varphi'' < 0$ (condition of convexity of the velocity profile).

By interchanging the positions of the argument and function in (3.24), it is found that

$$\frac{\frac{d^2\eta}{d\varphi^2}}{\frac{d\eta}{d\varphi}} = \varkappa\Psi, \tag{3.26}$$

the first integral of which is the equation

$$\frac{d\eta}{d\varphi} = C_1 \exp(\varkappa\zeta \int \Psi\, d\bar{u}). \tag{3.27}$$

In order to determine the integration constant C_1 it is necessary to be given the value of the derivative $d\varphi/d\eta$ at the edge of the laminar sublayer on the side of the turbulent core. The simplest assumption which can be made here is that this quantity has the same value as in an incompressible fluid, i.e., that

$$[\varphi'(\eta)]_{\eta_l+0} = f = \frac{1}{\varkappa\alpha};$$

in other words, it is assumed that $\varphi'(\eta_L + 0)$ is independent of compressibility and heat transfer (α is the empirical laminar sublayer constant, η_L is the coordinate of the edge of the laminar sublayer). This assumption leads to the following result:

$$\frac{d\eta}{d\varphi} = \frac{1}{f}\exp\left(\varkappa\zeta\int_{\bar{u}_l}^{\bar{u}}\Psi\,d\bar{u}\right). \tag{3.28}$$

Here $\bar{u}_L = u_L/U_e$ is the dimensionless velocity at the edge of the laminar sublayer (the determination of this quantity will be given later). /111

By carrying out the integration in (3.28) and determining the integration constant from the conditions at the edge of the laminar sublayer ($\bar{u} = \bar{u}_L$ at $\eta = \eta_L$), an expression is obtained for the velocity profile in the turbulent core

$$\eta = \eta_l + \frac{\zeta}{f}\int_{\bar{u}_l}^{\bar{u}}\exp\left(\varkappa\zeta\int_{\bar{u}_l}^{\bar{u}}\Psi\,d\bar{u}\right)d\bar{u}. \tag{3.29}$$

Here Ψ is expressed by equation (3.25). In the laminar sublayer it is possible to use the linear relationship

$$\varphi = \eta, \tag{3.30}$$

for the velocity profile, from which an expression for the velocity at the edge of the laminar sublayer is obtained*:

*A detailed derivation of equations (3.30) and (3.31), and a consideration of the problems of determining the thickness of the laminar sublayer and of the effects of various factors on the sublayer parameters will be given in Section 13.

$$\bar{u}_2 = \frac{\varphi_2}{\zeta} = \frac{\eta_2}{\zeta} = \frac{\alpha}{\zeta}. \tag{3.31}$$

Thus the derivative $\frac{d\eta}{d\varphi}(\bar{u})$ which is required for determining the Reynolds number Re ** (equation 3.22) can be expressed in the turbulent core by equation (3.28) and in the laminar sublayer, according to (3.30), by the equation

$$\frac{d\eta}{d\varphi} = 1. \tag{3.32}$$

Returning now to the expression for Re** (equation (3.22)), it can be seen that in evaluating the integral on the right side of this equation, the integration range, strictly speaking, should be divided into two sections: the laminar sublayer ($0 \leq \bar{u} \leq \bar{u}_L$) and the turbulent core ($\bar{u}_L \leq \bar{u} \leq 1$), and in each of these the separate values of $d\eta/d\varphi$ should be substituted, using equation (3.32) in the first zone and equation (3.28) in the second. However, such an evaluation, which would lead to quite a complicated expression for Re**, is not necessary when the relative thickness of the laminar sublayer is not very large [$(\delta_L/\delta) < 0.10 - 0.15$]. /112
In this case, it is possible to omit the first zone, and to extend the second zone to the wall. Calculations show that at large values of the friction parameter ζ the error involved in this approximation is negligible. Using this procedure, the expression for $d\eta/d\varphi$ in equation (3.28) is substituted into (3.22), as a result of which the following expression is obtained for the Reynolds number Re **:

$$\mathrm{Re}^{**} = \frac{\mu_w}{\mu_e}\frac{\zeta^2}{f}\int_0^1 \Phi(\bar{u}) \exp\left(\varkappa\zeta \int_{\bar{u}_2}^{\bar{u}} \Psi(\bar{u})\, d\bar{u}\right) d\bar{u}. \tag{3.33}$$

Here the following notation * has been introduced:

$$\Phi(\bar{u}) = \frac{\rho}{\rho_w}\bar{u}(1-\bar{u}). \tag{3.34}$$

Later it is more convenient to write (3.33) in the form

$$\mathrm{Re}^{**} = \exp[-\varkappa\zeta I(\bar{u}_2)]\frac{\mu_w}{\mu_e}\frac{\zeta^2}{f}\int_0^1 \Phi(\bar{u}) \exp[\varkappa\zeta I(\bar{u})]\, d\bar{u}, \tag{3.35}$$

*In the general case the function Φ depends on the two variables x and u, since $\rho = \rho(x, u)$. However, according to the approximation made earlier, according to which $\rho \approx \rho(\bar{u})$, it is seen that $\Phi \approx \Phi(\bar{u})$.

where

$$I(\bar{u}) = \int_0^{\bar{u}} \Psi(\bar{u})\, d\bar{u} = \int_0^{\bar{u}} \sqrt{\frac{\rho/\rho_w}{\tau/\tau_w}}\, d\bar{u}, \tag{3.36a}$$

$$I(\bar{u}_l) = \int_0^{\bar{u}_l} \Psi(\bar{u})\, d\bar{u} = \int_0^{\bar{u}_l} \sqrt{\frac{\rho/\rho_w}{\tau/\tau_w}}\, d\bar{u}. \tag{3.36b}$$

Use is made of the assumption (3.1) for the shear stress τ in the boundary layer (the basis of this assumption was given in Section 10). In this case, /113

$$I(\bar{u}) = \int_0^{\bar{u}} \sqrt{\frac{\rho}{\rho_w}}\, d\bar{u}. \tag{3.37}$$

In determining $I(\bar{u}_L)$ it is assumed approximately that the density in the laminar sublayer is a constant quantity, equal to the density at the wall ρ_w. In this case, bearing equation (3.31) in mind, it is found that

$$I(\bar{u}_l) = \bar{u}_l = \frac{\alpha}{\zeta}. \tag{3.38}$$

In evaluating the integral appearing in the expression (3.35), use is made of the fact that the value of ζ is significantly greater than unity ($\zeta \gg 1$). In this case, the integral can be represented in the form of an asymptotic series obtained as a result of integration by parts:

$$\int \Phi(\bar{u}) \exp[\varkappa\zeta I(\bar{u})]\, d\bar{u} = \frac{\exp[\varkappa\zeta I(\bar{u})]}{\varkappa\zeta\Psi}\left(\Phi - \frac{F_1}{\varkappa\zeta} + \frac{F_2}{\varkappa^2\zeta^2} - \frac{F_3}{\varkappa^3\zeta^3} + \ldots\right). \tag{3.39}$$

Here

$$\left.\begin{aligned} \Psi &= \left(\frac{\rho}{\rho_w}\right)^{1/2}, \quad F_1 = \frac{1}{\Psi}\left(\Phi' - \frac{\Phi\Psi'}{\Psi}\right), \\ F_2 &= \frac{1}{\Psi^3}\left(\Phi'' - \frac{\Phi\Psi'' + 3\Phi'\Psi'}{\Psi} + \frac{3\Phi\Psi'^2}{\Psi^2}\right), \\ F_3 &= \frac{1}{\Psi^3}\left(\Phi''' - \frac{6\Phi''\Psi' + 4\Phi'\Psi'' + \Phi\Psi'''}{\Psi} + \right. \\ &\quad \left. + \frac{15\Phi'\Psi'^2 + 10\Phi\Psi'\Psi''}{\Psi^2} - \frac{15\Phi\Psi'^3}{\Psi^3}\right). \end{aligned}\right\} \tag{3.40}$$

The primes denote differentiation with respect to $\bar{u}$.

The values of the functions $\Phi(\bar{u})$ and $\Psi(\bar{u})$ and their derivatives can be determined at $\bar{u} = 1$:

$$\left.\begin{aligned} &\Phi(1) = 0; \qquad \Phi'(1) = -\frac{\rho_e}{\rho_w}; \\ &\Phi''(1) = -2\left(\frac{\rho}{\rho_w}\right)'_e - 2\left(\frac{\rho_e}{\rho_w}\right); \\ &\Psi(1) = \left(\frac{\rho_e}{\rho_w}\right)^{1/2}; \quad \Psi'(1) = \frac{1}{2}\left(\frac{\rho}{\rho_w}\right)'_e\left(\frac{\rho_e}{\rho_w}\right)^{-1/2}. \end{aligned}\right\} \tag{3.41}$$

The need to calculate the values of the functions Φ and Ψ and their derivatives at $\bar{u} = 0$ does not arise, since it is immediately obvious that the contribution of the series (3.39) at $\bar{u} = 0$ to the value of the integral is very much smaller than the contribution of the series at $\bar{u} = 1$ owing to the presence of a large exponential multiplier in the second case. Bearing in mind equations (3.37), (3.38), (3.40) and (3.41), the definite integral appearing in the right-hand part of (3.35) can be evaluated by using the relationship (3.39). If we confine our attention to the terms containing $\varkappa^3\xi^3$ in the denominator, the following expression is obtained for Re **: /114

$$\mathrm{Re}^{**} = \frac{e^{-\varkappa z}}{fx^2}\cdot\frac{\mu_w}{\mu_e}\exp\left[\varkappa\zeta\int_0^1\left(\frac{\rho}{\rho_w}\right)^{1/2}d\bar{u}\right]\times \left[1-\frac{2+\frac{1}{2}\left(\frac{\rho_w}{\rho_e}\right)\left(\frac{\rho}{\rho_w}\right)'_e}{\left(\frac{\rho_e}{\rho_w}\right)^{1/2}\varkappa\zeta}\right]. \tag{3.42}$$

Another Reynolds number is introduced, formed from the displacement thickness δ^* (equation 2.77):

$$\mathrm{Re}^{*} = \frac{U_e\rho_e\delta^*}{\mu_e}. \tag{3.43}$$

By following the same path as in the determination of Re**, it is found that

$$\mathrm{Re}^{*} = \frac{e^{-\varkappa z}}{fx^2}\frac{\mu_w}{\mu_e}\exp\left[\varkappa\zeta\int_0^1\left(\frac{\rho}{\rho_w}\right)^{1/2}d\bar{u}\right]\left[1+\left(\frac{\rho}{\rho_w}\right)'_e\left(\frac{\rho_e}{\rho_w}\right)^{-1} - \frac{1}{\varkappa\zeta}\left(\frac{\rho_e}{\rho_w}\right)^{-3/2}\left[\frac{1}{2}\left(\frac{\rho}{\rho_w}\right)'_e + \left(\frac{\rho}{\rho_w}\right)''_e - \frac{3}{2}\left(\frac{\rho}{\rho_w}\right)'^2_e\left(\frac{\rho_e}{\rho_w}\right)^{-1}\right]\right]. \tag{3.44}$$

By forming the ratio Re*/Re**, an expression is obtained for the shape parameter $H^* = \delta^*/\delta^{**}$:

$$H^* = \left\{1 + \left(\frac{\rho}{\rho_w}\right)_c' \left(\frac{\rho_e}{\rho_w}\right)^{-1} - \frac{1}{\varkappa\zeta}\left(\frac{\rho_e}{\rho_w}\right)^{-3/2}\left[\frac{1}{2}\left(\frac{\rho}{\rho_w}\right)_e' + \left(\frac{\rho}{\rho_w}\right)_c'' - \frac{3}{2}\left(\frac{\rho}{\rho_w}\right)_e'^2\left(\frac{\rho_e}{\rho_w}\right)^{-1}\right]\right\}\left\{1 - \frac{1}{\varkappa\zeta}\left(\frac{\rho_e}{\rho_w}\right)^{-1/2}\left[2 + \frac{1}{2}\left(\frac{\rho_w}{\rho_e}\right)\left(\frac{\rho}{\rho_w}\right)_c'\right]\right\}^{-1}. \quad (3.45)$$

Equation (3.42), which relates the Reynolds number Re**(3.17) to the friction parameter ζ (3.8), is in essence a "resistance law". It is important to note that this law is obtained without any assumptions as to the nature of the change of density in the boundary layer, and can be used for solving problems in flows on impermeable surfaces with arbitrary changes of density in the boundary layer. /115

Passing now to the establishment of the relationships which are required later to link the density and velocity, it can be noted that from the equation of state (1.86) and the condition that the pressure is constant across the boundary layer, the following simple relationship can be obtained between the density and the temperature:

$$\frac{\rho}{\rho_w} = \left(\frac{T}{T_w}\right)^{-1}. \quad (3.46)$$

In its simplest form the relationship between the temperature and velocity in the boundary layer is obtained by assuming that the Prandtl number Pr and its turbulent analog Pr_T are equal to unity, while the specific heat capacity of the gas is constant. In this case there is a special integral energy equation known as the Crocco integral

$$\frac{T}{T_w} = 1 - \omega\bar{u} - \beta\bar{u}^2. \quad (3.47)$$

Here

$$\left.\begin{aligned}\omega &= 1 - \frac{T_e^*}{T_w}, \quad \beta = \frac{\gamma-1}{2}M_e^2\frac{T_e}{T_w},\\ T_e^* &= T_e\left(1 + \frac{\gamma-1}{2}M_e^2\right)\end{aligned}\right\} \quad (3.48)$$

(T_e^* is the stagnation temperature).

Sometimes in order to take into account differences in the Prandtl numbers (Pr and Pr_T) from unity a recovery coefficient r* is introduced artificially into

*For a more detailed discussion of the recovery coefficient in a turbulent boundary layer, see Section 15.

the expressions for ω and β (3.48). In this case,

$$\left.\begin{aligned} \omega &= 1 - \frac{T_r}{T_w}, \qquad \beta = r\frac{\gamma-1}{2} M_e^2 \frac{T_e}{T_w}, \\ T_r &= T_e\left(1 + r\frac{\gamma-1}{2} M_e^2\right) \end{aligned}\right\} \tag{3.49}$$

(T_r is the recovery temperature).

This change in the form of the Crocco integral is based on simple arguments, /116
according to which the coefficient ω must tend to zero in the absence of heat transfer between the gas and the wall regardless of the values of the Prandtl numbers (Pr, Pr_T). For Prandtl numbers different from unity this condition can be satisfied only if T_e^* in the equation for ω (3.48) is taken to mean the equilibrium temperature of the thermally insulated wall T_r. As a consequence of this, it is necessary to introduce the recovery coefficient r in the expression for β (3.48) in order to satisfy the condition at the outer edge ($T = T_e$ at $\bar{u} = 1$); as a result, β assumes the form (3.49).

By using the equations (3.47) and (3.46), the required relationship between the density and velocity in the boundary layer is

$$\frac{\rho}{\rho_w} = (1 - \omega\bar{u} - \beta\bar{u}^2)^{-1}. \tag{3.50}$$

By substituting the relationships (3.50) and (3.37) and carrying out the integrations, the following very important expression for the function $I(\bar{u})$ is obtained:

$$I(\bar{u}) = \frac{1}{\sqrt{\beta}}\left(\arcsin\frac{\sqrt{\beta}\,\bar{u} + \frac{\omega}{2\sqrt{\beta}}}{\sqrt{1 + \frac{\omega^2}{4\beta}}} - \arcsin\frac{\frac{\omega}{2\sqrt{\beta}}}{\sqrt{1 + \frac{\omega^2}{4\beta}}}\right). \tag{3.51}$$

It should also be noted that the function $I(\bar{u})$ appears as the power on an exponent in equation (3.42) and (3.44), and by carrying out the equations required in the right-hand part of these equations, using (3.50), the following expressions are obtained for Re** and Re*:

$$\mathrm{Re}^{**} = \frac{e^{-\varkappa z}}{f\varkappa^2}\frac{\mu_w}{\mu_e}\exp[\varkappa\zeta I(1)]\left[1 - \frac{2 - 1{,}5\,\omega - \beta}{\varkappa\zeta\sqrt{1 - \omega - \beta}}\right], \tag{3.52}$$

$$\mathrm{Re}^{**} = \frac{e^{-\varkappa z}}{f\varkappa^2}\frac{\mu_w}{\mu_e}\exp\left[\varkappa\zeta I(1)\right]\left[\frac{1+\beta}{1-\omega-\beta}\right]\times$$
$$\left[1-\frac{\beta\left(3-1{,}5\omega-\beta+\frac{\omega}{2\beta}\right)}{\varkappa\zeta(1+\beta)\sqrt{1-\omega-\beta}}\right]. \qquad (3.53)$$

Here /117

$$I(1) = \frac{1}{\sqrt{\beta}}\left(\arcsin\frac{\sqrt{\beta}+\frac{\omega}{2\sqrt{\beta}}}{\sqrt{1+\frac{\omega}{4\beta}}} - \arcsin\frac{\frac{\omega}{2\sqrt{\beta}}}{\sqrt{1+\frac{\omega^2}{4\beta}}}\right). \qquad (3.54)$$

By forming the ratio of the equations (3.53) and (3.52), an expression is obtained for the form parameter $H^* = \delta^*/\delta^{**}$:

$$H^* = \frac{(1+\beta)\left[1-\frac{\beta\left(3-1{,}5\,\omega-\beta+\frac{\omega}{2\beta}\right)}{\varkappa\zeta(1+\beta)\sqrt{1-\omega-\beta}}\right]}{(1-\omega-\beta)\left[1-\frac{2-1{,}5\,\omega-\beta}{\varkappa\zeta\sqrt{1-\omega-\beta}}\right]}. \qquad (3.55)$$

In the limiting case of the flow of an incompressible gas ($\beta = 0$) and in the absence of heat transfer ($\omega = 0$), we obtain the expression

$$H_0^* = \frac{1}{1-\frac{2}{\varkappa\zeta_0}}, \qquad (3.56)$$

which gives a value of $H_0^* = 1.36 - 1.23$ at Reynolds numbers of $10^5 - 10^7$, which is in good agreement with experiments.

Once the resistance law (3.52) is available to form the link between the Reynolds number Re**(3.17) based on the momentum loss thickness and the friction parameter ζ (3.8), it is not difficult to establish (using the momentum equation in the form (3.20)) the required relationship between the friction coefficient c_f and the Reynolds number Re_x (3.18) based on the local value of the coordinate at the point on the plate. In establishing this relationship, it is convenient to use a rougher approximation for Re**, neglecting the second term on the right-hand side of equation (3.52) in comparison with the first. This approximation makes it possible to simplify the final equation for the friction coefficient c_f considerably. The error caused by this simplification in the formula for c_f is compensated to a

considerable extent by an appropriate choice of the interaction constant*. By substituting this "rough" expression for Re** into equation (3.20) and carrying out the integration with the boundary condition $Re_x = 0$ at $\xi = 0$ (the condition that the turbulent boundary layer begins at the leading edge of the plate), it is found to this degree of approximation that

/118

$$C_1 \frac{e^{-\varkappa\alpha}}{f\varkappa^2} \frac{\mu_w}{\mu_e} \frac{\rho_e}{\rho_w} \zeta^2 \exp[\varkappa\zeta I(1)] = Re_x. \tag{3.57}$$

The constant C_1 is introduced into (3.57) to "compensate" for the approximation made in determining Re**.

On converting from ξ to c_f in equation (3.57) according to (3.8) by using equation (3.50) and taking logarithms, it is found that

$$\varkappa(\lg e)\sqrt{2}\sqrt{1-\omega-\beta}\, I(1)(c_f)^{-1/2} = 2\lg(Re_x c_f) - \lg\left(\frac{\mu_w}{\mu_e}\right) + C_2, \tag{3.58}$$

where I(1) is given by equation (3.54) and

$$C_2 = -\lg\left[\frac{C_1 2e^{-\varkappa\alpha}}{f\varkappa^2}\right].$$

By substituting $\varkappa = 0.4$ into (3.58) and determining the constant C_2 from the condition that $\omega = \beta = 0$, equation (3.58) can be converted into von Kármán's formula for an incompressible fluid

$$\frac{0{,}242}{\sqrt{c_{f0}}} = 0{,}41 + \lg(Re_x c_{f0}), \tag{3.59}$$

and the following expression is obtained for the local skin friction coefficient on a flat plate in a compressible gas

*It may be noted that a similar approach is used in the derivation of the well-known formula of von Kármán for the friction coefficient on a flat plate in an incompressible fluid. See, for instance, [20], vol. II.

$$\frac{0{,}242\sqrt{1-\omega-\beta}}{\sqrt{c_f}\sqrt{\beta}}\left(\arcsin\frac{\sqrt{\beta}+\frac{\omega}{2\sqrt{\beta}}}{\sqrt{1+\frac{\omega^2}{4\beta}}}-\arcsin\frac{\frac{\omega}{2\sqrt{\beta}}}{\sqrt{1+\frac{\omega^2}{4\beta}}}\right)=$$
$$0{,}41+\lg(\mathrm{Re}_x c_f)-\lg\left(\frac{\mu_w}{\mu_e}\right). \qquad (3.60)$$

In order to calculate the dynamic viscosity of the gas, it is necessary to use either Sutherland's formula (1.75) or a power law /119

$$\frac{\mu}{\mu_e}=\left(\frac{T}{T_e}\right)^n, \qquad (3.61)$$

where the exponent n is usually taken to be equal to 0.76.

Let us now pass on to the determination of the mean skin friction coefficient:

$$c_F=\frac{1}{\mathrm{Re}_x}\int_0^{\mathrm{Re}_x} c_f d\,\mathrm{Re}_x. \qquad (3.62)$$

The integral momentum relationship in the form (3.19) is used here, transforming it first to the form

$$\frac{\rho_w}{\rho_e}\frac{1}{\zeta^2}d\,\mathrm{Re}_x=d\,\mathrm{Re}^{**}. \qquad (3.63)$$

The left side of equation (3.63) is converted from ζ to c_f by using equation (3.8) and carrying out the integration with the condition $\mathrm{Re}^{**}=0$ at $\mathrm{Re}_x=0$, using equation (3.62), to give

$$c_F\,\mathrm{Re}_x=2\,\mathrm{Re}^{**}. \qquad (3.64)$$

By substituting the "rough" value Re** (3.52) into the right-hand side of (3.64), it is found that

$$c_F\,\mathrm{Re}_x=C_3\frac{2e^{-\varkappa x}}{f\varkappa^2}\frac{\mu_w}{\mu_e}\exp\left[\varkappa\zeta I(1)\right]. \qquad (3.65)$$

The constant C_3 is introduced here, as in equation (3.57), to "compensate" for the roughness of the expression for Re**.

By comparing equation (3.65) with equation (3.57), converted to the form

$$c_f \mathrm{Re}_x = C_1 \frac{2e^{-\varkappa z}}{\sqrt{\varkappa}} \frac{\mu_w}{\mu_e} \exp[\varkappa \zeta I(1)],$$

it is not difficult to see that with the large values of the parameter ζ being considered here, the coefficients c_F and c_f differ by a constant quantity. As a result, it can be concluded that the expression for the mean friction coefficient will have the form (3.60), but with a different constant, i.e., /120

$$\frac{0{,}242\sqrt{1-\omega-\beta}\,I(1)}{\sqrt{\beta}\sqrt{c_F}} = \lg(\mathrm{Re}_x c_F) - \lg\left(\frac{\mu_w}{\mu_e}\right) + C_4. \qquad (3.66)$$

The constant C_4 is determined from the requirement that for $\omega = \beta = 0$, equation (3.66) should reduce to the von Kármán relationship for the mean skin friction coefficient in an incompressible fluid, i.e., to

$$\frac{0{,}242}{\sqrt{c_F}} = \lg(\mathrm{Re}_x c_F). \qquad (3.67)$$

After determining the constant C_4, the following final formula is obtained for the mean skin friction coefficient:

$$\frac{0{,}242\sqrt{1-\omega-\beta}}{\sqrt{c_F}\sqrt{\beta}}\left(\arcsin\frac{\sqrt{\beta}+\frac{\omega}{2\sqrt{\beta}}}{\sqrt{1+\frac{\omega^2}{4\beta}}} - \arcsin\frac{\frac{\omega}{2\sqrt{\beta}}}{\sqrt{1+\frac{\omega^2}{4\beta}}}\right) = \lg(\mathrm{Re}_x c_F) - \lg\left(\frac{\mu_w}{\mu_e}\right). \qquad (3.68)$$

Two special cases of practical importance of flow along a flat plate will now be considered.

Thermally insulated plate. In this case, $T_w = T_r$, $\omega = 0$,

$$\beta = \frac{\frac{\gamma-1}{2}M_e^2}{1+\frac{\gamma-1}{2}M_e^2} \quad \text{for} \quad \mathrm{Pr} = \mathrm{Pr}_T = 1, \qquad (3.69a)$$

$$\beta = \frac{r\frac{\gamma-1}{2}M_e^2}{1+r\frac{\gamma-1}{2}M_e^2} \quad \text{for} \quad \mathrm{Pr} \neq \mathrm{Pr}_T \neq 1. \tag{3.69b}$$

Equation (3.60) for the local friction coefficient and equation (3.68) for the mean friction coefficient can be transformed respectively to /121

$$\frac{0{,}242}{\sqrt{c_f}}\sqrt{\frac{1-\beta}{\beta}}\arcsin\sqrt{\beta} = 0{,}41 + \lg(\mathrm{Re}_x c_f) - \lg\left(\frac{\mu_r}{\mu_e}\right) \tag{3.70}$$

and

$$\frac{0{,}242}{\sqrt{c_F}}\sqrt{\frac{1-\beta}{\beta}}\arcsin\sqrt{\beta} = \lg(\mathrm{Re}_x c_F) - \lg\left(\frac{\mu_r}{\mu_e}\right). \tag{3.71}$$

Plate with heat transfer to a stream of incompressible fluid. In this case, by letting the value of β tend to zero it is found that

$$\frac{0{,}484\,(\sqrt{1-\omega}+\omega-1)}{\sqrt{c_f\omega}} = 0{,}41 + \lg(\mathrm{Re}_x c_f) - \lg\left(\frac{\mu_w}{\mu_e}\right), \tag{3.72}$$

$$\frac{0{,}484\,(\sqrt{1-\omega}+\omega-1)}{\sqrt{c_F\,\omega}} = \lg(\mathrm{Re}_x c_F) - \lg\left(\frac{\mu_w}{\mu_e}\right). \tag{3.73}$$

In nonexplicit form, these equations give the friction coefficients as functions of the parameters of the approaching stream and the conditions at the wall; as a result, they are not always convenient to use in practice. By means of some simple rearrangements, it is not difficult to show that these relationships can be made explicitly. For this purpose it is necessary to return to equation (3.57), which in the case of flow of an incompressible fluid in the absence of heat transfer between the gas and the wall reduces to the form

$$C_1\frac{e^{-\varkappa\alpha}}{f\varkappa^2}\zeta_0^2 e^{\varkappa\zeta_0} = \mathrm{Re}_x. \tag{3.74}$$

By dividing the two sides of equation (3.57) by the two sides of equation (3.74), it is found that

$$\left(\frac{\zeta}{\zeta_0}\right)^2 \exp\left[\varkappa\zeta I(1) - \varkappa\zeta_0\right] = \frac{\mu_e \rho_w}{\mu_w \rho_e}. \tag{3.75}$$

By converting equation (3.75) from ζ to c_f using relationship (3.8) and taking logarithms leads to

$$-\lg\frac{c_f}{c_{f0}} + FK\sqrt{\frac{c_{f0}}{c_f}} = F + G, \tag{3.76}$$

where /122

$$F = \frac{0{,}242}{\sqrt{c_{f0}}}, \tag{3.77}$$

$$G = \lg\left(\frac{\mu_e}{\mu_w}\right), \tag{3.78}$$

$$K = \sqrt{\frac{1-\omega-\beta}{\beta}}\left(\arcsin\frac{\sqrt{\beta}+\frac{\omega}{2\sqrt{\beta}}}{\sqrt{1+\frac{\omega^2}{4\beta}}} - \arcsin\frac{\frac{\omega}{2\sqrt{\beta}}}{\sqrt{1+\frac{\omega^2}{4\beta}}}\right). \tag{3.79}$$

For determining the friction coefficient c_{f_0} it is possible to use either von Kármán's formula, (3.59) or the simpler explicit relationship

$$c_{f0} = 0{,}0263\,\mathrm{Re}_x^{-1/7}, \quad c_{f0} = 0{,}085\,\mathrm{Re}_x^{-0{,}29-0{,}01\lg \mathrm{Re}_x} \quad [45] \tag{3.80}$$

Equations (3.76) can be reduced to a transcendental equation with one parameter. For this purpose, this equation is rewritten in the form

$$2\lg\frac{1}{\sqrt{\frac{c_f}{c_{f0}}}} + \frac{FK}{\sqrt{\frac{c_f}{c_{f0}}}} = F + G$$

and then 2 lg(FK/2) is added to both sides of the resulting equation, giving

$$\lg\left(\frac{FK}{2\sqrt{\frac{c_f}{c_{f0}}}}\right) + \frac{FK}{2\sqrt{\frac{c_f}{c_{f0}}}} = \lg\frac{FK}{2} + \frac{F+G}{2}. \tag{3.81}$$

By introducing the notation

$$N = \frac{FK}{2\sqrt{\frac{c_f}{c_{f0}}}}, \tag{3.82}$$

$$Q = \lg \frac{FK}{2} + \frac{F+G}{2}, \tag{3.83}$$

the following equation is obtained in place of (3.81): /123

$$\lg N + N = Q. \tag{3.84}$$

Thus, the expression for the friction coefficient can be written in the form

$$\frac{c_f}{c_{f0}} = \left(\frac{FK}{2N}\right)^2, \tag{3.85}$$

where the values of F and K are determined from equations (3.77) and (3.79), while the value of N is obtained by solving equation (3.84). The determination of the value of N presents no particular difficulty and can be carried out by means of a table of logarithms to base 10 or a graph.

If a power relationship of the type (3.61) is assumed for the dynamic viscosity, the expression for the function G, which is needed together with F and K to determine N, assumes the form

$$G = n \lg \left(\frac{T_e}{T_w}\right). \tag{3.86}$$

It is interesting to note that by using Prandtl's formula (2.68) instead of the von Kármán formula (2.69) for the friction coefficient, the same expression (3.85) is obtained, except that in place of (3.86), G must be given by

$$G = \left(n + \frac{1}{2}\right) \lg \left(\frac{T_e}{T_w}\right). \tag{3.87}$$

On considering equation (3.85), it can be noted that at large Reynolds numbers the value of the ratio c_f/c_{f_0} depends only slightly on the Reynolds number. Actually, as the Reynolds number tends to infinity ($Re_x \to \infty$), or, what is the same thing, $F \to \infty$, the following limiting equation is obtained for the ratio c_f/c_{f_0}:

$$\frac{c_f}{c_{f0}} = K^2, \tag{3.88}$$

The value of K expressed by equation (3.79) depends only on the compressibility of the medium (β) and heat transfer (ω), but not on the Reynolds number. /124

The fact that a limiting formula (3.88) exists was established and then widely used for setting up semiempirical methods of calculating turbulent boundary layers in the work of S. S. Kutateladze, A. I. Leont'ev, et al., [51, 52].

When equation (3.85) is used for calculating the friction coefficient, it is useful to consider special cases, as earlier.

In the case of a thermally insulated plate ($\omega = 0$), the coefficient β is given by equations (3.69a) and (3.69b), and the function K has the form

$$K = \sqrt{\frac{1-\beta}{\beta}} \arcsin \sqrt{\beta}. \tag{3.89}$$

In an incompressible liquid in the presence of heat transfer, the value of β tends towards zero, giving

$$K = \frac{2(\sqrt{1-\omega} + \omega - 1)}{\omega}. \tag{3.90}$$

For calculating the mean friction coefficient of a flat plate, it is not difficult to establish the validity of a formula which agrees in form with equation (3.85), i.e.,

$$\frac{c_F}{c_{F0}} = \left(\frac{FK}{2N}\right)^2, \tag{3.91}$$

where K and N are expressed as previously by equations (3.79) and (3.84), and the quantity F has the form

$$F = \frac{0{,}242}{\sqrt{c_{F0}}}. \tag{3.92}$$

In order to determine the friction coefficient c_{F_0} it is possible to use either the von Kármán formula (3.67) or the simpler power law relationship /125

$$c_{F0} = 0{,}0307\, \mathrm{Re}_x^{-1/7}. \tag{3.93}$$

The equations (3.85) and (3.91) obtained above make it possible to calculate the ratios between the local and mean friction coefficients at given values of the Mach number M_e, the temperature factor T_w/T_r, and the Reynolds number Re_x to the local and mean friction coefficients in an incompressible fluid ($M_e = 0$, $T_w/T_r = 1$) at the same value of the Reynolds number. However, in some cases, and particularly in the evaluation of experimental data, it is more convenient to use as the characteristic Reynolds number the Reynolds number formed from the momentum loss thickness Re **. This is the case, for example, when it is difficult to determine the origin of the boundary layer on the tube wall, so that it is impossible to use the Reynolds Re_x formed from the local value of the coordinate. In such a case, it is convenient in comparing theory with experiments to have the ratios c_f/c_{f0}, in which the values of c_f, c_{f0} and c_F, c_{F0} are evaluated at the same values of the Reynolds number Re**.

In order to obtain these relationships, we must return to the expression for the Reynolds number Re** (3.53), which in the case of the flow of an incompressible fluid reduces to the form

$$\mathrm{Re}^{**} = \frac{e^{-\varkappa\alpha}}{f\varkappa^2} e^{\varkappa\zeta_0}\left(1 - \frac{2}{\varkappa\zeta_0}\right). \tag{3.94}$$

Just as in the case of establishing relationships (3.85) and (3.91), it is convenient to use a rough approximation for the Reynolds number Re**, according to which the terms containing $1/\zeta$ ($1/\zeta_0$) are neglected compared to unity in the right-hand parts of equations (3.52) and (3.94). Thus, by proceeding as before and dividing both sides of equation (3.52) by both sides of equation (3.94) and then converting from ζ to c_f by means of equation (3.8), simple rearrangement gives /126

$$\left(\frac{c_f}{c_{f0}}\right)_{\mathrm{Re}^{**}} = \left(\frac{K}{1 + \frac{G}{F}}\right)^2, \tag{3.95}$$

where the functions F, K and G are given by the equations (3.77) - (3.79).

The expression for $(c_F/c_{F0})_{\mathrm{Re}^{**}}$ has the same form as (3.95), except that in this case the function F is given by equation (3.92).

If the Reynolds number Re**in equation (3.95) tends to infinity, the limiting formula obtained earlier, equation (3.88), is obtained.

Let us now go on to the determination of the velocity profile in the boundary layer. In the laminar sublayer the velocity profile is described by the linear relationship (3.30). In order to establish the velocity profile in the turbulent core of the boundary layer, we return to equation (3.29), first transforming it to the form

$$\eta = \eta_L + \frac{\zeta}{f}\exp\left[-\varkappa\zeta\int_0^{\bar{u}_L}\Psi\,d\bar{u}\right]\left\{\int_0^{\bar{u}}\exp\left[\varkappa\zeta\int_0^{\bar{u}}\Psi\,d\bar{u}\right]d\bar{u} - \int_0^{\bar{u}_L}\exp\left[\varkappa\zeta\int_0^{\bar{u}}\Psi\,d\bar{u}\right]d\bar{u}\right\}. \qquad (3.96)$$

Here the quantity Ψ is given by equation (3.25).

If it is assumed, as earlier, that the approximation (3.1) is satisfactory for the shear stress, and if the density is constant and equal to its value at the wall in the laminar sublayer (for $0 \leq \bar{u} \leq \bar{u}_L$), it is found from the previous equation:

$$\eta = \frac{e^{-\varkappa\zeta}}{f}\int_0^{\bar{u}}\exp\left[\varkappa\zeta I(\bar{u})\right]d\bar{u}. \qquad (3.97)$$

Here $I(\bar{u})$ is given by equation (3.51).

On substituting the value of $I(\bar{u})$ from equation (3.51) into the expression (3.97) and performing the integration, the following expression is obtained for the velocity profile in the turbulent core: /127

$$\eta = \frac{e^{-\varkappa\alpha}}{f\varkappa}\left(\frac{\sqrt{1-\omega\bar{u}-\beta\bar{u}^2}+\frac{\beta}{\varkappa\zeta}\bar{u}+\frac{\omega}{2\varkappa\zeta}}{1+\frac{\beta}{\varkappa^2\zeta^2}}\right)\times \exp\left[\frac{\varkappa\zeta}{\sqrt{\beta}}\left(\arcsin\frac{\sqrt{\beta}\,\bar{u}+\frac{\omega}{2\sqrt{\beta}}}{\sqrt{1+\frac{\omega^2}{4\beta}}}-\arcsin\frac{\frac{\omega}{2\sqrt{\beta}}}{\sqrt{1+\frac{\omega^2}{4\beta}}}\right)\right]. \qquad (3.98)$$

After substituting the corresponding values of the empirical constants ($\alpha = 11.5$, $\varkappa = 0.4$, $f = 1/\varkappa\alpha = 0.218$) into (3.98) and taking logarithms, the velocity profile reduces to the following form

$$\frac{\zeta}{\sqrt{\beta}}\left(\arcsin\frac{\sqrt{\beta}\,\bar{u}+\frac{\omega}{2\sqrt{\beta}}}{\sqrt{1+\frac{\omega^2}{4\beta}}}-\arcsin\frac{\frac{\omega}{2\sqrt{\beta}}}{\sqrt{1+\frac{\omega^2}{4\beta}}}\right)+ 5{,}75\lg\left[\left(1+\frac{6{,}25\beta}{\zeta^2}\right)^{-1}\left(\sqrt{1-\omega\bar{u}-\beta\bar{u}^2}+\frac{2{,}5\beta\bar{u}}{\zeta}+\frac{1{,}25\omega}{\zeta}\right)\right] = 5.75\lg\eta + 5.5. \qquad (3.99)$$

In the limiting case of flow of an incompressible fluid ($\beta = 0$) and in the absence of heat transfer ($\omega = 0$), equation (3.99) reduces to the well known logarithmic velocity profile

$$\varphi = 5{,}75 \lg \eta + 5{,}5. \tag{3.100}$$

If equation (3.52) is used for the Reynolds number Re**, the velocity profile expression can be readily rearranged to the following form, which is useful in selected practical cases:

$$\frac{\zeta}{\sqrt{\beta}}\left(\arcsin\frac{\sqrt{\beta}\,\bar{u}+\frac{\omega}{2\sqrt{\beta}}}{\sqrt{1+\frac{\omega^2}{4\beta}}}-\arcsin\frac{\frac{\omega}{\sqrt{\beta}}}{\sqrt{1+\frac{\omega^2}{4\beta}}}\right)+5{,}75\times$$
$$\lg\frac{0{,}4\zeta\left(\sqrt{1-\omega\bar{u}-\beta\bar{u}^2}+\frac{2{,}5\beta\bar{u}}{\zeta}+\frac{1{,}25\omega}{\zeta}\right)}{\left(1+\frac{6{,}25\beta}{\zeta^2}\right)\left(\sqrt{1-\omega-\beta}-\frac{5}{\zeta}+\frac{3{,}75\omega}{\zeta}+\frac{2{,}5\beta}{\zeta}\right)\sqrt{1-\omega-\beta}}=$$
$$5{,}75\lg\left(\frac{y}{\delta^{**}}\right). \tag{3.101}$$

The semiempirical method of calculating friction in a turbulent boundary layer on a flat plate which has been discussed above is illustrated by the graphs given in Figs. 23 - 26. At the same time, the experimental data of various authors are also given for comparison. /128

Figure 23 shows the calculated results for local friction coefficients on a thermally insulated plate for three Reynolds numbers: 10^6, 10^7, 10^8. The curve calculated from the limiting formula (3.88) is denoted by ∞. In addition to the experimental points of authors whose work was considered in Section 11, Fig. 23 also shows the points obtained from Lipmann and Dhavan [53].

Figure 24 shows the calculated results for the mean friction factors on a thermally insulated surface. Apart from the experimental points from the work previously discussed, use has also been made of the results obtained by Pappas [54]. It should be noted that here (and in Fig. 23), the experimental points of Coles lie above the calculated curves.

Figure 25 gives the calculated results for the local friction coefficients for a plate exchanging heat with the gas (heat flux directed from the gas to the wall).

Figure 26 gives the results of calculations of the ratio of the local friction coefficient in a compressible gas to the friction coefficient in an incompressible fluid, where both coefficients are evaluated at the same value of the Reynolds number formed from the momentum loss thickness (equation (3.95)). As well as the experimental points from the paper of Hill considered in Section 11, Fig. 26 also gives experimental points at $M_e = 10$ from a more recent paper by the same author [55].

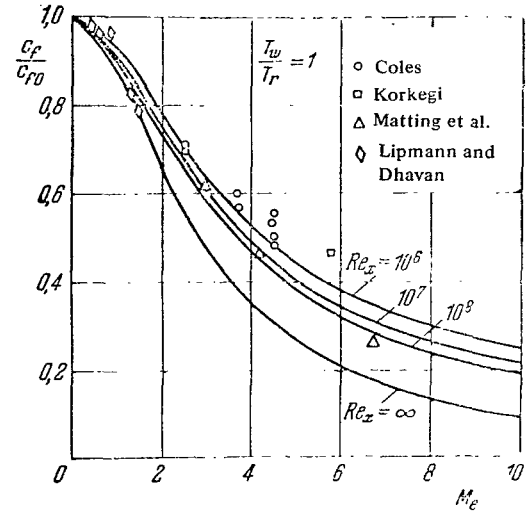

Figure 23.

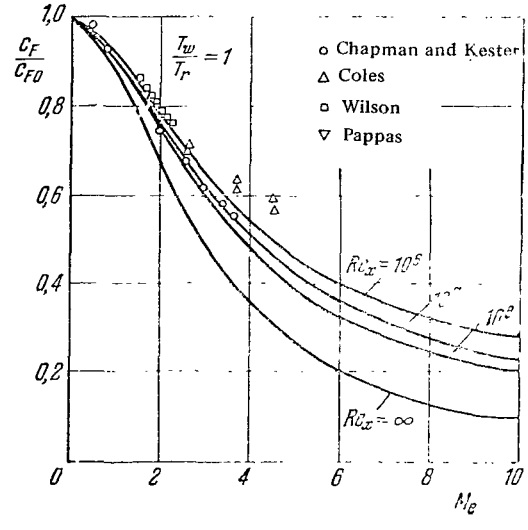

Figure 24.

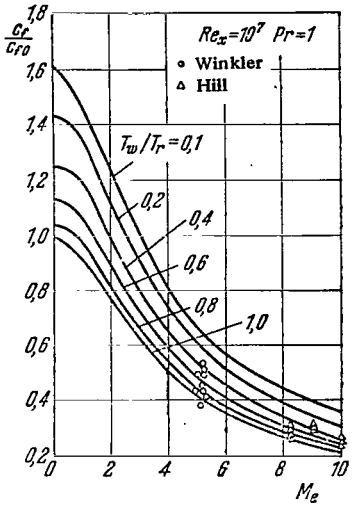

Figure 25.

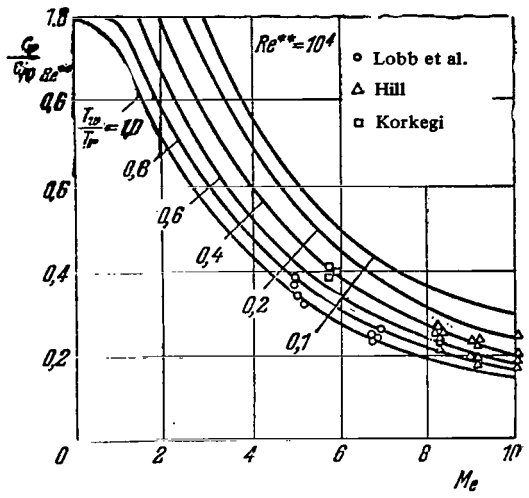

Figure 26.

Figure 27 shows a comparison of the form parameter H* calculated by equation (3.55) with the value of this same form parameter obtained in the experiments of Pappas [54]. As can be seen from the graphs, the agreement between the calculated and experimental data becomes better as the Reynolds number increases.

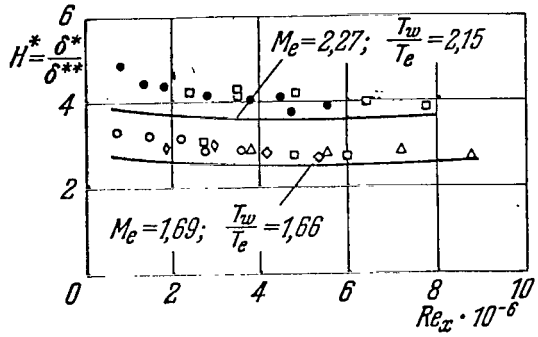

Figure 27.

Figure 17 shows the calculated velocity profiles as well as the experimental velocity profiles obtained in Hill's experiments. The solid lines show the velocity profiles calculated from equation (3.30) (laminar sublayer) and equation (3.99) (turbulent core). The dashed lines show the logarithmic velocity profiles in an /131

incompressible fluid calculated from equation (3.100). Comparison of the solid curves with the experimental points indicates that the effects of compressibility and the temperature factor on the form of the velocity profile have been correctly taken into account quantitatively in equation (3.99). Complete agreement of the calculated and experimental velocity profiles can scarcely be expected bearing in mind some of the simplifying assumptions made in setting up the present method of calculation. (This is particularly true of assumption (3.1) as to the constancy of the shear stress across the boundary layer).

13. The effects of compressibility and heat transfer on the laminar sublayer.

The problem of determining the thickness of the laminar sublayer and the velocity at its outer boundary is a very important one in turbulent boundary layer theory, since the selection of these parameters has an appreciable effect on the "laws" for drag and heat transfer. It will be recalled that in the turbulent boundary layer theory for incompressible fluids the laminar sublayer thickness is determined from simple dimensional considerations. Actually, if it is assumed that the motion in the laminar sublayer is determined by the shear stress at the wall τ_w, the viscosity μ, and the density ρ of the medium, it follows from dimensionality considerations that [17]

/132

$$\delta_L = \alpha \frac{\nu}{\sqrt{\tau_w/\rho}}, \qquad \nu = \frac{\mu}{\rho}; \tag{3.102}$$

where α is a dimensionless empirical constant.

The value of the constant α cannot be obtained theoretically, and must be determined from experiments. Measurements carried out by Nikuradze during the flow of water in long cylindrical tubes showed that the value of α was close to 11.5. Subsequent measurements by other authors have led to values of α lying between 10 and 13.5.

The assumption of the constancy of the shear stress in the sublayer ($\tau = \text{const} = \tau_w$) and Newton's formula (equation 3.105) for friction leads to a linear velocity distribution in the laminar sublayer:

$$u = \frac{\tau_w}{\mu} y. \tag{3.103}$$

In terms of the universal coordinates, this equation assumes the form

$$\varphi = \eta, \tag{3.30}$$

and according to equation (3.102), it is found that at the edge of the sublayer*

$$\eta_1 = \frac{\delta_1 \sqrt{\frac{\tau_w}{\rho}}}{\nu} = \alpha. \tag{3.104}$$

When flow in the turbulent boundary layer of a compressible gas is considered, it is obvious that on the basis of the same dimensional considerations a formula similar to (3.102) must be obtained. However, as a result of the variation of ρ and μ across the thickness of the sublayer, the problem remains unclear as to how the value of the viscosity and the density in this formula should be selected. It is also not clear if the empirical constant α depends on the Mach number and temperature factor. It is usually assumed that μ and ρ is equation (3.102) should be taken at some "distinguishing" temperature, or the results obtained over the entire thickness of the sublayer should be directly averaged. For example, in the papers of Wilson and van Driest to which reference has already been made, the wall temperature was selected as the characterizing temperature. /133

In the paper of L.E. Kalikhman [25] the following averaging procedure was used for the viscosity

$$\mu_{av} = \mu_w \frac{T_{av}}{T_w},$$

$$T_{av} = \frac{\int_0^{\delta_1} \rho u T \, dy}{\int_0^{\delta_1} \rho u \, dy},$$

while for the density and velocity he used

$$\rho_{av} u_{av} \delta_1 = \int_0^{\delta_1} \rho u \, dy.$$

*From equations (3.104) and (3.30) it is not difficult to obtain the relationship $\rho u_L \delta_L / \mu = \alpha$, which is why certain authors regard the quantity α^2 as a critical Reynolds number (Re_{cr}) governing the transition from laminar flow in the sublayer to turbulent flow in the core.

Examples could be given of still other methods of averaging, but it is scarcely necessary to list these at present. It is quite obvious that at present it is not possible to solve uniquely the problem how to select the "defining" temperature or the rule to be used for averaging. As mentioned above, this fact also leads to a wide variety of methods for determining the thickness of the laminar sublayer. As is always the case in such situations, the criterion for judging the validity of the selection of the "defining" temperature or the averaging rule must be comparison with experiments. However, the absence of a sufficient quantity of experimental data makes it impossible to carry out this comparison at present. Until sufficient experimental data are accumulated, the preference in selecting among the hypotheses of the "defining" temperature (or method of averaging) must obviously be given to the one which leads to the simplest results. /134

The flow in the laminar sublayer of the compressible gas can be described most simply by taking the wall temperature as the "defining" temperature. In this case the velocity profile is described by the same linear relationship (3.30) as is valid for an incompressible fluid. The experimental data given in Section 11 for velocity profiles indicate that this relationship is well satisfied at supersonic gas velocities.

The methods indicated above for taking into account the effects of compressibility and heat transfer on the parameters of the laminar sublayer by means of selecting a suitable "defining" temperature or method of averaging over the thickness of the sublayer do not make it possible to carry out a detailed analysis of the problem. Much more information on the velocity profile in the laminar sublayer can be obtained if the actual change in the gas viscosity with temperature across the sublayer can be allowed for. This has been done in the work of Czarnecki and Monta [56]. Following these authors, Newton's formula for the shear stress

$$\tau = \mu \frac{\partial u}{\partial y} \tag{3.105}$$

is written in the form

$$\tau = \tau_w \left(\frac{\mu}{\mu_w}\right) \frac{d\varphi}{d\eta}, \tag{3.106}$$

where φ and η are the universal coordinates defined by relationship (3.8).

If the assumptions are made that the shear stress is constant over the thickness of the sublayer (3.1), that there is a power dependence of viscosity on temperature (3.61), and that Crocco's integral (3.47) can be used to interrelate the temperature and viscosity, it is possible to obtain from equation (3.106) the following expression for the velocity profile in the laminar sublayer:

$$\eta = \int_0^{\varphi} \left[1 - \frac{\omega}{\zeta}\varphi - \frac{\beta}{\zeta^2}\varphi^2\right]^n d\varphi, \tag{3.107}$$

where ω, β and ζ are given by equations (3.49) and (3.8).

The results of calculations by equation (3.107) for a Mach number $M_e = 9$, Reynolds numbers $Re_x = 10^6$, 10^7 and 10^8 and two values of the temperature factor $T_w/T_e = 15.1$ (thermally insulated surface) and $T_w T_e = 2.6$ (strongly cooled surface) are shown in Fig. 28. From Fig. 28 it can be seen that on the thermally insulated plate, the compressibility has a quite feeble effect on the shape of the velocity profile: all the curves for the three Reynolds numbers fall close to the curve $\varphi = \eta$. As a result, the value of the coordinate η_L marking the edge of the laminar sublayer is close to its value in the incompressible fluid ($\eta_L = 10 - 11$). On the strongly cooled plate ($T_w/T_e = 2.6$) the velocity profiles becomes more gradual, and are appreciably displaced relative to the profile $\varphi = \eta$. In this case, the value of the coordinate η_L increases appreciably*. /136

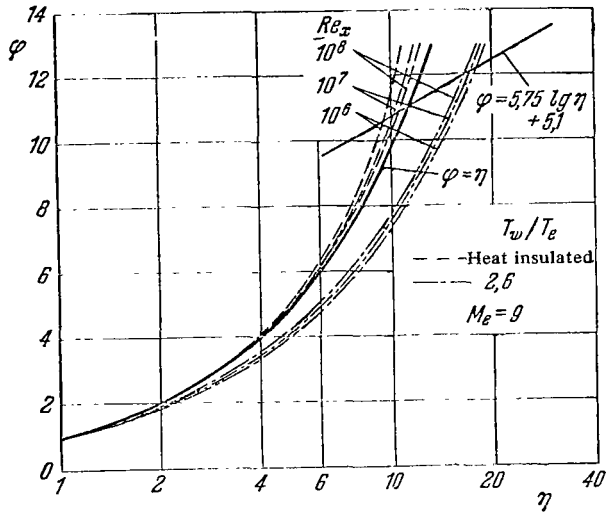

Fig. 28.

*It should be noted here that the estimation of the effect of compressibility and heat transfer on the magnitude of the coordinate η_L which is made here is not exact, since the value of the coordinate η_L was obtained in the work of Czarnecki and Monta was obtained as a result of merging the velocity profile (3.107) in the laminar sublayer with the logarithmic velocity profile for an incompressible fluid. This fact makes it impossible to make a quantitative evaluation on the basis of a similar type of analysis, but this analysis is definitely useful for explaining the tendencies and the nature of the effect of compressibility and heat transfer over the thickness of the laminar sublayer. Naturally, the establishment of quantitative relationships for the change of thickness of the laminar sublayer η_L as a function of the Mach number and temperature factor is possible only experimentally at present.

L. M. Zÿsina-Molozhen and I. A. Soskova [28] arrived at similar results, using a linear dependence of viscosity on temperature (n = 1). In this case, the velocity profile has the form

$$\eta = \varphi\left[1 - \frac{\omega}{\zeta}\frac{\varphi}{2} - \frac{\beta}{\zeta^2}\frac{\varphi^2}{3}\right], \qquad (3.108)$$

where ω and β are given by equation (3.48). Using the profile (3.108) in the laminar sublayer and the van Driest velocity profile [22] in the turbulent core, these workers were able by merging these profiles to determine the value of η_L for various values of the Mach number and temperature factor (Fig. 29, in which 2 represents the experimental data of Lobb, Winkler and Persch for $M_\infty = 5$; 1 and 3 represent the experimental data of L. M. Zÿsina-Molozhen and I. N. Soskova for $M_\infty = 1.45$ and $M_\infty = 0.2$ respectively). As can be seen from Fig. 29, the value of η_L increases markedly in the case of strong cooling*. A similar tendency was noted in the work of Lobb, Winkler and Persch (Fig. 21) as well as in the experiments of Hill, as can be seen from the same Fig. 21, which did not show this phenomenon. It follows that on thermally insulated surfaces and during heat transfer from the surface to the gas the value of η_L is close to its value for the incompressible fluid. A definite decision on the effect of heat transfer and compressibility on the parameter η_L can obviously only be made, however, after a sufficiently large quantity of experimental data has been collected. Until this problem is solved

/137

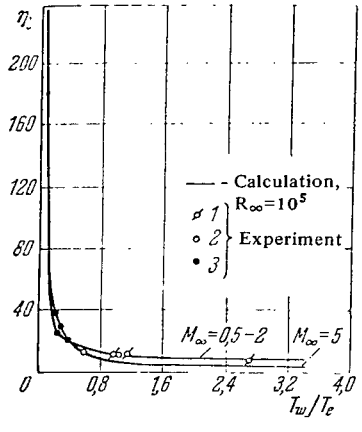

Fig. 29.

*In spite of the fact that the use of the van Driest velocity profile is more natural than the logarithmic velocity profile in an incompressible fluid, the note made earlier in connection with Fig. 28 is also valid in the present case.

experimentally it will obviously be necessary to assume for $\eta_L = \alpha$ the value of the parameters obtained in experiments with incompressible fluids, i.e., $\alpha = 11.5$.

14. Empirical methods of calculating drag on a flat plate*

This method is based on the assumption that the following functional relationship applies:

$$\frac{1}{2} c_f F_c = \psi^{**} (\mathrm{Re}^{**} F_{\mathrm{Re}^{**}}), \tag{3.109}$$

where the function ψ^{**} depends only on the Reynolds number Re^{**} formed from the momentum loss thickness, while the functions F_c and $R_{\mathrm{Re}}{}^{**}$ are such that

$$\left.\begin{aligned} F_c &= F_c\left(M_e, \frac{T_w}{T_e}\right) = 1, \\ F_{\mathrm{Re}^{**}} &= F_{\mathrm{Re}^{**}}\left(M_e, \frac{T_w}{T_e}\right) = 1 \end{aligned}\right\} \quad \text{for} \quad M_e = 0 \text{ and } \frac{T_w}{T_e} = 1. \tag{3.110}$$

The arguments leading to the relationship (3.109) are obvious if this relationship is given in the form /138

$$\left(\frac{c_f}{c_{f0}}\right)_{\mathrm{Re}^{**}} = \frac{F_{\mathrm{Re}^{**}}}{F_c}, \tag{3.111}$$

where

$$c_{f0} = 2\psi^{**}\mathrm{Re}^{**}. \tag{3.112}$$

By comparing equation (3.111) with equation (3.95) in section 12, it is seen that in contrast to (3.95), the right-hand part of (3.111) is independent of the Reynolds number Re^{**}, which takes place at sufficiently large Reynolds numbers (see the limiting formula (3.88)).

In order to establish the relationship between the friction coefficient c_f and the Reynolds number formed from the distance from the leading edge of the plate Re_x, use is made of the integral momentum equation (3.20) written in the form

$$\mathrm{Re}_x = \int_0^{\mathrm{Re}^{**}} \frac{2}{c_f} d\mathrm{Re}^{**}. \tag{3.113}$$

*See the paper by Spalding and Chi [18] discussed earlier in this chapter.

By multiplying both sides of this equation by $F_{Re^{**}}/F_c$, we have

$$\frac{F_{Re^{**}}}{F_c} Re_x = \int_0^{F_{Re^{**}}Re^{**}} \frac{2}{c_f F_c} d(F_{Re^{**}}Re^{**}). \tag{3.114}$$

By introducing the notation

$$F_{Re_x} = \frac{F_{Re^{**}}}{F_c} = F_{Re_x}\left(M_e, \frac{T_w}{T_e}\right) \tag{3.115}$$

and noting that according to (3.109) there is a unique relationship between $(c_f F_c)$ and $(F_{Re^{**}}Re^{**})$, it can be concluded that the following relationship exists

$$\frac{1}{2} c_f F_c = \psi_x (Re_x F_{Re_x}), \tag{3.116}$$

where the function ψ_x depends only on the Reynolds number Re_x, and is independent of the Mach number M_e and the temperature factor T_w/T_e, while /139

$$F_{Re_x} = F_{Re_x}\left(M_e, \frac{T_w}{T_e}\right) = 1 \quad \text{for } M_e = 0, \frac{T_w}{T_e} = 1. \tag{3.117}$$

In a similar way, it can be found that

$$\frac{1}{2} c_F F_c = \bar{\psi}(Re_x F_{Re_x}), \tag{3.118}$$

where $\bar{\psi}$ is once again independent of M_e and T_w/T_e.

Equations (3.116) and (3.118) can be represented in the form

$$\left(\frac{c_f}{c_{f0}}\right)_{Re_x} = \frac{F_{Re_x}}{F_c}, \tag{3.119}$$

$$\left(\frac{c_F}{c_{F0}}\right)_{Re_x} = \frac{F_{Re_x}}{F_c}. \tag{3.120}$$

By comparing equations (3.119) and (3.120) with their analogy (3.95), it can be seen that in contrast to (3.95), the right-hand parts of (3.119) and (3.120) are not dependent on the Reynolds number Re_x. As a result, in the present method of

calculation, the following ratios must be equal

$$\left(\frac{c_f}{c_{f0}}\right)_{Re_x} = \left(\frac{c_F}{c_{F0}}\right)_{Re_x}.$$

In order to determine the functions ψ^{**}, ψ_x and $\bar{\psi}$ the authors used the relationships

$$Re^{**} = \frac{1}{6}\zeta_0^2 + \frac{1}{\varkappa\alpha}\left[\left(2 - \frac{2}{\varkappa\zeta_0}\right)\exp(\varkappa\zeta_0) + \frac{2}{\varkappa\zeta_0} + 1 - \frac{1}{6}(\varkappa\zeta_0)^2 - \frac{1}{12}(\varkappa\zeta_0)^3 - \frac{1}{40}(\varkappa\zeta_0)^4 - \frac{1}{180}(\varkappa\zeta_0)^5\right], \quad (3.121)$$

$$Re_x = \frac{1}{12}\zeta_0^2 + \frac{1}{\varkappa\alpha}\left[(6 - \varkappa\zeta_0 + (\varkappa\zeta_0)^2\exp\varkappa\zeta_0 - 6 - 2\varkappa\zeta_0 - \frac{1}{12}(\varkappa\zeta_0)^4 - \frac{1}{20}(\varkappa\zeta_0)^5 - \frac{1}{60}(\varkappa\zeta_0)^6 - \frac{1}{252}(\varkappa\zeta_0)^7\right], \quad (3.122)$$

$$\frac{1}{2}c_{F0} = \frac{Re^{**}}{Re_x}, \quad (3.123)$$

where $\varkappa = 0{,}4$, $\alpha = 12$, $\zeta_0 = \sqrt{2/c_{f0}}$.

The form of one of the two unknown functions F_c and $F_{Re^{**}}$ (or F_{Re_x}) which determines the friction coefficient, and hence the function F_c was selected on the basis of an analysis of existing semi-empirical methods of calculation. The analysis of the semi-empirical methods carried out by the authors showed that the highest accuracy is given by the methods whose results can be represented in the form (3.111), (3.119) or (3.120), leading to the following expression for F_c: /140

$$F_c = \frac{1}{K^2}, \quad (3.124)$$

where K is expressed by equation (3.79), and the coefficients ω and β appearing in (3.79) are given by equation (3.49). In other words, the function F_c is obtained in exactly the same way as was used in the semi-empirical method proposed in Section 12.

The second unknown function $F_{Re^{**}}$ was determined empirically by using experimental data on the friction coefficient. It was assumed that the function $F_{Re^{**}}$ had the form

$$F_{Re^{**}} = \left(\frac{T_w}{T_e}\right)^p \left(\frac{T_r}{T_w}\right)^q. \quad (3.125)$$

The arguments leading to equation (3.125) were also obtained on the basis of an analysis of existing semi-empirical methods.

By using the functions $\psi_{Re^{**}}$, ψ_x, $\bar{\psi}$ and F_c determined above and numerous experimental values, the authors of this method obtained the values of p and q from the condition that the least mean-square value of the following quantity should result:

$$\frac{(c_{f,\,exp} - c_{f,\,theor})}{c_{f,\,theor}}.$$

As a result, it was found that p = -0.702, and q = 0.772. The corresponding expression for $F_{Re^{**}}$ was found to be

$$F_{Re^{**}} = \left(\frac{T_w}{T_e}\right)^{-0,702}\left(\frac{T_r}{T_w}\right)^{0,772}. \qquad (3.126)$$

In the case of flow along a thermally insulated wall, /146

$$F_{Re^{**}} = \left(\frac{T_w}{T_e}\right)^{-0,702}. \qquad (3.127)$$

Comparison of this method with the experimental data provided by this author showed that the method gives the smallest value of the mean square error (9.9%) compared with the other methods.

In order to simplify the calculations, the auxiliary functions which are required have been tabulated (Tables 9-11).

The procedure for carrying out the calculations by the proposed method reduces to the following. At given values of the Mach number M_e and the temperature factor T_w/T_e, the function F_c is determined from Table 9. The function $F_{Re^{**}}$ is then determined from equation (3.126) or Table 10, and then F_{Re_x} is found from equation (3.115). Finally, from the given value of the Reynolds number (Re^{**} or Re_x) and the previously determined functions F_{Re_x} (or $F_{Re^{**}}$) and F_c, the values of c_f and c_F are determined from Table 11.

This method of calculating friction on a flat plate in a turbulent boundary layer does not involve any new physical hypotheses. The expression for the function F_c was taken to be the same as that obtained by semi-empirical means in Section 12. The function $F_{Re^{**}}$ was determined purely empirically. On the whole, this method can be recommended as a simple engineering method of calculating friction on a flat plate.

TABLE 9. Values of the Function F_c for Various Values of M_e and T_w/T_e

T_w/T_e \ M_e	0	1	2	3	4	5	6	7
0,05	0,3743	0,4036	0,4884	0,6222	0,7999	1,0184	1,2759	1,5713
0,1	0,4331	0,4625	0,5477	0,6829	0,8628	1,0842	1,3451	1,6444
0,2	0,5236	0,5530	0,6388	0,7756	0,9584	1,1836	1,4491	1,7534
0,3	0,5989	0,6283	0,7145	0,8523	1,0370	1,2649	1,5337	1,8418
0,4	0,6662	0,6957	0,7821	0,9208	1,1069	1,3370	1,6083	1,9194
0,5	0,7286	0,7580	0,8446	0,9839	1,1713	1,4031	1,6767	1,9903
0,6	0,7873	0,8168	0,9035	1,0434	1,2318	1,4651	1,7405	2,0564
0,8	0,8972	0,9267	1,0137	1,1544	1,3445	1,5802	1,8589	2,1785
1	1,0000	1,0295	1,1167	1,2581	1,4494	1,6871	1,9674	2,2913
2	1,4571	1,4867	1,5744	1,7176	1,9130	2,1572	2,4472	2,7809
3	1,8660	1,8956	1,9836	2,1278	2,3254	2,5733	2,8687	3,2092
4	2,2500	2,2796	2,3678	2,5126	2,7117	2,9621	3,2611	3,6066
5	2,6180	2,6477	2,7359	2,8812	3,0813	3,3336	3,6355	3,9847
6	2,9747	3,0044	3,0927	3,2384	3,4393	3,6930	3,9971	4,3493
8	3,6642	3,6938	3,7823	3,9284	4,1305	4,3863	4,6937	5,0505
10	4,3311	4,3608	4,4493	4,5958	4,7986	5,0559	5,3657	5,7259
12	4,9821	5,0117	5,1003	5,2470	5,4504	5,7088	6,0204	6,3832
14	5,6208	5,6505	5,7391	5,8860	6,0898	6,3491	6,6621	7,0271
16	6,2500	6,2797	6,3683	6,5153	6,7196	6,9795	7,2937	7,6603
18	6,8713	6,9010	6,9897	7,1368	7,3413	7,6019	7,9170	8,2851
20	7,4861	7,5157	7,6045	7,7517	7,9564	8,2175	8,5334	8,9027
25	9,0000	9,0297	9,1184	9,2658	9,4711	9,7330	10,0505	10,4222
30	10,4886	10,5183	10,6071	10,7546	10,9602	11,2228	11,5415	11,9149

Table 9 (Continued)

T_{10}/T_e \ Me	8	9	10	11	12	13	14	15
0,05	1,9041	2,3738	2,6803	3,1233	3,6027	4,1186	4,6707	5,2591
0,1	1,9812	2,3552	2,7660	3,2134	3,6976	4,2180	4,7748	5,3680
0,2	2,0958	2,4756	2,8925	3,3462	3,8366	4,3636	4,9269	5,5267
0,3	2,1882	2,5723	3,9937	3,4522	3,9974	4,4782	5,0475	5,6523
0,4	2,2732	2,6569	3,0829	3,5443	4,0435	4,5794	5,1518	5,7608
0,5	2,3429	2,7336	3,1620	3,6276	4,1303	4,6697	5,2458	5,8584
0,6	2,4115	2,8049	3,2362	3,7048	4,2105	4,7531	5,3324	5,9483
0,8	2,5379	2,9360	3,3721	3,8459	4,3570	4,9051	5,4901	6,1117
1	2,6542	3,0562	3,4966	3,9748	4,4905	5,0434	5,6333	6,2599
2	3,4564	3,5725	4,0282	4,5228	5,0556	5,6263	6,2345	6,8801
3	3,5029	4,0184	4,4846	4,9904	5,5335	6,1187	6,7401	7,3993
4	3,9684	4,4290	4,9030	5,4176	5,9719	6,5653	7,1972	7,8673
5	4,3772	4,8174	5,2979	5,8196	6,3817	6,9833	7,6240	8,3033
6	4,7477	5,1905	5,6764	6,2041	6,7727	7,3814	8,0297	8,7169
8	5,4549	5,9050	6,3994	6,9368	7,5191	8,1365	8,7972	9,4977
10	6,1347	6,5904	7,0913	7,6363	8,2241	8,8539	9,5247	10,2259
12	6,7955	7,2556	7,7618	8,3123	8,9077	9,5452	10,2245	10,9449
14	7,4422	7,9058	8,4164	8,9727	9,5734	10,2174	10,9040	11,6321
16	8,0779	8,5444	9,0587	9,6194	10,2251	10,6748	11,5676	12,3026
18	8,7045	9,1737	9,6912	10,2556	10,8657	11,5204	12,2187	12,9598
20	9,3238	9,7952	10,3154	10,8832	11,4971	12,1562	12,8595	13,6059
25	10,8467	11,3225	11,8482	12,4227	13,0446	13,7128	14,4263	15,1841
30	12,3418	12,8209	13,3509	13,9305	14,5586	15,2339	15,9556	16,7225

TABLE 10. Values of the Function $F_{Re^{**}}$ for Various Values of M_e and T_w/T_e

T_w/T_e \ M_e	0	1	2	3	4	5	6	7
0,05	82,7405	93,8950	125,3092	173,1153	234,1633	306,3489	388,2642	478,9229
0,1	29,7852	33,8006	45,1092	62,3185	84,2949	110,2803	139,7684	172,4040
0,2	10,7221	12,1676	16,2385	22,4336	30,3447	39,6990	50,3142	62,0625
0,3	6,8983	6,6934	8,9323	12,3407	16,6926	21,8384	27,6779	34,1406
0,4	3,8598	4,3801	5,8456	8,0757	10,9236	14,2910	18,1123	22,3414
0,5	2,2779	3,1524	4,2071	5,8121	7,9618	10,2853	13,0355	16,0792
0,6	2,1233	2,4095	3,2157	4,4424	6,0091	7,8615	9,9636	12,2900
0,8	1,3395	1,5768	2,1043	2,9071	3,9323	5,1445	6,5201	8,0425
1	1,0000	1,1348	1,5145	2,0923	2,8301	3,7025	4,6926	5,7883
2	0,3600	0,4085	0,5452	0,7532	1,0183	1,3328	1,6892	2,0837
3	0,1980	0,2247	0,2999	0,4143	0,5604	0,7332	0,9292	1,1462
4	0,1296	0,1471	0,1963	0,2711	0,3667	0,4798	0,6081	0,7501
5	0,0933	0,1058	1,1412	0,1951	0,2639	0,3453	0,4377	0,5398
6	0,0713	0,0809	0,1080	0,1491	0,2017	0,2639	0,3345	0,4126
8	0,0466	0,0523	0,0706	0,0976	0,1320	0,1727	0,2189	0,2700
10	0,0336	0,0381	0,0508	0,0702	0,0950	0,1243	0,1575	0,1943
12	0,0257	0,0291	0,0389	0,0537	0,0726	0,0950	0,1204	0,1485
15	0,0204	0,0232	0,0310	0,0428	0,0579	0,0757	0,0959	0,1183
16	0,0168	0,0191	0,0254	0,0351	0,0475	0,0622	0,0788	0,0972
18	0,0141	0,0160	0,0214	0,0295	0,0400	0,0523	0,0662	0,0817
20	0,0121	0,0137	0,0183	0,0253	0,0342	0,0447	0,0567	0,0700
25	0,0087	0,0099	0,0132	0,0182	0,0246	0,0322	0,0408	0,0503
30	0,0066	0,0075	0,0101	0,0139	0,0188	0,0246	0,0312	0,0385

Table 10 (Continued)

T_w/T_e \ M_e	8	9	10	11	12	13	14	15
0,05	577,5949	683,7162	796,8344	916,5768	1042,629	1174,722	1312,620	1456,116
0,1	207,9243	246,1261	286,8467	329,9519	375,3286	422,8793	472,5207	524,1767
0,2	74,8492	88,6012	103,2599	118,7770	135,1119	152,2295	170,0993	188,6946
0,3	41,1745	48,7395	56,8032	65,3392	74,3250	83,7414	93,5716	103,8009
0,4	26,9444	31,8949	37,1718	42,7577	48,6380	54,8000	61,2328	67,9268
0,5	19,3920	22,9549	26,7527	30,7729	35,0050	39,4398	44,0696	48,8873
0,6	14,8221	17,5454	20,4482	23,5210	26,7557	30,1455	33,6842	37,3665
0,8	9,6995	11,4816	13,3812	15,3920	17,5088	19,7271	22,0428	24,4525
1	6,9808	8,2634	9,6305	11,0777	12,6012	14,1977	15,8643	17,5986
2	2,5130	2,9747	3,4668	3,9878	4,5362	5,1109	5,7109	6,3352
3	1,3824	1,6364	1,9071	2,1937	2,4954	2,8115	3,1416	3,4850
4	0,9046	1,0708	1,2480	1,4355	1,6330	1,8398	2,0553	2,2809
5	0,6511	0,7707	0,8982	1,0332	1,1752	1,3241	1,4796	1,6413
6	0,4976	0,5891	0,6862	0,7897	0,8983	1,0121	1,1309	1,2545
8	0,3256	0,3855	0,4493	0,5168	0,5878	0,6623	0,7401	0,8210
10	0,2344	0,2774	0,3233	0,3719	0,4231	0,4767	0,5326	0,5909
12	0,1791	0,2121	0,2471	0,2843	0,3234	0,3643	0,4071	0,4516
14	0,1427	0,1690	0,1969	0,2265	0,2576	0,2903	0,3244	0,3598
16	0,1172	0,1388	0,1617	0,1860	0,2116	0,2384	0,2664	0,2955
18	0,0985	0,1167	0,1359	0,1564	0,1779	0,2004	0,2239	0,2484
20	0,0844	0,0999	0,1164	0,1339	0,1523	0,1716	0,1917	0,2127
25	0,0607	0,0719	0,0838	0,0964	0,1096	0,1235	0,1380	0,1531
30	0,0464	0,0549	0,0640	0,0737	0,0838	0,0944	0,1055	0,1170

TABLE 11. Values of the Functions $F_{c^c f}$, $F_{c^c F}$, $F_{Re^{**}Re^{**}}$ and $F_{Re_x Re_x}$

$F_{c^c f}$	$F_{c^c F}$	$F_{Re^{**}Re^{**}}$	$F_{Re_x Re_x}$	$F_{c^c f}$	$F_{c^c F}$	$F_{Re^{**}Re^{**}}$	$F_{Re_x Re_x}$
0,0010	0,001117	$2,878 \cdot 10^7$	$5,758 \cdot 10^{10}$	0,0060	0,008205	233,0	$5,679 \cdot 10^4$
0,0015	0,001716	$3,955 \cdot 10^5$	$4,610 \cdot 10^8$	0,0065	0,009105	177,6	$3,901 \cdot 10^4$
0,0020	0,002333	$5,425 \cdot 10^4$	$4,651 \cdot 10^7$	0,0070	0,010012	140,4	$2,796 \cdot 10^4$
0,0025	0,002967	$1,386 \cdot 10^4$	$9,340 \cdot 10^6$	0,0075	0,011014	114,4	$2,078 \cdot 10^4$
0,0030	0,003621	5030	$2,778 \cdot 10^6$	0,0080	0,012016	95,62	$1,592 \cdot 10^4$
0,0035	0,004299	2233	$1,062 \cdot 10^6$	0,0085	0,01304	92,49	$1,251 \cdot 10^4$
0,0040	0,005006	1208	$4,828 \cdot 10^5$	0,0090	0,01409	73,91	$1,006 \cdot 10^4$
0,0045	0,005747	716,0	$2,492 \cdot 10^5$	0,0095	0,01516	62,55	$8,253 \cdot 10^3$
0,0050	0,006526	462,3	$1,417 \cdot 10^5$	0,0100	0,01624	55,87	$6,883 \cdot 10^3$
0,0055	0,007345	319,4	$8,697 \cdot 10^4$	0,0105	0,01732	50,46	$5,826 \cdot 10^3$

15. Relationship between friction and heat transfer on a flat plate (Reynolds' analogy). Recovery coefficient.

According to Fourier's law, the specific heat flux between a gas and wall can be represented in the form:

$$q_w = \left(\lambda \frac{\partial T}{\partial y}\right)_w. \tag{3.128}$$

By converting this equation from temperatures to enthalpies $\left(h = \int_0^T c_p dT\right)$, and carrying out some simple rearrangements, it is found that /147

$$q_w = \left(\frac{\lambda}{c_p}\frac{\partial h}{\partial y}\right)_w = \frac{\tau_w}{\mathrm{Pr}}\frac{h_e}{U_e}\left(\frac{\partial \bar{h}}{\partial \bar{u}}\right)_w. \tag{3.129}$$

Here

$$\bar{h} = \frac{h}{h_e}, \quad \bar{u} = \frac{u}{U_e}. \tag{3.130}$$

In order to determine the derivative $(\partial \bar{h}/\partial \bar{u})$, we return to the energy equation in terms of Crocco's variables, equation (2.65) [22]. In the present case of flow along a flat plate placed at zero angle of attack $(dp/d\xi = 0)$, and assuming a a homogeneous gas $(\partial c_i/\partial u = 0)$, this equation assumes the form

$$\rho u(\mu + \varepsilon)\frac{\partial h}{\partial \xi} + \left(1 - \frac{1}{\mathrm{Pr}_m}\right)\tau\frac{\partial \tau}{\partial u}\frac{\partial h}{\partial u} - \tau^2\left[1 + \frac{\partial}{\partial u}\left(\frac{1}{\mathrm{Pr}_m}\frac{\partial i}{\partial u}\right)\right] = 0. \tag{3.131}$$

Here $\mathrm{Pr}_m = \mathrm{Pr}$ in the laminar sublayer, and $\mathrm{Pr}_m = \mathrm{Pr}_T$ in the turbulent core (see equations (1.103 and 2.33)).

A further simplifying assumption is made that the enthalpy h is a function only of the velocity u and is independent of the longitudinal coordinate ξ, i.e., $h = h(u)$. As a basis for this assumption it can be pointed out it is exactly satisfied if the Prandtl number and its turbulent analog are equal to unity. This is satisfied if the Prandtl number and its turbulent analog are equal to unity. This is the case when the Crocco integral occurs. Consequently, it can be expected that for small deviations of the Prandtl number and its turbulent analog from unity, the dependence of the enthalpy on the longitudinal coordinate will be insignificant. If this assumption is made $(\partial h/\partial \xi = 0)$, (3.131) can be rewritten as

$$\left(\frac{\bar{h}'}{\mathrm{Pr}_m}\right)' + (1 - \mathrm{Pr}_m)\frac{\bar{\tau}'}{\bar{\tau}}\left(\frac{\bar{h}'}{\mathrm{Pr}_m}\right) = -\frac{U_e^2}{h_e}. \tag{3.132}$$

Here

$$\bar{\tau} = \frac{\tau}{\tau_w},$$

and the primes denote derivatives with respect to the dimensionless velocity $\bar{u}$. The boundary conditions for equation (3.132) are of the form /148

$$\left.\begin{aligned} \bar{h} &= \bar{h}_w \quad \text{at} \quad \bar{u} = 0, \\ \bar{h} &= 1 \quad \text{at} \quad \bar{u} = 1. \end{aligned}\right\} \tag{3.133}$$

By integrating equation (3.132) once, it is found that

$$\frac{h_1}{\mathrm{Pr}_m} = \exp\left\{-\int_1^{\bar{\tau}}(1-\mathrm{Pr}_m)\frac{d\bar{\tau}}{\bar{\tau}}\right\} \times \left[\left(\frac{\bar{h}'}{\mathrm{Pr}_m}\right)_w - \frac{U_e^2}{h_e}\int_0^{\bar{u}}\exp\left(\int_1^{\bar{\tau}}(1-\mathrm{Pr}_m)\frac{d\bar{\tau}}{\bar{\tau}}\right)d\bar{u}\right]. \tag{3.134}$$

Integration of (3.134) leads to the relationship

$$\bar{h}(\bar{u}) = \bar{h}_w + \frac{(\bar{h}')_w}{\mathrm{Pr}_m S(\bar{u})} - \frac{U_e^2}{h_e} R(\bar{u}), \tag{3.135}$$

where

$$S(\bar{u}) = \left\{\int_0^{\bar{u}}\mathrm{Pr}_m \exp\left[-\int_1^{\bar{\tau}}(1-\mathrm{Pr}_m)\frac{d\bar{\tau}}{\bar{\tau}}\right]d\bar{u}\right\}^{-1}, \tag{3.136}$$

$$R(\bar{u}) = \int_0^{\bar{u}}\mathrm{Pr}_m \exp\left[-\int_1^{\bar{\tau}}(1-\mathrm{Pr}_m)\frac{d\bar{\tau}}{\bar{\tau}}\right] \times \left\{\int_0^{\bar{u}}\exp\left[\int_1^{\bar{\tau}}(1-\mathrm{Pr}_m)\frac{d\bar{\tau}}{\bar{\tau}}\right]d\bar{u}\right\}d\bar{u}. \tag{3.137}$$

Bearing in mind the second of the boundary conditions (3.133), an expression is obtained from equation (3.134) for the derivative $(\bar{h}')_w$ which is required for determining the heat flux:

$$(\bar{h}')_w = \mathrm{Pr}_m S(1)\left[1 - \bar{h}_w + \frac{U_e^2}{h_e} R(1)\right]. \tag{3.138}$$

Substituting the expression (3.138) into the expressions (3.134) and (3.129), it is found that /149

$$\bar{h}(\bar{u}) = \bar{h}_w - (\bar{h}_w - 1)\frac{S(1)}{S(\bar{u})} + \frac{U_e^2}{h_e}\left[\frac{S(1)}{S(\bar{u})}R(1) - R(\bar{u})\right], \tag{3.139}$$

$$q_w = -\tau_w S(1)\left[h_e + 2R(1)\frac{U_e^2}{2} - h_w\right]\frac{1}{U_e}. \tag{3.140}$$

The quantity

$$H_r = h_e + 2R(1)\frac{U_e^2}{2} \tag{3.141}$$

is usually termed the equilibrium enthalpy of a thermally insulated surface, or the recovery enthalpy. The factor

$$r = 2R(1), \tag{3.142}$$

which appears the expression for the equilibrium enthalpy (3.141) is termed the recovery coefficient. The recovery coefficient characterizes the difference between the value of the equilibrium enthalpy H_r and the enthalpy of adiabatic and isentropic retardation of the gas, $H_e = h_e + U_e^2/2$, or in other words, it characterizes the non-adiabaticity of the flow processes in the boundary layer.

Now we introduce the dimensionless heat transfer coefficient (Stanton number):

$$c_h = \frac{q_w}{\rho_e U_e (H_r - h_w)}. \tag{3.143}$$

Then, using the expression for the local friction coefficient c_f (equation (2.85)), the following expression is obtained from equation (3.140):

$$\frac{2c_h}{c_f} = S(1). \tag{3.144}$$

The quantity S(1) is termed the Reynolds analogy parameter.

Thus, in order to calculate the local flux density q_w it is necessary to know the recovery coefficient r, the Reynolds analogy parameter S(1), and the local friction coefficient c_f: /150

$$q_w = \frac{c_f}{2}\rho_e U_e S(1)\left(h_e + r\frac{U_e^2}{2} - h_w\right). \tag{3.145}$$

The recovery coefficient. It follows from equations (3.142) and (3.137) that the general expression for the recovery coefficient for variable Prandtl number Pr_m is

$$r = 2\int_0^1 Pr_m \exp\left[-\int_1^{\bar{\tau}} (1 - Pr_m)\frac{d\bar{\tau}}{\bar{\tau}}\right] \times \left\{\int_0^{\bar{u}} \exp\left[\int_1^{\bar{\tau}} (1 - Pr_m)\frac{d\bar{\tau}}{\bar{\tau}}\right] d\bar{u}\right\} d\bar{u}. \tag{3.146}$$

If the generalized Prandtl number Pr_m can be regarded as constant over the boundary layer cross-section, equation (3.146) can be considerably simplified, and after some rearrangements assumes the form

$$r = 2\,Pr_m \int_0^1 \bar{\tau}^{-Pr_m+1}\left(\int_0^{\bar{u}} \bar{\tau}^{-Pr_m+1} d\bar{u}\right) d\bar{u}. \tag{3.147}$$

When the generalized Prandtl number is equal to unity ($Pr_m = 1$), which means that in the two-layer Prandtl model for the turbulent boundary layer the Prandtl number Pr is constant and equal to unity in the laminar sublayer while its turbulent analog Pr_T is constant and equal to unity in the turbulent core, the recovery factor becomes equal to unity (r = 1), as follows from equation (3.147). In this case the equilibrium enthalpy of the heat insulated surface is equal to the enthalpy of an adiabatic and isentropic retardation of the gas: $H_r = H_e$. Thus it is only when $Pr = Pr_T = 1$ that the motion in the boundary layer can be compared with adiabatic motion.

When $Pr_m = \text{const} \neq 1$, it can be seen from equation (3.147) that to determine the recovery coefficient it is necessary to know the distribution of the shear stresses across the boundary layer $\bar{\tau} = \bar{\tau}(\bar{u})$.

At present, (as already noted in Section 10), there is only a very small amount of information available on the nature of this distribution even in the case of the flow of incompressible fluids. According to the experimental data of Klebanoff which is shown in Fig. 2, the dependence of the shear stress on the transverse coordinate is close to linear and can be described approximately by equation (3.2). The dependence of the shear stress on velocity in the turbulent core of the boundary layer can be given approximately in the form shown in Fig. 3 and described by equation (3.5). As can be seen from Fig. 3, for a value of $\zeta_0 = 30$ and the range of velocities $0 \leqslant \bar{u} \leqslant 0.8$, the shear stress varies in the range $0.9 \leqslant \bar{\tau} \leqslant 1$, which makes it possible to assume approximately that the shear stress in the boundary layer is constant and equal to its value at the wall. If this assumption is made, then within the framework of the two-zone model, equation (3.147) leads to the following expression for the recovery coefficient

$$r = Pr_T - (Pr_T - Pr)\,\bar{u}_L^2. \tag{3.148}$$

/151

where $\bar{u}_L$ is the dimensionless velocity at the edge of the laminar sublayer defined by equation (3.31). It should be noted that in obtaining equation (3.148) the integration interval $0 \leqslant \bar{u} \leqslant 1$ was divided into two zones: $0 \leqslant \bar{u} < \bar{u}_L$ for the laminar sublayer, where $Pr_m = Pr$, and $\bar{u}_L \leqslant \bar{u} \leqslant 1$ for the turbulent core, where $Pr_m = Pr_T$*.

Unfortunately, up to the present time there are no sufficiently reliable data on the turbulent Prandtl number. Attempts to determine the value of Pr_T directly from velocity and temperature profile measurements during the flow of air in tubes and channels have led to values of Pr_T which are a little smaller than unity. However, in the case of heat transfer to liquid metals, values of the turbulent Prandtl number $Pr_T > 1$ are found. This difference of Pr_T from unity is obviously caused by different effects of the process of molecular transport within the turbulent transport elements (the ultimate packets of the gas which take part in turbulent mixing) on the mechanisms of momentum and heat transport. The certain degree of ambiguity in the value of Pr_T is sometimes used to obtain better agreement between theory and experiment by means of a suitable choice of the value of the Prandtl number. Until there is a final experimental solution of the problem of what the value of Pr_T really is, it follows that its value must be taken as unity, as has been done by several investigators. /152

Assuming that $Pr_T = 1$ in the expression for the recovery coefficient (3.148), it is found that**

$$r = 1 - (1 - Pr)\,\bar{u}_L^2. \tag{3.149}$$

For Prandtl numbers close to unity and over the range of velocities at the edge of the laminar sublayer from $\bar{u}_L = 0.2$ to 0.8, equation (3.149) can be replaced simple formula to an accuracy of ± 10%:

$$r = 1 - (1 - Pr)\,\bar{u}_L^2 \simeq Pr^{1/3}. \tag{3.150}$$

---

*It is appropriate to note here that differences of the Prandtl number from unity leads within the two-layer model of the turbulent boundary layer leads to the situation that the thicknesses of the dynamic and thermal sublayers appear to be different. To allow strictly for this difference leads to important difficulties arising in the calculation of heat transfer, but this does not appear to be necessary at Prandtl numbers which do not differ too much from unity. In this connection it can be noted that heat transfer calculations based on the Prandtl two-layer model of the boundary layer usually leads to satisfactory results at Prandtl numbers close to unity. At Prandtl number which are significantly different from unity, the more complicated three-layer model due to von Kármán gives better results. For a discussion of this, and also for information on the calculation of heat transfer at very small values of the Prandtl number, see [57].

**The first expression for the recovery coefficient analogous to equation (3.149) was obtained by M. F. Shirokov [58].

When Pr = 0.72 (air), equation (3.150) leads to a value of the recovery coefficient r = 0.895, which is in good agreement with the experimental data, as will be shown below.

Apart from the use of the two-layer model and these very simplest assumptions as to the shear stress distribution in the boundary layer, attempts have been made to compute recovery coefficients using the more complicated von Kármán three-layer model [59]. /153

It may be noted that according to this model [60] the velocity profile in the turbulent boundary layer of an incompressible fluid is divided into three zones: 1) the laminar sublayer, in which

$$\varphi = \eta \text{ for } 0 \leqslant \eta \leqslant 5; \tag{3.151a}$$

2) the transition (buffer) zones, within which

$$\varphi = 5\left[1 + \ln\frac{\eta}{5}\right] \text{ for } 5 \leqslant \eta \leqslant 30; \tag{3.151b}$$

3) the completely turbulent region:

$$\varphi = 5{,}5 + 2{,}5 \ln \eta \text{ for } \eta \geqslant 30. \tag{3.151c}$$

In the work of van Driest which is being considered [59] the shear stress is assumed to be constant and equal to the value at the wall in the forst two zones. In the third zone the shear stress distribution is taken to be of the form (3.5). The final formula obtained by van Driest for calculating the recovery coefficient is

$$\begin{aligned} r = \mathrm{Pr}_T\Bigg[1 + \frac{2}{\varkappa}\sqrt{\frac{c_{f0}}{2}}(1 - \mathrm{Pr}_T)\left\{\frac{\pi^2}{6} + \frac{3}{2}(1 - \mathrm{Pr}_T)\right\} + \\ 25\,\frac{c_{f0}}{2}\left\{\frac{\mathrm{Pr}}{\mathrm{Pr}_T} - 1 + 2\ln\left[1 + \frac{5}{6}\left(\frac{\mathrm{Pr}}{\mathrm{Pr}_T} - 1\right)\right] + \right. \\ \left. (\ln 6)\ln\left[1 + \frac{7}{8}\left(\frac{\mathrm{Pr}}{\mathrm{Pr}_T} - 1\right)\right] - (\ln 6)\ln\left[1 + \frac{1}{4}\left(\frac{\mathrm{Pr}}{\mathrm{Pr}_T} - 1\right)\right]\right\}\Bigg] \end{aligned} \tag{3.152}$$

As follows from what has been said above, this equation is valid for the case of flow of incompressible fluids. As van Driest showed, equation (3.152) can be generalized to cover the case of motion of a compressible gas (without heat transfer) if we introduce instead of c_{fo} the quantity c_f multiplied by the factor $(1 + r\frac{\gamma - 1}{2}M_e^2)$, where c_f is taken to be the local friction coefficient for the compressible gas. When calculations were carried out by equation (3.152) it appeared that if the friction coefficient for an incompressible stream, c_{fo}, was used and a value of the turbulent Prandtl number of 0.86 was assumed, then for the Reynolds number range $10^5 \leqslant \mathrm{Re}_x \leqslant 10^8$, the /154

recovery coefficient would be a constant quantity equal to 0.88. The value of the Prandtl number was assumed equal to 0.71.

The attempt to take into account the effect of compressibility on the value of r in equation (3.152) by introducing into this equation the friction coefficient c_f for the compressible stream and the multiplier $(1 + r\frac{\gamma-1}{2}M_e^2)$ on c_f gives a value of the recovery coefficient which is only slightly dependent on the Mach number (for $0 < M_e < 5$) (see Fig. 30). Two calculated curves are given in Fig. 30. The first curve (1) was calculated for wind tunnel conditions (stagnation temperature $T_e^* = 311^\circ K$). Van Driest explains the difference between these curves as being due to the different natures of the changes in the molecular Prandtl number in the wind tunnel and in free flight.

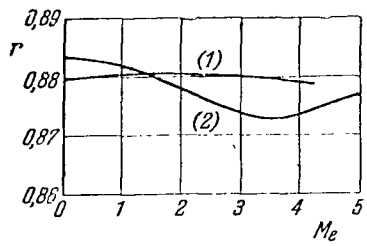

Figure 30.

Experimental data on the recovery coefficient. The first measurements of the recovery coefficient were made more than a quarter century ago. In a paper by L. Crocco, published in 1941 [61], it was shown as a result of experimental investigations of turbulent boundary layers in supersonic streams that the recovery coefficient varied over the range 0.91-0.98, with a noticeable dependence of r on the Mach number M_e. /155

Later a whole series of experimental investigations were made to determine the recovery coefficient. The results of some of these investigations carried out in the years 1949-1952 are shown in Table 12, which is taken from the paper by Kaye [62]. /156

More precise measurements of the recovery coefficient have been made in the course of the last 10-15 years.

The experiments of Pappas [54]. In these experiments, measurements were made of the surface temperatures of thermally insulated plates and the Mach number at the outer edge of the boundary layer. The recovery coefficients were calculated from the formula

$$r = \frac{T_r}{T_e^*}\frac{1 + 0{,}2M_e^2}{0{,}2M_e^2} - \frac{1}{0{,}2M_e^2}, \qquad (3.153)$$

TABLE 12.

Author	Year	Model	$Re_x \cdot 10^{-6}$	M_e	r
Uimbrou	1949	cone, paraboloid	2,7 4,8 —	2 1,5 2,0	0,885 ± 0.008 0,902 ± 0.005 0,894 ± 0,008
Stolder, Rubezin, Tendelend	1950	plate	7	2,4	(0,884÷0,897) ± ±0,007
Khilton	1951	plate	10	2,0	0,830 ± 0.004
Éber	1952	cone, cone-cylinder	1,0 0,25	2,87 4,25	0,92 0,97
Klirs, Sternberg	1952	cone, cone-cylinder	7	2÷3,4	0,882 ± 0,007
Sléḱ	1952	plate	3	2,4	0,906
Staŷn, Sherer	1952	10° cone, 40° cone-cylinder	0,4÷4 0,3÷1	2÷3,8 3÷3,8	0,882 ± 0.008 0,885 ± 0,011

where T_e^* is the temperature of the adiabatically and isentropically retarded gas. Measurements were carried out at Mach numbers of $M_e = 1.69$ and 2.27. The Reynolds number varied from 10^6 to 10^7. The results of the measurements are shown in Figs. 31 and 32. As can be seen from the figures, the recovery coefficient decreases as the Reynolds number increases from about 0.90 to 0.89; in most of the experiments the points fall close to the value 0.89.

The experiments of Shoulberg, Hill & Rivas [63]. In these experiments, measurements were made of the recovery coefficient on a flat plate in a wind tunnel. The measurement procedure and method of calculation were the same as in the work of Pappas considered above. Measurements were carried out over the following ranges of the Mach and Reynolds numbers: $1.9 \leqslant M_e \leqslant 3.14$ and $4 \cdot 10^6 \leqslant Re_x \leqslant 17 \cdot 10^6$. The experimental results are shown in Figs. 33 and 34. It can be seen from Fig. 33 that as the Reynolds number increases the recovery coefficient slowly decreases. Although this decrease is only about 0.5% over this range of the Reynolds number, there is nevertheless quite a clear tendency for r to decrease. As regards the effect of the Mach number on the recovery coefficient, Fig. 34 shows that there is no effect

/157

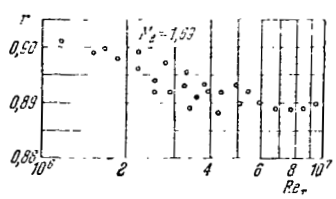

Figure 31.

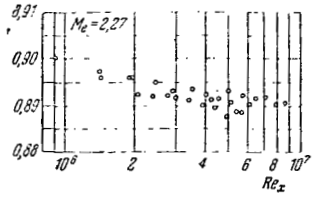

Figure 32.

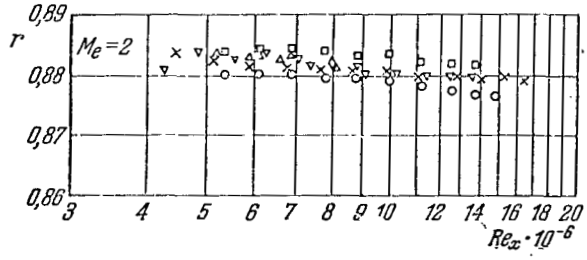

Figure 33.

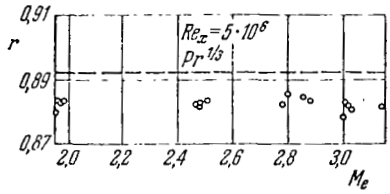

Figure 34.

/158

of M_e over the range investigated. The values of the measured recovery coefficients (Fig. 33) were about 1% smaller than the values calculated by equation (3.150), in which the Prandtl number was determined at the wall temperature $T_w = T_r$.

The experiments of Tendeland [64]. Measurements were carried out on the surface of a cylinder model with a conical front (cylinder diameter was 2 inches, cylinder length was 14.75 inches, and the cone had an included angle of 20°) during the flow past the model of air at Mach numbers $M_\infty = 3$, 3.44, 4.08, 4.56 and 5.04. The local Reynolds numbers calculated on the basis of 1 foot (Re_x/foot) were respectively 3×10^6, 4×10^6, 3.6×10^6, 2.8×10^6 and 2.3×10^6. The recovery coefficients were calculated from the values of the temperature measured along the model under equilibrium conditions. After making corrections for the relatively small radiation losses

to the cool side walls of the wind tunnel using the local temperature values, the local values of the Mach number M_e and the values of the stagnation temperatures were used for determining the local values of the recovery coefficients.

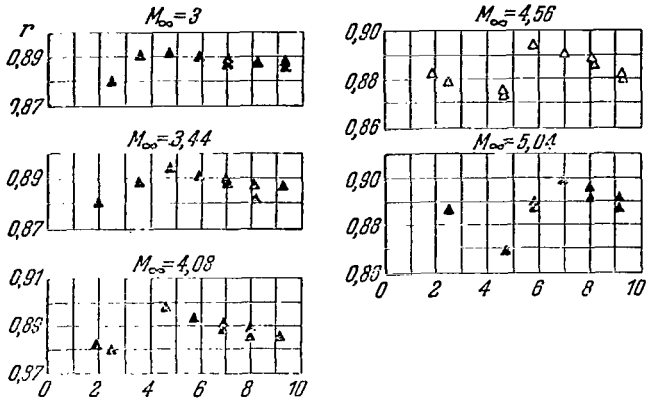

Figure 35.

The measured results are shown in Fig. 35. The distance from the nose of the model (in diameters) is plotted along the abscissa. On considering these graphs it can be seen that for $M_\infty = 3.00$, 3.44 and 4.08, the recovery coefficients vary from about 0.88 to 0.89, while the value of r for the conical section was rather smaller than the value of r for the cylindrical part of the model. For $M_\infty = 4.56$ and 5.04 the value of r close to the junction of the nose and cylindrical section fell appreciably. /159 This phenomenon was explained by the author as being caused by the presence of a considerable pressure drop at the junction and a temperature gradient along the model axis which led to a reduction in temperature, and, as a result of this, to considerable errors in determining r for the junction region.

The experiments of Adcock, Peterson & McRee [65]. This work presents the results of an experimental investigation of the turbulent boundary layer on a cylinder at a Mach number $M_e = 6$ and at Reynolds numbers (formed from the distance from the leading edge) in the range $5 \leqslant Re_x \cdot 10^{-6} \leqslant 33$. The dependence of the recovery coefficient on the distance from the leading edge of the model is shown in Fig. 36. As in the case of the work by Pappas and Shoulberg et al., a tendency for the value of r to decrease with increase of the Reynolds number is observed. In the range of Reynolds numbers investigated the values of the recovery coefficients fell in the range $0.875 \leqslant r \leqslant 0.895$.

In summarizing the experimental data of the various authors given above, the conclusion can be reached that the recovery coefficient depends very slightly on the local Reynolds number Re_x and is independent of the Mach number. Over the range

of Reynolds and Mach numbers investigated (up to $M_e = 6$), the values of the recovery coefficient fell in the range $0.88 \leqslant r \leqslant 0.90$. It may be mentioned that there is satisfactory agreement between the Van Driest formula (3.152) and the experimental data over the range of Mach numbers being considered. /160

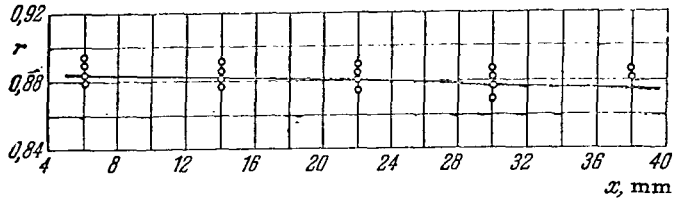

Figure 36.

In order to develop a sufficiently reliable theoretical method for calculating the recovery coefficients at supersonic velocities it is necessary to carry out detailed experimental investigations of the structure of the laminar sublayer and the transitional (buffer) layer, and also of the shear stress distribution in turbulent boundary layers at these velocities.

Until a satisfactory theory for calculating recovery coefficients is set up and experimental data are obtained at high supersonic velocities, it can be assumed in practical calculations that $0.88 \leqslant r \leqslant 0.90$.

Parameter of the Reynolds analogy. A general expression for the coefficient of the Reynolds analogy can be seen from equations (3.144) and (3.136) to have the form

$$\frac{2c_h}{c_f} = \left\{\int_0^1 \mathrm{Pr}_m \exp\left[-\int_1^{\bar{\tau}} (1 - \mathrm{Pr}_m)\frac{d\bar{\tau}}{\bar{\tau}}\right] d\bar{u}\right\}^{-1}. \qquad (3.154)$$

If the generalized Prandtl number Pr_m is constant, equation (3.154) becomes

$$\frac{2c_h}{c_f} = \left(\mathrm{Pr}_m \int_0^1 \bar{\tau}^{\mathrm{Pr}_m - 1} d\bar{u}\right)^{-1}. \qquad (3.155)$$

When the generalized Prandtl number is equal to unity ($\mathrm{Pr}_m = 1$), then the use of the assumption

$$\mathrm{Pr} = \mathrm{Pr}_T = 1$$

within the framework of the two-layer Prandtl model reduces equation (3.155) to the classical expression for the Reynolds analogy

$$c_h = \frac{1}{2} c_f. \tag{3.156}$$

When $Pr_m = \text{const} \neq 1$, it is necessary in order to determine the parameter of the Reynolds analogy to be given the shear stress distribution in the boundary layer $\bar{\tau}(\bar{u})$, just as in the case of determining the recovery coefficient r. With the assumption (3.1) ($\tau = \text{const} = \tau_w$) and using the two-layer model for the turbulent boundary layer, the following expression is obtained from equation (3.155) for the Reynolds analogy parameter: /161

$$\frac{2c_h}{c_f} = [Pr_T - (Pr_T - Pr)\bar{u}_L]^{-1}. \tag{3.157}$$

If the turbulent Prandtl number is taken to be unity ($Pr_T = 1$), equation (3.157) assumes the form

$$\frac{2c_h}{c_f} = [1 - (1 - Pr)\bar{u}_L]^{-1}. \tag{3.158}$$

For changes of $\bar{u}_L$ in the range 0.4 to 0.9 and Prandtl numbers close to unity, equation (3.158) can be replaced (to within an accuracy of ± 10%) by the much simpler formula

$$\frac{2c_h}{c_f} = [1 - (1 - Pr)\bar{u}_L]^{-1} \approx Pr^{-2/3}. \tag{3.159}$$

When Pr = 0.72, equation (3.159) gives a value of $2c_h/c_f = 1.24$. Using the same assumptions which were used in obtaining equation (3.152) for the recovery coefficient, Van Driest [59] obtained the following parameter for the Reynolds analogy parameter:

$$\frac{2c_h}{c_f} = \frac{1}{Pr_T}\left[1 + 5\sqrt{\frac{c_f}{2}}\left\{\frac{1}{5\varkappa}(1 - Pr_T)\left[\frac{\pi^2}{6} + \frac{3}{2}(1 - Pr_T)\right] + \frac{Pr}{Pr_T} - 1 + \ln\left[1 + \frac{5}{6}\left(\frac{Pr}{Pr_T} - 1\right)\right]\right\}\right]^{-1}. \tag{3.160}$$

As the author noted, this formula is valid for $0.7 \leqslant Pr_T \leqslant 1$. As in the calculation of r using equation (3.152), it is recommended that a value of the turbulent Prandtl number of 0.86 he used in this equation.

In order to allow for the effects of compressibility and heat transfer on the Reynolds analogy parameter, Van Driest suggests that it is necessary to introduce

a multiplier $(T_w/T_e)\left(1 + r\frac{\gamma-1}{2}M_e^2\right)$, on c_f, while c_f itself is taken to be the local friction coefficient in the compressible gas.

The results of calculating the quantity $2c_h/c_f$ from formula (3.160) for the conditions in a wind tunnel ($T_e^* = 338^\circ K$, curve 1) and free flight conditions ($T_e = 500^\circ K$, curve 2) and various values of the Mach number are shown in Fig. 37. Figure 38 shows the results of calculations by equations (3.157), (3.158), (3.159) and (3.160) as functions of the Reynolds number in incompressible fluid streams. /162

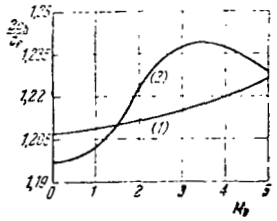

Figure 37.

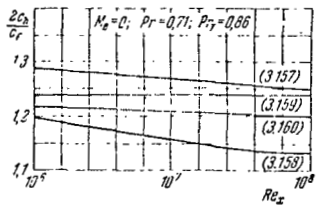

Figure 38.

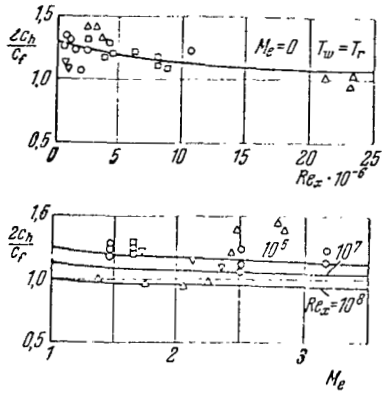

Figure 39.

In order to evaluate the accuracy of the formulas given above, let us now turn our attention to experimental data.

Experimental data on the Reynolds analogy parameter $2c_h/c_f$. The experimental data on heat transfer and friction obtained by various authors up to 1954 were evaluated by Seiff [68]. By analyzing the results of his evaluation (see Fig. 39), Seiff

concluded that in the turbulent boundary layer the experimental data could be represented as follows with an accuracy of 15-20%: /163

$$\frac{2c_h}{c_f} = \mathrm{Pr}^{-0,57} \qquad (3.161)$$

or

$$\frac{2c_h}{c_f} = 1,22.$$

It should be noted that the experimental data used by Seiff were obtained over the range of Mach numbers $0 \leqslant M_e \leqslant 4$.

As a result of the small number of experimental data and their low accuracy, Seiff was not able to establish a relationship between the Reynolds analogy parameter $2c_h/c_f$ and the Reynolds number, Mach number and temperature factor.

Quite recently on the basis of analyzing experiments on the direct and simultaneous measurement of the local values of the heat flux and friction, L. V. Kozlov [66] proposed the following more accurate dependence of the Reynolds analogy parameter on the parameters mentioned above:

$$\frac{2c_{hw}}{c_{fw}} = \mathrm{Pr}_w^{-0,57}\, 0,695\, \mathrm{Re}_{xw}^{0,09-0,01 \lg \mathrm{Re}_{xw}} \left(\frac{T_r}{T_e}\right)^{-0,09}. \qquad (3.162)$$

With $T_r/T_e = 1$, $M_e = 0$ and $Re_{xw} = 4.73 \times 10^6$, equation (3.162) reverts to equation (3.161), which is well confirmed by numerous experiments on the flow of incompressible fluids in pipes and over flat plates.

Equation (3.162) was obtained by L. V. Kozlov over the following ranges of the parameters: $1.7 \leqslant M_e \leqslant 4$; $5 \times 10^5 < Re_{xw} < 2 \times 10^7$; $0.5 \leqslant T_w/T_r \leqslant 1$. The effects of the individual parameters on the ratio $2c_h/c_f$ can be seen from Fig. 40, where, as in Fig. 39, all the curves were obtained by calculation from equation (3.162) with c_h and c_f determined for the conditions at the edge of the boundary layer.

From a consideration of Figs. 40 and 39 it follows that as the Mach and Reynolds numbers increase the quantity $2c_h/c_f$ decreases, and approaches a value close to /164 unity. The fact that at large Mach numbers the Reynolds analogy parameter is close to unity is also indicated by the experimental data obtained by Hill on a flat plate for $8 \leqslant M_e \leqslant 10$ (Fig. 41). As can be seen from Fig. 41, the value of the parameter $2c_h/c_f$ lies in the range $0.9 \leqslant 2c_h/c_f \leqslant 1.1$.

The review of the experimental and theoretical data shows that in spite of certain advances in this field, the problem of the relationship between heat transfer and friction in general requires further theoretical and experimental work.

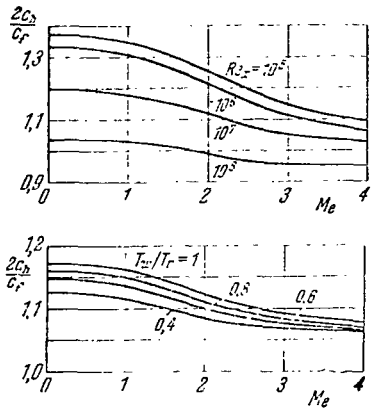

Figure 40.

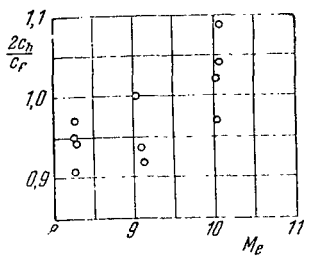

Figure 41.

16. The turbulent boundary layer on a cone at zero angle of attack.

Apart from flow close to a flat plate, the simplest case for theoretical analysis is flow along a cone placed at zero angle of attack, as long as the angle of the cone vertex is such that the leading shock wave remains attached (Fig. 42). In this case the motion of the gas after the shock wave is "conical", and the pressure on the surface of the cone is constant. This fact relates the flow in the boundary layer on a cone to the flow near a flat plate. As Van Driest has shown [67], there is a simple approximate rule for converting the local friction coefficient on a plate into the corresponding coefficient on a cone. /165

In order to establish this rule, let us turn our attention to the integral momentum relationship (2.80). In the case of flow along a cone with an impermeable surface ($v_w = 0$) this relationship assumes the form

$$\frac{d\delta^{**}}{dx} + \frac{\delta^{**}}{x} = \frac{\tau_w}{\rho_e U_e^2}. \qquad (3.163)$$

Here it must be remembered (see Fig. 42) that $r_w = x \sin \theta$; θ is the half-angle of the cone. Equation (3.163) is easily transformed to the form

$$\mathrm{Re}_x \, d\,\mathrm{Re}_x = \frac{\rho_e}{\rho_w} \zeta^2 d\,(\mathrm{Re}^{**}\,\mathrm{Re}_x). \tag{3.164}$$

where the parameter ζ is given by equation (3.8), and the Reynolds numbers Re_x and Re** are defined by equations (3.18) and (3.17).

If it is assumed that the mechanisms of flow in the boundary layers around a cone and plate are the same (both are gradientless flows, i.e., dp/dx = 0), it can be expected that the functional relationships for the velocity profile and momentum loss thickness on these bodies will also be the same. In this case, equation (3.152) can be used for the Reynolds number Re**, since this was obtained for the flat plate. If the rougher approximation is used (as in Section 12), i.e., if the second term on the right side of equation (3.52) is discarded, we have

$$\mathrm{Re}^{**} = \frac{e^{-\varkappa x}}{f\varkappa^2} \cdot \frac{\mu_w}{\mu_e} \exp\left[\varkappa \zeta I\,(1)\right]. \tag{3.165}$$

After substituting Eq. (3.165) into equation (3.164) and carrying out the integration to the same degree of accuracy as in Section 12, an equation analogous to equation (3.57) is obtained for the cone:

$$C_1 \frac{e^{-\varkappa x}}{f\varkappa^3} \frac{\mu_w}{\mu_e} \frac{\rho_e}{\rho_w} \zeta^2 \exp\left[\varkappa \zeta I\,(1)\right] = \frac{1}{2} \mathrm{Re}_x. \tag{3.166}$$

Since the parameter ζ is equivalent to the local friction coefficient c_f (see equation (3.81)), it follows from a comparison of equations (3.166) and (3.57) that there is a simple rule according to which the local friction coefficient for a cone is equal to the value of this coefficient for a flat plate calculated at a Reynolds number Re_x equal to a half of this number for the cone, and the same values of the temperature factor and Mach number at the outer edge of the boundary layer. /166

If the local friction coefficients on a cone and plate are compared at the same values of the Reynolds number and the same values of the temperature factor and Mach number at the outer edge of the layer, it is found that these coefficients are 10-15% higher for the cone than for the flat plate.

An analysis of the relationships between the local and averaged friction coefficients on a cone and plate by means of the integral momentum relationship and power relationships for the velocity profile and resistance law was carried out by Bradfield [69]. As a result, the following relationship was obtained

$$\frac{c_{fc}}{c_{fpl}} = \left[\frac{2\,(n+2)}{n+1}\right]^{\frac{2}{n+3}}, \tag{3.167}$$

where 1/n is the exponent on the expression for the velocity profile $u/U_e = (y/\delta)^{1/n}$. When n = 7, equation (3.167) gives $c_{fc}/c_{fpl} = 1.18$, and when n varies over the range from 5 to 10, the ratio c_{fc}/c_{fpl} varied from 1.13 to 1.23.

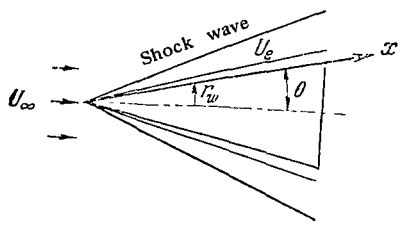

Figure 42.

For the mean friction coefficient it was found that /167

$$c_{Fc}/c_{Fpl} = 2\left[\frac{n+1}{2(n+2)}\right]^{\frac{n-1}{n+3}}. \qquad (3.168)$$

When $5 < n < 10$, it follows from equation (3.168) that $1.035 < c_{Fc}/c_{Fpl} < 1.065$; when n = 7, $c_{Fc}/c_{Fpl} = 1.05$.

Apart from this analysis, Bradfield's paper also gives the measured results for the local friction coefficients on a cone with a half-angle of 15° at a Mach number $M_e = 3.7$ and various values of the Reynolds number. The measured results are shown in Fig. 43 (open circles); the solid circles indicate the results obtained by Coles [36] on a flat plate under the same conditions, and the dashed line represents the relationship $c_{fc} = 1.18c_{fpl}$. As can be seen from Fig. 43, the friction on the cone is about 28% higher than that on the plate. Obviously both Van Driest's rule and Bradfield's relationship (3.167) lead to friction values on the cone which are rather lower than those actually prevailing.

Obviously more detailed conclusions on this problem can only be reached after further experimental data become available.

17. The turbulent boundary layer in the presence of a longitudinal pressure drop.

The problem of calculating the turbulent boundary layer in the presence of an arbitrary distribution of the longitudinal velocity at the outer edge of the layer includes a particularly difficult part of this problem - the determination of the position /168 of the point (or line) of separation. Even in the case of the flow of an incompressible fluid this is far from being completely solved. (See, for instance, [70]).

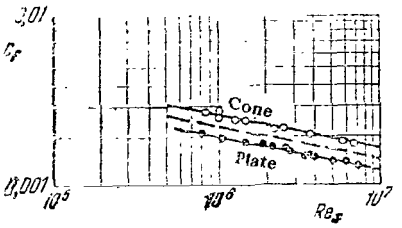

Figure 43.

The presence of compressibility and heat transfer effects between the gas and wall complicate this problem still further, leading to additional difficulties whose nature was described in the previous sections. Existing methods of calculating turbulent boundary layers in high-velocity gas streams in the presence of longitudinal pressure drops and heat transfer between the gas and wall are usually generalizations and further developments of the methods for calculating turbulent boundary layers in incompressible liquids. A characteristic of most of these methods is the use of integral relationships (for momentum, energy, and moment of momentum). Usually the number of unknowns in these integral relationships exceeds the number of equations. In these methods it is therefore very important to select a family of velocity and temperature profiles which can be used for substitution in the integral relationships instead of the actual other unknowns. Under the present state of the theory, this selection presents a difficult problem. Apart from applying the Prandtl-von Kármán semi-empirical theory of turbulence, it is sometimes possible to use for describing velocity fields power-law type formulas with constant [30] or variable exponents depending on various parameters.

A detailed development of a semi-empirical method of calculating turbulent boundary layers in a gas in the presence of heat transfer and an arbitrary pressure distribution in the external stream has been given in the monograph by L. E. Kalikhman [71]. In this method, which is based on applying the formulas of Prandtl's semi-empirical theory, calculation of friction and heat transfer in the boundary layer is reduced to solving the linear differential equations, which are approximately equivalent to the integral relationships for momentum and energy; auxiliary tables and graphs are used to convert the functions found to those required (i.e., the friction and heat transfer coefficients). /169

Another method of calculating turbulent boundary layers on curvilinear surfaces which is essentially similar to the semi-empirical method is due to S.S. Kutateladze and A.I. Leont'ev [72]; this is based on applying the limiting laws for friction and heat transfer.

The work of McLafferty and Barber [73] and Sasman and Cresci [74] can be mentioned as examples of the semi-empirical approach to the present problem. In the latter of these papers the Ludwieg-Tillmann empirical formula from the theory of turbulent boundary layers in incompressible fluids is used as the resistance law to establish the relationship between the resistance coefficient and the momentum loss thickness δ^{**} and the form parameter $H^* = \delta^*/\delta^{**}$. The generalization of this formula

to the case of flow with variable density was accomplished by the method of a defining temperature proposed by Eckert [75]. In the work of Sasman and Cresci the characteristics of the turbulent boundary layer were obtained on the basis of simultaneously solving the integral relationships for the momentum and moment of momentum.

Of the other methods proposed for calculating turbulent boundary layers in the presence of longitudinal pressure drops, mention can be made of the method developed by V.M. Ievlev [23, 76].

Leaving the details to the original sources, it can be mentioned that the feature characteristic of most of the methods is the use of single-parametric families of velocity profiles. This fact is obviously one of the main reasons leading to the unsatisfactory nature of these methods of calculating boundary layers in the zones before separation. The development of two- and multi-parametric methods is in its early stages at present. /170

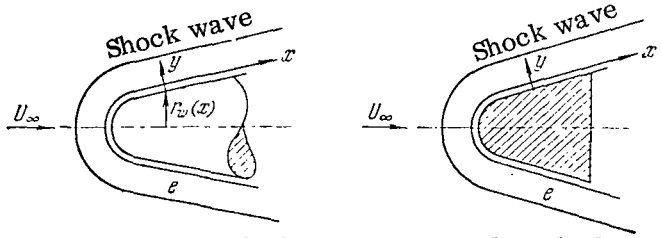

Axisymmetric body Plane body

Figure 44.

On evaluating the state of this problem as a whole, it can be stated that the existing methods for calculating turbulent boundary layers in supersonic gas streams with arbitrary pressure distributions in the external stream and heat transfer between the gas and wall lead to more or less satisfactory results only in cases when the longitudinal pressure drop does not have a large effect on the form of the velocity profile.

Bearing in mind what has been said above, we will confine ourselves here to a discussion of the method of calculation, in which allowance is made for the effect of the longitudinal pressure drop on friction only by means of the integral momentum relationship, while the direct effects of the pressure drop on the velocity profile are neglected. The assumptions made, as shown by the experiments, are approximately valid for flows with negative or small positive pressure gradients. The last limitation means essentially that pre-separation and separated flows have to be excluded from our consideration. /171

Methods of calculation based on linearization of the integral momentum relationship. Let us consider the flow along a curvilinear surface of a steady gas stream (Fig. 44). A curvilinear system of coordinates is used. The position of a point in the stream is characterized by the coordinate x measured along the surface from the stagnation point, and a coordinate y measured normal to the surface.

Let us now return to the integral momentum relationship (2.80), which is the case of flow near an impermeable surface ($v_w = 0$) assumes the form

$$\frac{d\delta^{**}}{dx} + \frac{U_e'}{U_e}(2 + H^* - M_e^2)\delta^{**} + \frac{(r_w^{\nu})'}{r_w^{\nu}}\delta^{**} = \frac{\tau_w}{\rho_e U_e^2}. \tag{3.169}$$

Later it is convenient to write equation (3.169) in rather different form, which is obtained after eliminating from the equation M_e^2 by means of equation (2.79). Omitting the simple rearrangements, it is found finally that

$$\frac{1}{\rho_e U_e}\frac{d}{dx}(\rho_e U_e \delta^{**}) + \delta^{**}\left[\frac{U_e'}{U_e}(1 + H^*) + \frac{(r_w^{\nu})'}{r_w^{\nu}}\right] = \frac{1}{\zeta^2}\frac{\rho_w}{\rho_e}. \tag{3.170}$$

Here ζ is given by equation (3.8).

Following the example used in the work of L. E. Kalikhman to which reference was made earlier in this Section, a new variable is introduced:

$$z = \rho_e U_e \delta^{**} \zeta^2. \tag{3.171}$$

The first term in the left-hand part of equation (3.170) can be rearranged using equation (3.171) to the form

$$\frac{1}{\rho_e U_e}\frac{d}{dx}(\rho_e U_e \delta^{**}) = \frac{1}{\rho_e U_e \zeta^2 A}\frac{dz}{dx}. \tag{3.172}$$

The notation is then introduced

$$A = \frac{d\ln z}{d\ln(\rho_e U_e \delta^{**})} = 1 + \frac{2}{\dfrac{d\ln(\rho_e U_e \delta^{**})}{d\ln\zeta}}. \tag{3.173}$$

By using equation (3.172), the integral momentum relationship (3.170) becomes /172

$$\frac{dz}{dx} + A\left[\frac{U_e'}{U_e}(1 + H^*) + \frac{(r_w^{\nu})'}{r_w^{\nu}}\right] z = \rho_w U_e A. \tag{3.174}$$

It is appropriate to note that the differential equation (3.174) for the function z is as exact as the initial equation (3.169).

Before passing on to the problem of considering the integration of equation (3.174), it is necessary to establish the dependence of the parameters A and H* which appear in this equation on the unknown function z. In order to establish this relationship it is necessary to have a resistance "law", i.e., a relationship between the momentum loss thickness δ^{**} and the friction ζ. Since we are here considering only flows in which the direct effect of the longitudinal pressure gradient on the shape of the velocity profile is small, it is obvious that it is possible to use as the resistance law the one established in Section 12 for the flat plate (3.52). It is only necessary to bear in mind that the parameters $U_e(x)$, $\omega(x)$, $\beta(x)$, etc., at the outer edge of the boundary layer will be variable quantities in the case now being considered. The "rough" expression for the resistance law is used, as in Section 12, neglecting for sake of simplicity the second term in the square brackets in equation (3.52). In order to compensate for the error introduced by this approximation, a constant C_1 is introduced in the resistance law; a suitable choice of this constant makes the results obtained more precise (it should be mentioned that von Kármán used a similar approach in deriving the resistance formula (3.59)). The resistance law transformed in this way has the form

$$\delta^{**} = C_2 \frac{\mu_w}{\rho_e U_e} \exp[\varkappa\zeta I(1)], \quad C_2 = C_1 \frac{e^{-\varkappa\alpha}}{f\varkappa^2}. \tag{3.175}$$

where the quantity I(1) is given by equation (3.54), and ω and β, which appear in equation (3.54) are given by equations (3.48) and (3.49).

By substituting the expression for the momentum loss thickness (3.175) into equation (3.174), a relationship is obtained between the function z and the friction parameter ζ: /173

$$z = C_2 \mu_w \zeta^2 \exp[\varkappa\zeta I(1)]. \tag{3.176}$$

As equation (3.176) shows, the dependence of the friction parameter ζ on the function z is essentially logarithmic, which makes it possible to confine our attention to approximate methods of evaluating the function z(x). In consequence, in calculating the parameter H* it is possible to use the expression for the flat plate (3.55), which is satisfactory within the limits of the approximate approach being used here.

The expression for the function A, equation (3.173) assumes the following form after substituting the resistance law (3.175) into it:

$$A = 1 + \frac{1}{\varkappa\zeta I(1)}. \tag{3.177}$$

The dependence of the functions H* and A on the friction parameter ζ, and consequently through equation (3.176) on the unknown function z, leads to the integration of the very complex non-linear equation (3.174) in order to establish this function. There are grave difficulties in integrating this equation exactly, and this is not necessary, as will be shown below. Simplifications can be effected as a result of the fact that the functions H* and A depend only very slightly on the friction parameter ζ. This fact makes it possible to confine our attention to the approximate determination of H* and A at values of the parameter ζ calculated from the formula for the flat plate (Section 12). As regards the parameters β and ω (see equations (3.48), (3.49)), on which (together with the parameter ζ) H* and A depend, their values can be evaluated at each cross-section of the boundary layer from the local values of the Mach number M_e and the temperature factor T_w/T_e. Thus, before starting the integration of equation (3.174), the functions A and H* can be regarded as known functions of the longitudinal coordinate x.

This approximate method of determining the parameters A and H* should not lead to appreciable errors in the determination of the function z(x) using equation (3.174), according to the evaluations carried out below. /174

Let us determine the value of the parameter A for the case of flow of an incompressible fluid along a flat plate under isothermal conditions. By noting that in this case I(1) = 1 and using the resistance formula (3.80), it is found from equation (3.177) that

$$A = 1 + \frac{2}{\varkappa\zeta_0} = 1 + 3.54\sqrt{c_{f0}} = 1 + 0.575\mathrm{Re}_x^{-1/14}. \qquad (3.178)$$

It follows from equation (3.178) that as the Reynolds number changes by two orders of magnitude (from 10^5 to 10^7), the value of A will change by 6% (from 1.25 to 1.18). In the general case of flow of a compressible gas in the presence of heat transfer between the gas and the wall, the variation of the parameter A will not be too great under real conditions.

The results of calculating the parameter H* according to equation (3.55) for the case of flow of an air stream along a flat plate with

$$M_e = 1.69, \quad T_w/T_e = 1.66 \text{ and } M_e = 2.27, \quad T_w/T_e = 2.15$$

are shown in Fig. 27. The experimental points obtained by Pappas for these same flow conditions are also shown. It is clear from Fig. 27 that the parameter H* depends only very slightly on the Reynolds number, and consequently on the friction parameter ζ. The fact that H* depends only feebly on the parameter ζ is well confirmed by experimental data in the case of flow of an incompressible liquid along a flat plate. Thus, the measurements of Schlutz-Grunow [77] and Hama [78] on smooth plates showed that as the parameter ζ_0 varied from 18-30, the parameter H* changed from 1.5 to 1.25. The results of applying equation (3.55) to the flow of an incompressible fluid also gives satisfactory agreement with the experimental data.

The results of this analysis for determining the parameters H* and A can be represented in the form /175

$$\left.\begin{aligned} H^*\left[M_e, \frac{T_w}{T_e}, \zeta\left(M_e, \frac{T_w}{T_e}, \mathrm{Re}_x\right)\right] \\ \approx H^*\left[M_e, \frac{T_w}{T_e}, \zeta_{\mathrm{pl}}\left(M_e, \frac{T_w}{T_e}, \mathrm{Re}_x\right)\right], \\ A\left[M_e, \frac{T_w}{T_e}, \zeta\left(M_e, \frac{T_w}{T_e}, \mathrm{Re}_x\right)\right] \\ \approx A\left[M_e, \frac{T_w}{T_e}, \zeta_{\mathrm{pl}}\left(M_e, \frac{T_w}{T_e}, \mathrm{Re}_x\right)\right]. \end{aligned}\right\} \quad (3.179)$$

In these equations the subscript pl indicates that the quantities on which it appears are determined from the formulas obtained for flow along flat plates.

If the approximate method of determining the parameters H* and A given in equation (3.179) is used, the problem of determining the function z(x) is reduced to integrating the following linear, 1st-order differential equation with variable coefficients:

$$\frac{dz}{dx} + P(x)z = Q(x), \quad (3.180)$$

where

$$P(x) = A\left[\frac{U_e'}{U_e}(1 + H^*) + \frac{(r_w^{\nu})'}{r_w^{\nu}}\right], \quad Q(x) = \rho_w U_e \zeta. \quad (3.181)$$

On integrating equation (3.180) it is found that

$$z = \exp\left[-\int_{x_t}^{x} P(x)\,dx\right]\left\{\int_{x_t}^{x} Q(x)\exp\left[\int_{x_t}^{x} P(x)\,dx\right]dx + C\right\}. \quad (3.182)$$

Here x_t is the coordinate of the point of transition from a laminar to a turbulent boundary layer. The integration constant C is determined as usual from the condition that the values of the momentum loss thickness δ^{**} at the transition point must match. As a result, it is found that /176

$$\begin{aligned} z = \exp\left[-\int_{x_t}^{x} P(x)\,dx\right] \\ \times\left\{\int_{x_t}^{x} Q(x)\exp\left[\int_{x_t}^{x} P(x)\,dx\right]dx + \rho_{et}U_{et}\zeta_t\delta_t^{**}\right\}, \end{aligned} \quad (3.183)$$

in which the parameters ζ_t and δ_t^{**} are to be determined from laminar boundary layer theory.

If the laminar section is absent ($\delta_t^{**} = 0$ when $x_t = 0$), equation (3.183) can be somewhat simplified to

$$z = \exp\left[-\int_0^x P(x)\,dx\right]\int_0^x Q(x)\exp\left[\int_0^x P(x)\,dx\right]dx. \qquad (3.184)$$

The quadratures appearing in equations (3.183) and (3.184) can be obtained numerically or by graphical integration.

In the flow along a flat plate at zero angle of attack ($dU_e/dx = 0$, $\nu = 0$), equation (3.184) can be converted by applying (3.181) and 3.177) to

$$z = \rho_e U_e \int_0^x A\,dx = \rho_e U_e \int_0^x \left[1 + \frac{2}{\varkappa\zeta} I(1)\right]dx. \qquad (3.185)$$

In the case of the flow of an incompressible fluid the expression (3.178) can be used for A, after which the integral in the right-hand side of equation (3.185) can be easily evaluated, giving

$$z_0 = \rho_e U_e x\,(1 + 0{,}62\,\mathrm{Re}_x^{-1/14}). \qquad (3.186)$$

As the Reynolds number (Re_x) varies from 10^5 to 10^7, the expression in round brackets in equation (3.186) changes from 1.27 to 1.20. As a result, to a sufficiently high degree of accuracy it can be assumed that

$$z_0 = 1{,}24\rho_e U_e x. \qquad (3.187)$$

Once equation (3.183) (or equation (3.184)) has been used to determine the distribution of the parameter z(x) over the surface of the body, it is possible to find from equation (3.176) the dependence of the friction parameter ζ on the longitudinal coordinate, and then to find the friction coefficient $c_f(x)$ by means of equation (3.8). However, it is inconvenient to use equation (3.176) directly, due to the necessity of solving a logarithmic equation. In order to simplify the process of calculating the friction it is necessary to carry out certain transformations on equation (3.176). /177

By taking logarithms of equation (3.176) and converting from ζ to c_f using equation (3.8), it is found that

$$\varkappa\sqrt{2}(\lg e)\left(\frac{\rho_w}{\rho_e}\right)^{1/2} I(1)\,c_f^{-1/2} + 2\lg(c_f^{-1/2}) = C_3 + \lg\left(\frac{\rho_e}{\rho_w}\frac{z}{\mu_w}\right),$$
$$C_3 = \lg C_2.$$

By carrying out some simple operations in this equation and introducing the notation

$$K = \left(\frac{\rho_w}{\rho_e}\right)^{1/2} I(1), \tag{3.188}$$

it is found that

$$\frac{0{,}242K}{\sqrt{c_f}} + 2\lg\frac{1}{\sqrt{c_f}} = C_3 + \lg\left(\frac{\rho_e}{\rho_w}\frac{z}{\mu_w}\right). \tag{3.189}$$

The value of the constant C_3 is determined from the condition that equation (3.189) must agree with von Kármán's formula (3.59) for a flat plate in an incompressible fluid. By making use of equation (3.187) and carrying out this matching of equations (3.189) and (3.59), it is found that $C_3 = 0.30$. Equation (3.189) can then be reduced to an equation with one parameter. If both sides of this equation are divided by two, and lg (0.121K) is added to both sides, it is found that

$$N + \lg N = -0{,}767 + \lg\left(K\sqrt{\frac{\rho_e}{\rho_w}\frac{z}{\mu_w}}\right), \tag{3.190}$$

where

$$N = \frac{0{,}121K}{\sqrt{c_f}}. \tag{3.191}$$

If equation (3.191) is rearranged to extract c_f, it is found that /178

$$c_f = \left(\frac{0{,}121K}{N}\right)^2. \tag{3.192}$$

The determination of the function N from equation (3.190) when the right-hand part is known can be carried out with tables of logarithms to base ten.

A still greater simplfication of the calculation procedure can be achieved by replacing the left side of equation (3.190) by a simpler approximate expression. Calculations show that over the range of values of N from 1 to 4 (which in flow over a flat plate corresponds to the following changes in the Reynolds number, Mach number and temperature factor: $10^5 \leqslant \mathrm{Re}_x \leqslant 10^8$; $0 \leqslant M_e \leqslant 10$; $0.1 \leqslant T_w/T_r \leqslant 1$) it is possible to represent the left-hand side of equation (3.190) with sufficient accuracy by

$$N + \lg N = 0{,}15 + 1{,}2N. \tag{3.193}$$

The maximum error involved in this approximation is 5% at N = 1, and the mean error varies from 2 to 1%.

By using equation (3.193), the following expression is obtained after some computation for the friction coefficient instead of equation (3.192):

$$c_f = \left[\frac{0{,}145K}{\lg\left(0{,}242K\sqrt{\frac{\rho_e}{\rho_w}\frac{z}{\mu_w}}\right)}\right]^2. \qquad (3.194)$$

In concluding the discussion of this method of calculation, it can be noted that one of the functions which govern the friction (N) is related to z by a relationship which is close to logarithmic. This fact justifies the approximate method assumed here for determining z on the basis of linearizing the integral momentum relationship.

To conclude, a brief list of the main steps in the calculation according to this procedure is given below:

1. The quantities $\beta(x)$ and $\omega(x)$ are determined from equations (3.48) and (3.49) for the given parameters of the external stream ($M_e(x)$ and $T_e(x)$) and the conditions at the wall (T_w). The recovery coefficient r in equation (3.49) can be assumed equal to 0.89. /179

2. From the known values of $\beta(x)$ and $\omega(x)$ and the local value of Reynolds number $Re_x = U_e\rho_e x/\mu_e$ and equation (3.85), the local friction coefficient on a plate $c_{f\,pl}$ is calculated, from which the friction parameter $\zeta_{pl}(x)$ is obtained by using equation (3.8). In passing, the functions required subsequently are also determined: I(1) (equation (3.54)) and K(x) (equation (3.79)). The ratio of densities ρ_w/ρ_e is determined from equation (3.50), and the viscosity μ from equation (3.61).

3. The values of H*(x) and A(x) are determined from the known values of $\beta(x)$, $\omega(x)$ and $\zeta_{pl}(x)$ using equations (3.55) and (3.177).

4. The coefficients P(x) and Q(x) are calculated from equation (3.181). To do this the values of $U_e(x)$, $U'_e(x)$, $r_w(x)$ and $r'_w(x)$ must be known.

5. The function z(x) is calculated from relationship (3.183) (or (3.184) if the laminar and transitional zones of the boundary layer are absent). The quadratures appearing in equation (3.183) (or (3.184)) are determined numerically, or by graphical integration.

6. The distribution of the local friction coefficient $c_f(x)$ along the surface of the body is then calculated from equation (3.194). If the friction coefficient is to be determined from the more precise formula (3.192), it is necessary in advance to calculate the function N(x) from equation (3.190) from the known value of

the right-hand side. The solution of equation (3.190) is carried out by using tables of logarithms to base ten.

The following quantities must be given in the form of initial data: $U_e(x)$, $U'_e(x)$, $r_w(x)$, $r'_w(x)$, $T_e(x)$ and T_w. Instead of the quantities $U_e(x)$ and $U'_e(x)$, it is possible to give the Mach number at the outer edge of the boundary layer $M_e(x)$ and its derivative with respect to the longitudinal coordinate, $M'_e(x)$, which are related to the velocities through equation (2.83).

From the distribution $c_f(x)$ obtained as a result of the calculations it is possible to derive the friction coefficient evaluated on the basis of the parameters of the approaching stream:

$$c_{f\infty} = \frac{2\tau_w}{\rho_\infty U_\infty^2} = c_f \frac{\rho_e}{\rho_\infty}\left(\frac{U_e}{U_\infty}\right)^2. \qquad (3.195)$$

The method of successive approximations. On the basis of the same initial premises as in the previous method, i.e., considering only the flow with an averaged longitudinal pressure drop, the following method of calculation can be proposed on the basis of a simple transformation of the integral momentum relationship to a form which makes it possible to calculate the friction by the method of successive approximations. A similar transformation was first used in the work of K.K. Fedyaevskiĭ and A.S. Ginevskiĭ [79] for calculating friction in a turbulent boundary layer of an incompressible fluid; it was then used by Yu.V. Lapin for calculating friction in compressible gases [80]. /180

Let us return to the momentum equation (3.170). By introducing into this equation the new variables

$$\theta = \rho_e U_e \delta^{**} e^{\Omega}, \qquad \Omega = \int_{x_l}^{x} \left[\frac{U'_e}{U_e}(1 + H^*) + \frac{(r_w^\nu)'}{r_w^\nu}\right] dx, \qquad (3.196)$$

it is converted to the form

$$\frac{d\theta}{dx} = \frac{e^{\Omega}}{\zeta^2}\rho_w U_e. \qquad (3.197)$$

By integrating equation (3.197) and then converting from θ to δ^{**}, it is found that

$$\rho_e U_e \delta^{**} = e^{-\Omega}\left(\int_{x_l}^{x} \frac{e^{\Omega}}{\zeta^2}\rho_w U_e dx + \rho_{el} U_{el} \delta_l^{**}\right), \qquad (3.198)$$

where the subscript t denotes parameters at the transition point from a laminar to a turbulent layer, so that the quantity δ_t^{**} is determined from laminar boundary layer theory.

On substituting the equation for the momentum loss thickness (3.175) into the left part of (3.198), it is found then that /181

$$C_2\mu_w \exp[\varkappa\zeta I(1)] = e^{\Omega}\left(\int_{x_t}^{x} \frac{e^{\Omega}}{\zeta^2}\rho_w U_e dx + \rho_{et}U_{et}\delta_t^{**}\right). \qquad (3.199)$$

When logarithms are taken in (3.199) and a conversion from ζ to c_f is made by using equation (3.8), the following relationship is obtained after several simple rearrangements:

$$\frac{0{,}242K}{\sqrt{c_f}} = C_3 + E, \qquad (3.200)$$

where K is given by equation (3.79) and the function E, which itself involves the unknown friction coefficient c_f, has the form

$$E = \lg\left[\frac{e^{-\Omega}}{\mu_w}\left(\frac{1}{2}\int_{x_t}^{x} e^{\Omega}\rho_e U_e c_f dx + \rho_{et}U_{et}\delta_t^{**}\right)\right]. \qquad (3.201)$$

The value of the constant C_3 can be taken to be the same as in the previous section, i.e., $C_3 = 0.3$. Bearing this in mind, it is not difficult to obtain from relationship (3.200) the following expression for the friction coefficient:

$$c_f = \left(\frac{0{,}242K}{0{,}3 + E}\right)^2. \qquad (3.202)$$

When the laminar and transitional zones of the boundary layer are absent ($x_t = 0$, $\delta_t^{**} = 0$) the expression for the function E is simplified and assumes the form

$$E = \lg\left(\frac{1}{2}\frac{e^{-\Omega}}{\mu_w}\int_0^x c_f\rho_e U_e e^{\Omega}dx\right). \qquad (3.203)$$

The exponent Ω, which is given by the second of the equations in (3.196), contains the parameter $H^* = \delta^*/\delta^{**}$. As in the previous method the calculation of this parameter can be carried out by equation (3.55).

Equation (3.202) makes it possible to use the method of successive approximations for calculating friction. As the zeroth approximation for the friction coefficient c_f it is natural to take the value of this coefficient for the

flat plate, i.e., $c_f^{(0)} = c_{f\ pl}$. The calculation of $c_{f\ pl}$ for given parameters at the outer edge of the boundary layer can be carried out by the method discussed in Section 12. After determining $c_f^{(0)}(x)$, the following quantities are determined in turn: $\zeta^{(0)}(x)$ by means of equation (3.8), $H^{*(0)}$ from equation (3.55) $\Omega^{(0)}(x)$ from equation (3.196), $E^0(x)$ from equation (3.201) (or (3.203)), $c_f^{(1)}(x)$ from equation (3.202), etc. /182

The fact that the unknown function c_f occurs in the right-hand side of equation (3.203) within the integral and logarithm signs ensures that the iteration process usually converges rapidly.

In conclusion, it can be noted that as the calculations have shown, both the methods proposed in the present Section for calculating turbulent boundary layers (the method based on linearization of the integral momentum relationship, and the method of successive approximations) lead to similar results. Tests of the use of these methods for calculating friction coefficients in the pre-separation zone of flow showed that in these cases the friction coefficients are appreciably overestimated.

18. The turbulent layer on a sphere

Among the bodies with various shapes of the front sections, the greatest interest to engineers and investigators centers around bodies with spherical surfaces. This interest arises because of the wide occurrence of blunt shapes in practical structures in aviation equipment. One of the main advantages of blunt bodies over pointed shapes is that the specific heat flux to a blunt body is significantly smaller than on a sharp body. For laminar flow conditions in the boundary layer in the neighborhood of the forward stagnation point, the heat flux to the wall appears to be inversely proportional to the square root of the radius of curvature: $q_w \sim 1/\sqrt{R}$.

At present the problem of flow in a laminar boundary layer in the neighborhood of the forward stagnation point of a blunt body at supersonic velocities has been studied very thoroughly both experimentally and theoretically. /183

Much less work has been done on turbulent flow on blunt bodies along which supersonic streams flow. This is explained by the fact that at the forward stagnation point and in its immediate vicinity the flow conditions in the boundary layer always remain laminar because of the small values of the Reynolds number. If the laminar nature of the flow is also retained further along the flow contour, the maximum value of the heat flux is reached at the forward stagnation point. However, the existing experimental data show that the laminar nature of the flow in the boundary layers on blunt bodies is not always retained further away. In particular, the experimental data of Stetson [81] indicate the possibility of a transition of the laminar layer into a turbulent one in the neighborhood of the sonic point (line) (the sonic point (line) is the name given to the point (or line) at which the velocity at the outer edge of the boundary layer becomes equal to the local velocity of sound). In this case, the maximum heat flux occurs in the

vicinity of the sonic point (line). This is the reason for the existence of particular interest in turbulent boundary layers on blunt bodies.

Of the wide class of bodies with blunt shapes, the flow patterns close to bodies with spherical surfaces have been most studied. A schematic representation of the flow picture close to a sphere is given in Fig. 45. During the flow of a supersonic stream around a spherical body a detached shock wave is formed ahead of it. In passing through the shock wave in the neighborhood of the forward stagnation the stream is slowed down to zero velocity, and is then accelerated close to the body, reaching the local velocity of sound at some line (the sonic line). Experiments and theoretical calculations show that the sonic line occurs close to the point with the angular coordinate $\vartheta = 45°$. /184

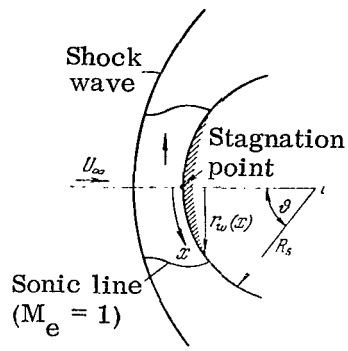

Figure 45.

Theoretical calculations of the flow close to the forward stagnation point on a sphere have been carried out in particular by Li Ting-Yi and Geiger [82]; experimental studies have been made by Korobkin and Gruenewald [83]. As a result of the investigation of Li Ting-Yi and Geiger it was found that the velocity gradient of the external stream at the forward stagnation point on a sphere is

$$\beta_s = \left(\frac{dU_e}{dx}\right)_s = \frac{U_\infty}{R_s}\sqrt{\frac{\rho_\infty}{\rho_s}\left(2 - \frac{\rho_\infty}{\rho_s}\right)}, \qquad (3.204)$$

where R_s is the radius of curvature of the body at the forward stagnation point; ρ_∞ is the gas density in the approaching stream (before the density jump); ρ_s is the gas density after the density jump line. It follows from the theory of density jump lines that the ratio of densities before and after the density jump line depends on

the Mach number of the approaching stream, and is given by the equation

$$\frac{\rho_s}{\rho_\infty} = \frac{(\gamma+1)M_\infty^2}{(\gamma-1)M_\infty^2+2}\left[1+\frac{\gamma-1}{2}\frac{(\gamma-1)M_\infty^2+2}{2\gamma M_\infty^2-(\gamma-1)}\right]^{\frac{1}{\gamma-1}}. \qquad (3.205)$$

Figure 46 shows the results of calculating the parameter $2R_s/U_\infty\,(dU_e/dx)_s$ from equations (3.204) and (3.205). The experimental data of Korobkin and Gruenewald are also shown. The agreement between the theory and experiments can be regarded as good.

It can be seen from Fig. 47 that as the Mach number M_∞ increases, the parameter $2R_s/U_\infty\,(dU_e/dx)_s$ tends asymptotically to some limiting values which depends on the value of the adiabatic factor γ.

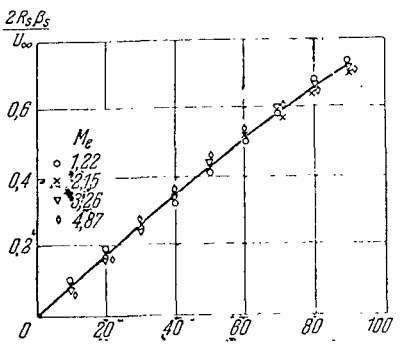

Figure 46.

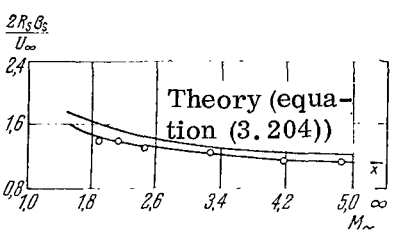

Figure 47.

It should be noted that for Mach numbers $M_\infty > 4$ it is possible to calculate the value of the parameter $(dU_e/dx)_s$ very accurately using an improved form of Newton's formula [84]. In this case, the velocity gradient at the critical point is given by the equation /185

$$\beta_s = \left(\frac{dU_e}{dx}\right)_s = \frac{1}{R_s}\sqrt{\frac{2(p_s - p_\infty)}{\rho_s}}. \qquad (3.206)$$

Apart from the value of the velocity gradient at the forward stagnation point, in our case it is also of interest to determine the change in the stream velocity along the surface of the sphere, particularly in the region of the sonic point. Experimental data on the velocity distributions along spheres were obtained by Korobkin and Gruenewald over the range of Mach numbers in the approaching stream of 1.22 to 4.87 (Fig. 46), and these indicated that the dependence of the velocity on the longitudinal coordinate was close to linear: $U_e \sim x$. The velocity gradient along the surface of the sphere appears to be very similar to the value of this parameter at the stagnation point. From evaluations carried out by Sibulkin [85], the differences in the velocity gradients at the forward stagnation points do not exceed 3% (at $\gamma = 1.4$). All the data presented make it possible to conclude that the velocity distribution of the stream along the sphere surface $0 \leqslant \vartheta \leqslant 90°$) can be well described by the linear relationship: /186

$$U_e = \left(\frac{dU_e}{dx}\right)_s x = \beta_s x.$$

The quantity $(dU_e/dx)_s$ can be determined either from equation (3.204) or from the graph shown in Fig. 47, or from equation (3.206) if the Mach number is $M_\infty > 4$.

Calculation of friction on a sphere. Let us now proceed to the calculation of the distribution of friction along the surface of a sphere. For this purpose a method of calculation is used which is based on linearization of the momentum equation (Section 17), with some preliminary simplifying assumptions relative to the behavior of the parameter H* and the function A; these are regarded as constant quantities. By considering equations (3.55) and (3.173) it is not difficult to arrive at a basis for this simplifications. Actually, it follows from results of analyses carried out in the previous Section that the quantities H* and A depend very slightly on the friction parameter ζ. It can therefore be expected that if the compressibility parameter β and the heat transfer parameter ω (see equations (3.48) or (3.49)) vary little along the surface, then H* and A will also vary little. In the present case of friction on a sphere, the compressibility parameter β is small, since the Mach number at the outer edge of the boundary layer does not exceed the value of 1.5 to 2. The previously mentioned fact that the Mach number M_e reaches a value equal to unity at the point with the angular

coordinate $\vartheta = 45°$ is important in this connection. It follows that the effect of the compressibility parameter on the values of H* and A will be small. As regards the heat transfer parameter ω, its value may be quite large. However, if the wall temperature is constant, the change in the value of this parameter along the surface of the sphere will be insignificant, since the temperature at the outer edge of the boundary layer along the sphere changes little. Thus, in the present case of flow close to a sphere there is every reason to assume that the quantities H* and A are constants. If it is assumed approximately in addition that $r_w(x) \approx x$, the coefficients P(x) and Q(x) in equation (3.180), which are given by equation (3.181), assume the form

/187

$$P(x) = A(2 + H^*)\frac{1}{x}, \qquad Q(x) = \rho_e \beta_s A x. \tag{3.207}$$

By substituting the values of these coefficients into the expression for the function z (equation (3.183)), it is found after evaluating the quadratures that

$$z = \left(\frac{x}{x_t}\right)^{-A(2+H^*)} \left[\frac{\beta_s \rho_w A x_t^2}{A(2 + H^*) + 2}\left[\left(\frac{x}{x_t}\right)^{A(2+H^*)+2} - 1\right] + \rho_e U_{et}\zeta_t^2 \delta_t^{**}\right]. \tag{3.208}$$

If the laminar and transitional sections of the boundary layer are absent ($x_t = 0$, $U_{et} = 0$), equation (3.208) can be somewhat simplified, and assumes the form

$$z = \frac{\beta_s \rho_w A}{A(2 + H^*) + 2} x^2. \tag{3.209}$$

Once the function z(x) has been obtained, it is not difficult to use equations (3.192) or (3.194) of the previous Section to calculate the distribution of the surface friction coefficient $c_f(x)$.

For a completely turbulent boundary layer the following expression can be obtained for the local friction coefficient after substituting equation (3.209) into equation (3.194):

$$c_f = \frac{0{,}29K}{[\lg\{0{,}0586K^2 \mathrm{Re}_x (\mu_e/\mu_w)^{A[A(2+H^*)+2]^{-1}}\}]^2}, \tag{3.210}$$

where

$$\mathrm{Re}_x = \frac{\beta_s \rho_e x^2}{\mu_e}, \tag{3.211}$$

and the quantities K, H* and A are given respectively by equations (3.188), (3.55) and (3.177).

For convenience in carrying out calculations, Fig. 48 gives the relationship between the group $\frac{A}{A(2+H^*)+2}$ and the temperature factor T_w/T_e for Mach numbers $M_e = 0.2$. The nature and limits of this complex confirm the assumptions made as to the constancy of the quantities A and H*. It should be noted that the group $\frac{A}{A(2+H^*)+2}$ depends not only on the parameters T_w/T_e and M_e, but also on the Reynolds number. However, this dependence appears to be extremely feeble, and so the graphs shown in Fig. 48 (constructed for $Re_x = 10^7$; r = 0.89) can be used with a high degree of accuracy over a wide range of Reynolds numbers (approximately from 10^5 to 10^9). /188

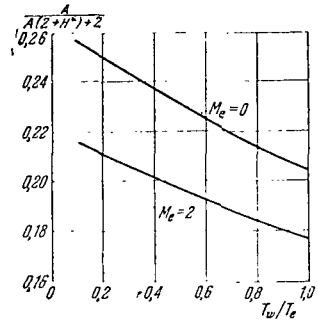

Figure 48.

Figures 49 and 50 show the results of calculating the distributions of some of the parameters and the local friction coefficients on the surface of a sphere for various flow conditions*.

The calculations whose results are shown in Fig. 49 were carried out for the conditions of flow around a sphere of diameter d = 2 m in the case of a gas stream with a Mach number $M_\infty = 3$ at a height of 20 km (with respect to standard atmosphere). The surface of the sphere is assumed to be thermally insulated. These figures show the distributions of the Mach number M_e and the Reynolds number Re_x (see equation (3.211)) at the outer edge of the boundary layer. The variation of the Reynolds number is characterized by the presence of a maximum, caused by the fact that in the initial section the predominant factor governing the increase of the Reynolds number is the increase of the longitudinal coordinate x, while

*The calculations were carried out at the request of the author by G. V. Semenova.

in the subsequent sections it is the gas density ρ, which decreases sharply as a result of the isentropic expansion of the stream along the sphere surface. Figure 49 also shows the distribution of the local friction coefficient c_f on the surface of the sphere (see equation (3.210)), and the distribution of $c_{f\infty}$ (see equation (3.195)). The curve for the variation of the friction coefficient $c_{f\ pl}$ is also shown; this is calculated from the flat-plate formulas for local values of the Mach number M_e and the Reynolds number Re_x at the outer edge of the boundary layer. /189

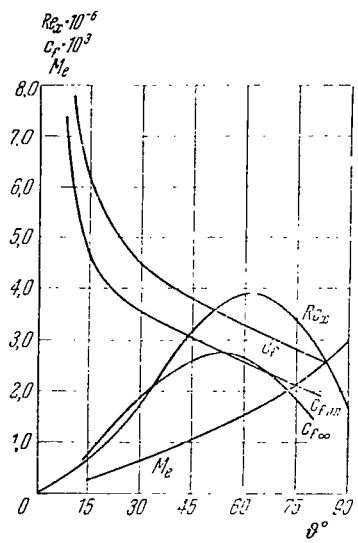

Figure 49.

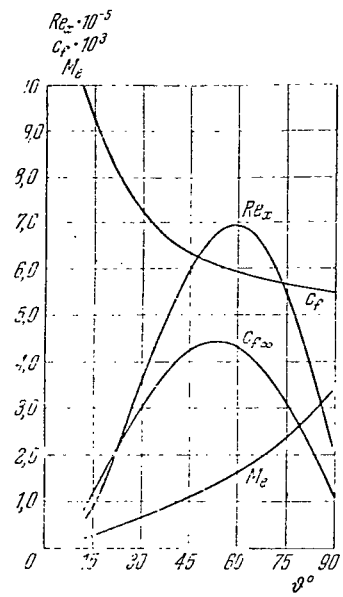

Figure 50.

Figure 50 shows the analogous results obtained for calculations of the flow around a sphere of diameter d = 1.07 m of a stream with a Mach number $M_\infty = 11$ at a height of 25 km and with a value of the temperature factor $T_w/T_{eo} = 0.327$ (T_{eo} is the stagnation temperature).

It can be seen from Figs. 49 and 50 that in both of the cases considered for flow around a sphere, the local friction coefficient $c_{f\infty}$ defined in terms of the parameters of the approaching stream (see equation (3.195)) reaches a maximum in the zone of the flow adjacent to the sonic line.

Calculation of heat transfer on a sphere. After determining the friction coefficient by the method described above it is possible by applying Reynolds analogy

(equation (3.144)) to obtain the local heat transfer coefficient (Stanton number). /190
By using Reynolds analogy, the expression obtained for the local heat flux is

$$q_w = \frac{1}{2} c_f \rho_e U_e S(1) \left(h_e + r \frac{U_e^2}{2} - h_w \right). \qquad (3.145)$$

Here S(1) and r are the Reynolds analogy parameter and the recovery coefficient. The values of these parameters can be obtained from equations (3.150) and (3.159). When these formulas and equation (3.207) are used, the following expression is obtained for the heat flux on the sphere:

$$q_w = \frac{1}{2} c_f \mathrm{Pr}^{-2/3} \rho_e \beta_s x \left(h_e + \frac{1}{2} \mathrm{Pr}^{1/3} \beta_s^2 x^2 - h_w \right). \qquad (3.212)$$

Apart from this method, there is a whole series of other approximate methods of calculating heat transfer on spherical surfaces. The results of some of these are given below:

Van Driest [86] used a power-law type velocity profile with an exponent of 1/7, and obtained the following expression for the local heat transfer coefficient:

$$c_{h\infty} = 0{,}042\, \mathrm{Pr}^{-2/3} \left(\frac{\beta_s d}{U_\infty} \right)^{4/5} \left(\frac{\rho_\infty U_\infty d}{\mu_\infty} \right)^{-1/5} \left(\frac{\rho_e}{\rho_\infty} \right)^{4/5} \left(\frac{\mu_e}{\mu_\infty} \right)^{1/5} \left(\frac{x}{d} \right)^{3/5}, \qquad (3.213)$$

where the heat flux is given by the equation

$$q_w = c_{h\infty} \rho_\infty U_\infty (H_r - h_w). \qquad (3.214)$$

It should be noted that equation (3.213) was obtained under the assumption that the turbulent boundary layer started at the forward stagnation point.

Arthur and Williams [87] used van Driest's formula (3.213) and a power dependence of viscosity on temperature, $\mu \sim T^{0.76}$, and the assumption that there /191
was an isentropic distribution of gas around the surface of the sphere, and found that in this case the maximum value of the heat transfer coefficient $(c_{h\infty})_{max}$ is reached at the point x/d = 0.322, which corresponds to the angular position $\vartheta = 37°$. The maximum heat flux for Pr = 0.75 appears to be equal to

$$(q_w)_{max} = 0{,}0195 \left(\frac{\beta_s d}{U_\infty} \right)^{4/5} \left(\frac{\rho_s}{\rho_\infty} \right)^{4/5} \left(\frac{\mu_s}{\mu_\infty} \right)^{1/5} \times \left(\frac{\rho_\infty U_\infty d}{\mu_\infty} \right)^{-1/5} \rho_\infty U_\infty (H_r - h_w), \qquad (3.215)$$

where the subscript s denotes parameters at the forward stagnation point.

Sibulkin [85] investigated heat transfer at the sonic point, and obtained an expression equivalent to equation (3.213). Like van Driest, Sibulkin used a power-law velocity profile. For calculating the friction, he used the power formula of Blasius, which is widely used in the theory of turbulent boundary layers in incompressible fluids, in which the flow parameters were evaluated by the nominal temperature method of Eckert [75].

In concluding the present section we will give the formula for calculating turbulent heat transfer in the neighborhood of the stagnation point of an axisymmetric body which was proposed by V.S. Avduevskiĭ [88]:

$$q_w = 3600 g c_l \rho_e \beta_s x \, 0{,}040 \left(\frac{\beta_s x^2 \rho_e}{\mu_e}\right)^{-0{,}2} \times \left(\frac{T_w}{T_r}\right)^{-0{,}16} \mathrm{Pr}^{0{,}6} (T_r - T_w) \quad \frac{\text{kcal}}{\text{m}^2\,\text{hr}}. \tag{3.216}$$

Equation (3.216) was obtained by solving the integral energy relation using the experimental relationship between the heat flux and local characteristics of the boundary layer established for a flat plate. In deriving equation (3.216) it was assumed that $\rho_e(x) = \text{const}$. /192

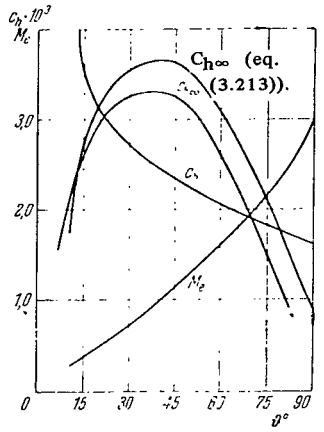

Figure 51.

Figures 51 and 52 present the results of calculating the heat transfer coefficients c_h and $c_{h\infty}$ on the surface of a sphere for the flow conditions indicated in the explanations of Figs. 49 and 50 respectively. The local heat transfer coefficient c_h, defined in terms of the parameters at the outer edge of the boundary

layer (see equation (3.143)) was calculated according to equation (3.159). The local heat transfer coefficient $c_{h\infty}$ is defined by the relationship $c_{h\infty} = c_h \frac{\rho_e}{\rho_\infty} \frac{U_e}{U_\infty}$.

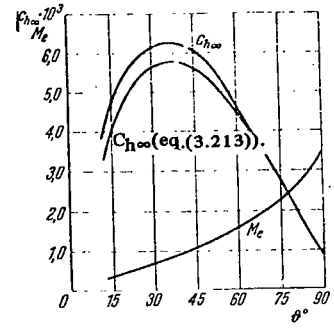

Figure 52.

Figures 51 and 52 also gives the distribution of the local heat transfer coefficients $c_{h\infty}$ obtained from van Driest's formula (3.213). As can be seen from the figures, the two methods lead to similar results. The maximum heat transfer rate occurs close to the sonic line.

CHAPTER IV.

THE TURBULENT BOUNDARY LAYER IN DISSOCIATING GASES

19. Some remarks on the thermodynamic properties of air at high temperature*

/193

The increase in the velocities of flying equipment from small subsonic to moderate supersonic velocities has made it necessary to take into account the dependence of the gas density and transport properties (viscosity and thermal conductivity) on temperature in calculating these motions. The specific heat capacity of air at high temperatures increases as a result of disturbances of the vibratory degrees of freedom (Fig. 53). However, if the temperature difference in the boundary layer is not very large, it is possible in carrying out approximate calculations to assume that the heat capacity of air is constant, with the value corresponding to some mean temperature of the stream.

Methods of calculating turbulent boundary layers on bodies of different shapes based on the assumption of constancy of the gas heat capacity have been considered in the previous chapter.

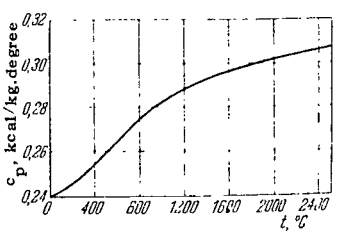

Figure 53.

/194

Any further increase in the velocities of flying equipment is accompanied by such increases in the gas temperature that in addition to variation of the density and transport coefficients, the necessity may arise to take into account the dependence of the heat capacity on temperature. In this case, it must be remembered that the absolute value of the temperature is not of primary importance, but rather the temperature drop in the boundary layer (in other words, the difference between the maximum and minimum temperatures). The calculation of gas flows with variation of the heat capacity can be carried out both on the basis of the generalized methods considered in the previous chapter (in many cases, such generalizations can be formally reduced to a replacement of temperatures by enthalpies) and by using methods which will be developed in the present chapter.

---

* For details of the thermodynamic properties of gases at high temperatures, see [89].

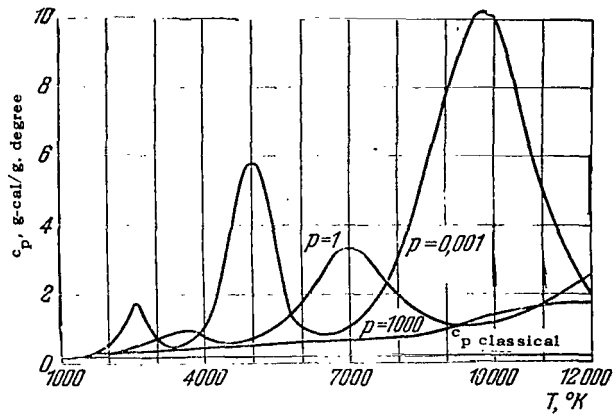

Figure 54.

The transition to hypersonic velocities causes such large increases in the gas temperature that thermochemical processes can begin to occur in the gas; these include dissociation of the gas molecules, ionization of atoms, and the formation of oxides, radiations, etc. Figure 54 gives a representation of the /195
effects of these processes on the "effective" heat capacity of air under equilibrium conditions [90]; the graphs give the dependence of the heat capacity c_p on temperature at various pressures (the "effective" heat capacity usually means the heat capacity at which, together with the usual heat capacity, the thermal effects of the thermochemical processes occurring in the gas are taken into account).

Figure 55, which is taken from the same work by E. V. Stupochenko et al., gives the calculated mole concentrations under conditions of thermodynamic equilibrium of the molecular and atomic components of air and electrons as functions of the temperature at three values of the pressure, p = 0.001, 1 and 1000 atm. As can be seen from Fig. 55, at high temperatures air represents a multicomponent mixture consisting of molecules of oxygen O_2, nitrogen N_2, nitric oxide NO, atoms of oxygen O, nitrogen N, argon Ar, and electrons e^-. In addition to these components in the mixture there are positively charged ions of oxygen O^+, nitrogen N^+, nitric oxide NO^+ (the concentrations of these components is not shown in Fig. 55).

Over wide ranges of temperature and pressure the concentrations of argon and nitric oxide do not exceed 1%, so that in carrying out approximate calculations, the presence of these components can be neglected.

Calculations of the equilibrium state of air show [91] that as a result of the considerable difference in the dissociation energies of oxygen and nitrogen (5.08 ev for O_2 and 9.756 ev for N_2), the dissociation of oxygen in mainly completed before the beginning of the dissociation of nitrogen. In addition, because of the high ionization potentials for oxygen and nitrogen (13.62 ev for O and 14.55 ev for N) the dissociation of the molecules of oxygen and nitrogen is essentially complete before ionization of the O and N atoms begins.

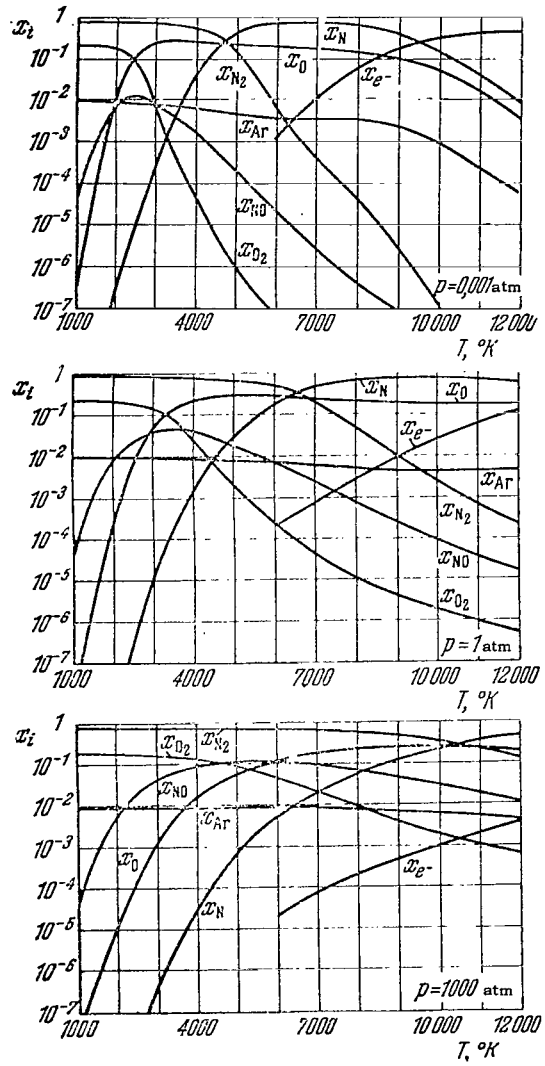

Figure 55.

These features of the chemical reactions occurring in air at high temperatures makes it possible to distinguish approximately several temperature and pressure zones for each of which one or other of the reactions ic characteristic (Fig. 56) *. The separation into zones as indicated in Fig. 56 makes it possible to greatly simplify the calculation of air flows at high temperatures. /197

*Figure 56, which was compiled by Hansen, is to be found in the book by Dorrens [92].

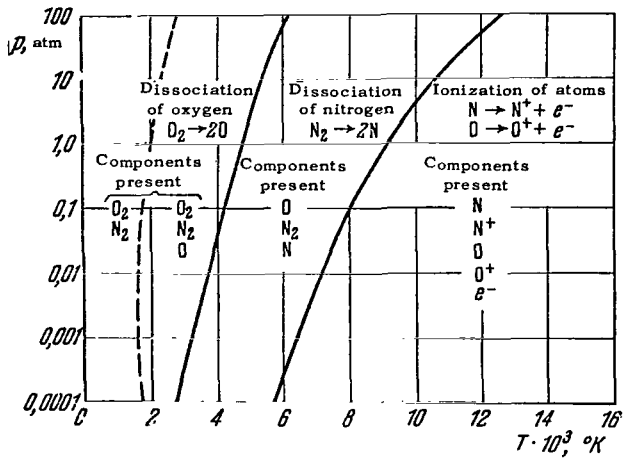

Figure 56.

In the present chapter we will consider methods of calculating turbulent boundary layers for the flow regimes in which the effects of ionization processes can be neglected (see Fig. 56).

20. Some information on the kinetics of chemical reactions

/198

In the present section some of the information required in the subsequent development on the formal kinetics of homogeneous chemical reactions will be given [93], in particular, information on the kinetics of the dissociation reactions of the main constituents of air (oxygen and nitrogen). Here we will also give a description of the model of the "ideal dissociating gas" proposed by Lighthill [94] which has been widely used in gas-dynamic investigations, as well as the model of the partially disturbed dissociating gas. Brief information will also be presented on the kinetics of heterogeneous (surface) chemical reactions.

Some definitions. The processes of chemical interaction between particles in a gas mixture are the result of collisions of the reacting particles. Depending on the type of system in which the reactions occur, they may be of two types, homogeneous and heterogeneous.

Reactions occurring in a single medium (for instance, in a mixture of reacting gases or in a solution) are termed homogeneous. Usually homogeneous reactions are taken to mean those occurring in a finite volume of gas, solution, etc.; if the gases participating in the reaction are contained in a vessel, the rate of a homogeneous reaction is independent of the size of the vessel surface. The dissociation reaction of molecules of oxygen and nitrogen at high temperatures can be regarded as an example of a homogeneous reaction.

Reactions occurring in a nonhomogeneous medium, on surfaces adjacent to the reacting materials, are termed heterogeneous, as are those in which the reactants are in different phases, for instance, solid and gaseous (reactions of

recombinations of atoms on catalytic walls), liquid and gaseous (reaction combustions of hydrocarbons on surface films of melts of certain materials used for the thermal protection of space equipment), etc. Heterogeneous reactions usually include all those reactions occurring in narrow zones (compared with the volume occupied by the gas) such as might occur in the contacting of previously unmixed reacting gases. In the limiting case, when the rate of the chemical reaction is infinitely large compared with the rate of diffusion (the rate of supply and removal or reagents and reaction products), this zone can be regarded as a surface (the reaction front). As an example of such a reaction it is possible to give the case of the oxidation (combustion) reaction of a gaseous fuel during the flow of an air stream heated to a high temperature around a carbon wall. In this case, the gaseous carbon formed as a result of sublimation of the solid carbon diffuses from the wall surface to the outer edge of the boundary layer against the oxygen, which is diffusing in the opposite direction. If the temperature in the boundary layer is sufficiently high, the rate of the oxidation (combustion) reaction of the carbon will be very large, and the reaction zone (combustion front) will be so shallow compared with the thickness of the boundary layer that such reactions can in practice be regarded as heterogeneous reactions. /199

A reaction is termed endothermic if it proceeds with the absorption of heat (for example, the dissociation reaction of oxygen molecules), and it is termed exothermic if it proceeds with the liberation of heat (for example, the recombination reaction of oxygen atoms).

The law of mass action. Each chemical reaction proceeds according to a law of constant proportions, and in the general case can be described by the following stoichiometric equation:

$$\sum_{k=1}^{N} \nu_k' A_k' \underset{k''}{\overset{k'}{\rightleftarrows}} \sum_{k=1}^{N} \nu_k'' A_k'', \tag{4.1}$$

where ν_k' and ν_k'' are the stoichiometric coefficients for the reagents (prime) and the reaction products (double prime), respectively. The A_k's are the chemical symbols of the reacting materials; N is the total number of chemical components; k' and k'' are the rate constants for the forward and reverse reactions, respectively, which are functions of temperature. /200

The main relationship describing the rate of a chemical reaction (the rate of formation or consumption of the i^{th} component is the relationship given by the law of mass action. According to the law of mass action, the rate of formation of a chemical material is proportional to the product of the concentrations of the reacting materials, and each of the concentrations appears raised to some power equal to the stoichiometric coefficient. According to this law, the rate at which the reaction proceeds from left to right for the equation of the chemical reaction described above can be represented in the form

$$\left(\frac{d[n_i]}{dt}\right)' = k'(T) \prod_{k=1}^{N} [n_k]^{\nu_k'}, \tag{4.2}$$

while the rate of the reaction from the right to left is given by the equation

$$\left(\frac{d[n_i]}{dt}\right)'' = k''(T)\prod_{k=1}^{N}[n_k]^{\nu_k''}. \qquad (4.3)$$

Here $[n_i]$ denotes the number of moles of component i per unit volume. The derivative $d[n_i]/dt$ expresses the rate of change of the number of moles of the i^{th} component per unit volume as a result of the occurrence of the chemical reaction. It should be noted that equations (4.2) and (4.3) are written for calculations on the basis of 1 mole.

If the reaction is such that the reactants are present on the left and right of the reaction equation, the expression for the reaction rate can be written as

$$\left(\frac{d[n_i]}{dt}\right)' = (\nu_i'' - \nu_i')k'(T)\prod_{k=1}^{N}[n_k]^{\nu_k'}, \qquad (4.4)$$

$$\left(\frac{d[n_i]}{dt}\right)'' = (\nu_i'' - \nu_i')k''(T)\prod_{k=1}^{N}[n_k]^{\nu_k''}. \qquad (4.5)$$

These equations are written for calculations with $(\nu_i'' - \nu_i')$ moles.

The overall rate of formation of the i^{th} component will be equal to the difference between the rates of the forward and reverse reactions: /201

$$\frac{d[n_i]}{dt} = (\nu_i'' - \nu_i')k'(T)\prod_{k=1}^{N}[n_k]^{\nu_k'} - (\nu_i'' - \nu_i')k''(T)\prod_{k=1}^{N}[n_k]^{\nu_k''}. \qquad (4.6)$$

At chemical equilibrium there is no change in the composition of the medium, i.e., the rates of the forward and reverse reactions become equal $(d[n_i]/dt = 0)$; in this case, therefore:

$$\frac{k'(T)}{k''(T)} = \prod_{k=1}^{N}[n_k^{(e)}]^{\nu_k''-\nu_k'} = K_n(T), \qquad (4.7)$$

where $K_n(T)$ is the equilibrium constant, and the superscript e denotes the equilibrium value of $[n_k]$.

Equation (4.7) is the most general equation for determining the composition of the reaction products when chemical equilibrium is reached. This equation interrelates the ratio of the kinetic parameters k' and k'' to the equilibrium constant $K_n(T)$, which can be calculated accurately by applying thermodynamic and quantum-mechanical methods.

By using equation (4.7), equation (4.6) can also be written in the form

$$\frac{d[n_i]}{dt} = (\nu_i'' - \nu_i')\, k'(T) \prod_{k=1}^{N} [n_k]^{\nu_k'} \left[1 - \frac{1}{K_n(T)} \prod_{k=1}^{N} [n_k]^{\nu_k'' - \nu_k'}\right]. \qquad (4.8)$$

If several reactions occur simultaneously in the system, it is necessary to use the principle of independence of the individual reactions in order to calculate the overall rate of formation of the i^{th} component. According to this principle, if several reactions occur in the system, each of them will proceed independently of the others, and each will obey the law of mass action. The total rate of formation of the i^{th} component is equal to the sum of the rates of formation of this component in each of the reactions:

$$\frac{d[n_i]}{dt} = \sum_{s=1}^{a} \left(\frac{d[n_i]}{dt}\right)_s = \sum_{s=1}^{a} (\nu_{is}'' - \nu_{is}')\, k_s' \prod_{k=1}^{N} [n_k]^{\nu_{ks}'} \left[1 - \frac{1}{K_{ns}} \prod_{k=1}^{N} [n_k]^{\nu_{ks}'' - \nu_{ks}'}\right], \qquad (4.9)$$

/202

where a is the number of independent reactions, s is the reaction number.

For an ideal gas whose state is described by Clapeyron's equation,

$$[n_i] = \frac{p_i}{RT}. \qquad (4.10)$$

Here p_i is the partial pressure of the i^{th} component, R is the universal gas constant (if $[n_i]$ is measured in mole/cm^3, and the pressure in atmospheres, the gas constant is $R = 82.05$ cm$^3 \cdot$ atm $\cdot$ mole$^{-1} \cdot$ °K^{-1}).

In the equilibrium state

$$[n_i^{(e)}] = \frac{p_i^{(e)}}{RT}. \qquad (4.11)$$

Apart from the equilibrium constant K_n expressed in terms of the numbers of moles (equation (4.7)), use is frequently made in chemical kinetics of another equilibrium constant K_p expressed in terms of the partial pressures:

$$K_p = \prod_{k=1}^{N} (p_k^{(e)})^{\nu_k'' - \nu_k'}. \qquad (4.12)$$

Bearing in mind equation (4.11), it is not difficult to see that the equilibrium constants K_n and K_p are interrelated by the equation

$$K_n = K_p (RT)^{-\Delta\nu}, \quad \Delta\nu = \sum_{k=1}^{N} (\nu_k'' - \nu_k'). \qquad (4.13)$$

The ratio of the number of moles of the i^{th} component per unit volume (or the partial pressure of the i^{th} component) to the total number of moles per unit volume (or to the total pressure of the mixture) is termed the molal concentration of the i^{th} component: /203

$$x_i = \frac{[n_i]}{[n]} = \frac{p_i}{p}. \qquad (4.14)$$

Here $[n] = \sum_{i=1}^{N} [n_i]$ is the total number of moles per unit volume, and p is the pressure of the gas mixture.

The expression for the equilibrium constants in terms of the equilibrium molal concentrations is

$$K_x = \prod_{k=1}^{N} (x_k^{(e)})^{\nu_k'' - \nu_k'}. \qquad (4.15)$$

Analogously, it is possible to introduce an equilibrium constant expressed in terms of the equilibrium mass concentrations:

$$K_c = \prod_{k=1}^{N} (c_k^{(e)})^{\nu_k'' - \nu_k'}. \qquad (4.16)$$

Here

$$c_k = \frac{\rho_k}{\rho}, \quad \rho_k = \frac{p_k}{RT} M_k = [n_k] M_k. \qquad (4.17)$$

By using these relationships, it is not difficult to show that the following interrelationships exist among the equilibrium constants:

$$\frac{k'}{k''} = K_n = K_p (RT)^{-\Delta\nu} = K_x \left(\frac{p^{(e)}}{RT}\right)^{\Delta\nu} = K_c (\rho^{(e)})^{\Delta\nu} \left[\prod_{k=1}^{N} (M_k)^{\nu_k'' - \nu_k'}\right]^{-1}. \qquad (4.18)$$

It can be seen from equations (4.15) and (4.16) that the equilibrium constants K_x and K_c are always dimensionless parameters. As regards K_n and K_p (equations (4.7) and (4.12)), these equilibrium constants are dimensionless only when $\Delta\nu = 0$. In order to be able to use any of the equilibrium constants given above in the expression for the rate of a chemical reaction (equation (4.8)), it is useful to note that the group /204

$$\frac{k''}{k'} \prod_{k=1}^{N} [n_k]^{\nu_k'' - \nu_k'}$$

must always be dimensionless.

By introducing the following quantities by analogy with the equilibrium constants

$$K_n^* = \prod_{k=1}^{N} [n_k]^{\nu_k'' - \nu_k'}, \quad K_p^* = \prod_{k=1}^{N} (p_k)^{\nu_k'' - \nu_k'},$$
$$K_x^* = \prod_{k=1}^{N} (x_k)^{\nu_k'' - \nu_k'}, \quad K_c^* = \prod_{k=1}^{N} (c_k)^{\nu_k'' - \nu_k'},$$

it is found that

$$\frac{k''}{k'} \prod_{k=1}^{N} [n_k]^{\nu_k'' - \nu_k'} = \frac{K_n^*}{K_n} = \frac{K_p^*}{K_p} = \frac{K_x^*}{K_x} = \frac{K_c^*}{K_c} \left(\frac{\rho}{\rho^{(e)}}\right)^{\Delta\nu} = \frac{K_\alpha^*}{K_\alpha}$$
$$(\alpha = n,\ p,\ x). \qquad (4.19)$$

By using equations (4.19), the following equivalent expressions can be obtained for the rate of the chemical reaction:

$$\frac{d[n_i]}{dt} = (\nu_i'' - \nu_i') k' \left(1 - \frac{K_\alpha^*}{K_\alpha}\right) \prod_{k=1}^{N} [n_k]^{\nu_k'}$$
$$= (\nu_i'' - \nu_i') k' (RT)^{-\alpha} \left(1 - \frac{K_\alpha^*}{K_\alpha}\right) \prod_{k=1}^{N} (p_k)^{\nu_k'} = \qquad (4.20)$$

$$= (\nu_i'' - \nu_i')\, k' [n]^{\sigma} \left(1 - \frac{K_\alpha^*}{K_\alpha}\right) \prod_{k=1}^{N} (x_k)^{\nu_k'}$$

$$= (\nu_i'' - \nu_i')\, k' \rho^{\sigma} \left(1 - \frac{K_\alpha^*}{K_\alpha}\right) \prod_{k=1}^{N} \left(\frac{c_k}{M_k}\right)^{\nu_k'},$$

$$\sigma = \sum_{k=1}^{N} \nu_k'. \qquad (4.20 \text{ Cont'd})$$

Equilibrium constants. Statistical thermodynamics [95, 96] leads to the following expression for the equilibrium constant: /205

$$\ln K_p = -\frac{\Delta E_0}{RT} + \sum_{k=1}^{N} \nu_k'' \ln Q_p(A_k'') - \sum_{k=1}^{N} \nu_k' \ln Q_p(A_k'), \qquad (4.21)$$

where

$$\Delta E_0 \equiv \sum_{k=1}^{N} \nu_k'' E_0(A_k'') - \sum_{k=1}^{N} \nu_k' E_0(A_k') \qquad (4.22)$$

is the difference between the energies of the reaction products and the energies of the reacting materials at a point with zero temperature, while the reacting materials and reaction products are considered to be in a state with unit concentration at normal pressure; Q_p is the sum of the states for the gas with unit pressure; E_c is the energy of the gas at absolute zero.

The sum of the states for the gas with unit pressure is related to a fundamental quantity in statistical thermodynamics, the total sum of states Q, by the equation

$$Q_p = pQ. \qquad (4.23)$$

The sum of states Q is expressed as follows:

$$Q = \sum_i g_i e^{-\frac{\varepsilon_i}{kT}}, \qquad (4.24)$$

where ε_i is the energy of the particles in the i^{th} state; g_i is the statistical weighting or degree of degeneration of the energy levels, i.e., the number of states of particles with energy levels close to ε_i.

According to modern concepts, the energy of a gas molecule can be made up of an energy of translational motion ε_t, an energy of rotational motion ε_r, an

energy of intramolecular vibration, i.e., vibrations of atoms or groups of atoms in the molecule, ε_v, an energy of electronic excitation ε_e, and an energy of nuclear excitation. For the temperatures which are encountered in gas dynamics, the energy of nuclear excitation can be neglected. If it is assumed that interrelationships among the various forms of energy are absent, the sum of states can be represented by /206

$$Q = Q^t Q^r Q^v Q^e. \tag{4.25}$$

The factors on the right-hand side of equation (4.25) are the respective sums of states connected with the translational, rotational, vibrational and electronic energy levels. It can be shown by the methods of statistical thermodynamics that for biatomic molecules these factors are

$$Q^t_{A_2} = \left(\frac{2\pi m_{A_2} kT}{h^2}\right)^{3/2} \frac{RT}{p}, \tag{4.26a}$$

$$Q^r_{A_2} = \frac{1}{2}\frac{8\pi IkT}{h^2} = \frac{1}{2}\frac{T}{T_r}, \tag{4.26b}$$

$$Q^v_{A_2} = \left(1 - e^{\frac{h\nu}{kT}}\right)^{-1} = \left(1 - e^{-\frac{T_v}{T}}\right)^{-1}, \tag{4.26c}$$

$$Q^e_{A_2} = \sum_{i=0}^{\infty} g_i e^{-\frac{\varepsilon_i}{kT}}. \tag{4.26d}$$

Here m_{A_2} is the mass of the molecule, I is the moment of inertia of the molecule; h is Planck's constant; ν is the frequency of the vibration; T_r is a characteristic temperature for rotation, T_v is a vibrational characteristic temperature.

The expression for $Q^r_{A_2}$ is given for a biatomic molecule consisting of single atoms. For monoatomic particles, which do not have rotational and vibrational degrees of freedom, the corresponding sum of states assumes a value equal to unity. The sums of states for the translational and electronic degrees of freedom of monoatomic particles have the same forms as equations (4.26a) and (4.26d), except that in equation (4.26a) it is necessary to replace m_{A_2} by m_A.

Rate constants for homogenous reactions. An expression for the rate constant of a chemical reaction can be obtained only on the basis of the collision theory (Arrhenius' theory) [97, 98], or from the theory of absolute reaction rates [99] (sometimes the absolute reaction rate theory is termed the method of activated complexes). /207

The collision theory, which is an integral part of formal kinetics, does not consider the mechanism of the collisions, but gives only a quantitative description of the results of particle interactions. The collision theory was founded by Arrhenius. According to Arrhenius, all reactions occur through an intermediate stage related to the formation of active molecules, i.e., molecules possessing an amount of energy sufficient to overcome an energy barrier. For this elementary act of the chemical reaction to occur, it is necessary for the molecules of the reacting materials to approach each other. This is so regardless of whether the process involves the liberation or the absorption of energy; as a rule, as the molecules approach each other, repulsion forces occur, and to overcome these some definite energy is required. In order to illustrate this, Fig. 57 shows a sketch of how the energy of a reacting system varies. The potential energy of the system is plotted along the ordinate, while along the abscissa is plotted a coordinate characterizing the relative positions of the atoms. Region I corresponds to the initial particles, region II to the activated particles, and region III to the reaction products.

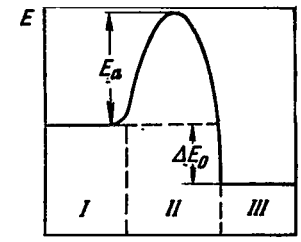

Figure 57.

The energy difference between the initial and final states of the system is equal to the energy effect of the reaction (ΔE_0). E_a is the energy of activation, i.e., the minimum value of the overall energy of the colliding molecules which is required for them to enter into reaction with each other. /208

The reaction rate constants are directly related to the numbers of collisions of activated molecules, and so the value of this constant is made proportional to the Boltzmann factor, $\exp(-E_a/RT)$. The problems of which collisions must be regarded as active ones must be solved experimentally. Comparison of the calculations based on various hypotheses with experimental data showed that for simple molecules only those collisions in which the components of the kinetic energies of the relative motion along the line of the centers exceeds the activation energy can be regarded as active collisions. In this case, the following expression is obtained for the reaction rate constant (see also [98]):

$$\bar{k} = 2r_{12}^2\left(\frac{2\pi kT}{\bar{m}}\right)^{1/2}\exp\left(-\frac{E_a}{RT}\right) = b(T)\exp\left(-\frac{E_a}{RT}\right)$$
$$(\bar{k} = k', k'').$$

Here r_{12} is the sum of the radii of the colliding particles; $\bar{m} = \left(\frac{1}{m_1} + \frac{1}{m_2}\right)^{-1}$ is the reduced mass of the particles; k is Boltzmann's constant.

This expression for the reaction rate constant does not always lead to results which are in good agreement with experiments, particularly if the reaction involves complex molecules. The explanation is that not all the active collisions lead to chemical changes. In order to take this fact into account, it is necessary

to introduce an additional factor P in the expression for the reaction rate constant which expresses the probability that an active collision will be succeeded by a chemical change. (P is sometimes termed the steric factor). In this case the expression for k assumes the form

$$\bar{k} = Pb(T)\exp\left(-\frac{E_a}{RT}\right). \qquad (4.27)$$

If all the active collisions lead to reactions, P = 1. In reactions in which complex molecules play a part, P can be very small (of the order of 10^{-8}). /209

Instead of equation (4.27) it is more usual to use the expression

$$\bar{k} = Z(T)\exp\left(-\frac{E_a}{RT}\right), \qquad (4.28)$$

which Arrhenius introduced in practice. The value of the pre-exponential factor Z(T) is usually determined experimentally, and for some not too complex reactions it can be computed on the basis of the absolute reaction rate theory *.

Heterogeneous chemical reactions**. In chemical kinetics the term "heterogeneous" refers to reactions which occur on interfaces or boundaries. Depending on the nature of the participation of the surface in the reaction, the heterogeneous reactions which are of greatest interest fall into two types.

In one case, the surface plays the part of a catalyst for reactants which are in the gas phase. In this case, the products of the heterogeneous catalytic reaction do not contain elements appearing in the composition of the surface. In the course of such reactions, neither the properties of the catalyst nor the shape of the calalytic surface varies. The reaction of catalytic recombination of atoms can be mentioned as an example of such a reaction.

In the second case, the surface takes a direct part in the reaction. The combustion of carbon surfaces around which a stream of high-temperature air flows can be mentioned as an example. In such a process, the shape of the surface may change as a result of the combustion products being carried away by the air stream.

The chemical processes in heterogeneous reactions are localized in a thin (monomolecular) layer at the surface. The volume of this layer is determined by the size of the surface and the dimensions of the reacting molecules. This monomolecular layer is held on the surface by the forces of chemical adsorption, /210

*A discussion of the absolute reaction rate theory is outside the scope of the present book. Readers who are interested in this theory are recommended to consult the monograph of Glasstone, Laidler and Eyring [99].

** For this problem, the paper of Rosner [100] is recommended; this contains a review and an extensive bibliography.

which are similar in nature to the forces of valency bonds (physical, or van der Waals, adsorption seldom leads to heterogeneous reactions).

The processes in a reaction occurring on a solid wall can be divided into the following stages: 1) transport of the reacting materials to the surface; 2) chemical adsorption of the reacting materials onto the surface; 3) chemical reaction among the reacting materials adsorbed on the surface, or between adsorbed components and components in the gas phase; 4) desorption of the reaction products from the surface; 5) removal of the reaction products from the surface.

By way of an example, let us consider the surface reactions of recombination and dissociation of oxygen. One of the possible mechanisms for this reaction, which is named the Langmuir-Hinshelwood reaction [101], can be described by the following system of equations:

$$O + W \rightleftarrows OW, \tag{4.29}$$

$$OW + OW \rightleftarrows O_2 + W + W. \tag{4.30}$$

Equation (4.29) describes the adsorption (forward reaction) and desorption (reverse reaction) of oxygen atoms. W denotes the so-called active parts of the wall, and OW the adsorbed atoms of oxygen, i.e., the atoms chemically bound to the surface. Equation (4.30) describes the reaction between neighboring adsorbed atoms, as a result of which molecules of oxygen are formed and liberated (desorbed), setting free active sites (W).

Another possible mechanism of the reaction (sometimes termed the Ridil-Ely mechanism [101]) is described by the relationships /211

$$O + W \rightleftarrows OW, \tag{4.29}$$

$$O + OW \rightleftarrows O_2 + W. \tag{4.31}$$

Equation (4.31) describes the reaction between adsorbed atoms of oxygen and oxygen atoms from the gas phase.

In both the first and second cases the rate at which the reaction occurs depends on the type of surface and the conditions on it.

In order to simplify the calculations, it is usually assumed in gas dynamic applications that the adsorption reaction occurs very rapidly, and so does not control the rate of the reaction as a whole. In this case, the reactions of types (4.30) and (4.31) control the overall rate. Schematically, both reactions can be represented in the form

$$A_i \underset{k_{wj}}{\overset{k_{wi}}{\rightleftarrows}} A_j, \tag{4.32}$$

where k_{wi} and k_{wj} are the rate constants of the forward and reverse surface catalytic reactions. The expression for the rate of formation of the component A_i given by formal kinetics can then be represented in the form

$$g_{A_i w} = \frac{d[A_i]_w}{dt} = k_{wi}[A_i]_w^{n_i} - k_{wj}[A_j]_w^{n_j}, \tag{4.33}$$

where n_i and n_j are the orders of the forward and reverse reactions; $[A_i]_w$ and $[A_j]_w$ are the concentrations of the reacting materials and the reaction products at the wall. The dimensions of the rate constant k_{wi} (or k_{wj}) depend on the dimensions of the reactant concentration and concentration of the reactant products.

By introducing the equilibrium constant

$$K_w = \frac{k_{wj}}{k_{wi}} = \frac{\{[A_i]_w^{n_i}\}^{(e)}}{\{[A_j]_w^{n_j}\}^{(e)}} \tag{4.34}$$

(here the superscript (e) refers to parameters in the state of thermodynamic equilibrium) equation (4.33) can be rearranged to the form /212

$$g_{A_i w} = \frac{d[A_i]_w}{dt} = k_{wi}\{[A_i]_w^{n_i} - K_w[A_j]_w^{n_j}\}. \tag{4.35}$$

Under steady-state conditions, the rate of formation of each component is equal to the diffusion flux of this component to the surface:

$$j_{A_i w} = -k_{wi}\{[A_i]_w^{n_i} - K_w[A_j]_w^{n_j}\}. \tag{4.36}$$

Equation (4.36) can be used as a boundary condition in solving boundary layer problems in the presence of surface catalytic reactions.

In many cases, the dependence of the constants k_{wi} on temperature is well described by Arrhenius' law:

$$k_{wi} = k_{0i}\exp\left(-\frac{E_{aw}}{RT_w}\right). \tag{4.37}$$

Here k_{oi} is a constant for the reagent - catalyst system studied; E_{aw} is the energy of activation. The ratio of E_{aw} to the universal gas constant R can be regarded as a "characteristic" temperature T_{aw} of the particular system of reactants and catalyst.

The kinetics of dissociation and recombination reactions in air. Under normal conditions air behaves as a mixture of mainly diatomic molecules of oxygen and nitrogen.

The concentrations of carbon dioxide gas, water vapor, argon and other trace materials are so small that their presence in the air can be neglected in most practical cases.

Over the temperature range from 2000 to 8000°K triatomic components, such as O_3, NO_2 and some other polyatomic oxides of nitrogen, play no important part, nor do ionization processes. The following are the main reactions in this temperature range [102]: /213

$$\left.\begin{array}{l} O_2 + X \rightleftarrows O + O + X, \\ N_2 + X \rightleftarrows N + N + X, \\ N_2 + O \rightleftarrows NO + N, \\ NO + O \rightleftarrows O_2 + N, \\ N_2 + O_2 \rightleftarrows NO + NO, \\ NO + X \rightleftarrows N + O + X. \end{array}\right\} \qquad (4.38)$$

Here X denotes a catalytic particle.

Of these six reactions, the last four, which involve NO, play a secondary role compared with the first two, since the equilibrium concentrations of nitric oxide are usually small (less than 1%). In carrying out approximate calculations, therefore, when the main objective is to obtain overall characteristics (friction, heat flux), it is possible in many cases to confine our attention to the first two reactions. It was also mentioned above that molecular oxygen is almost completely dissociated (bearing in mind the equilibrium dissociation) before nitrogen begins to dissociate. This fact makes it possible to regard air as a binary mixture of atoms and molecules. In this case, it is only necessary to make allowances for the differences in the dissociation energies of oxygen and nitrogen.

For nonequilibrium dissociation, the binary model for air may in some cases show inadequacy as a result of differences in the rate constants for recombination k_r for reactions in which various catalytic particles (X) take part. The values of the constant k_r for various reactions and various catalytic particles are given in Table 13, which is taken from the paper of Chung [103]. As can be seen from Table 13, the main scheme according to which the dissociation reactions occur can be written in the form

$$A_2 + X \underset{k_r(X)}{\overset{k_d(X)}{\rightleftarrows}} A + A + X. \qquad (4.39)$$

Here A_2 denotes a diatomic molecule, A denotes an atom, and X denotes a catalytic particle (atom or molecule). /214

Table 13

Reaction	D, ev	X	$2k_r$, $cm^2/mole^2 \cdot sec$
$O_2 + X \underset{k_r}{\rightleftarrows} O + O + X$	5,1	O	$0{,}25 \cdot 10^{20} \cdot T^{-3/2}$
		O_2	$0{,}8 \cdot 10^{20} \cdot T^{-3/2}$
		N_2	$6{,}19 \cdot 10^{15} \cdot T^{-1/2}$
		N, NO	$3{,}02 \cdot 10^{15} \cdot T^{-1/2}$
$N_2 + X \underset{k_r}{\rightleftarrows} N + N + X$	9,8	N	$2{,}36 \cdot 10^{21} \cdot T^{-3/2}$
		N_2	$2{,}76 \cdot 10^{16} \cdot T^{-1/2}$
		O_2, O, NO	$1{,}09 \cdot 10^{16} \cdot T^{-1/2}$
$NO + X \underset{k_r}{\rightleftarrows} N + O + X$	6,5	NO	$2 \cdot 10^{21} \cdot T^{-3/2}$
		O, N, O_2, N_2	$1{,}02 \cdot 10^{20} \cdot T^{-3/2}$
$O + N_2 \underset{k_r}{\rightleftarrows} NO + N$	3,3		$1{,}62 \cdot 10^{13}$ $\frac{cm^3}{mole \cdot sec}$

Dissociation and recombination processes which occur according to the scheme $A_2 \rightleftarrows A + A$, i.e., without the participation of particles X, play no important part. The rate of the forward reaction appears to be small, since the direct breakdown of a strongly excited molecule is not very probable. The rate of the reverse reaction is also small, since the molecules which are formed as a result of the combination of two atoms possess very high energies. As a result, most of such molecules dissociate after first colliding with other particles.

From the information in Table 13 it is clear that the rate constants for the recombination of oxygen and nitrogen differ appreciably from one another depending on the type of catalytic particle (X) participating in the reaction. The reaction rate constants, which are distinguished only by the type of the catalytic particle, depend only on the temperature and are interrelated by relationships which arise from the principle of local equilibrium /215

$$\frac{k_d(T, X)}{k_r(T, X)} = K_n(T), \tag{4.40}$$

where $K_n(T)$ is the equilibrium constant given by equation (4.7).

By using the relationships obtained earlier in this section, it is not difficult to write an equation for the mass rate of formation of an atomic component w_A during the occurrence of reactions described by the stoichiometric relationship (4.39). If the mixture consists of N components, then in the general case the mass rate of formation w_A can be obtained, according to the principle of independence of reactions (equation (4.9)), by summing the rates of formation in each

of the reactions (in this case, the number of reactions s is equal to the number of components N). For subsequent use, it is convenient to determine an expression for w_A in terms of the mass concentrations of the components. Thus, in order to obtain the rate of formation $d[n_A]/dt$, it is possible to use the last part of equation (4.20), and for the equilibrium constant and the ratio K*/K, equation (4.16) and the last of equation (4.19) are used. By remembering that for all N reactions of the type (4.39), which differ only through the catalytic particles X, and whose stoichiometric coefficients are the same and equal to $\nu'_{A_2} = 1$, $\nu'_X = 1$, $\nu'_A = 0$, ν''_{A_2}, $\nu''_X = 1$, $\nu''_A = 2$, and also that

$$\sigma = \sum_{k=1}^{N} \nu_k' = 2, \quad \Delta\nu = \sum_{k=1}^{N} (\nu_k'' - \nu_k') = 1.$$

it is found that

$$w_A = \sum_{s=1}^{N} w_{A_s} = M_A \sum_{s=1}^{N} \left(\frac{d[n_A]}{dt} \right)_s = \rho^2 c_{A_2} \left(1 - \frac{1}{K_c} \frac{c_A^2}{c_{A_2}} \frac{\rho}{\rho^{(e)}} \right) \sum_{s=1}^{N} k_{d_s} \frac{c_{X_s}}{M_{X_s}} \quad . \tag{4.41}$$

Both here and subsequently, the superscript e denotes an equilibrium parameter; /216
c_{Xs} is the mass concentration of the catalytic component (X) in the s^{th} reaction; N is the number of components in the reaction.

Sometimes it is more convenient to express the rate of formation of an atomic component w_A not in terms of the dissociation rate constant k_{ds}, as in equation (4.41), but in terms of the recombination rate constant k_{rs}. In this case, by using equation (4.40) and the relationship between the constants K_n and K_c given by equation (4.18), it is not difficult to show that

$$w_A = 2M_A^{-1}\rho^3 c_{A_2} \left(K_c \frac{\rho^{(e)}}{\rho} - \frac{c_A^2}{c_{A_2}} \right) \sum_{s=1}^{N} k_{r_s} \frac{c_{X_s}}{M_{X_s}}. \tag{4.42}$$

The equilibrium constant K_c which is defined in the general case by equation (4.16) assumes the following form for the reaction (4.39):

$$K_c = \frac{c_A^{(e)^2}}{c_{A_2}^{(e)}}. \tag{4.43}$$

In order to determine the equilibrium constant we have to return to equation (4.21). For the reaction (4.39), this equation assumes the form

$$\ln K_p = -\frac{\Delta E_0}{RT} + 2\ln Q_p(A) - \ln Q_p(A_2). \tag{4.44}$$

The expression for the sum of the states of the molecules ((4.26)) and atoms is now substituted into the previous equation (the sum of the states related to the translational energy levels for an atom, Q_A^t, is expressed in the same way as $Q_{A_2}^t$, except that m_{A_2} must be replaced by m_A). After making this substitution and converting from K_p to K_c by equation (4.18), it is found that

$$K_c = \frac{\exp\left(-\frac{T_d}{T}\right)}{\rho^{(c)}}\left\{m_A\left(\frac{\pi m_A k}{h^2}\right)^{3/2}(T_r T_v^{1/2})\left(\frac{T}{T_v}\right)^{1/2}\left[1 - \exp\left(-\frac{T_v}{T}\right)\right]\frac{(Q_A^e)^2}{Q_{A_2}^e}\right\}. \tag{4.45}$$

Here T_d is the characteristic dissociation temperature, equal to /217

$$T_d = \frac{D}{\frac{R}{2M_A}}, \qquad D = \frac{\Delta E_0}{2M_A}, \tag{4.46}$$

where D is the dissociation energy per unit mass of the molecule, ΔE_0 is the dissociation energy per mole of the initial material (molecule).

Thus, to determine the equilibrium constant K_c it is necessary to know the characteristic temperatures: the value for dissociation T_d, the vibrational value T_v, the rotational, T_r, and also the electronic sum of states for the main components of the air. Data on these characteristic temperatures are given in Table 14 [104].

Table 14.

	M_i, $\frac{g}{mole}$	m_i, g	T_d, °K	T_v, °K	T_r, °K
O_2	32	$5{,}312\cdot10^{-23}$	59 000	2270	2,08
N_2	28	$4{,}648\cdot10^{-23}$	113 200	3390	2,89

The electronic sums of states are described as follows (see the work of Hansen [104] to which reference has already been made):

$$\left.\begin{aligned} Q^e_{O_2} &= 3 + 2\exp\left(-\frac{11\,390}{T}\right) + \exp\left(-\frac{18\,990}{T}\right), \\ Q^e_O &= 5 + 3\exp\left(-\frac{223}{T}\right) + \exp\left(-\frac{326}{T}\right) \\ &\quad + 5\exp\left(-\frac{22\,800}{T}\right) + \exp\left(-\frac{48\,600}{T}\right), \\ Q^e_{N_2} &= 1, \\ Q^e_N &= 4 + 10\exp\left(-\frac{27\,700}{T}\right) + 6\exp\left(-\frac{41\,500}{T}\right). \end{aligned}\right\} \quad (4.47)$$

It follows from equation (4.47) that over the range of temperatures being considered (2000 - 8000°K) the ratios of the electronic sums of states for nitrogen and oxygen, which are required for calculating the equilibrium constants, vary insignificantly; it can therefore be assumed approximately /218

$$\frac{(Q^e_O)^2}{Q^e_{O_2}} = 27, \qquad \frac{(Q^e_N)^2}{Q^e_{N_2}} = 16. \quad (4.48)$$

If the assumption (4.48) is made that the ratios of the electronic sums of states are constant (this assumption is fulfilled to a high degree of accuracy for nitrogen, and the error does not exceed 10 - 12% for oxygen), the expression for the equilibrium constants (4.45) can be written as follows:

$$K_c = 2\frac{\rho_d}{\rho^{(e)}}\left(\frac{T}{T_v}\right)^{1/2}\left[1 - \exp\left(-\frac{T_v}{T}\right)\right]\exp\left(-\frac{T_d}{T}\right). \quad (4.49)$$

Here

$$\rho_d = \frac{m_A}{2}\left(\frac{\pi m_A k}{h^2}\right)^{3/2}(T_r T_v^{1/2})\frac{(Q^e_A)^2}{Q^e_{A_2}} \quad (4.50)$$

is the so-called characteristic density. A dissociating gas whose equilibrium constant is described by equation (4.49) (ρ_d = constant) is termed a "partially excited dissociating gas" [105]. When the conditions of equation (4.48) are satisfied, ρ_d = 151 g/cm^3 for oxygen; for nitrogen under the same conditions, ρ_d = 107 g/cm^3 [105].

Calculation of the group

$$\rho_{dL} = 2\rho_d\left(\frac{T}{T_v}\right)^{1/2}\left[1 - \exp\left(-\frac{T_v}{T}\right)\right], \quad (4.51)$$

which appears in the right-hand part of equation (4.49) shows that for gases such as oxygen and nitrogen, the quantity ρ_{dL} varies relatively little over a wide

range of temperatures. This can be seen from Table 15, taken from the paper of Lighthill [94].

Table 15.

T, °K		1000	2000	3000	4000	5000	6000	7000
ρ_{dL}, $\frac{g}{cm^3}$	O_2	145	170	166	156	144	133	123
	N_2	113	135	136	133	128	123	118

This peculiarity in the variation of ρ_{dL} was used by Lighthill, who proposed an "ideally dissociating gas" model, in which one of the main assumptions is that the quantity ρ_{dL} is constant. Like ρ_d, this quantity has the dimensions of a density. The quantity ρ_{dL} has been termed the characteristic density of an ideally dissociating gas. For oxygen and nitrogen the values of ρ_{dL} can be taken as 150 g/cm^3 and 130 g/cm^3 respectively (other properties of an ideally dissociating gas and those of partially excited dissociating gases will be considered in a later section). Thus, for an ideally dissociating gas, equation (4.49) for the equilibrium constant K_c will assume the following form when equation (4.51) is used

$$K_c = \frac{\rho_{dL}}{\rho^{(c)}} \exp\left(-\frac{T_d}{T}\right) \qquad (\rho_{dL} = \text{const}). \tag{4.52}$$

By now substituting equation (4.52) for the equilibrium constant K_c into equations (4.41) and (4.42), the following equivalent relationships are obtained for determining the mass rates of formation of the atomic components:

$$w_A = \rho^2 c_{A_2}\left[1 - \frac{\rho}{\rho_{dL}} \exp\left(\frac{T_d}{T}\right)\frac{c_A^2}{c_{A_2}}\right]\sum_{s=1}^{N} k_{ds}\frac{c_{X_s}}{M_{X_s}}, \tag{4.53}$$

$$w_A = 2\rho^2 c_{A_2} M_A^{-1}\left[\frac{\rho_{dL}}{\rho}\exp\left(-\frac{T_d}{T}\right) - \frac{c_A^2}{c_{A_2}}\right]\sum_{s=1}^{N} k_{rs}\frac{c_{X_s}}{M_{X_s}}. \tag{4.54}$$

For binary mixtures consisting of atoms and molecules of a single gas ($c_A + c_{A_2} = 1$), the last expressions become: /220

$$w_A = \rho^2(1 - c_A)M_A^{-1}\left[1 - \frac{\rho}{\rho_{dL}}\exp\left(\frac{T_d}{T}\right)\frac{c_A^2}{1 - c_A}\right] \times\left[k_d(A)c_A + \frac{1}{2}(1 - c_A)k_d(A_2)\right], \tag{4.55}$$

$$w_A = 2\rho^3(1 - c_A) M_A^{-2} \left[\frac{\rho_{dL}}{\rho} \exp\left(-\frac{T_d}{T}\right) - \frac{c_A^2}{1 - c_A} \right] \times \left[k_r(A) c_A + \frac{1}{2}(1 - c_A) k_r(A_2) \right]. \quad (4.56)$$

When the difference in the rate constants for dissociation (or, what is the same thing, for recombination) is small, it is possible to stop at the introduction of one constant, and equations (4.55) and (4.56) can be written in the form

$$w_A = \frac{1}{2}\rho^2(1 - c_A^2) M_A^{-1} k_d \left[1 - \frac{\rho}{\rho_{dL}} \exp\left(\frac{T_d}{T}\right) \frac{c_A^2}{1 - c_A} \right]. \quad (4.57)$$

$$w_A = \rho^3(1 - c_A^2) M_A^{-2} k_r \left[\frac{\rho_{dL}}{\rho} \exp\left(-\frac{T_d}{T}\right) - \frac{c_A^2}{1 - c_A} \right]. \quad (4.58)$$

By using equations (4.43) and (4.45), it is not difficult to represent the last two expressions for the mass rates of formation of the atomic component in the form

$$w_A = \frac{1}{2}\rho^2 M_A^{-1} k_d \left(1 - \frac{c_A^2}{c_A^{(e)^2}} \right), \quad (4.59)$$

$$w_A = \rho^3 M_A^{-2} k_r (1 + c_A) \frac{c_A^{(e)^2} - c_A^2}{1 - c_A^{(e)^2}}. \quad (4.60)$$

By equating the right-hand parts of equations (4.59) and (4.60), and making some simple rearrangements, an expression is obtained for the equilibrium constant:

$$K_n = \frac{k_d}{k_r} = \frac{4p}{RT} \frac{c_A^{(e)^2}}{1 - c_A^{(e)^2}}. \quad (4.61)$$

In the general case, the reaction rate constants depend on the temperature according to Arrhenius' law (see equation (4.28)), i.e., they increase exponentially with temperature. The rate constant for the recombination of atoms is an exception to this rule, since the recombination reaction occurs without requiring activation energy ($E_{ar} = 0$). The expression for the recombination rate constant has the form /221

$$k_r = Z_r(T). \quad (4.62)$$

For the recombination reactions occurring in air, k_r is closely approximated by a power relationship in temperature (see Table 12),

Table 17

	Reaction	X	k_i, $cm^3/mole \cdot sec$
1)	$O_2 + X \rightarrow \rightarrow O + O + X$, $\Delta E_0 = 118$ kcal/mole	O_2	$5{,}2 \cdot 10^{10} T^{1/2} \left(\frac{\Delta E_0}{RT}\right)^3 \exp\left(\frac{-\Delta E_0}{RT}\right)$
		N_2	$2{,}5 \cdot 10^{11} T^{1/2} \left(\frac{\Delta E_0}{RT}\right)^{1,5} \exp\left(\frac{-\Delta E_0}{RT}\right)$
		O	$6{,}25 \cdot 10^{12} T^{1/2} \left(\frac{\Delta E_0}{RT}\right)^{1,5} \exp\left(\frac{-\Delta E_0}{RT}\right)$
		N, NO	$k_i(O_2)$
		Ar	$4{,}2 \cdot 10^{11} T^{1/2} \left(\frac{\Delta E_0}{RT}\right) \exp\left(\frac{-\Delta E_0}{RT}\right)$
2)	$N_2 + X \rightarrow \rightarrow N + N + X$, $\Delta E_0 = 225$ kcal/mole	N_2	$4{,}25 \cdot 10^{11} T^{1/2} \left(\frac{\Delta E_0}{RT}\right)^{1,2} \exp\left(\frac{-\Delta E_0}{RT}\right)$
		N	$1{,}85 \cdot 10^{12} T^{1/2} \left(\frac{\Delta E_0}{RT}\right)^{1,5} \exp\left(\frac{-\Delta E_0}{RT}\right)$
		O_2, NO, O	$k_i(N_2)$
		Ar	$6{,}8 \cdot 10^{11} T^{1/2} \left(\frac{\Delta E_0}{RT}\right)^{1,5} \exp\left(\frac{-\Delta E_0}{RT}\right)$
3)	$NO + X \rightarrow \rightarrow N + O + X$, $\Delta E_0 = 150$ kcal/mole	O_2, N_2, Ar	$7 \cdot 10^{10} T^{1/2} \left(\frac{\Delta E_0}{RT}\right)^2 \exp\left(\frac{-\Delta E_0}{RT}\right)$
		NO, O, N	$20k_i$ (Ar)
4)	$O + N_2 \rightarrow \rightarrow NO + N$		$7 \cdot 10^{18} \exp T\ (-75\,500/RT)$
	$N + O_2 \rightarrow \rightarrow NO + O$		$1{,}3 \cdot 10^{10} T \exp(-7100/RT)$
	$N_2 + O_2 \rightarrow \rightarrow NO + NO$		$9{,}1 \cdot 10^{24} T^{-5/4} \exp(128\,500/RT)$

At moderate wall temperatures, reactions of the type (4.32) are first order, so that n = 1.

It follows from equation (4.65) that when $k_w = 0$,

$$(\partial [c_A]/\partial y)_w = 0,$$

which corresponds to a chemically isolated (absolutely noncatalytic) surface; when $k_w \rightarrow \infty$, $c_{Aw} \rightarrow 0$, which corresponds to an absolutely catalytic surface.

$$k_r = A_r T^{-n} \qquad (0 \leqslant n \leqslant 2). \tag{4.63}$$

The equilibrium constants K_n for the important reactions occurring in air at temperatures from 3000 to 8000°K have been approximated by Rei [102] by relationships of the form

$$K_n = AT^n \exp\left(-\frac{\Delta E_0}{RT}\right).$$

The results of the approximations (error less than 10%) are given in Table 16.

Table 16

Reaction	Equilibrium constant K_n	Dimensions
$O_2 + X \rightleftarrows O + O + X$	$1{,}2 \cdot 10^7 T^{-1/2} \exp(-118\,000/RT)$	mole/cm^3
$N_2 + X \rightleftarrows N + N + X$	$18 \exp(-224\,900/RT)$	mole/cm^3
$NO + X \rightleftarrows N + O + X$	$4{,}0 \exp(-150\,000/RT)$	mole/cm^3
$N_2 + O \rightleftarrows NO + N$	$4{,}5 \exp(-75\,000/RT)$	1
$NO + O \rightleftarrows O_2 + N$	$0{,}24 \exp(-32\,020/RT)$	1
$N_2 + O_2 \rightleftarrows NO + NO$	$19 \exp(-42\,980/RT)$	1

Table 17 gives the values of the rate constants of the reactions occurring in air which are recommended in the monograph by E. V. Stupochenko et al. [106].

In the general case, the boundary conditions on a catalytic wall have the form of equation (4.36). For catalytic recombination reactions the conditions on the surface are usually far from thermodynamic equilibrium, $[A]_w \gg [A]^{(e)}$, and so the second term in the right-hand part of equation (4.36) can be neglected in comparison with the first. In this case, equation (4.36) becomes

/223

$$J_{A_i w} = -k_w (\rho c_A)_w^n. \tag{4.64}$$

By using equation (1.57) for the diffusion flux of the i^{th} component, equation (4.64) can be converted to the form

$$\left(\rho \mathcal{D}_i \frac{\partial c_A}{\partial y}\right)_w = k_w (\rho c_A)_w^n. \tag{4.65}$$

Here k_w is the rate constant for the catalytic recombination, which depends on the temperature according to Arrhenius' law, equation (4.37); n is the order of the reaction.

At present there is only very limited information available on the reaction rate constants for the catalytic recombination of nitrogen and oxygen on various surfaces. Some of the available results are shown in Fig. 58, which is taken from the work of Coulard [107]. On the abscissa of this figure is plotted the catalytic capability γ_w, which is related to the constant k_w through the relationship

$$\gamma_w = k_w\left(\frac{2\pi M_A}{RT}\right). \tag{4.66}$$

On the ordinate is shown the wall temperature T_w. On the same figure are shown lines of constant values of k_w, which are practically the same for nitrogen and oxygen. /224

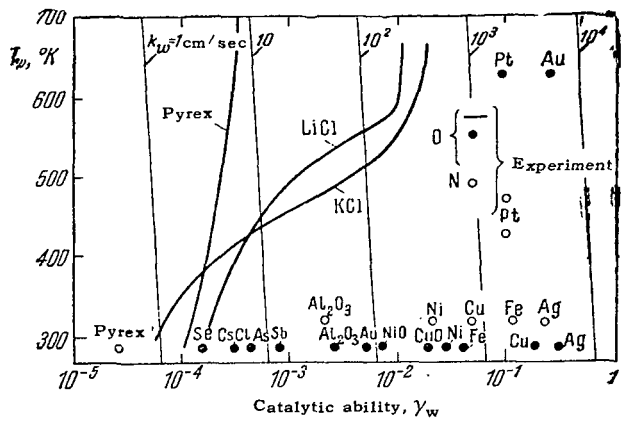

Figure 58.

It should be noted that the data given in Fig. 58 were obtained for the recombination of pure nitrogen and oxygen. The processes of catalytic recombination of mixtures of nitrogen and oxygen have been studied even less.

21. The properties of partially excited dissociating and ideally dissociating gases

In the previous section, an expression was obtained for the equilibrium constant of a partially excited dissociating gas (4.9) and for an ideally dissociating gas (4.52), as well as for the mass rate of formation of atomic components.

For a partially excited dissociating gas consisting of atoms and molecules (binary mixture), the equilibrium composition can be determined from the following relationship:

$$\frac{c_A^{(e)2}}{1-c_A^{(e)}} = 2\frac{\rho_d}{\rho^{(e)}}\left(\frac{T}{T_v}\right)^2\left[1-\exp\left(-\frac{T_v}{T}\right)\right]\exp\left(-\frac{T_d}{T}\right), \tag{4.67}$$

which is obtained from equations (4.43) and (4.49). The value of the characteristic density ρ_d, which is given in the general case by equation (4.50), can be assumed to be $\rho_d(O_2) = 151$ g/cm^3 for oxygen and $\rho_d(N_2) = 107$ g/cm^3 for nitrogen. /225

For an ideally dissociating gas, it follows from equation (4.43) and equation (4.52) that

$$\frac{c_\Lambda^{(e)2}}{1 - c_\Lambda^{(e)}} = \frac{\rho_{dL}}{\rho^{(e)}} \exp\left(-\frac{T_d}{T}\right), \tag{4.68}$$

where ρ_{dL} is given by equation (4.51).

For oxygen, it can be assumed that $\rho_{dL} = 150$ g/cm^3, and for nitrogen that $\rho_{dL} = 130$ g/cm^3.

For the subsequent treatment it is useful to consider the thermodynamic properties of dissociating gases.

Statistical thermodynamics leads to the following expressions for the enthalpy and internal energy of a gas mixture:

$$h = \sum_i c_i h_i = \sum_i c_i \left[\frac{R}{M_i} T^2 \left(\frac{\partial \ln Q_{ip}}{\partial T}\right) + h_i^0\right], \tag{4.69}$$

$$E = \sum_i c_i E_i = \sum_i c_i \left[\frac{R}{M_i} T^2 \left(\frac{\partial \ln Q_{ic}}{\partial T}\right) + h_i^0\right]. \tag{4.70}$$

Here Q_{ip} is the sum of the states of the i^{th} component of the gas mixture at unit pressure, which is given by equations (4.23) - (4.26); Q_{ic} is the sum of the states of the i^{th} component of a gas mixture with unit concentration:

$$Q_{ic} = \frac{p}{RT} Q_i, \tag{4.71}$$

Q_i is given by equations (4.24) - (4.26); h_i^0 is the energy of formation of the i^{th} component per unit mass at a temperature equal to absolute zero.

For a binary mixture of atoms and molecules with unexcited electronic states, substitution of Q_{ip} and Q_{ic} into equations (4.69) and (4.70) respectively given: /226

$$h = \left[\frac{7}{2} + \frac{3}{2}c_A + (1 - c_A)\frac{\frac{T_v}{T}}{e^{T_v/T} - 1}\right]\frac{R}{2M_A}T + c_A D, \tag{4.72}$$

$$E = \left[\frac{5}{2} + \frac{1}{2}c_A + (1 - c_A)\frac{\frac{T_v}{T}}{e^{T_v/T} - 1}\right]\frac{R}{2M_A}T + c_A D. \tag{4.73}$$

In these expressions for the enthalpy and internal energy of a partially excited dissociating gas, the third terms in the square brackets expresses the contribution of the vibratory degrees of freedom to the enthalpy and internal energy. As the temperature varies from 0 to ∞, the values of these terms varies from 0 to $(1 - c_A)$. The maximum contribution of the oscillatory degrees of freedom occurs when $c_A = 0$, and consists of about 20% of the total enthalpy and 30% of the entire internal energy.

At high temperatures, when dissociation becomes appreciable, equations (4.72) and (4.73) can be simplified by putting $[T_V/T]\,[\exp(T_V/T) - 1] = 1/2$. According to this simplification, which, like the simplification of a constant characteristic density ($\rho_{dL} = \text{const}$), is based on Lighthill's model of an ideally dissociating gas, it is assumed that regardless of temperature, the gas molecules are excited with respect to their vibratory degrees of freedom by a value equal to a half of the value of the "classical" vibratory excitation of the molecules. At high temperatures this assumption does not lead to appreciable error, since as the temperature increases, the concentration of the molecules $(1 - c_A)$ decreases, and the contribution of the term $c_A D$ increases. Thus, for an ideally dissociating gas we will have

$$h = (4 + c_A)\frac{R}{2M_A}T + c_A D, \tag{4.74}$$

$$E = 3\frac{R}{2M_A}T + c_A D. \tag{4.75}$$

Also, by having an expression for the enthalpy and internal energy of a partially excited dissociating gas and an ideally dissociating gas, it is possible to define an "effective" specific heat capacity of the gas at constant pressure or at constant volume. /227

According to these definitions, the specific heat capacities of a gas mixture at constant pressure and at constant volume are equal to

$$c_p = \left(\frac{\partial h}{\partial T}\right)_p, \quad c_v = \left(\frac{\partial E}{\partial T}\right)_\rho. \tag{4.76}$$

By substituting into (4.76) the expressions for h and E (4.69) and (4.70) and making use of equation (4.67), the expressions for the "effective" specific heat capacities of a partially excited dissociating gas in a state of equilibrium are found to be

$$\frac{c_p}{\frac{R}{2M_A}} = \frac{7}{2} + \frac{3}{2}c_A + (1 - c_A)\frac{\frac{T_v}{T}}{1 - e^{-T_v/T}} + \frac{1}{2}c_A(1 - c_A^2)\left(\frac{3}{2} + \frac{T_d}{T} - \frac{\frac{T_v}{T}}{1 - e^{-T_v/T}}\right)^2, \tag{4.77}$$

$$\frac{c_v}{\frac{R}{2M_A}} = \frac{5}{2} + \frac{1}{2}c_A + (1 - c_A)\frac{\frac{T_v}{T}}{1 - e^{-T_v/T}} + \frac{c_A(1 - c_A)}{2 - c_A}\left(\frac{1}{2} + \frac{T_d}{T} - \frac{\frac{T_v}{T}}{1 - e^{-T_v/T}}\right)^2. \tag{4.78}$$

In a similar way, using equations (4.68) and (4.74) - (4.76), an "effective" specific heat capacity for an ideally dissociating gas is obtained for the case of thermodynamic equilibrium: /228

$$\frac{c_p}{\frac{R}{2M_A}} = 4 + c_A + \frac{1}{2}c_A(1 - c_A^2)\left(1 + \frac{T_d}{T}\right)^2, \tag{4.79}$$

$$\frac{c_v}{\frac{R}{2M_A}} = 3 + \frac{c_A(1 - c_A)}{2 - c_A}\left(\frac{T_d}{T}\right)^2. \tag{4.80}$$

It is clear from the last two equations that the assumption that there is a constant excitation of the vibratory degrees of freedom leads to the ratio of specific heats in an ideally dissociating gas before the onset of dissociation being equal to $c_p/c_v = 1.33$ and not 1.4, as in the case of real diatomic gases in the absence of excitation of the vibratory degrees of freedom. In addition, it is not difficult to conclude that in an ideally dissociating gas, the specific heat capacities at constant volume per unit masses of molecules and atoms are the same; $c_{vA} = c_{vA_2}$, since the number of degrees of freedom of the molecules (six) is just twice as large as the number of degrees of freedom of the atoms (three).

In various gas dynamic studies, including investigations of boundary layers in dissociating gases, it is useful to introduce a characteristic pressure of an ideally dissociating gas, p_d:

$$p_d = \frac{R}{2M_A} \rho_{dL} T_d. \qquad (4.81)$$

Values of p_d for oxygen and nitrogen are presented in Table 18, along with other quantities which determine the properties of ideally dissociating oxygen and nitrogen.

Table 18.

	T_d, °K	ρ_{dL}, g/cm^3	p_d, atm
O_2	59 000	150	$2{,}3 \cdot 10^7$
N_2	113 200	130	$4{,}1 \cdot 10^7$

An expression for the determination of the equilibrium concentration of atoms in an ideally dissociating gas as a function of temperature can be easily obtained from equation (4.68) if use is made of the equation of state for a binary mixture, which can be rearranged by use of equation (4.81) to the form /229

$$\frac{p}{p_d} = \frac{\rho}{\rho_{dL}} \frac{T}{T_d} (1 + c_A). \qquad (4.82)$$

By eliminating the density ρ between equations (4.68) and (4.82), it is found after some simple rearrangements that

$$c_A = \left[1 + \frac{p}{p_d} \frac{T_d}{T} \exp \frac{T_d}{T}\right]^{-1/2}. \qquad (4.83)$$

To conclude this section, results of calculations of the equilibrium concentrations of oxygen atoms are given in Fig. 59 for a pressure p = 1 atm and various temperatures for an ideally dissociating gas (dashed curve, calculated from equation (4.83) with $\rho_{dL} = 150$ g/cm^3) and a partially excited dissociating gas (solid curve, calculated from equation (4.67) with $\rho_d = 151$ g/cm^3). As can be seen from Fig. 59, which is taken from the work of Glass and Takano [105], the difference between the equilibrium concentrations of an ideally dissociating and a partially excited dissociating gas is quite small.

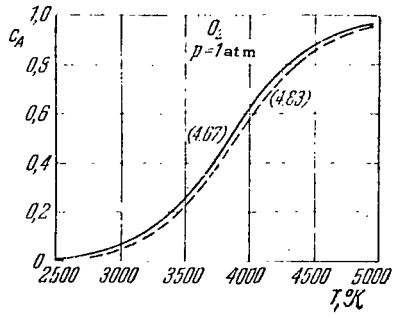

Figure 59.

22. Formulation of the problem of the turbulent boundary layer in a dissociating gas

Some remarks on the dynamic structure of the turbulent boundary layer at large supersonic velocities. The results of velocity profile measurements in turbulent boundary layers on a flat plate at large Mach numbers (up to $M_e = 10$) and various values of the temperature factor (see section 11) showed that in terms of the universal coordinates the velocity profile was satisfactorily described by a linear relationship in the laminar sublayer, while the turbulent core (or at least, the inner part of it) was logarithmic. /230

As already mentioned, it is characteristic of velocity profiles at large Mach numbers that the extent of the transition (buffer) zone between the laminar sublayer and the turbulent core is reduced. The buffer zone essentially disappears completely, and the transition from the laminar sublayer to the core becomes quite sharp.

Another important feature of the velocity profiles at large Mach numbers is the increase in the relative thickness of the laminar sublayer as the Mach number increases. It is well known that in incompressible fluids the thickness of the laminar sublayer does not exceed 2 - 3% of the total boundary layer thickness. According to Hill's data, presented in section 11, at $M_e = 9$ the sublayer thickness can make up about 15% of the total boundary layer thickness.

These features of the experimental velocity profiles at large supersonic velocities must, of course, be taken into account in setting up semiempirical methods of calculating turbulent boundary layers. Even the possibility of setting up semiempirical methods of calculating turbulent boundary layers at large supersonic velocities is largely based on the existence of a sufficiently extensive logarithmic section of the velocity profile in the turbulent core. The presence of such a section makes it possible to apply the semiempirical formulas of Prandtl and von Kármán to the calculation of turbulent boundary layers at large Mach numbers, since, as shown in section 10, these formulas always lead to a logarithmic velocity profile, regardless of the distribution of density in the boundary layer.

A sharp transition from the laminar sublayer to the turbulent core (disappearance of the buffer layer) confirms the applicability of the Prandtl two-layer model (laminar sublayer - turbulent core) in the theory of turbulent boundary layers at large supersonic velocities. /231

Finally, the last of these features of the velocity profiles at large supersonic velocities (the increase of the relative thickness of the laminar sublayer) indicates that the part played by the laminar sublayer in heat and mass transfer processes in the boundary layer must increase. A result of this is that in calculating heat and mass fluxes it is necessary to take into account the molecular thermal and diffusional properties of the sublayer quite accurately (i.e., to allow for the Prandtl and Schmidt numbers being different from unity). As regards the calculation of friction at large supersonic velocities, it is obvious that here it is possible to confine our attention to flow in the laminar sublayer, assuming that the Prandtl and Schmidt numbers are equal to unity.

The turbulent boundary layer equations in a dissociating gas. The general turbulent boundary layer equations in a multicomponent mixture of chemically reacting gases have been obtained in Chapter II. In the present chapter we will consider only steady flow in the boundary layer, assuming that the turbulent Prandtl and Schmidt numbers are equal to unity.

The main equations can be written in the following form:

continuity:

$$\frac{\partial}{\partial x}(\rho u r_w^{\nu}) + \frac{\partial}{\partial y}(\rho v r_w^{\nu}) = 0, \tag{4.84}$$

momentum:

$$\rho u \frac{\partial u}{\partial x} + \rho v \frac{\partial u}{\partial y} = -\frac{dp}{dx} + \frac{\partial}{\partial y}\left[(\mu + \varepsilon)\frac{\partial u}{\partial y}\right], \tag{4.85}$$

energy:

$$\rho u \frac{\partial H}{\partial x} + \rho v \frac{\partial H}{\partial y} = \frac{\partial}{\partial y}\left(\varepsilon \frac{\partial H}{\partial y}\right) + \frac{\partial}{\partial y}\left\{\frac{\mu}{\mathrm{Pr}}\left[\frac{\partial H}{\partial y} + \sum_i (\mathrm{Le}_i - 1) h_i \frac{\partial c_i}{\partial y} + (\mathrm{Pr} - 1)\frac{\partial}{\partial y}\left(\frac{u^2}{2}\right)\right]\right\}, \tag{4.86}$$

conservation of the i^{th} component:

$$\rho u \frac{\partial c_i}{\partial x} + \rho v \frac{\partial c_i}{\partial y} = \frac{\partial}{\partial y}\left(\varepsilon \frac{\partial c_i}{\partial y}\right) + \frac{\partial}{\partial y}\left(\frac{\mu}{\mathrm{Sc}_i}\frac{\partial c_i}{\partial y}\right) + w_i, \tag{4.87}$$ /232

equation of state:

$$p = \rho RT \sum_i \frac{c_i}{M_i}. \tag{4.88}$$

The total enthalpy H is defined by the equations

$$H = h + \frac{u^2}{2}, \quad h = \sum_i c_i h_i, \quad h_i = \int_0^T c_{pi} dT + h_i^0. \tag{4.89}$$

For an impermeable wall, the velocity boundary conditions have the usual form

$$\left.\begin{aligned} u = v = 0 \quad &\text{at} \quad y = 0, \\ u \to U_e \quad &\text{at} \quad y \to \infty. \end{aligned}\right\} \tag{4.90}$$

The boundary condition for the total enthalpy is not difficult to obtain from equation (4.89). At the wall we have

$$H = h_w = \sum_i c_{iw} \int_0^{T_w} c_{pi} dT + \sum_i c_i h_i^0 \quad \text{at} \quad y = 0, \tag{4.91}$$

and at the outer edge of the boundary layer

$$H \to H_e = h_e + \frac{U_e^2}{2} = \sum_i c_{ie} \int_0^{T_e} c_{pi} dT + \sum_i c_{ie} h_i^0 + \frac{U_e^2}{2} \tag{4.92}$$

$$\text{at} \quad y \to \infty.$$

The concentrations of component i at the wall, c_{iw}, and at the edge of the boundary layer, c_{ie}, appear in the boundary conditions for the total enthalpy, (4.91) and (4.92). The concentration of the i^{th} component at the outer edge is usually known from the solution of the outer stream, so that the boundary condition for the concentration at the outer edge has the form

$$c_i \to c_{ie} \quad \text{at} \quad y \to \infty. \tag{4.93}$$

In the general case, in the presence of catalytic reactions on the surface, the concentration at the wall c_{iw} is not known in advance, and must be calculated in the course of solving the problem using the boundary condition (4.36) (for air with not too high wall temperatures, this condition can be simplified to the form

/233

(4.65)). The concentration boundary condition on the wall becomes definite in two limiting cases: 1) when the wall is absolutely noncatalytic ($k_{wi} = 0$); in this case it follows from the condition (4.36) that

$$\frac{\partial c_i}{\partial y} = 0 \qquad \text{at} \quad y = 0; \tag{4.94}$$

2) when the wall is absolutely catalytic ($k_{wi} \to \infty$); in this case if follows from the same condition (4.36) that

$$c_i = c_i^{(e)} \qquad \text{at} \quad y = 0. \tag{4.95}$$

For air at not too high wall temperatures, $c_A^{(e)} = 0$ at $y = 0$, and so condition (4.95) can be simplified to the form

$$c_i = 0 \qquad \text{at} \quad y = 0. \tag{4.96}$$

In studying turbulent boundary layers it is convenient in many cases to use the energy equation and the equation for conservation of the i^{th} component in terms of Crocco variables, (2.63), (2.64). In what follows, flow in the turbulent boundary layer will be considered in the framework of the two-layer Prandtl model (laminar sublayer - turbulent core), and so it is convenient to express these equations separately for the sublayer and core, bearing in mind the assumption made earlier in this chapter that the turbulent Prandtl and Schmidt numbers are equal to unity.

In the laminar sublayer we will have:

energy equation:

$$\rho u \frac{\mu}{\tau}\frac{\partial H}{\partial \xi} + \left(\frac{\partial \tau}{\partial u} - \frac{dp}{d\xi}\frac{\mu}{\tau}\right)\frac{\partial H}{\partial u} = \frac{\partial}{\partial u}\left\{\tau\left[\frac{1}{\mathrm{Pr}}\frac{\partial H}{\partial u} + \frac{1}{\mathrm{Pr}}\sum_i (\mathrm{Le}_i - 1) h_i \frac{\partial c_i}{\partial u} + \left(1 - \frac{1}{\mathrm{Pr}}\right) u\right]\right\}, \tag{4.97}$$

equation for conservation of component i: /234

$$\rho u \frac{\mu}{\tau}\frac{\partial c_i}{\partial \xi} + \left(\frac{\partial \tau}{\partial u} - \frac{dp}{d\xi}\frac{\mu}{\tau}\right)\frac{\partial c_i}{\partial u} = \frac{\mu}{\tau} w_i + \frac{\partial}{\partial u}\left(\frac{\tau}{\mathrm{Sc}_i}\frac{\partial c_i}{\partial u}\right). \tag{4.98}$$

In the turbulent core the energy equation and the conservation equation for the i^{th} component become, in Crocco variables:

$$\rho u \frac{\partial H}{\partial \xi} - \frac{dp}{d\xi}\frac{\partial H}{\partial u} = \frac{\tau^2}{\varepsilon}\frac{\partial^2 H}{\partial u^2}, \tag{4.99}$$

$$\rho u \frac{\partial c_i}{\partial \xi} + \frac{dp}{d\xi} \frac{\partial c_i}{\partial u} = w_i + \frac{\tau^2}{\varepsilon} \frac{\partial^2 c_i}{\partial u^2}. \qquad (4.100)$$

The boundary conditions for equations (4.97) - (4.100) can be written as

$$\left.\begin{aligned} H = h_w, \quad c_i = c_{iw} \qquad & \text{at} \quad u = 0; \\ H \to H_e, \quad c_i \to c_{ie} \qquad & \text{at} \quad u \to U_e. \end{aligned}\right\} \qquad (4.101)$$

It is pertinent to note that the comments made at the beginning of this section concerning concentration boundary conditions at the wall remain valid here also.

The Damköhler number. Frozen equilibria in nonequilibrium flows. The nature of the flow in a boundary layer during the occurrence of chemical reactions in the external stream and in the boundary layer itself depends on the ratio of the rates of diffusion and of the chemical processes.

Let us return to the equation for the conservation of an atomic component, equation (4.87), which was set up for a binary mixture, for simplicity, consisting of atoms and molecules. Equation (4.60) is used as an expression for the mass rate of formation of the atomic component. By substituting this expression into the conservation equation, it is found that

$$\rho u \frac{\partial c_A}{\partial x} + \rho v \frac{\partial c_A}{\partial y} = \frac{\partial}{\partial y}\left[\left(\frac{\mu}{Sc} + \varepsilon\right)\frac{\partial c_i}{\partial y}\right] + \rho^3 M_A^2 k_r (1 + c_A) \frac{c_A^{(e)^2} - c_A^2}{1 - c_A^{(e)^2}}.$$

This equation can be converted into dimensionless form by introducing a characteristic dimension of the flow, L, as a length scale, the velocity of the on-flowing stream U_∞ as a velocity scale, and the density and viscosity ρ_∞ and μ_∞ as measures of the density and viscosity. After several rearrangements it is found that

/235

$$\bar{\rho}\bar{u}\frac{\partial c_A}{\partial \bar{x}} + \bar{\rho}\bar{v}\frac{\partial c_A}{\partial \bar{y}} - \frac{1}{Re_L}\frac{\partial}{\partial \bar{y}}\left[\left(\frac{\bar{\mu}}{Sc} + \bar{\varepsilon}\right)\frac{\partial c_A}{\partial \bar{y}}\right] = Da \cdot \bar{\rho}^3 (1 + c_A) \frac{c_A^{(e)^2} - c_A^2}{1 - c_A^{(e)^2}}.$$

Here

$$Re_L = \frac{\rho_\infty U_\infty L}{\mu_\infty}, \qquad Da = \frac{\dfrac{L}{U_\infty}}{\dfrac{1}{\rho_\infty^2 M_A^2 k_r}}.$$

The dimensionless group Da which appears in the right-hand part of this equation is known as the Damköhler number. It is not difficult to explain the significance of the Damköhler number by considering separately the numerator and denominator in the last equation. Actually, it is readily seen that the quantity L/U_∞, which appears in the numerator, characterizes the time for which a particle remains in the boundary layer (t_{stream}). The quantity in the denominator,

$1/\rho_\infty^2 M_A^{-2} k_r = t_{chem}$ also has the dimensions of time. This quantity characterizes the lifetime of an atom, and is the characteristic time which determines the rate at which chemical processes are occurring.

Thus, the Damköhler number represents a ratio of two characteristic times: the time for which particles remain in the stream (the diffusion time), and the time for the chemical reaction to occur, i.e.,

$$Da = \frac{t_{stream}}{t_{chem}} = \frac{\frac{L}{U_\infty}}{\frac{1}{\rho_\infty^2 M_\Lambda^{-2} k_r}}. \qquad (4.102)$$

If $Da \to 0$, the time for the chemical reaction to occur is much larger than the time for which particles remain in the stream ($t_{chem} \gg t_{stream}$), and as a result, the effect of the chemical reaction in the gas phase on the flow in the boundary layer is insignificant. In this case, the mixture of gases in the boundary layer can be regarded as chemically inert, and the boundary layer as chemically "frozen". In this case the dissociation products (atoms) appear in the boundary layer only as a result of their diffusion from the outer stream. For a chemically frozen boundary layer the conservation equation of the boundary layer is simplified, since the term expressing the mass rate of formation of the i^{th} component is equal to zero ($w_i = 0$). /236

If the Damköhler number is very large, $Da \to \infty$, the time for the occurrence of the chemical reaction is much smaller than the time for which the particles remain in the boundary layer ($t_{chem} \ll t_{stream}$), and consequently at each point in the boundary layer it will be possible to establish local thermochemical equilibrium. The concentration distribution of each component will not depend on transport processes (convection and diffusion), and will depend only on the local values of the temperature and pressure. In this case the need for a conservation equation for the i^{th} component disappears, and the concentration distribution is determined from the condition $w_i = 0$ (the sign of the equation should not be confused with the sign of the identity in the case of frozen flow). A boundary layer in which thermochemical equilibrium is established is termed an "equilibrium" boundary layer.

When the Damköhler number is finite in size, the rates of the chemical processes and the transport processes may be quantities of the same order ($t_{stream}/t_{chem} - 1$), so that the thermochemical state of the boundary layer will differ from equilibrium. For sake of brevity, such boundary layers will be referred to as "nonequilibrium" boundary layers. In order to determine the concentration fields in this case it is necessary to use the conservation equations for the individual components in their general form.

23. Velocity profiles, integral thicknesses, and friction on a flat plate

Returning to Section 12, it is not difficult to see that many of the results obtained there are also valid in the case of flow of a dissociating gas around a flat plate. Actually, the expressions for the velocity profiles in the turbulent core (equation (3.28)) which were obtained from the von Kármán formula without any assumptions as to the nature of the density changes in the turbulent core can still be used for calculating the velocity profiles on a plate in the presence of dissociation. Making use of the assumption (3.1), according to which friction τ is constant across the boundary layer and equal to τ_w, this expression becomes /237

$$\eta = \eta_1 + \frac{\zeta}{f}\int_{\bar{u}_1}^{\bar{u}} \exp\left[\varkappa\zeta\int_{\bar{u}_1}^{\bar{u}} \sqrt{\frac{\rho}{\rho_w}}\,d\bar{u}\right]d\bar{u}. \tag{4.103}$$

From equation (4.103), the value of the derivative $d\eta/d\varphi$ in the turbulent core, which is needed later, is found to be

$$\frac{d\eta}{d\varphi} = \frac{1}{f}\exp\left(\varkappa\zeta\int_{\bar{u}_1}^{\bar{u}} \sqrt{\frac{\rho}{\rho_w}}\,d\bar{u}\right). \tag{4.104}$$

For the velocity profile in the laminar sublayer, it is possible to use a linear relationship, just as in Section 12:

$$\varphi = \eta. \tag{4.105}$$

The basis of this relationship was given from the consideration of experimental data in Sections 11 and 13.

In the laminar sublayer the derivative $d\eta/d\varphi$ is obviously

$$\frac{d\eta}{d\varphi} = 1. \tag{4.106}$$

In order to determine the Reynolds numbers formed from the momentum loss thickness and the displacement thickness, and the form parameter

$$H^* = \delta^*/\delta^{**}$$

equations (3.42), (3.44) and (3.45) can be used; these equations were derived in Section 12 for any arbitrary density distribution in the boundary layer.

For convenience, the following expressions are introduced here: /238

$$
\left.
\begin{aligned}
\mathrm{Re}^{**} &= \frac{e^{-\varkappa\alpha}}{fx^2}\frac{\mu_w}{\mu_e}\exp\left[\varkappa\zeta\int_0^1\left(\frac{\rho}{\rho_w}\right)^{1/2}d\bar{u}\right] \\
&\quad\times\left[1-\frac{2+\frac{1}{2}\frac{\rho'(1)}{\rho_e}}{\varkappa\zeta\left(\frac{\rho_e}{\rho_w}\right)^{1/2}}\right], \\
\mathrm{Re}^{*} &= \frac{e^{-\varkappa\alpha}}{fx}\frac{\mu_w}{\mu_e}\exp\left[\varkappa\zeta\int_0^1\left(\frac{\rho}{\rho_w}\right)^{1/2}d\bar{u}\right] \\
&\quad\times\left[1+\frac{\rho'(1)}{\rho_e}-\frac{1}{\varkappa\zeta}\left(\frac{\rho_w}{\rho_e}\right)^{1/2}\right. \\
&\quad\left.\times\left(\frac{1}{2}\frac{\rho'(1)}{\rho_e}+\frac{\rho''(1)}{\rho_e}-\frac{3}{2}\frac{\rho'(1)^2}{\rho_e^2}\right)\right], \\
H^{*} &= \left[1+\frac{\rho'(1)}{\rho_e}-\frac{1}{\varkappa\zeta}\left(\frac{\rho_w}{\rho_e}\right)^{1/2}\right. \\
&\quad\left.\times\left(\frac{1}{2}\frac{\rho'(1)}{\rho_e}+\frac{\rho''(1)}{\rho_e}-\frac{3}{2}\frac{\rho'(1)^2}{\rho_e^2}\right)\right] \\
&\quad\times\left[1-\frac{2+\frac{1}{2}\frac{\rho'(1)}{\rho_e}}{\varkappa\zeta\left(\frac{\rho_e}{\rho_w}\right)^{1/2}}\right]^{-1}.
\end{aligned}
\right\} \qquad (4.107)
$$

Here,

$$
\rho'(1) = \left(\frac{d\rho}{d\bar{u}}\right)_{\bar{u}=1}, \qquad \rho''(1) = \left(\frac{d^2\rho}{d\bar{u}^2}\right)_{\bar{u}=1}.
$$

It is not difficult to see that for calculating friction only the formulas derived in Section 12 need be used. The only thing lacking to apply these relationships to actual situations is the velocity dependence of the gas density in the boundary layer. This comment refers to the function K, which for an arbitrary density distribution in the boundary layer assumes the form

$$
K = \int_0^1\left(\frac{\rho}{\rho_e}\right)^{1/2}d\bar{u}. \qquad (4.108)
$$

The form of the functions F, G and N which are required for calculating the friction remain unchanged in the present case being considered of the flow of a dissociating gas. For convenience, a collection of all the relationships required for calculating friction can be presented: /239

$$
\left.
\begin{aligned}
&\left(\frac{c_f}{c_{f0}}\right) = \left(\frac{FK}{2N}\right)^2, \\
&F = 0{,}242\,c_{f0}^{-1/2}, \quad G = \lg\left(\frac{\mu_e}{\mu_w}\right), \\
&N + \lg N = \lg\frac{FK}{2} + \frac{1}{2}(F+G).
\end{aligned}
\right\} \qquad (4.109)
$$

It may be mentioned that the local friction coefficient c_{fo} on a plate along which an incompressible fluid flows can be evaluated either by von Kármán's formula, (3.59), or by equation (3.80). The dynamic viscosity can be determined from the power formula, equation (3.61). The function N is easily calculated from the last of equations (4.109) by using tables of logarithms to base 10.

In a similar way, generalizations can be made of all the formulas obtained in Section 12 for the calculation of local and average friction to allow for the flow of a dissociating gas. The effect of the thermochemical state of the flow on the resistance in the boundary layer obviously appears through the dependence $\rho(u)$ and also through the viscosity μ. Thus, the problem of calculating drag reduces to establishing the dependences of temperature and density on velocity.

The establishment of these relationships for frozen, equilibrium and non-equilibrium flows in the boundary layer will be dealt with the next Sections of this chapter.

24. Flow along a flat plate at Schmidt and Prandtl numbers equal to unity

Relationship between the velocity profile and total enthalpy. Let us consider flow along a flat plate ($dp/dx = 0$) of a supersonic gas stream, (see Fig. 22). The Prandtl and Schmidt numbers (and consequently, the Lewis number also), will be regarded as equal to unity. In this case, the differential equations for momentum (4.85), energy (4.86), and conservation of the i^{th} component (4.87) /240 assume the form

$$\rho u \frac{\partial u}{\partial x} + \rho v \frac{\partial u}{\partial y} = \frac{\partial}{\partial y}\left[(\mu + \varepsilon)\frac{\partial u}{\partial y}\right], \tag{4.110}$$

$$\rho u \frac{\partial H}{\partial x} + \rho v \frac{\partial H}{\partial y} = \frac{\partial}{\partial y}\left[(\mu + \varepsilon)\frac{\partial H}{\partial y}\right], \tag{4.111}$$

$$\rho u \frac{\partial c_i}{\partial x} + \rho v \frac{\partial c_i}{\partial y} = \frac{\partial}{\partial y}\left[(\mu + \varepsilon)\frac{\partial c_i}{\partial y}\right] + w_i. \tag{4.112}$$

From equations (4.110) and (4.111) and the boundary conditions (4.101), it follows that the velocity and total enthalpy fields are similar:

$$\frac{u}{U_e} = \frac{H - h_w}{H_e - h_w}. \tag{4.113}$$

By solving equation (4.113) for H, it is found that

$$H = h_w + (H_e - h_w)\bar{u} \qquad \left(\bar{u} = \frac{u}{U_e}\right). \tag{4.114}$$

Equilibrium flow of an ideally dissociating gas. In the case of total thermochemical equilibrium, the concentration of atomic components of a mixture is uniquely determined by the local values of the temperature and pressure. The

relationship between the concentration and pressure and temperature for an ideally dissociating gas is given by equation (4.83). As a result of the constancy of the pressure across the boundary layer, the pressure p in this equation can be put equal to the pressure at the outer edge of the boundary layer, p_e. As a result, it is found that

$$c_\Lambda = \left[1 + \frac{p_e}{p_d}\frac{T_d}{T}\exp\frac{T_d}{T}\right]^{-1/2}. \tag{4.115}$$

Here p_d and T_d are the characteristic pressure and temperature (values of these quantities are given for oxygen and nitrogen in Table 18).

The relationships between the velocity, temperature and concentration profiles are easily obtained by substituting into the left-hand part of equation (4.114) the expressions for the enthalpy of an ideally dissociating gas, equation (4.74). After making this substitution and some rearrangements, it is found that /241

$$\bar{\beta}\bar{u}^2 - (\overline{H}_e - \bar{h}_w)\bar{u} - \bar{h}_w + 4\overline{T} + c_\Lambda(1 + \overline{T}) = 0. \tag{4.116}$$

where

$$\left.\begin{aligned} \bar{\beta} &= \frac{U_e^2}{2D}, \\ \bar{h}_w &= \frac{h_w}{D} = c_{\Lambda w} + (4 + c_{Aw})\,\overline{T}_w, \\ \overline{H}_e &= \frac{H_e}{D} = c_{\Lambda e} + (4 + c_{Ae})\,\overline{T}_e + \bar{\beta}, \\ \overline{T} &= \frac{T}{T_d}. \end{aligned}\right\} \tag{4.117}$$

Equations (4.115) and (4.116) make it possible to establish a relationship between the velocity and the temperature and concentration. By substituting equation (4.115) into equation (4.116), the following quadratic equation in the dimensionless velocity is obtained:

$$\bar{\beta}\bar{u}^2 - a\bar{u} + b = 0. \tag{4.118}$$

Here

$$\left.\begin{aligned} a &= \overline{H}_e - \bar{h}_w, \\ b &= 4\overline{T} + (1 + \overline{T})\left[1 + \bar{p}_e\,\overline{T}^{-1}\exp\left(\frac{1}{\overline{T}}\right)\right] - \bar{h}_w, \\ \bar{p}_e &= \frac{p_e}{p_d}. \end{aligned}\right\} \tag{4.119}$$

When equation (4.118) is solved for $\bar{u}$, it is found that

$$\bar{u} = \frac{a \pm \sqrt{a^2 - 4\bar{\beta}b}}{2\bar{\beta}}. \qquad (4.120)$$

The sign in front of the root in equation (4.120) is selected from the condition $\bar{u} \leq 1$.

Once the relationship between the velocity and temperature is established with equation (4.120), equation (4.115) can be used to find the relationship between the velocity and temperature.

The density distribution in the boundary layer is easily determined in terms of known temperatures and concentrations using the relationship /242

$$\frac{\rho}{\rho_e} = \left(\frac{T}{T_e}\right)^{-1} \frac{1 + c_{Ae}}{1 + c_A}, \qquad (4.121)$$

which is obtained from the equation of state (4.88) if the condition that the pressure is constant across the boundary layer is taken into account.

The local friction coefficient can be determined from the density distribution and equations (4.108) and (4.109).

Frozen flow of an ideally dissociating gas on a catalytic plate. In frozen flow the rate of chemical reaction is negligibly small compared with the rate of diffusion ($w_A \equiv 0$), so that the concentration distribution as a whole is determined by diffusion processes.

The equation for the conservation of the atomic components (4.112) assumes the following form in the present case:

$$\rho u \frac{\partial c_A}{\partial x} + \rho v \frac{\partial c_A}{\partial y} = \frac{\partial}{\partial y}\left[(\mu + \varepsilon) \frac{\partial c_A}{\partial y}\right]. \qquad (4.122)$$

In this case the need for a conservation equation for the molecular component c_{A_2} disappears, since for binary mixtures, $c_{A_2} = 1 - c_A$.

From equations (4.110) and (4.122) and the boundary condition (4.101) it follows that the velocity and concentration fields are similar:

$$\frac{u}{U_e} = \frac{c_A - c_{Aw}}{c_{Ae} - c_{Aw}}. \qquad (4.123)$$

The boundary condition (4.65) can be used for determining the concentration of atoms at the wall; if the order of the catalytic reaction is taken to be unity

(which occurs for air at not too large values of the wall temperature), the condition can be simply rearranged to give

$$\tau_w \left(\frac{dc_A}{d\bar{u}}\right)_w = \rho_w k_w U_e c_{Aw}. \tag{4.124}$$

If the derivative $(dc_A/d\bar{u})_w$ is determined from equation (4.123), the following expression is obtained for the concentration at the wall from equation (4.124): /243

$$c_{Aw} = c_{Ae}(1 + A_w)^{-1}, \quad A_w = \frac{\rho_w k_w U_e}{\tau_w}. \tag{4.125}$$

When $k_w = 0$, which corresponds to the case of an absolutely noncatalytic wall, $c_{Aw} = c_{Ae}$, i.e., the concentration of atoms in the boundary layer is constant over the cross section and is equal to the value at the outer edge of the boundary layer (this corresponds to equation (4.123)).

When $k_w \to \infty$, which corresponds to the case of an absolutely catalytic wall, $c_{Aw} \to 0$, i.e., all the atoms which diffuse to the wall recombine there.

By solving equation (4.123) for c_A, a dependence of the concentration of atoms on the velocity is obtained

$$c_A = c_{Aw} + (c_{Ae} - c_{Aw})\bar{u}. \tag{4.126}$$

Then by substituting equation (4.126) into equation (4.116), and solving for the temperature, it is found that

$$\bar{T} = \frac{T}{T_d} = \frac{[\bar{h}_w + (\bar{H}_e - \bar{h}_w)\bar{u} - (c_{Ae} - c_{Aw})\bar{u} - \bar{\beta}\bar{u}^2 - c_{Aw}]}{[1 + c_{Aw} + (c_{Ae} - c_{Aw})\bar{u}]}. \tag{4.127}$$

Here $\bar{\beta}$, $\bar{h}_w$, $\bar{H}_e$ are given by equation (4.117), and c_{Aw} is given by equation (4.125).

The density and friction can be determined from equations (4.121) and (4.108), (4.109).

Nonequilibrium flow of an ideally dissociating gas [108]. In order to determine the dependence of the density on velocity it is necessary to establish relationships between the temperature and velocity and concentration, and between the concentration and velocity and temperature. The dependence of the temperature on the velocity and concentration is not difficult to obtain from equation (4.116), which was obtained without any assumptions as to the thermochemical state of the flow in the boundary layer, by solving it for the temperature:

$$\overline{T} = [\overline{h}_w + (\overline{H}_e - \overline{h}_w)\,\overline{u} - \overline{\beta}\,\overline{u}^2 - c_A]\,[4 + c_A]^{-1}. \qquad (4.128)$$

/244

In order to establish the relationship between the concentration and the velocity and temperature it is necessary to return to the conservation equation of the atomic components, written in terms of Crocco variables. These equations can easily be obtained from equations (4.98) and (4.100) by substituting in them $dp/d\xi = 0$, $Sc_i = 1$. By combining in this way the simplified forms of equations (4.98) and (4.100) it is found that

$$\rho u \frac{\partial c_A}{\partial \xi} = \frac{\tau^2}{\mu + \varepsilon} \frac{\partial^2 c_A}{\partial u^2} + w_A. \qquad (4.129)$$

For simplicity it will be assumed that the concentration is a function only of the velocity u, and is independent of the longitudinal coordinate ξ, i.e., $\partial c_A / \partial \xi = 0$ (an implicit dependence on the physical coordinate x is retained, since $c_A = c_A\,[u(x, y)]$). As a basis for this assumption it can be noted that it is strictly satisfied if the motion in the boundary layer is frozen or of the equilibrium type (see the previous subsections of the present section). Consequently, it can be expected that the explicit dependence $c_A(\xi)$ will be sufficiently feeble that it can be neglected *.

With this assumption, equation (4.129) becomes

$$\frac{d^2 c_A}{du^2} = -\frac{\mu + \varepsilon}{\tau^2} w_A. \qquad (4.130)$$

By integrating equation (4.130) twice and evaluating the integration constants from the conditions at the wall, it is found that

/245

$$c_A = c_{Aw} + \left(\frac{dc_A}{du}\right)_w u - \int_0^u du \int_0^u \frac{\mu + \varepsilon}{\tau^2} w_A\, du. \qquad (4.131)$$

By using the boundary condition (4.124) and the conditions at the outer edge of the boundary layer ($c_A = c_{Ae}$ when $u = U_e$), a relationship is obtained for determining the concentration of atoms at the wall in the presence of a surface catalytic reaction:

---

*The principle proposed here as the basis for considering nonequilibrium flow can be termed the principle of local similarity for a turbulent boundary layer by analogy with the well known principle introduced by L. Liz for practical calculations of laminar boundary layers. According to this principle, the concentration and temperature (enthalpy) profiles at each cross section can be regarded as being similar to the velocity profile.

$$c_{Aw}=\left(c_{Ae}+\int_0^{U_e} du \int_0^u \frac{\mu+\varepsilon}{\tau^2} w_A\, du\right)(1+\Lambda_w)^{-1}, \tag{4.132}$$

where A_w is determined from equation (4.125).

Later it is more convenient to write equation (4.131) in the following form, which is easily obtained by using the condition at the outer edge of the boundary layer:

$$c_A = c_{Aw} + [c_{Ae} - c_{Aw} + I(1)]\,\bar{u} - I(\bar{u}). \tag{4.133}$$

Here

$$I(\bar{u}) = U_e^2 \int_0^{\bar{u}} d\bar{u} \int_0^{\bar{u}} \frac{\mu+\varepsilon}{\tau^2} w_A\, d\bar{u}. \tag{4.134}$$

It follows from equation (4.133) that when the effect of the nonequilibrium nature of the dissociation process on the concentration distribution of atoms in the boundary layer is taken into account, this is equivalent to evaluating the value of $I(\bar{u})$. In the special case of frozen flow in the boundary layer ($w_A = 0$), $I(\bar{u}) = 0$, and the concentration distribution of the atoms in the boundary layer is given by equation (4.126).

For determining the value of $I(\bar{u})$, it can be written in the form

$$I(\bar{u}) = U_e^2 \int_0^{\bar{u}} d\bar{u} \int_0^{\bar{u}} \frac{w_A\, d\bar{u}}{\tau_w \left(\frac{\partial u}{\partial y}\right)}. \tag{4.135}$$

By converting the part of equation (4.135) within the integral sign to the universal coordinates (3.8) and substituting the expression for the mass rate of formation of the atomic component w_A from equation (4.60), it is found that /246

$$I(\bar{u}) = \frac{\zeta^4}{\mathrm{Re}_{xw}} \frac{\rho_w}{\rho_d} \int_0^{\bar{u}} d\bar{u} \int_0^{\bar{u}} C_r \left(\frac{\rho}{\rho_w}\right)^3 (1+c_A) \frac{c_A^{(e)'} - c_A^2}{1 - c_A^{(e)^2}} \frac{d\eta}{d\varphi}\, d\bar{u}. \tag{4.136}$$

Here

$$C_r = \frac{\frac{x}{U_e}}{\frac{m_A^2}{k_r \rho_d \rho_w}}, \qquad \mathrm{Re}_{xw} = \frac{U_e \rho_w x}{\mu_w}. \tag{4.137}$$

It is not difficult to see that the quantity C_r represents the Damköhler number, equation (4.102). The physical significance of this quantity was considered in detail in Section 22. When dissociation reactions are being considered, C_r is sometimes termed the recombination parameter. If this parameter is large, the flow will be of the equilibrium type, and if it is small, of the frozen type.

The quantity $d\eta/d\varphi$ which appears in equation (4.136) is defined by equation (4.104) in the turbulent core and by equation (4.106) in the laminar sublayer. The friction parameter ζ is given by equation (3.8), and the equilibrium concentration of atoms $c_A^{(e)}$ is found from equation (4.68).

The method of successive approximations is used for calculating the concentration profiles from equation (4.133). Preliminary calculations are made of the boundary layer characteristics $c_A(u)$, $T(u)$, $\rho(u)$, c_f and ζ for frozen and equilibrium flow (see the previous parts of the present Section). As a zero approximation for the concentration of atoms it is possible to assume either the concentration of atoms in a frozen flow (the parameters of a frozen flow are subsequently denoted by the superscript f), i.e., $c_A^{(0)} = c_A^{(f)}$, or by the arithmetic mean of the concentrations in frozen and equilibrium flow, i.e., $c_A^{(0)} = 1/2\,(c_A^{(f)} + c_A^{(e)})$ where the superscript e denotes an equilibrium quantity. The dependence of concentration on velocity is determined from equation (4.133) to a first approximation to give $c_A^{(1)}$, and then the temperature and density $T^{(1)}$ and $\rho^{(1)}$ are determined from equations (4.128) and (4.121). From the known density distributions according to equations (4.109), (3.8), (4.104) and (4.106), the values of $c_f^{(1)}$, $\zeta^{(1)}$, $(d\eta/d\varphi)^{(1)}$, etc., are determined. /247

Figures 60 - 64 show the calculated results for the boundary layer flow on a wedge of half-angle 30° along which oxygen flows at U_∞ = 7 km/sec with a pressure and temperature in the approaching stream of $p_\infty = 2.85 \cdot 10^{-4}$ atm and T = 220°K *. The wall temperature was assumed to be 720°K. The values of the characteristic parameters and the recombination rate constant for oxygen were taken to have the values given in Tables 18 and 14. In these figures, the letters (e), (f) and (ne) refer respectively to the equilibrium, frozen, and nonequilibrium types of flows in the boundary layer.

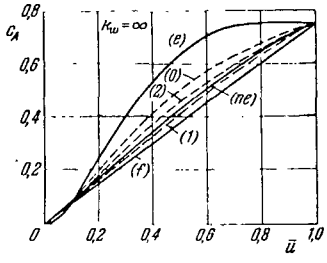

Figure 60.

*The calculations were carried out by O. K. Zakharova at the request of the author.

Figure 60 shows the dependence of the concentration of oxygen atoms on the velocity over the cross section of the boundary layer on an absolutely catalytic wall ($k_w = \infty$). In order to illustrate the process of convergence of the method of calculating a nonequilibrium flow, this figure also shows the curves (dashed) which are obtained in the various approximations (the numbers on the curves indicate the numbers of the approximations). As can be seen from Fig. 60, the convergence of the method is quite satisfactory.

For the same flow conditions, Fig, 61 shows the dependence of the temperature on the velocity in the boundary layer; Fig. 62 gives the velocity profiles for equilibrium , frozen and nonequilibrium flows in the boundary layer (see equations (4.103) and (4.105)). In addition, the velocity profile in an incompressible fluid is also shown in Fig. 62 (see equation (3.4)); this profile is indicated by nc. /248
Also given is a velocity profile calculated for the same external conditions and conditions on the surface of the wedge as used for curves (e), (f) and (ne), but without taking dissociation in the boundary layer into account (see equation (3.99)). This profile is indicated by (c). The curves in Fig. 62 were obtained for $k_w = \infty$.

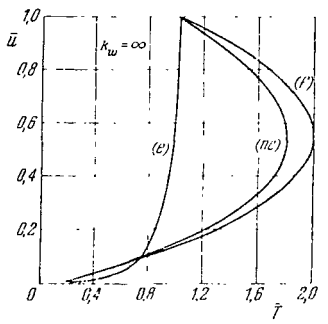

Figure 61.

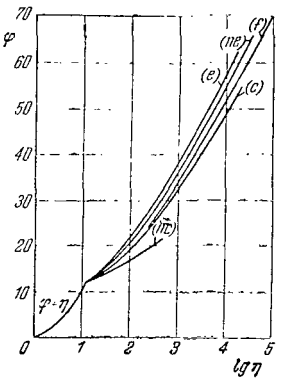

Figure 62.

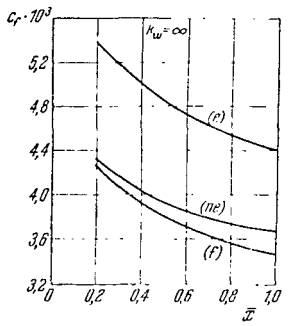

Figure 63.

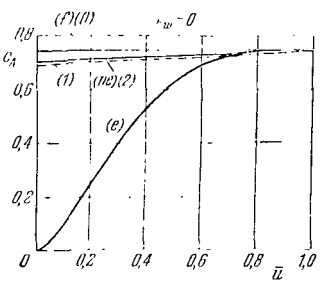

Figure 64.

Figure 63 shows graphs of the local friction coefficient on a wedge as functions of the longitudinal coefficient. It can be seen from the figure that in this case the friction in equilibrium flow appreciably exceeds (by about 1.3 times) the friction in frozen flow. This illustrates that in computing drag it is necessary to quite accurately take into account the nature of the thermodynamic processes taking place in the boundary layer. /249

Figure 64 gives the concentration of oxygen atoms in the boundary layer as a function of the velocity in the boundary layer on an absolutely noncatalytic surface ($k_w = 0$). The concentration distribution in a frozen stream was used as the zeroth approximation for calculating nonequilibrium flow in this case. It can be seen from this figure (notation is the same as in Fig. 60) that making allowance for nonequilibrium dissociation leads to a considerable change in the concentration profile compared with frozen flow.

The method for calculating friction in an ideally dissociating gas which has been proposed in this section can be generalized if required to the case of flow of a partially excited dissociated gas, the properties of which were described in Section 21.

25. Heat and mass transfer in a boundary layer on a flat plate at Prandtl and Schmidt numbers different from unity

It has been already mentioned (Section 22) that as a result of the increase in relative thickness of the laminar sublayer in hypersonic flows, molecular heat conduction and diffusion play an increasingly important part in heat and mass transfer processes in turbulent boundary layers. In some cases, this circumstance makes it necessary to take into account quite accurately the thermal and diffusional properties in determining heat and mass transfer to surfaces.

To a first approximation, these effects can be taken into account by giving up the assumption that the Prandtl and Schmidt numbers are equal to unity, assuming that these numbers are constant over the thickness of the laminar sublayer and equal to their values at the wall. However, if the laminar sublayer occupies a substantial part of the total turbulent boundary layer (20 - 30% or more), this approximation becomes inadequate. Actually, the Prandtl and Schmidt numbers in dissociating air depend on the degree of dissociation. Approximate evaluations made by Dorrens [92] for dissociating oxygen led to the following dependences for these criteria on the degree of dissociation: /250

$$\mathrm{Pr} = \mathrm{Pr}_0 \frac{(1 + 0{,}25\, c_O)(1 + c_O)}{1 + 1{,}62\, c_O}, \quad \mathrm{Sc} = \mathrm{Sc}_O (1 + c_O). \tag{4.138}$$

Here c_O is the concentration of atomic oxygen. From these relationships it is not difficult to evaluate the dependence of the Lewis number on the degree of dissociation:

$$\mathrm{Le} = \mathrm{Le}_0 \frac{1 + 0{,}25\, c_O}{1 + 1{,}62\, c_O}. \qquad (4.139)$$

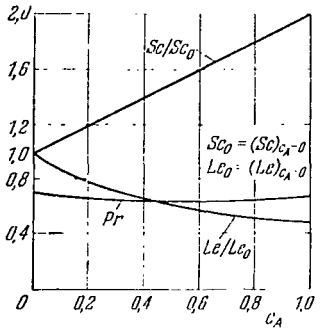

Figure 65.

The results of calculations carried out according to these formulas are shown in Fig. 65. It can be seen that the Prandtl number varies relatively little with change in the degree of dissociation. At the same time, the Schmidt number varies by a factor of almost two. Subsequent comparison of these relationships with more accurate results showed that this type of behavior of the Prandtl and Schmidt numbers is retained for air also. Thus, if in the laminar sublayer the change in concentration of atoms is such that the Schmidt number is subject to considerable change over the thickness of the sublayer, it becomes necessary to take these changes into account.

Within the framework of the two-layer model of the turbulent boundary layer, the difference of the Prandtl and Schmidt numbers from unity leads to the fact that the thicknesses of the laminar sublayers for the dynamic, thermal and diffusion boundary layers are all different in the general case. It is not difficult to show that by using the equations of motion, energy and conservation of the i^{th} component in the laminar sublayer that /251

$$\eta_{1t} = \frac{\eta_1}{\sqrt{\mathrm{Pr}}}, \quad \eta_{1d} = \frac{\eta_1}{\sqrt{\mathrm{Sc}}}. \qquad (4.140)$$

The subscripts "t" and "d" refer respectively to "thermal" and "diffusional" conditions.

By considering (4.140) it can be seen that if Pr < 1 and Sc < 1 (which occurs in dissociating air), the thicknesses of the thermal and diffusional laminar sublayers will be larger than the thickness of the dynamic sublayer. In this case the thermal and diffusional sublayers occupy a part of the turbulent core with the logarithmic velocity profile (Fig. 66). Bearing this fact in mind, it is not difficult to evaluate the difference in the dimensionless velocities at the edges of the dynamic, thermal and diffusion boundary sublayers. Actually, if the velocity profile of an incompressible fluid (3.100) is assumed approximately for the turbulent core, and equation (4.140) is used, it is found that

$$\varphi_{1t} = \varphi_1 - 2{,}875 \lg \mathrm{Pr}, \quad \varphi_{1d} = \varphi_1 - 2{,}875 \lg \mathrm{Sc}. \qquad (4.141)$$

Assuming that Pr = 0.72, Sc = 0.5, $\varphi_1 = 11.5$, it is found that

$$\frac{\varphi_{1t}}{\varphi_1} = 1{,}03, \qquad \frac{\varphi_{1d}}{\varphi_1} = 1{,}07.$$

This approximate analysis shows that when Pr < 1 and Sc < 1 (for air), there is no need to take into account differences in the velocities at the edges of the dynamic, thermal and diffusion laminar sublayers, and, as a result, equation (3.31) can be used for determining these velocities.

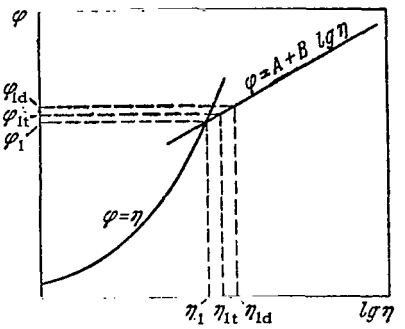

Figure 66.

Relation of total enthalpy to velocity and concentration. Reynolds analogy. Enthalpy of recovery. In order to establish an approximate relationship between the total enthalpy, the velocity, and concentration, let us return to the energy equations in terms of Crocco variables, (4.97) and (4.99). /252

For a flat plate ($dp/d\xi = 0$), and this equation assumes the form

$$\rho u \frac{\mu}{\tau}\frac{\partial H}{\partial \xi} + \frac{\partial \tau}{\partial u}\frac{\partial H}{\partial u} = \frac{\partial}{\partial u}\left\{\tau\left[\frac{1}{\mathrm{Pr}}\frac{\partial H}{\partial u} + \frac{1}{\mathrm{Pr}}\sum_i (\mathrm{Le}_i - 1) h_i \frac{\partial c_i}{\partial u} + \left(1 - \frac{1}{\mathrm{Pr}}\right) u\right]\right\} \qquad (4.142)$$

in the laminar sublayer, and

$$\rho u \frac{\partial H}{\partial \xi} = \frac{\tau^2}{\varepsilon}\frac{\partial^2 H}{\partial u^2} \qquad (4.143)$$

in the turbulent core.

Some further simplifying assumptions can be made; it will be assumed that the total enthalpy is a function of the longitudinal velocity only, i.e., H = H(u). On the basis of this assumption, it can be noted that it is exactly satisfied if the Prandtl and Schmidt numbers are exactly equal to unity. In this case, as was shown in the previous section, there is an integral energy equation (4.119) similar to the Crocco integral. It can therefore be expected that at small deviations of the Prandtl and Schmidt numbers from unity the dependence of the total enthalpy on the longitudinal coordinate H(ξ) will be quite feeble.

Apart from this assumption, it is also assumed, as previously, that the shear stress is constant across the layer, i.e., that $\tau = \text{const} = \tau_w$.

With the use of these assumptions, equations (4.142) and (4.143) assume the following forms:

$$\frac{d}{du}\left[\frac{dH}{du}+\sum_i(\mathrm{Le}_i-1)h_i\frac{\partial c_i}{\partial u}+(\mathrm{Pr}-1)u\right]=0, \tag{4.144}$$

$$\frac{d^2H}{du^2}=0. \tag{4.145}$$

By integrating equation (4.144) and determining the integration constant from the condition at the wall ($q = q_w$ when $u = 0$), it is found that /253

$$\frac{dH}{du}+\sum_i(\mathrm{Le}_i-1)h_i\frac{\partial c_i}{\partial u}+(\mathrm{Pr}-1)u=\frac{\mathrm{Pr}\,q_w}{\tau_w}. \tag{4.146}$$

Here

$$q_w=\frac{\tau_w}{\mathrm{Pr}}\left[\frac{dH}{du}+\sum_i(\mathrm{Le}_i-1)h_i\frac{\partial c_i}{\partial u}\right]_w \tag{4.147}$$

is the heat flux at the wall. It is easy to see that equation (4.147) follows from the definition of the heat flux in a multicomponent mixture, equation (1.79), if only the transport of energy due to thermal conduction and mass diffusion are taken into account.

By integrating (4.146) from 0 to u, and determining the integration constant from the condition that $H = H_w$ when $u = 0$, a relationship is obtained between the total enthalpy and the velocity and concentration in the laminar sublayer:

$$H=h_w+\mathrm{Pr}\frac{2c_h}{c_f}(H_r-H_w)\bar{u}-\sum_i(\mathrm{Le}_i-1)\int_0^{\bar{u}}h_i\frac{\partial c_i}{\partial\bar{u}}d\bar{u}+\frac{1}{2}(1-\mathrm{Pr})U_e^2\bar{u}^2. \tag{4.148}$$

Here $2c_h/c_f$ is the Reynolds analogy parameter

$$c_h=\frac{q_w}{\rho_e U_e(H_r-h_w)}, \tag{4.149}$$

c_h is the dimensionless heat transfer coefficient (Stanton number), H_r is the equilibrium enthalpy of a thermally insulated wall, or the recovery enthalpy (the definitions of H_r and $2c_h/c_f$ will be given below.

In the turbulent core the dependence of the total enthalpy on the velocity and concentration is found by integrating equation (4.145) twice. The first integration

constant is found by assuming that the heat flux is constant across the boundary layer and equal to its value at the wall, i.e., $q = \text{const} = q_w$. The second integration constant is found from the condition at the outer edge, $H \to H_e$ when $u \to U_e$. As a result it is found that /254

$$H = H_e - \frac{2c_h}{c_f}(H_r - h_w)(1 - \bar{u}). \tag{4.150}$$

Let us consider further the case when heat transfer between the gas and the wall is absent ($h_w = H_r$). By equating the total enthalpies from equations (4.148) and (4.150) at the edge of the laminar sublayer and solving the equation which is obtained for H_r, it is found that

$$H_r = h_e + \mathrm{Pr}^{1/3}\frac{U_e^2}{2} + \sum_i(\mathrm{Le}_i - 1)\int_0^{\bar{u}_1} h_i\frac{\partial c_i}{\partial \bar{u}}\,d\bar{u}. \tag{4.151}$$

It should be noted that in obtaining equation (4.151), use was made of the approximate relationship (3.150). The expression (4.151) for the recovery enthalpy H_r is quite general in the sense that it can be used for calculating equilibrium, frozen and nonequilibrium flows.

If the recovery coefficient r is introduced as in a homogeneous gas, i.e.,

$$H_r = h_e + r\frac{U_e^2}{2} \tag{4.152}$$

an expression is obtained by comparing equations (4.151) and (4.152) for the recovery coefficient in a multicomponent gas mixture:

$$r = \mathrm{Pr}^{1/3} + 2\sum_i(\mathrm{Le}_i - 1)\int_0^{\bar{u}_1}\frac{h_i}{U_e^2}\frac{\partial c_i}{\partial \bar{u}}\,d\bar{u}. \tag{4.153}$$

For determining the Reynolds analogy parameter the total enthalpies according to equations (4.148) and (4.150) are equated, and the resulting equation is solved for this parameter, giving /255

$$\frac{2c_h}{c_f} = \mathrm{Pr}^{-2/3}(H_r - h_w)^{-1}\left[h_e + \mathrm{Pr}^{1/3}\frac{U_e^2}{2} - h_w + \sum_i(\mathrm{Le}_i - 1)\int_0^{\bar{u}_1} h_i\frac{\partial c_i}{\partial \bar{u}}\,d\bar{u}\right]. \tag{4.154}$$

The approximate relationships (3.150) and (3.159) are used in deriving equation (4.154).

By using equations (4.149) and (4.154), an expression can be obtained for the heat flux at the wall:

$$q_w = \frac{1}{2} c_f \rho_e U_e \mathrm{Pr}^{-2/3} \left[h_e + \mathrm{Pr}^{1/3} \frac{U_e^2}{2} - h_w + \sum_i (\mathrm{Le}_i - 1) \int_0^{\bar{u}} h_i \frac{\partial c_i}{\partial \bar{u}} d\bar{u} \right]. \qquad (4.155)$$

From the definition of the total enthalpy, equation (4.89), and the condition that the specific heat capacities of the individual components are independent of temperature, an expression is found for the temperature:

$$T = \left(H - \sum_i c_i h_i^0 - \frac{u^2}{2} \right) \left(\sum_i c_i c_{pi} \right)^{-1}. \qquad (4.156)$$

The expressions obtained above for the total enthalpy in the laminar sublayer and turbulent core, the recovery coefficient, the Reynolds analogy parameter, the heat flux and the temperature all contain the so far unknown concentrations of the individual components. Thus, the problem reduces to determining the relationship between the concentration and the velocity in the laminar sublayer and in the turbulent core. The forms of these relationships are different depending on the thermodynamic state of the flow, i.e., depending on whether the flow is equilibrium, frozen, or nonequilibrium.

Equilibrium flow of an ideally dissociating gas [109]. Passing now to the consideration of the equilibrium flow of an ideally dissociating gas, it is useful to note that the difference in enthalpies of the atomic and molecular components can be regarded as approximately equal to the dissociation energy. Actually, bearing in mind that /256

$$h_A = \frac{10}{2} \left(\frac{R}{2M_A} \right) T + h_A^0, \qquad h_M = \frac{8}{2} \left(\frac{R}{2M_A} \right) T + h_M^0,$$

it is found that

$$h_A - h_M = \left(\frac{R}{2M_A} \right) T + (h_A^0 - h_M^0) = \left(\frac{R}{2M_A} \right) T + D \approx D. \qquad (4.157)$$

For gases such as oxygen and nitrogen, this assumption given by equation (4.157) does not lead to appreciable errors in calculation.

Taking equation (4.157) into account, the following expression is obtained from equation (4.148) for the total enthalpy in the laminar sublayer:

$$\bar{H} = \frac{H}{D} = \bar{h}_w + \mathrm{Pr} \frac{2c_h}{c_f} (\bar{H}_r - \bar{h}_w) \bar{u} + (1 - \mathrm{Pr}) \overline{\beta u^2} - (\mathrm{Le} - 1)(c_A - c_{Aw}). \qquad (4.158)$$

The dimensionless quantities $\bar{h}_w$, $\bar{H}_r$ and $\bar{\beta}$ are defined by equation (4.117).

The Reynolds analogy parameter $2c_h/c_f$ and the recovery enthalpy H_r, which in the general case are expressed by equations (4.154) and (4.151), become now

$$\frac{2c_h}{c_f} = \mathrm{Pr}^{-1/3}(\bar{H}_r - \bar{h}_w)^{-1}[\bar{h}_e + \bar{\beta}\mathrm{Pr}^{1/3} - \bar{h}_w + (\mathrm{Le} - 1)(c_{A1} - c_{Aw})], \tag{4.159}$$

$$\bar{H}_r = \frac{H_r}{D} = \bar{h}_e + \bar{\beta}\,\mathrm{Pr}^{1/3}[(\mathrm{Le} - 1)(c_{A1} - c_{Aw})]_r. \tag{4.160}$$

It should be noted that in equations (4.159) and (4.160) the subscript r indicates the parameters determined for the case when heat transfer between the gas and wall is absent.

In an ideally dissociating gas the expression for the heat flux (4.155) becomes /257

$$q_w = \frac{1}{2} c_f \rho_e U_e \mathrm{Pr}^{-2/3} D \times [\bar{h}_e + \bar{\beta}\,\mathrm{Pr}^{1/3} - \bar{h}_w + (\mathrm{Le} - 1)(c_{A1} - c_{Aw})]. \tag{4.161}$$

If use is made of the relationship (4.159), the total enthalpy in the turbulent core (4.150) can be written

$$\bar{H} = \frac{H}{D} = \bar{H}_e - \mathrm{Pr}^{-2/3}[\bar{h}_e + \bar{\beta}\mathrm{Pr}^{1/3} - \bar{h}_w + (\mathrm{Le} - 1)(c_{A1} - c_{Aw})](1 - \bar{u}). \tag{4.162}$$

Analogous rearrangements of the expressions for the total enthalpy in the laminar sublayer (4.158) lead to the following result:

$$\bar{H} = \frac{H}{D} = \bar{h}_w + \mathrm{Pr}^{1/3}[\bar{h}_e + \bar{\beta}\mathrm{Pr}^{1/3} - \bar{h}_w + (\mathrm{Le} - 1)(c_{A1} - c_{Aw})]\bar{u} + (1 - \mathrm{Pr})\bar{\beta}\bar{u}^2 - (\mathrm{Le} - 1)(c_A - c_{Aw}). \tag{4.163}$$

When $\mathrm{Pr} = \mathrm{Le} = 1$, equations (4.162) and (4.163) reduce to equation (4.114) of the previous section.

In the present case the dependence of the concentration of atoms on the pressure and temperature is expressed by equation (4.115).

Equations (4.162), (4.163), (4.156), and (4.115) make it possible in principle to calculate the dependence of the enthalpy, temperature and concentration

on the velocity in the boundary layer. However, for convenience in carrying out the calculations it is advisable to make some rearrangements. By substituting the expression for the enthalpy h (equation (4.74)) into the left-hand part of equation (4.163) and making some simple rearrangements and making use of equation (4.115), the following expression is obtained for the relative velocity $\bar{u}$:

$$\bar{\beta}\bar{u}^2 - a\bar{u} - b = 0, \tag{4.164}$$

where

$$\left.\begin{aligned} a &= \mathrm{Pr}^{-2/3}[\bar{h}_e + \bar{\beta}\mathrm{Pr}^{1/3} - \bar{h}_w + (\mathrm{Le}-1)(c_{A1} - c_{Aw})], \\ b &= \mathrm{Pr}^{-1}\left\{\bar{h}_w + (\mathrm{Le}-1)c_{Aw} - \mathrm{Le}\left[1 + \frac{p_e}{p_d}\frac{1}{\bar{T}}\exp\left(\frac{1}{\bar{T}}\right)\right]\right\}^{-1/2}, \\ \bar{T} &= \frac{T}{T_d}. \end{aligned}\right\} \tag{4.165}$$

/258

By solving equation (4.164), a relationship between the velocity and temperature in the laminar sublayer:

$$\bar{u} = \frac{a \pm \sqrt{a^2 + 4\bar{\beta}b}}{2\bar{\beta}}. \tag{4.166}$$

Similarly, by substituting equation (4.74) into the left part of equation (4.162) and making use of equation (4.115), an expression is obtained relating the temperature and the velocity in the turbulent core:

$$\bar{\beta}\bar{u}^2 - a\bar{u} - c = 0, \tag{4.167}$$

where a is given by the first part of (4.165), and c has the form

$$c = \bar{H}_e - a - 1\bar{T} - \left[1 + \bar{p}_e\bar{T}^{-1}\exp\left(\frac{1}{\bar{T}}\right)\right]^{-1/2}, \quad \bar{p}_e = \frac{p_e}{p_d}. \tag{4.168}$$

By solving equation (4.167) for $\bar{u}$, the dependence of temperature on velocity in the turbulent core becomes

$$\bar{u} = \frac{a \pm \sqrt{a^2 + 4\bar{\beta}c}}{2\bar{\beta}}. \tag{4.169}$$

In equations (4.166) and (4.169) the sign in front of the root is selected from the condition that $\bar{u} \leq 1$.

It is much simpler to determine the concentration and temperature during flow along a thermally insulated wall than in the case of a heat conducting wall, since the coefficient a in equations (4.166) and (4.169) tends to zero. In this case, the value of the temperature at the edge of the laminar sublayer is given by the condition

$$(\bar{\beta}\bar{u}_1^2 = b)_r, \qquad (4.170)$$ /259

where the dimensionless velocity at the edge of the laminar sublayer $\bar{u}_L$ is given by equation (3.31).

When calculations are being carried out by this procedure, it is necessary to have as initial data information on the parameters at the outer edge of the boundary layer (U_e, T_e, p_e) and at the wall (T_w). The concentration of atoms at the outer edge (c_{Ae}) must also be specified. If it is assumed that the external flow is in an equilibrium state, c_{Ae} can be determined for the given value of T_e and p_e from equation (4.115). Similarly, the concentration of atoms at the wall c_{Aw} can be determined from the known values T_w and p_e. In the case of thermochemical equilibrium being considered, the presence of catalytic processes on the wall occurring with a finite velocity will obviously not affect the concentration distribution in the boundary layer.

The calculation of the profiles of the parameters in the boundary layer according to the relationships derived above can be carried out by the method of successive approximations. The quantity which must be made more precise in the course of the calculation can be seen from equation (4.165) to be the concentration at the edge of the laminar sublayer, c_{AL}. As the zeroth approximation for c_{AL} it is possible to assume the value obtained from a calculation with Pr = Sc = 1 (see the previous Section). From the same calculation it is possible to obtain the value of the friction parameter ζ, which is required as a starting point for determining the velocity at the edge of the laminar sublayer $\bar{u}_L$ (equation (3.31)). In this connection it may be noted that usually it is not necessary to obtain successive approximations to $\bar{u}_L$, since the small differences of the Prandtl and Schmidt numbers from unity cause only small effects on the friction parameter ζ.

After determining $\bar{u}_L$, equation (4.166) is used for $0 < \bar{u} < \bar{u}_L$ and equation (4.169) for $\bar{u}_L < \bar{u} < 1$, making it possible to establish the relationship between the temperature and velocity in the boundary layer to the first approximation. In calculating flow along a plate at zero angle of attack, the value of the temperature in equations (4.165) and (4.168) must be selected in the range between the wall temperature and the stagnation temperature. In calculating flow along a plate at some angle of attack, when the temperature value in the boundary layer can be assumed equal to the temperature after the heat of the density jump, the temperature value must be selected in the range between the wall temperature and the temperature at the outer edge (in this case, the temperature in the boundary layer usually varies monotonically).

Once the relationship between the velocity and temperature is established with the use of equation (4.115), the relationship between the concentration and velocity can then be found, etc.

From the known distributions of the concentration and temperature, the dependence of density on velocity (equation (4.121)) can be found, and then the local friction coefficient (4.109)). Knowing the friction coefficient and the parameters at the wall, the edge of the laminar sublayer, and at the outer edge of the boundary layer, the heat flux can be determined from equation (4.161).

The Prandtl, Schmidt and Lewis numbers can be found for the given concentrations of atoms at the wall from the approximate formulas of Dorrance, equations (4.138) and (4.139), using $Pr_0 = 0.7$, $Sc_0 = 0.5$, $Le_0 = 1.4$.

Frozen flow of an ideally dissociating gas on a catalytic wall [110]. In the previous Section it was shown that in the case of frozen flow in a boundary layer ($w_A = 0$) and with the assumption that the Schmidt number is equal to unity, there is a special integral relationship for the conservation of the i^{th} component, equation (4.126), according to which the concentration depends only on the velocity, i.e., $c_A = c_A(u)$. In the case of frozen flow now being considered along a flat plate at Schmidt numbers different to unity, it will be assumed approximately that the concentration primarily depends only on the velocity and is independent of the longitudinal coordinate. It can be expected that when the deviation of the Schmidt number from unity is small, the dependence of the concentration on the longitudinal coordinate $c_A(\xi)$ will be quite feeble. In addition, the simplifying assumption (3.1) that the shear stress is constant across the boundary layer ($\tau = \text{const} = \tau_w$) is made. /261

Using these assumptions, the following equation is obtained from equations (4.98) and (4.100) for determining the concentration in the laminar sublayer and in the turbulent core:

$$\frac{d^2c_A}{d\bar{u}^2} = 0. \tag{4.171}$$

Equation (4.65) is used as a boundary condition for the concentration at the wall, assuming that the order of the catalytic reaction n is equal to unity. By making some simple rearrangements, this expression is reduced to the form

$$\tau_w \left(\frac{dc_A}{d\bar{u}}\right)_w = \rho_w k_w \,\mathrm{Sc}\, U_e c_{Aw}. \tag{4.172}$$

When equation (4.171) is integrated once and the equation (4.172) is used, it is found that

$$\frac{dc_A}{d\bar{u}} = \mathrm{Sc}\, A_w c_{Aw}, \qquad A_w = \frac{\rho_w k_w U_e}{\tau_w}. \tag{4.173}$$

When (4.173) is integrated and the integration constant is determined from the condition at the wall, ($c_A = c_{Aw}$ at $u = 0$), the concentration is found as a function of velocity in the laminar sublayer

$$c_A = c_{Aw}(1 + \mathrm{Sc}\, A_w \bar{u}). \tag{4.174}$$

The derivative of the concentration with respect to the dimensionless velocity at the edge of the laminar sublayer on the side of the turbulent core, $(dc_A/d\bar{u})_{\bar{u} = \bar{u}_L + 0}$, is found from the condition that the diffusion fluxes of the atomic component must be the same on both sides of the boundary between the core and the sublayer:

$$\left(\frac{dc_A}{d\bar{u}}\right)_{\bar{u}=\bar{u}_1+0} = \frac{A}{\mathrm{Sc}}\left(\frac{dc_A}{d\bar{u}}\right)_{\bar{u}=\bar{u}_1-0}. \tag{4.175}$$

Using this equation and the condition at the outer edge of the boundary layer, $c_A = c_{Ae}$ when $u = U_e$, a relationship between the concentration and velocity in the boundary layer (in the turbulent core):

$$c_A = c_{Ac} - c_{Aw} A_w (1 - \bar{u}). \tag{4.176}$$

By equating the concentration values from equations (4.173) and (4.176) at the edge of the laminar sublayer, an expression is obtained for the concentration of atoms at the wall as a function of the catalytic recombination parameter A_w: /262

$$c_{Aw} = c_{Ae}(1 + A_w \mathrm{Sc}^{2/3})^{-1}. \tag{4.177}$$

In the derivation of equation (4.177) use was made of the following approximation.

$$1 - (1 - \mathrm{Sc})\bar{u}_l \approx \mathrm{Sc}^{2/3}. \tag{4.178}$$

If Sc = 0.5, the error in calculating with equation (4.178) does not exceed ± 10% over the range $\bar{u}_L$ from 0.6 to 0.86.

Equations (4.174) and (4.176) can be rearranged to a form not containing the catalytic recombination parameter A_w by eliminating this parameter with the use of equation (4.177). After some simple rearrangements, this gives

$$\left.\begin{aligned} c_A &= c_{Aw} + \mathrm{Sc}^{1/3}(c_{Ae} - c_{Aw})\bar{u}, \\ c_A &= c_{Ae} - \mathrm{Sc}^{2/3}(c_{Ae} - c_{Aw})(1 - \bar{u}). \end{aligned}\right\} \tag{4.179}$$

The first of these equations is valid in the laminar sublayer, and the second in the turbulent core. When the Schmidt number is equal to unity, these equations reduce to equation (4.126) obtained earlier.

From equations (4.174), (4.176), and (4.177) it follows that when $k_w = 0$ (corresponding to flow along an absolutely noncatalytic wall), $c_{Aw} = c_{Ae}$, i.e., the concentration of atoms in the boundary layer is constant over the cross section and equal to the value at the outer edge. When $k_w \to \infty$, which corresponds to flow along an absolutely catalytic wall, $c_{Aw} = 0$, i.e., all the atoms diffusing into the layer recombine.

By using the equations (4.174) and (4.177), and also equations (4.160), (4.159) and (4.161), which are also valid in the case of frozen flow, expressions are obtained for the recovery enthalpy, the Reynolds analogy parameter and the heat flux in a frozen turbulent boundary layer on a flat plate with arbitrary catalytic properties on the surface: /263

$$\bar{I}_r = \bar{h}_e + \bar{\beta}\,\mathrm{Pr}^{1/3} + [(\mathrm{Le}^{2/3} - 1)\,\mathrm{Sc}^{1/3} c_{Ae}\psi_w]_r, \tag{4.180}$$

$$\frac{2c_h}{c_f} = \mathrm{Pr}^{-2/3}(\bar{I}_r - \bar{h}_w)^{-1} \times [\bar{h}_e + \bar{\beta}\,\mathrm{Pr}^{1/3} - \bar{h}_w + (\mathrm{Le}^{2/3} - 1)\,\mathrm{Sc}^{1/3} c_{Ae}\psi_w], \tag{4.181}$$

$$q_w = \frac{1}{2} c_f \rho_e U_e \mathrm{Pr}^{-2/3} D \times [\bar{h}_e + \bar{\beta}\,\mathrm{Pr}^{1/3} - \bar{h}_w + (\mathrm{Le}^{2/3} - 1)\,\mathrm{Sc}^{1/3} c_{Ae}\psi_w]. \tag{4.182}$$

In equations (4.180) to (4.182) the approximation

$$1 + (\mathrm{Le} - 1)\bar{u}_1 \approx \mathrm{Le}^{1/3}, \tag{4.183}$$

is used, and the following function is introduced:

$$\psi_w = \left(1 + \frac{1}{A_w \mathrm{Sc}^{2/3}}\right)^{-1}. \tag{4.184}$$

It is not difficult to see that for an absolutely catalytic wall ($k_w \to \infty$), the function $\psi_w \to 1$, while for an absolutely noncatalytic wall ($k_w = 0$), $\psi_w \to 0$.

If the effects of the catalytic wall on friction (c_f) and the Prandtl and Lewis numbers are not taken into account, by using equation (4.182) it is easy to obtain an equation giving the ratio of the heat flux for an arbitrary rate of the catalytic recombination to the heat flux on an absolutely catalytic wall:

$$\frac{q_w}{(q_w)_{k_w \to \infty}} = 1 - \frac{(\mathrm{Le}^{2/3} - 1)\,\mathrm{Sc}^{1/3} c_{Ae} D}{h_e + \mathrm{Pr}^{1/3}\frac{U_e^2}{2} + (\mathrm{Le}^{2/3} - 1)\,\mathrm{Sc}^{1/3} c_{Ae} D - h_w}(1 - \psi_w). \tag{4.185}$$

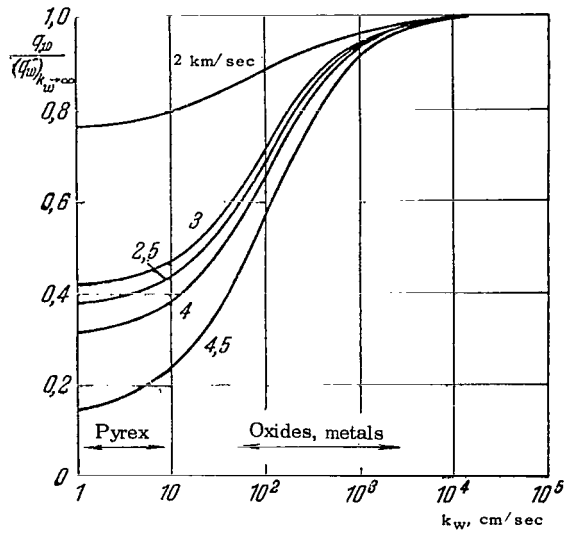

Figure 67.

Equation (4.185) makes it possible to evaluate the effect of the catalyzing ability of the wall on the value of the local heat flux. Figure 67, which is of an illustrative nature, shows the results of calculations according to equation (4.185) /264 for the flow of air along a flat plate. The calculations were carried out for a pressure corresponding to a height of 45 km above the surface of the earth and a wall temperature $T_w = 700°K$. Along the abscissa is plotted the rate constant of the catalytic recombination and ranges of the constant k_w for a series of materials are indicated (for details see Fig. 58). It can be seen from Fig. 67 that the catalyzing ability of the wall has a very powerful effect on the value of the heat flux. This fact makes it possible to conclude that by suitable selection of the material for lining the apparatus it will be possible to considerably decrease heat transfer to the surface. The fact that the curve for a flight velocity of 2.5 km/sec lies below the curve for 3 km/sec arises because nitrogen begins /265 to dissociate after all the oxygen in the outer stream is already dissociated *.

Let us establish a further relationship between the temperature and velocity. By substituting the expression for the enthalpy of an ideally dissociating gas, equation (4.74), into the left-hand part of equation (4.163) and solving the resulting equation for the temperature, the dependence of temperature on velocity in the laminar sublayer is found to be

$$\overline{T} = (4 + c_A)^{-1} \{\overline{h}_w + \mathrm{Pr}^{1/3}[\overline{h}_e + \overline{\beta}\,\mathrm{Pr}^{1/3} - \overline{h}_w + (\mathrm{Le}^{1/3} - 1)\,\mathrm{Sc}^{1/3} c_{Ae} \psi_w]\,\overline{u} - \mathrm{Pr}\,\overline{\beta}\overline{u}^2 + (\mathrm{Le} - 1)\,c_{Aw} - \mathrm{Le}\,c_A\}. \quad (4.186)$$

*Analogous results were obtained for the laminar boundary layer close to a forward stagnation point in the work of Goulard [107].

Here c_A and c_{Aw} are given by equations (4.174) and (4.177).

In a similar way an expression for the dependence of temperature on velocity in the turbulent core is obtained from equation (4.162):

$$\overline{T} = (1 + c_A)^{-1}\{\overline{H}_e - \overline{\beta u^2} - c_A - \mathrm{Pr}^{2/3}[\overline{h}_e + \overline{\beta}\,\mathrm{Pr}^{1/3} - \overline{h}_w + (\mathrm{Le}^{2/3} - 1)\,\mathrm{Sc}^{1/3} c_{Ac}\psi_w](1 - \bar{u})\}. \qquad (4.187)$$

Here c_A and c_{Aw} are given by equations (4.176) and (4.177).

The dimensionless quantities $\bar{h}_e$, $\bar{h}_w$, $\bar{\beta}$, $\bar{T}$ in equations (4.186) and (4.187) are given by equations (4.117) and (4.162). /266

From the known dependences of temperature on velocity and equation (4.121) it is possible to find the density as a function of velocity, which in turn makes it possible to determine the local friction coefficient by means of equation (4.109).

Suitable correlation equations for calculating the friction coefficients during frozen flow in a boundary layer were obtained by Dorrance [111] on the basis of friction calculations over the following wide ranges of the parameters ($10^5 \leq \mathrm{Re} \leq 10^8$; $0 \leq M_e \leq 4$; $0.04 \leq T_w/T_e \leq 1$). This formula has the form

$$\frac{c_f}{c_{f_0}} = 2\left(\frac{1 + c_{Ac}}{1 + c_{Aw}}\right)^{1/3} - 1. \qquad (4.188)$$

Here c_{fo} is the friction coefficient calculated without taking the effects of dissociation (but making allowances for the effects of the Mach number and temperature factor. The results obtained from equation (4.188) differ from the exact results by less than 4%. It follows from equation (4.188) that dissociation leads to changes in the friction coefficient which do not exceed ±22% of the value of c_{fo}. In addition it is easily seen from equation (4.188) that an increase in the catalyzing ability of the wall ($c_{Aw} \to 0$) leads to an increase in the friction coefficient. /267

Figures 68 - 72 show the results of calculations of the boundary layer characteristics during the flow of dissociating oxygen along a plate, using the methods given above [112].

Figures 68 and 69 show the local friction coefficient as a function of the Reynolds number for the two Mach numbers, $M_e = 4$ and $M_e = 10$. In the calculations it was assumed that $T_e = 3600°K$, $p_e = 1$ atm, $\mathrm{Pr} = 0.72$, $\mathrm{Le} = 1.4$, $c_{Aw} = 0$. The calculations of friction without taking dissociation into account were carried out by the method given in Section 12. As can be seen from the graphs, the friction coefficients for frozen gas flows differ from those calculated for the same conditions but in the absence of dissociation by no more than

20%, which is in good agreement with the results of Dorrance (equation (4.188)). In the case of equilibrium dissociation this difference can reach 40%.

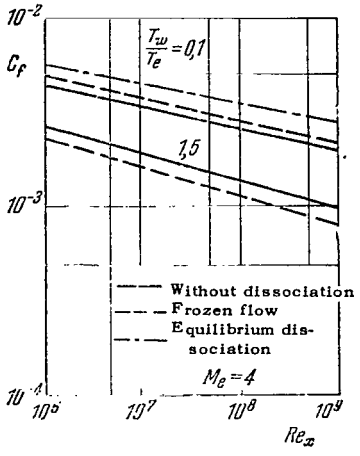

Figure 68.

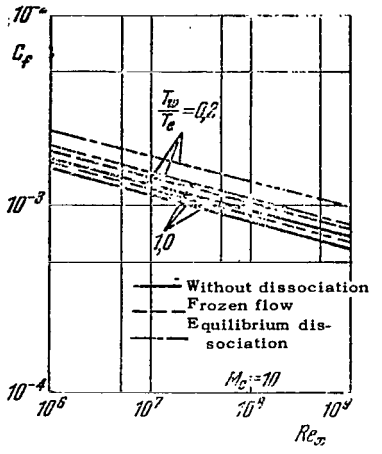

Figure 69.

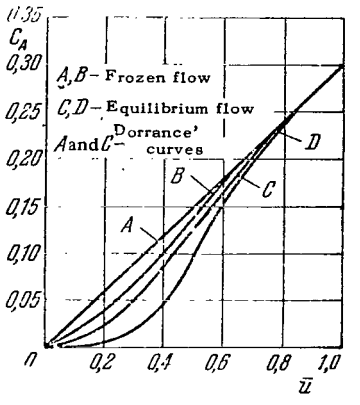

Figure 70.

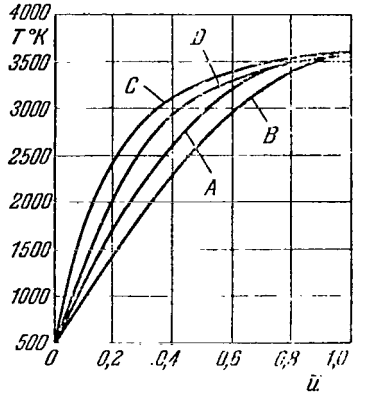

Figure 71.

Figures 70 and 71 show the concentration and temperature as functions of the velocity in frozen flow (curves A, B) and in equilibrium flow (curves C, D) in the boundary layer, calculated for the conditions: $M_e = 2.2$, $T_e = 3600°K$, $T_w = 500°K$, $c_{Ae} = 0.3$, $c_{Aw} = 0$. Curves A and C, which were obtained by Dorrance [113] are shown in Figs. 70 and 71 for comparison. The difference between curves B and D calculated by the procedure of the present Section and Dorrance' curves A and C is due to the fact that in his work Dorrance used relationships

between the total enthalpy, concentration and velocity which were obtained for Pr = Sc = 1 (equations (4.114) and (4.126)), so that in many ways Dorrance's method is analogous to the methods discussed in Section 24. Dorrance took into account the difference of the Prandtl and Schmidt numbers from unity only in setting up the expression for the Reynolds analogy parameter and by directly introducing the recovery coefficient. It should also be noted that in Dorrance's work the contribution of the vibratory degrees of freedom to the heat capacity of the molecules is not taken into account. /268

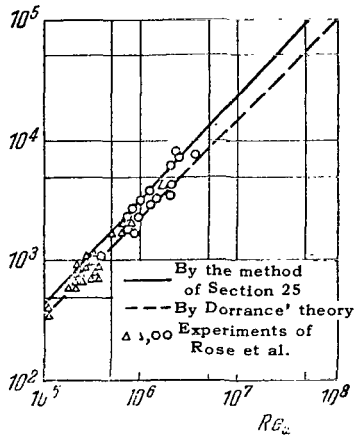

Figure 72.

Figure 72 shows the dependence of the heat transfer coefficient on the Reynolds number obtained by the method being discussed (frozen flow) for the conditions: $M_e = 2$, $T_w/T_e = 0.1$, $c_{Ae} = 0.31$ (the value of c_h^{-1} is plotted on the ordinate axis). For comparison, the relationship calculated by Dorrance (dashed line) is also given on the same figure. The differences between these theoretical relationships is due to the same reasons pointed out in considering Figs. 70 and 71, as well as the fact that in Dorrance's method the formula from the semiempirical Prandtl theory was used in calculating the friction, instead of the von Kármán formula which is used in the present method. Figure 72 also shows the experimental points obtained for heat transfer measurements by Rose et al. [114] on a cylinder with a spherical head. The measurements were carried out in the zone where the longitudinal pressure gradient was close to zero. The experimental points on the graph show a large degree of scatter; nevertheless, the agreement between the experimental data of the calculated results can be considered satisfactory. /269

Nonequilibrium flow of an ideally dissociating gas. The results of the calculations of equilibrium and frozen flow in boundary layers given in the subsections above show conclusively that the thermochemical state of the gas can have an appreciable effect on drag. It is obvious that the nature of the flow in the boundary layer will have an even more important effect in calculating the rate of heat transfer. Of course it is possible to estimate the heat flux at the surface of the body in the two limiting cases considered above - equilibrium and frozen flows. However, it is impossible to solve the problem of the nature of the flow in the boundary layer using the methods given in these sections. In many cases of practical importance it becomes necessary to evaluate heat transfer during the occurrence of dissociation reactions having finite velocities commensurate with the rate of diffusion, which leads to a nonequilibrium type of flow in the boundary layer. Nonequilibrium flow of an ideally dissociating gas was considered in the previous section assuming that the Schmidt and Prandtl numbers are equal to unity. As shown repeatedly above (Chapter III) it is necessary to take into account differences of the Prandtl and Schmidt numbers from unity in calculating heat transfer.

The general expressions for the heat flux q_w, recovery enthalpy H_r Reynolds analogy parameter $2c_h/c_f$, and the relationship between the total enthalpy and concentration and velocity for arbitrary Prandtl and Schmidt numbers were established at the beginning of the present section. In order to solve this problem it remains to establish the relationship between the concentration and velocity. There are reasons based on the arguments discussed during the consideration of nonequilibrium flow for $Pr = Sc = 1$ (Section 24) and for frozen flow for $Pr \neq Sc \neq 1$ (Section 25) for making the simplifying assumption that the concentration depends only on the velocity in the boundary layer and is independent of the longitudinal coordinate, i.e., $c_A = c_A(u)$. In addition the usual /270
assumption is made that the shear stress is constant across the boundary layer, i.e., $\tau = \text{const} = \tau_w$. With these assumptions, equations (4.98) and (4.100) assume the following forms:

$$\frac{d^2c_A}{du^2} = -\mathrm{Sc}\left(\frac{\mu}{\tau}\right)\frac{w_A}{\tau_w}, \quad \frac{d^2c_A}{du^2} = -\left(\frac{\varepsilon}{\tau}\right)\frac{w_A}{\tau_w}. \tag{4.189}$$

The first of these equations is valid in the laminar sublayer, and the second in the turbulent core. Integrating the first of the equations (4.189) using the boundary conditions (4.124), it is found that

$$\frac{dc_i}{d\bar{u}} = \mathrm{Sc}\,A_w c_{Aw} - \mathrm{Sc}\,I_1(\bar{u}). \tag{4.190}$$

Here

$$I_1(\bar{u}) = U_e^2\int_0^{\bar{u}}\left(\frac{\mu}{\tau}\right)\frac{w_A}{\tau_w}\,d\bar{u}, \tag{4.191}$$

and the quantity A_w is given by the second of equations (4.125).

It should be noted that the concentration of atomic components at the wall (c_{Aw}) is still an unknown quantity and will be determined later.

By integrating equation (4.190) and determining the integration constant from the condition at the wall ($c_A = c_{Aw}$ when $\bar{u} = 0$), the concentration distribution in the laminar sublayer is found as

$$c_A = c_{Aw}(1 + \mathrm{Sc}\,A_w\bar{u}) - \mathrm{Sc}\,I_1(\bar{u}), \tag{4.192}$$

where

$$I_1(\bar{u}) = U_e^2\int_0^{\bar{u}} d\bar{u}\int_0^{\bar{u}}\left(\frac{\mu}{\tau}\right)\frac{w_A}{\tau_w}d\bar{u}.$$

Let us now pass to the determination of the concentration profile in the turbulent core. By integrating the second of equations (4.189) once, it is found that

$$\frac{dc_A}{d\bar{u}} = \left(\frac{dc_A}{d\bar{u}}\right)_{\bar{u}=\bar{u}_1+0} - I_T(\bar{u}),$$

$$I_T(\bar{u}) = U_e^2 \int_{\bar{u}_1}^{\bar{u}} \left(\frac{\varepsilon}{\tau}\right)\frac{m_A}{\tau_w}\,d\bar{u}. \qquad (4.193)$$

Here $\bar{u}_L$ is the dimensionless velocity at the edge of the laminar sublayer, defined by equation (3.31). /271

The derivative of the concentration with respect to the dimensionless velocity at the edge of the laminar sublayer on the side of the turbulent core, $(dc_A/du)_{\bar{u}=\bar{u}_L+0}$, is determined from the condition that the diffusion fluxes of the atomic component on both sides of the interface between the sublayer and turbulent core (4.175) must be equal. Using this condition and equation (4.190), it is found that

$$\left(\frac{dc_A}{d\bar{u}}\right)_{\bar{u}=\bar{u}_1+0} = A_w c_{Aw} - I_1(\bar{u}_1). \qquad (4.194)$$

By substituting equation (4.194) into equation (4.193) and carrying out a further integration, and then determining the integration constant from the condition at the outer edge ($c_A = c_{Ae}$ when $\bar{u} = 1$), the concentration distribution in the turbulent core is found to be

$$c_A = c_{Ae} + I_T(1) - I_T(\bar{u}) - (1-\bar{u})[A_w c_{Aw} - I_1(\bar{u}_1)], \qquad (4.195)$$

where

$$I_T(\bar{u}) = U_e^2 \int_{\bar{u}_1}^{\bar{u}} d\bar{u} \int_{u_1}^{\bar{u}} \left(\frac{\varepsilon}{\tau}\right)\frac{m_A}{\tau_w}\,d\bar{u}.$$

By equating the concentration values from equations (4.192) and (4.195) at the boundary between the sublayer and turbulent core and solving the resulting equation for the concentration at the wall, the following expression is obtained:

$$c_{Aw} = (1 + Sc^{1/3}A_w)^{-1} \times [c_{Ae} + I_T(1) + Sc\, I_1(\bar{u}_1) + (1-\bar{u}_1) I_1(\bar{u}_1)]. \qquad (4.196)$$

Equation (4.178) is used in the derivation of (4.196).

The concentration distribution in the laminar sublayer (4.192) and in the turbulent core (4.195) are sometimes more convenient to use in a form not containing the catalytic recombination parameter A_w. By eliminating A_w from equations (4.192) and (4.195) using equation (4.196), we find for the laminar sublayer /272

$$c_A = c_{Aw} + \mathrm{Sc}^{1/3}(c_{Ae} - c_{Aw})\bar{u} + \mathrm{Sc}^{1/3}[I_T(1) + \mathrm{Sc}\, I_1(\bar{u}_1) + (1 - \bar{u}_1)\dot{I}_1(\bar{u}_1)]\bar{u} - \mathrm{Sc}\, I_1(\bar{u}), \tag{4.197}$$

and in the turbulent core

$$c_A = c_{Ae} - \mathrm{Sc}^{2/3}(c_{Ae} - c_{Aw})(1 - \bar{u}) + I_T(1) - I_T(\bar{u}) - \mathrm{Sc}^{2/3}[I_T(1) + \mathrm{Sc}\, I_1(\bar{u}_1)](1 - \bar{u}) + \mathrm{Sc}^{1/3}\bar{u}_1 \dot{I}_1(\bar{u}_1)(1 - \bar{u}). \tag{4.198}$$

In frozen flow ($w_A = 0$), the functions I_T, I_L and $\dot{I}_L$ tend to zero, and equations (4.197) and (4.198) reduce to equation (4.179) of the present section.

The dimensionless integral complexes I_L and I_T (4.192) and (4.195)) which appear in the concentration distributions characterize the overall "strength" of the sources of formation of atomic components included in some volume, the extent of which in the direction of the y axis is determined by the limits of integration, while the base area can be taken to be unity. The expressions for these complexes can be obtained similarly to the way in which the expression for the complex $I(\bar{u})$ (4.136) was obtained in the previous section. Omitting the simpler details, it need only be said that the final expressions for these complexes are:

$$I_1(\bar{u}) = \frac{\zeta^4}{\mathrm{Re}_{xw}} \frac{\rho_w}{\rho_d} \int_0^{\bar{u}} d\bar{u} \int_0^{\bar{u}} C_r \left(\frac{\rho}{\rho_w}\right)^3 (1 + c_A) \frac{c_A^{(e)2} - c_A^2}{1 - c_A^{(e)2}} \frac{d\eta}{d\varphi}\, d\bar{u}, \tag{4.199}$$

$$I_T(\bar{u}) = \frac{\zeta^4}{\mathrm{Re}_{xw}} \frac{\rho_w}{\rho_d} \int_{\bar{u}_1}^{\bar{u}} d\bar{u} \int_{\bar{u}_1}^{\bar{u}} C_r \left(\frac{\rho}{\rho_w}\right)^3 (1 + c_A) \frac{c_A^{(e)2} - c_A^2}{1 - c_A^{(e)2}} \frac{d\eta}{d\varphi}\, d\bar{u}. \tag{4.200}$$

Here ζ is the friction parameter (3.8), C_r is the recombination parameter (4.137), Re_{xw} is the Reynolds number (4.137), $d\eta/d\varphi$ is a quantity defined by equation (4.104) in the turbulent core and by equation (4.106) in the laminar sublayer. The equilibrium concentration of atoms $c_A^{(e)}$ is given by equation (4.68). /273

The complex $\dot{I}_L(\bar{u})$ which is still required for calculating the concentration distribution is given by

$$\dot{I}_1(\bar{u}) = \frac{dI_1(\bar{u})}{d\bar{u}}. \tag{4.201}$$

The value of the velocity at the edge of the laminar sublayer $\bar{u}_L$ can be found from equation (3.31).

The calculation of the concentration profiles by equations (4.197) and (4.198) or (4.192) and (4.195) can be carried out by the method of successive approximations. The calculation procedure is the same as in the calculation of nonequilibrium flow when $\mathrm{Pr} = \mathrm{Sc} = 1$ (see Section 14).

In equations (4.197) and (4.198) the first two terms in the right-hand parts give the contribution of diffusion to the concentration distribution, and all the remaining terms containing the complexes I_L, I_T, $\dot{I}_L$ characterize the contribution of the chemical reaction to this distribution. The interaction of the diffusion and chemical reaction on one another appears through the concentration at the wall, c_{Aw}, equation (4.196), which depends on the rates of both processes. The nature of the flow in the boundary layer is determined by the relative contributions of the diffusion and chemical reaction processes in the concentration distribution. With a value of the recombination parameter $C_r = \infty$, the contribution of the chemical process is infinitely large compared with the diffusion contribution (the sum of the terms containing the integral complexes in equations (4.197), (4.198) will be infinitely large compared with the diffusion term). In this case there will be equilibrium motion, and the concentration distribution can be determined from the condition $w_A = 0$. In the other limiting case when the recombination parameter is equal to zero ($C_r = 0$), the diffusion process will be controlling (frozen flow). This, the object of the calculation reduces to establishing the roles played by the diffusion process and chemical reaction in the transport processes in the boundary layer.

Once the concentration distributions (4.197), (4.198) are known, it is not difficult to obtain expressions for the Reynolds analogy parameter, the recovery enthalpy, and the heat flux during nonequilibrium flow in the boundary layer. /274
Equations (4.159) and (4.161) are used for this purpose, substituting in them the value of c_{AL} from (4.197).

As a result it is found that

$$\frac{2c_h}{c_f} = \mathrm{Pr}^{-2/3}(\bar{I}_r - \bar{h}_w)^{-1}\{\bar{h}_e + \bar{\beta}\,\mathrm{Pr}^{1/3} - \bar{h}_w + (\mathrm{Le}^{2/3} - 1)\,\mathrm{Sc}^{1/3}(c_{Ae} - c_{Aw}) + (\mathrm{Le}^{2/3} - 1)\,\mathrm{Sc}^{1/3}[I_T(1) + \mathrm{Sc}\,I_1(\bar{u}_1) + (1 - \bar{u}_1)\,\dot{I}_1(\bar{u}_1)] - (\mathrm{Le} - 1)\,\mathrm{Sc}\,I_1(\bar{u}_1)\}, \quad (4.202)$$

$$\bar{H}_r = \bar{h}_e + \bar{\beta}\,\mathrm{Pr}^{1/3} + \{(\mathrm{Le}^{2/3} - 1)\,\mathrm{Sc}^{1/3}(c_{Ae} - c_{Aw}) + (\mathrm{Le}^{2/3} - 1)\,\mathrm{Sc}^{1/3}[I_T(1) + \mathrm{Sc}\,I_1(\bar{u}_1) + (1 - \bar{u}_1)\,\dot{I}_1(\bar{u}_1)] - (\mathrm{Le} - 1)\,\mathrm{Sc}\,I_1(\bar{u}_1)\}_r, \quad (4.203)$$

$$q_w = \frac{1}{2}c_f\rho_e U_e\,\mathrm{Pr}^{-2/3}D\{\bar{h}_e + \bar{\beta}\,\mathrm{Pr}^{1/3} - \bar{h}_w + (\mathrm{Le}^{2/3} - 1)\,\mathrm{Sc}^{1/3}(c_{Ae} - c_{Aw}) + (\mathrm{Le}^{2/3} - 1)\,\mathrm{Sc}^{1/3}[I_T(1) + \mathrm{Sc}\,I_1(\bar{u}_1) + (1 - \bar{u}_1)\,\dot{I}_1(\bar{u}_1)] - (\mathrm{Le} - 1)\,\mathrm{Sc}\,I_1(\bar{u}_1)\}. \quad (4.204)$$

The value of the concentration at the wall in equations (4.202) - (4.204) is determined from equation (4.196), and the integral complexes I_T, I_L, I'_L by equations (4.199) - (4.201). The subscript r in equation (4.203) indicates the condition of a thermally insulated wall.

The enthalpy distribution in the boundary layer is determined from equation (4.163) in the laminar sublayer and (4.162) in the turbulent core after substituting in them from equations (4.197) and (4.198) respectively.

The temperature distribution corresponding to a given enthalpy distribution is not difficult to obtain from equation (4.74), which can be solved for the temperature. As a result it is found that

$$\overline{T} = (4 + c_A)^{-1}(\overline{H} - \overline{\beta u^2} - c_A). \qquad (4.205)$$

In addition, from equations (4.121) and (4.109) it is possible to determine the density in the boundary layer and the local friction coefficient on the wall.

Figure 73 gives the results of calculations of the local heat flux on a wedge with a half-angle of 30°, along which oxygen flows with a velocity of U_∞ = 7 km/sec at a temperature and pressure in the approaching stream of T = 220°K and $p_e = 2.85 \times 10^{-4}$ atm. The wall temperature was assumed equal to 720°K. The heat flux calculations for frozen (see equation (4.182); dotted lines) and nonequilibrium (see equation (4.204); solid curves) flow in the boundary layer were made for a series of values of the catalytic recombination parameter A_{w1} in the range 0 to ∞ (this parameter differs from the catalytic recombination parameter A_w (see equation (4.125)) used in this section only by having an additional multiplier ($A_{w1} = Sc^{2/3}A_w$)).

/275

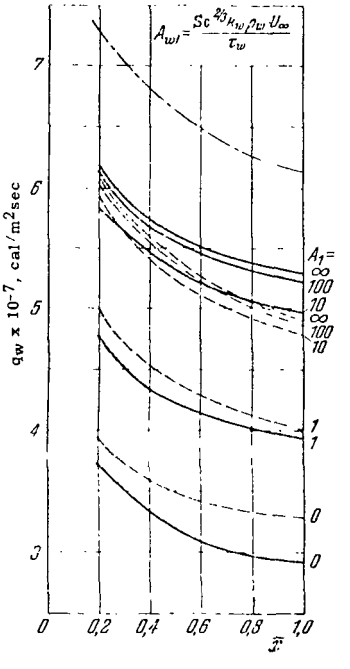

Figure 73.

It should be noted that a value of the parameter $A_{w1} = 0$ corresponds to flow along an absolutely noncatalytic surface, while a value of $A_{w1} = \infty$ corresponds to flow along an absolutely catalytic surface. The value of the heat flux during equilibrium flow (the chain-dotted curve) was determined from equation (4.161).

It should also be noted that the value of the local friction coefficient which is required for calculating the heat flux according to equations (4.161), (4.182) and (4.204) was calculated by the method proposed in the previous Section (i.e., with the assumption that the Prandtl and Schmidt numbers are constant and equal to unity).

26. Conclusions /276

It is not difficult to see that the methods for calculating friction and heat transfer in turbulent boundary layers of dissociating gases which are contained in this chapter represent further developments of the methods of calculating flows of homogeneous gases contained in Chapter III (Sections 12 and 15). In addition, it is also necessary to mention that there is a series of works by Soviet and foreign authors in which the approach to the problem of the turbulent boundary layer in a dissociating gas differs to a greater or lesser degree from the approach taken in this Chapter.

The case of equilibrium dissociation in a turbulent boundary layer on a flat plate was considered by S. I. Kosterin and Yu. A. Koshmarov [115]. As a basis for the investigation, they assumed a model of an ideally dissociating gas and the semiempirical theory of Prandtl. The Prandtl and Schmidt numbers and their turbulent analogs were assumed equal to unity. In many respects, the method of Kosterin and Koshmarov is analogous to the method proposed in Section 24.

The effect of equilibrium dissociation on friction and heat transfer on a flat plate with Prandtl and Schmidt numbers different to unity was considered in a paper by I. P. Ginzburg [116]. The semiempirical theory of Prandtl was used in this work for calculating friction.

A method for calculating skin friction and heat transfer on a flat plate for equilibrium and frozen flows was proposed by Dorrance. The main features of this method and some of the calculated results have been considered in Section 25 (see the discussion of Dorrance's results).

The calculation of heat transfer from a nonequilibrium turbulent boundary layer to a catalytic boundary surface was carried out by Kulgein [117]. In this paper the nonequilibrium nature of the dissociation process was taken into /277
account only in the laminar sublayer, while in the turbulent core the flow was assumed to be of the frozen type. Calculations of heat transfer for various flow conditions in the external stream and at the wall were carried out on a electronic computer.

The methods of calculating friction and heat transfer in an ideally dissociating gas (binary mixture of atoms and molecules) which are proposed in Sections 24 and 25 can be generalized without difficulty to the case of flowing multicomponent mixtures. With this in mind, in Section 25 particularly, expressions were obtained for the total enthalpy, Reynolds analogy parameter, recovery enthalpy and heat flux in a multicomponent mixture. The calculation of the concentration fields in equilibrium and frozen flows in multicomponent

mixture does not differ in principle from the calculations of the same fields in binary mixtures. In order to calculate nonequilibrium flows of multicomponent mixtures it is necessary to have data on the mass rates of formation of the components, which are contained in Section 20 of Chapter IV.

These methods are easily generalized to the flow of partially excited dissociating gases, the properties of which were described in detail in Sections 20, 21.

Finally, with the approximations made in Sections 17, 18, and using the formulas obtained in Sections 17, 18 of Chapter IV, it is possible to calculate friction and heat transfer in the presence of longitudinal pressure drops. The expressions for the integral thickness and the form parameter H* which are needed for this purpose are given in Section 23.

The almost complete absence of experimental data on the boundary layer characteristics in dissociating gases makes it impossible to carry out evaluations of the accuracy of the calculation methods proposed, but the good agreement between the calculated and experimental data in the absence of dissociation (Chapter III) provides confidence that the methods of Chapter IV, which are merely further developments of the methods of Chapter III, will also give satisfactory results.

CHAPTER V /278

TURBULENT BOUNDARY LAYERS IN THE PRESENCE OF MASS TRANSFER BETWEEN THE GAS AND A SOLID SURFACE

27. Introduction

In chapters III and IV we considered the properties of turbulent boundary layers formed on bodies of various shapes in the absence of mass transfer between the gas and the solid wall. Processes of mass transfer between the gas and surface begin to play an important part in the motion of bodies at very high supersonic velocities in the dense layers of the atmosphere. The powerful heating can lead to changes in the aggregate state of the solid: it can melt or evaporate, with subsequent entrainment of the surface material by the gas stream. The first information on mass transfer during the motion of bodies at very large supersonic velocities was obtained more than forty years ago in the study of meteorites. In the last decade, interest in this problem has increased still more as a result of the development of rocket and space technologies. The phenomena accompanying the heating of moving bodies at very high temperatures have been the subjects of careful experimental and theoretical investigations. One of the most important outcomes of these calculations was the establishment of the fact that it is possible to use special transferrable coatings for the thermal protection of the forward parts of rockets and other space apparatus. At the present it is obvious that thermal protection of hypersonic apparatus by means of transferrable coverings is the most effective method from the point of view of weight and constructional simplicity. An important part is played by mass transfer in the cooling of the walls of combustion chambers, supersonic air samplers, nozzles of rocket motors, etc.

As the heat protecting coverings wide use is made of constructional plastics, consisting mainly of thermo-reactive phenol-formaldehyde and epoxide melts [118]. /279

As fillers for reinforcing plastics, use is made of textolite, glass-textolite, asbestos, silicon, refractory oxides of magnesium, aluminum, nylon, terylene, and other materials.

There has recently been considerable interest in materials which break down at relatively low temperatures (up to 1000°K): Teflon, capron, polyethylene, and organic glasses. In the break-down of heat-protecting coverings made

of these materials, gases of various molecular weights appear in the boundary layer, and in many cases these lead to a powerful "injection effect", causing a reduction in the heat flux to the surface.

At present a large number of heat protecting materials have been studied and are widely used. However, in spite of the large number of these materials, it has been noted that the breakdown of heat-protecting coverings occurs mainly as a result of the following physico-chemical processes: surface pyrolysis of the binder, depolymerization, evaporation, sublimation, combustion, melting, or erosion. In many cases, beyond some definite rate the breakdown of the plastic covering reaches the rate of combustion of the coke residue of the binder material. At large percentage contents of glass and quartz fillers in the material, an important part is played by transport processes in the liquid phase. As an example of such heat-protecting coverings, mention may be made of asbestos-textolite coatings, in which the following processes are observed during heating: coke formation, dehydration of the asbestos, chemical interaction of the coke residue with oxygen and nitrogen, sublimation of the coke residue, spreading of the melt of silica fibres (SiO_2), and evaporation of the SiO_2 melt. As a result of these processes, the composition of the gas mixture in the boundary layer becomes very complicated [119]. Depending on the conditions, the mixture can contain the following components: O_2, O, N_2, N, C, C_2, C_3, CO, CO_2, CN, HCN, H_2, H, Si, SiO_2, SiO, SiC, SiC_2, Si_2C, etc. /280

The process of surface breakdown by means of these mechanisms, all together or only some of them, has been termed mass entrainment. One of the possible models by which the mass entrainment process occurs is shown in Fig. 74 a.

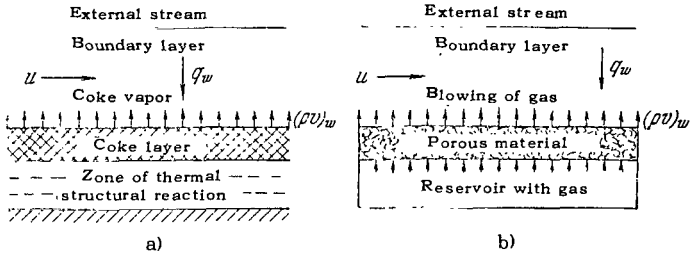

Figure 74.

In some cases, cooling of surfaces is effected by means of forced introduction of mass into the boundary layer through a porous wall (Fig. 74b). Air, water vapor, light gases (hydrogen, helium) and other gaseous and gas-forming materials can be used as the coolants in the porous cooling process *.

*A detailed description of the various methods of cooling surfaces subjected to high temperatures can be found in the book by Avduyevskiy and Danilov [120].

The presence of a transverse mass flux in the boundary layer caused by the injection of mass through the porous wall, sublimation of the solid surface, or evaporation of a liquid film causes a greater effect on the structure of the boundary layer (velocity profile, temperature profile, etc.) the more intense is this flux. Together with the change in the local characteristics of the boundary layer, changes also occur in its integral characteristics; blowing, in particular, usually leads to a decrease in friction and the heat flux at the wall. The only exception is in cases when the material introduced into the boundary layer enters into chemical reactions with the components of the main stream, and the heat liberated in this way may ultimately lead to an increase in the heat flux at the wall. The phenomena of reduction of the heat flux and friction during the injection of material into the boundary layer is sometimes termed the "blocking effect". /281

The present chapter is concerned with a consideration of some of the phenomena described above, and a discussion of the methods of calculating friction and heat transfer during injection of mass into the boundary layer. Friction will be considered close to a porous (or subliming) plate along which a supersonic gas stream flows, in the absence of chemical interaction between the injected material and the gas of the main stream.

In conclusion it can be mentioned that the solution of the problem being considered is still very far from being complete either experimentally or theoretically. Essentially only the first results have been obtained, and many theoretical and experimental aspects of the problem remain unclear. Bearing this in mind, it seems advisable to give a brief outline of the main directions in the development of this part of the turbulent boundary layer theory.

28. The main directions in the study of turbulent boundary layers in the presence of mass transfer between the gas and a surface.

This field of study has been developed mainly in the last ten to fifteen years. A knowledge of the work in this field indicates that its development has followed the same path as the development of turbulent boundary layer studies in compressible gases in the absence of mass transfer between the gas and a wall (some of the results of these studies were considered in Chapter III). Thus, three main directions of these studies can be mentioned: 1) the semiempirical approach, based on generalization of Prandtl's formula (2.68) or von Kármán's formula (2.69) in the case of flow of a compressible gas with mass transfer between the gas and wall (this approach can also be characterized as the approach based on the use of the logarithmic velocity profile); the semiempirical approach based on the use of a power-law velocity profile; 3) the empirical approach, based on the direct use of experimental data. /282

The first approach is the most highly developed at present. In most of the work on this approach the following expression is used for the shear stress in the boundary layer:

$$\tau = \tau_w + (\rho v)_w u. \qquad (5.1)$$

Here $(\rho v)_w$ is the mass flux of the material at the solid surface.

Equation (5.1) can be obtained easily from the following simple argument. The quantity $(\tau - \rho_w v_w u)$ can be expanded in a Taylor series, giving

$$\tau(\xi, y) - \rho_w v_w u(\xi, y) = \tau(\xi, 0) + \left[\frac{\partial}{\partial y}(\tau - \rho_w v_w u)\right]_{\substack{y=0 \\ \xi=0}} y + \ldots$$

Then, by noting that it follows that

$$\left[\frac{\partial}{\partial y}(\tau - \rho_w v_w u)\right]_{y=0} = 0,$$

from the equation of motion (2.52) for a flat plate and the second of the boundary conditions (2.73):

$$u \to U_e, \quad H \to H_e, \quad c_i \to c_{ie} \qquad \text{at } y \to \infty; \qquad (2.73)$$

which leads to equation (5.1). Equation (5.1) which is assumed for the shear stress essentially means that it is assumed that the mass flux of the material in the boundary layer is constant:

$$\rho v = \text{const} = (\rho v)_w.$$

It is not difficult to see that equation (5.1) leads to incorrect results at the outer edge of the boundary layer, where it is necessary to satisfy the conditions $\tau = 0$ when $u = U_e$.

The actual distribution of the shear stress in the boundary layer in the presence of blowing can be seen from Fig. 25 [121], which gives the results of shear stress measurements at various values of the blowing parameter B, defined by /283

$$B = \frac{2\rho_w v_w}{\rho_e U_e c_f} = \frac{\rho_w v_w U_e}{\tau_w}. \qquad (5.2)$$

The tangential stress distribution in Fig. 75 is shown as a function of the dimensionless distance from the wall y/δ, where δ is the boundary layer thickness. It can be seen from the Figure that in the absence of blowing (B = 0) the maximum shear stress occurs at the wall. As the blowing parameter increases, the shear stress at the wall decreases noticeably, and there is a considerable increase within the boundary layer, with a maximum in the zone adjacent to the wall. The same results, but recalculated in the form of a relationship $\tau/\tau_w = f(\bar{u})$,

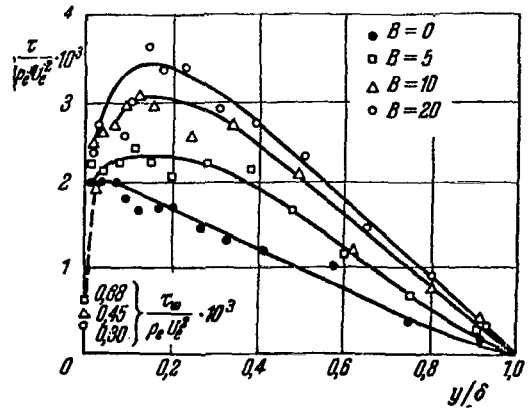

Figure 75.

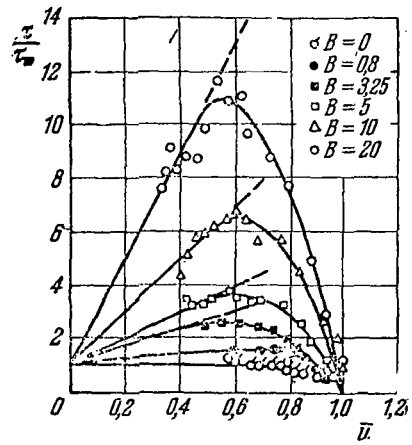

Figure 76.

are shown in Fig. 76. It can be seen that in the region $\bar{u} \leq 0.5$ the shear stress distribution is described well by equation (5.1) (dashed lines) in the form /284

$$\tau = \tau_w (1 + B\bar{u}). \qquad (5.3)$$

In spite of the fact that equation (5.3) describes the shear stress distribution in the outer region of the boundary layer poorly, it appears to be quite applicable for calculating the integral characteristics of the boundary layer (friction, displacement thickness, momentum loss thickness, etc.). This fact can be explained by arguments similar to those given in Section 10 in connection with equation (3.1).

By using equation (5.3), the following expressions for the velocity profiles in the turbulent core of the boundary layer can be obtained from Prandtl's equation (2.68) and von Kármán's formula (2.69):

$$\eta = \frac{1}{C_4} \exp\left[\varkappa\zeta \int \left(\frac{\frac{\rho}{\rho_w}}{1+B\bar{u}}\right)^{1/2} d\bar{u}\right], \tag{5.4}$$

$$\eta = C_5 + C_6\zeta \int \exp\left[\varkappa\zeta \int \left(\frac{\frac{\rho}{\rho_w}}{1+B\bar{u}}\right)^{1/2} d\bar{u}\right] d\bar{u}. \tag{5.5}$$

Here C_4, C_5, C_6 are integration constants, and η and ξ are expressed by equation (3.8).

It is not difficult to see that in the absence of blowing (B = 0) equations (5.4) and (5.5) reduce respectively to equations (3.6) and (3.7), which describe the velocity profiles in the turbulent core on an impermeable wall.

Equations (5.4) and (5.5) lead respectively to the following expressions for the momentum loss thickness: /285

$$\delta^{**} = \frac{\varkappa\zeta^2\mu_w}{\rho_e U_e C_4} \int_0^1 \left(\frac{\rho}{\rho_w}\right)^{3/2} \frac{\bar{u}(1-\bar{u})}{(1+B\bar{u})^{1/2}} \exp\left[\varkappa\zeta \int \left(\frac{\frac{\rho}{\rho_w}}{1+B\bar{u}}\right)^{1/2} d\bar{u}\right] d\bar{u}, \tag{5.6}$$

$$\delta^{**} = \frac{\zeta^2\mu_w C_6}{\rho_e U_e} \int_0^1 \left(\frac{\rho}{\rho_w}\right) \bar{u}(1-\bar{u}) \exp\left[\varkappa\zeta \int \left(\frac{\frac{\rho}{\rho_w}}{1+B\bar{u}}\right)^{1/2} d\bar{u}\right] d\bar{u}. \tag{5.7}$$

In the absence of blowing (B = 0) equations (5.6) and (5.7) reduce to equations (3.9) and (3.10) respectively *.

The difference between the work of different authors usually occurs in connection with the definition of the integration constant C_6 and with the method of evaluating the integrals in equations (5.6) and (5.7)**.

One of the first papers in which an analysis was made of turbulent boundary layers on a porous plate with injection of a material with the same physical properties as in the approaching stream was that of Dorrance and Dore [123, 124]. In this work the velocity profiles were determined on the basis of Prandtl's formula (see (5.4)), assuming that the shear stress distribution in the boundary layer was described by equation (5.3). The friction coefficient was found by the /286

*It should be noted that equations (5.6), (5.7), like (3.9), (3.10), are approximate, since they are obtained if the laminar sublayer is neglected, assuming that the turbulent core extends to the wall, which is valid when the laminar sublayer is relatively thin.

**A detailed analysis of these differences is to be found in the work of Spalding et al. [122].

usual method making use of the integral momentum relationship (2.80), which in the present case of flow along a flat plate becomes

$$\frac{d\delta^{**}}{dx} = \frac{c_f}{2}(1 + B). \tag{5.8}$$

The method of Dorrance and Dore was extended by V. P. Motulevich [125] to the case when the material injected into the boundary layer had different properties to those of the approaching stream. Later, Motulevich developed this method further to deal with sublimation of the plate surface, and improved it from the computational point of view [126, 127].

L. E. Kalikhman [128] studied the turbulent boundary layer in an incompressible fluid with mass injection of a material having the same physical properties as the gas wetting the surface. In this paper the solution was obtained on the basis of the semiempirical theory of Prandtl (2.68), using a boundary condition at the wall similar to the boundary condition in the boundary layer of a free jet, which is equivalent to assuming that there is no laminar sublayer close to the wall.

The question of what effect the Lewis and Prandtl numbers have on friction on a flat plate in the presence of blowing through a porous wall a material which is inert with respect to the gas in the main stream was studied in the paper by Ginzburg, Kocheryzhenkov and Mordvinova [129]. /287

Investigations of this problem on the basis of the limiting laws of friction and heat transfer have been made by Kutateladze and Leont'yev et al. [130, 131].

A semiempirical method of calculating turbulent boundary layers on a chemically active decomposing surface with applications to the calculation of the combustion of graphite surfaces was developed by Denison [132],

The second approach based on the use of the power-law type of expression for the velocity profile has had much less development up to the present. Of the papers using this approach, mention can be made of the work of V. D. Sovershennyi which considered flow on a permeable surface in the presence of a small longitudinal pressure gradient as well as flow along a porous plate.

The empirical method of calculating friction and heat transfer on a porous plate during the blowing of air into air was used by V. P. Mugalev [134]. This method is based on an analogy established experimentally by the author between friction with a positive longitudinal pressure gradient and friction on a porous plate in the presence of blowing. The analogy depends on the similarity of the velocity profiles in the boundary layer in these flows. By introducing the form parameter $f_w = (\rho_w v_w/\rho_e U_e)\,(\mathrm{Re}^{**})^{0.25}$, Mugalev reduced the integral momentum relationship to a form which made possible its linearization, similarly to the approach used in the well known method of L. G. Loytsyanskiy [135]. Subsequent calculations were carried out in the same way as calculations of boundary layers with longitudinal pressure drops. /288

An empirical method of calculating heat and mass transfer on a flat plate with and without chemical reactions in the boundary layer was developed by Spalding et al. [122]. To a certain extent this method is analogous to the method of Spalding and Chi for calculating friction on an impermeable plate which was considered in Section 14. As in the latter work, some of the functions were obtained on the basis of an analysis of semiempirical methods of calculation, and others on the basis of experimental data.

In order to calculate drag, heat transfer and the flow rate of the cooling material, tables and graphs were set up for a range of Mach numbers from 0 to 12 and temperature factors from $(T_w/T_\infty) = 0.05$ to 20. The injection of air, helium and hydrogen into air is considered. Two groups of tables are given for hydrogen, one taking combustion into account, and the other for the absence of combustion.

It should also be noted that the paper by Spalding, Auslander and Sundarom also contains a detailed analysis of many of the semiempirical methods and an extensive bibliography.

29. Experimental studies of turbulent boundary layers in the presence of mass transfer

Up to the present quite an extensive amount of experimental material has been accumulated on the effects of injecting various gases on the turbulent boundary layer characteristics (velocity and temperature profiles, friction, heat transfer, etc.). Most of the experimental data have been obtained for flows without longitudinal pressure gradients (plates, cones)*. Unfortunately, the considerable technical difficulties connected with carrying out these types of experiments have led to considerable errors (up to 100%) in some cases, as indicated by the very large scatter of the experimental points obtained by different authors under similar conditions. For a long time the main experimental method of determining local friction was the method based on measuring the velocity and temperature profiles. More exact direct methods of measuring local drag forces by means of "floating" elements, which have been widely used in studying flows on impermeable surfaces (see Section 11), are still relatively undeveloped. In a number of papers the various characteristics were not measured with sufficient accuracy. These circumstances have led to the situation that the effects of various parameters on friction and heat transfer still remain unclear, and in some cases the experimental data of different authors are contradictory. /289

In the present Section, we will consider the main results of the experimental investigations of boundary layer characteristics in the presence of blowing into supersonic streams. As usual, the measured results in subsonic streams will be introduced also in the combined graphs.

*It must be said that as a result of the effect of the thickened boundary layer on the external stream it is not by any means always possible to ensure gradientless flow in experiments with injection at large supersonic velocities. It may be noted in passing that the theory of interactions between turbulent boundary layers and hypersonic external streams has only just begun to be developed. See for instance [136].

The experiments of V. P. Mugalev [137-139] *. In his work, V. P. Mugalev obtained extensive information on the structure of flow in turbulent boundary layers in the presence of blowing, and on the effects of various parameters (the Reynolds and Mach numbers, Re_x, M_e, the properties of the injected gas, etc.) on heat transfer. In the experiments, measurements were made of the velocity, temperature, concentration and density profiles in the boundary layer and of heat transfer on a flat porous plate over a wide range of stream parameters and blowing intensities. /290

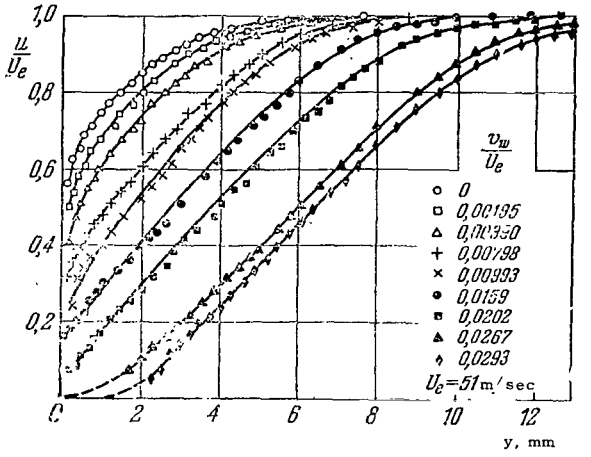

Figure 77.

Figure 77 shows the velocity profiles during the blowing of air into an air stream moving at subsonic velocities (U_e = 51 m/sec). It can be seen that as the blowing is increased, the velocity profiles are deformed, becoming less blunt. At large blowing intensities ($v_w/U_e > 0.02$) there is a point of inflection on the profiles, and the derivative $(\partial u/\partial y)_w$ tends to zero. From an analysis of the velocity profile changes, Mugalev concluded that at moderate blowing intensities (up to the appearance of the points of inflection on the profiles) the effect of blowing was similar to the effect of a longitudinal pressure gradient, while at larger blowing rates the velocity profiles became similar to jet profiles. /291

Figure 78 shows the velocity and temperature profiles obtained under the same conditions (M_e = 0.08) with the blowing of air. Along the ordinate axes of

*Most of the experimental material contained in the papers of Mugalev mentioned here, and the conclusions reached from this material, in particular, the conclusion that there is no appreciable effect of the Mach number on the relative heat flux to the wall during blowing, were obtained during the years 1955-1956.

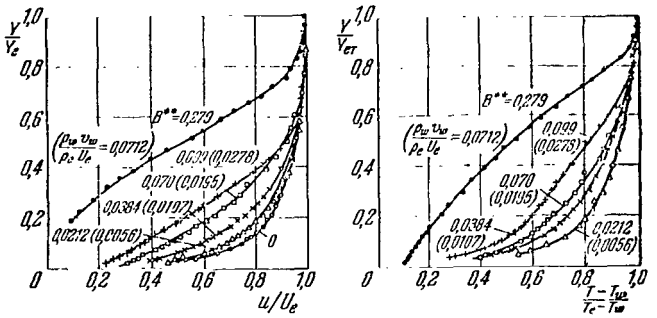

Figure 78.

these figures are plotted the quantities Y/Y_e and Y/Y_{eT}, where $Y = \int_0^y (\rho/\rho_{e(T)})dy$ so that Y_e and Y_{eT} are the coordinates of the edges of the dynamic and thermal boundary layers. The blowing parameter B** is expressed by the relationship

$$B^{**} = \frac{\rho_w v_w}{\rho_e U_e} \mathrm{Re}^{**0,25} \cdot \frac{T_w}{T_e}.$$

Comparison of the profiles of velocity and stagnation temperature difference indicates that these profiles are approximately similar. At the same time, at large values of the blowing parameter, the transfer of heat occurs rather more intensively than the transfer of momentum.

Figure 79 gives an analogous comparison of the profiles of velocity and relative concentration in the boundary layer during the blowing of carbon dioxide into an air stream; these were also obtained under similar conditions ($M_e = 2.5$, $T_w/T_{ro} = 1.1$). It can be seen from the figure that the velocity and concentration profiles are also approximately similar. /292

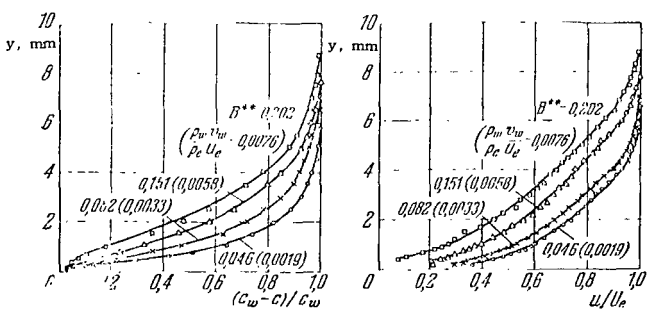

Figure 79.

Thus, in the case being considered it is possible to conclude that the injection of gas into the boundary layer has similar effects on the velocity, temperature and concentration profiles. At the same time, the author noted that strict similarity between these profiles was absent during blowing.

Experiments to measure heat transfer were carried out in a wind tunnel with injection of cold gases (helium, air, carbon dioxide, argon and krypton) into the boundary layer. The Mach and Reynolds numbers varied over the ranges $0 \leq M_e \leq 3.7$, $10^5 < Re_x \leq 10^7$, and the temperature factor varied from $T_w/T_{ro} = 0.5$ to 1. The heat transfer coefficients at the porous surface were determined on the basis of a heat balance equation from the measured values of the temperatures of the gas being injected and the wall, the flow rate of the gas being injected, and the parameters of the external flow.

The experimental results on the effects of blowing on heat transfer during the injection of various gases at various Mach numbers of the external stream are shown in Fig. 80, in which the conditions were: 1 - helium, $M_e = 2.5$; /293
2 - carbon dioxide, $M_e = 2.5$; 3 - argon, $M_e = 2.5$; 4 - krypton, $M_e = 2.5$; 5 - air, $M_e \approx 0$; 6 - air, $M_e = 2.5$; 7 - air, $M_e = 3.7$. In the estimation of the author, the maximum possible error in the experiment did not exceed 10 - 40% for $(M_1/M_2)^b B_{h0} \approx 0.5 - 5$.

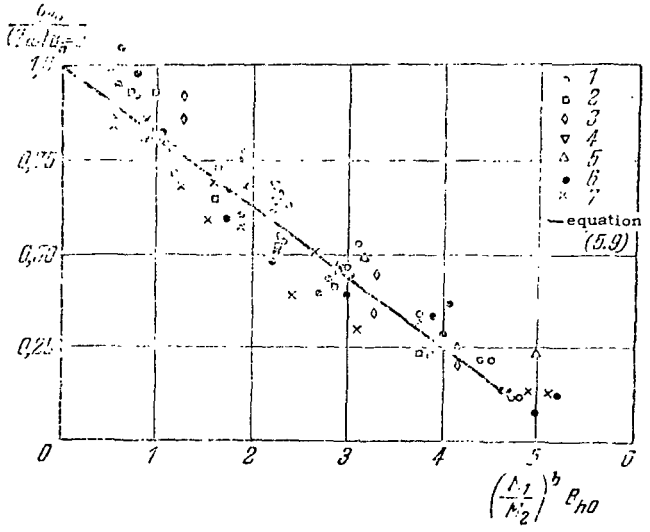

Figure 80.

On the basis of the data given in Fig. 80 it can be concluded that over the investigated ranges of the parameters M_e, Re_x and T_w/T_{ro}, these parameters have no effect on the dimensionless relationships

$$q_w/(q_w)_{B_h=0} = f_1(B_h) \text{ и } q_w/(q_w)_{B_h=0} = f_2(B_{h0}).$$

(Here $B_h = (\rho_w v_w)/\rho_e U_e c_h$; $B_{h0} = (\rho_w v_w)/\rho_e U_e (c_h)_{B_h=0}$; q_w, $(q_w)_{B_h=0}$ are the heat fluxes at the wall with and without blowing and T_w = idem.)

Based on an analysis of the experimental data on heat transfer, Mugalev proposed a simple approximate formula for calculating the heat flux: /294

$$\frac{q_w}{(q_w)_{B_h=0}} = 1 - 0{,}19\left(\frac{M_1}{M_2}\right)^b B_{h0}. \qquad (5.9)$$

Here M_1 and M_2 are the molecular weights of the gas at the external edge of the boundary layer and of the injected gas; $b = 0.35$ when $0.2 < (M_1/M_2) < 1$; $b = 0.7$ when $1 < (M_1/M_2) < 8$; $b = 1$ when $(M_1/M_2) = 14.5$. The approximate formula (5.9) is applicable when $q_w/(q_w)_{B_h=0} \geq 0.1$.

The experiments of Pappas and Okuno [140]. The dependence of the mean coefficients of friction and heat transfer, and the recovery coefficient and the Reynolds analogy parameter on the blowing of air, helium and Freon-12 through the porous wall of a cone with a vertex angle of 12° was investigated at Mach numbers of the air stream (on the cone) of 0.7, 3.67, 4.35 and a Reynolds number of the order of 9.5×10^6.

The results of the measurements made by Pappas and Okuno are shown in Figs. 81 - 89. The following notation is used on these figures: c_F - mean friction coefficient; c_H - mean heat transfer coefficient; $B_{F0} = 2\rho_w v_w/\rho_e U_e (c_F)_{B=0}$ is the blowing parameter for the supersonic stream; $B_{F0} = 2\rho_w v_w/\rho_\infty U_\infty (c_F)_{B=0}$ is the blowing parameter for a subsonic stream; U_e, ρ_e are the velocity and density at the edge of the boundary layer; M_e is the Mach number at the edge of the boundary layer (in the case of the subsonic flows, $M_e = M_\infty$); $r = (T_r - T_w)/(T_e^* - T_w)$ is the recovery coefficient; T_r is the recovery temperature; T_e^* is the stagnation temperature in the outer stream; $Re_x = U_e \rho_e x/\mu_e$ is the Reynolds number for the supersonic stream; $Re_x = U_\infty \rho_\infty x/\mu_\infty$ is the Reynolds number for a subsonic stream; x is the distance measured along the cone. The subscript "0" denotes parameters in the absence of blowing.

Figures 81 and 82 show the quantity $c_F/(c_F)_{B=0}$ on a thermally insulated surface as a function of the Mach number for various values of the blowing parameter B_{F0}. In addition, Fig. 82 also shows the experimental points of /296 Mickley and Davis [141], which were obtained as a result of measuring local friction coefficients from velocity profiles on a plate in an incompressible fluid. By considering Figs. 81 and 82 it can be concluded that the Mach number at the

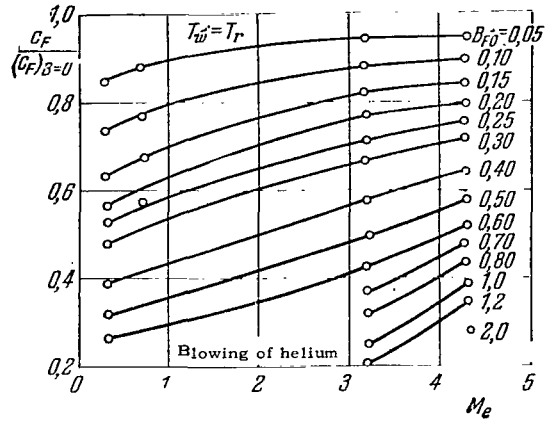

Figure 81.

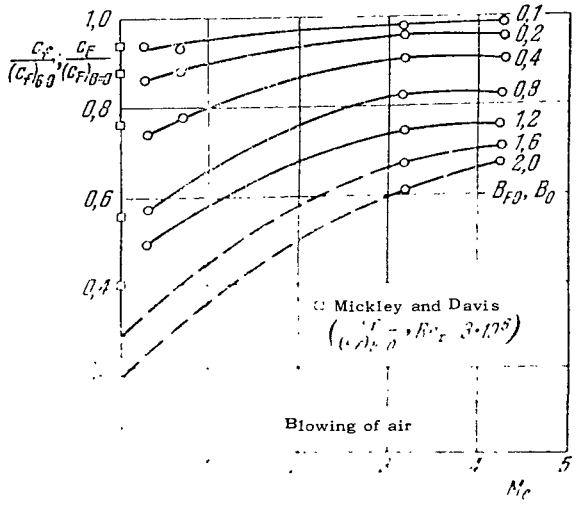

Figure 82.

outer edge of the boundary layer has a considerable effect on the ratio $c_F/(c_f)_{B=0}$. This effect increases as the blowing parameter B_{F_0} increases.

Figures 83 and 84 show the results of measurements of the heat transfer coefficient at various values of the injection intensities of helium, air and Freon-12 at $M_e = 3.67$ and 4.35. The same data for helium and air, supplemented by measured values at $M_e = 0.7$, are shown in terms of differenc coordinates in Figs. 85 and 86. From Figs. 85 and 86 it can be seen that over the

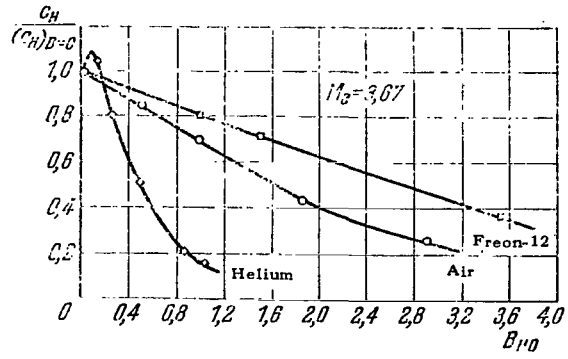

Figure 83.

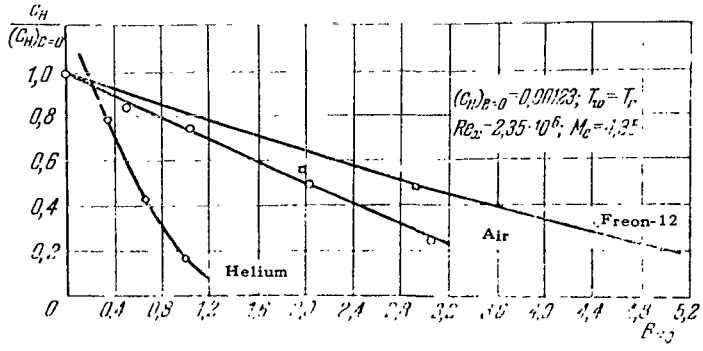

Figure 84.

range of Mach numbers M_e from 0.7 to 3.67, the effect of the Mach number on the ratio $c_H/(c_H)_{B=0}$ is small, which agrees with the data given above from the work of V. P. Mugalev. Over the range of Mach numbers from 3.67 to 4.35, the nature of this dependence changes quite sharply, which is in contradiction to other existing results, such as the results of the same authors in the range $0.7 \leq M_e \leq 3.67$.

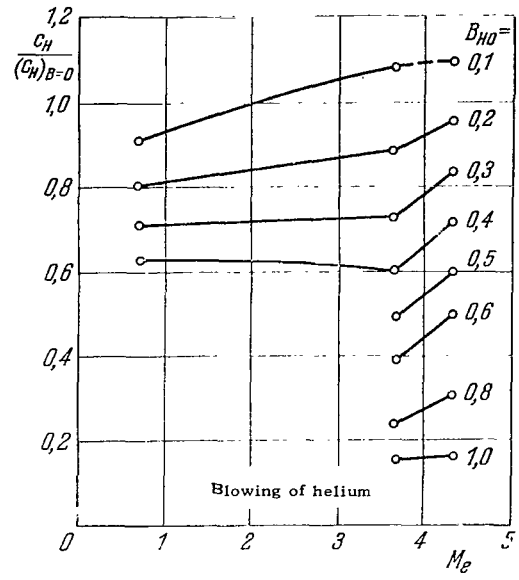

/298

Figure 85.

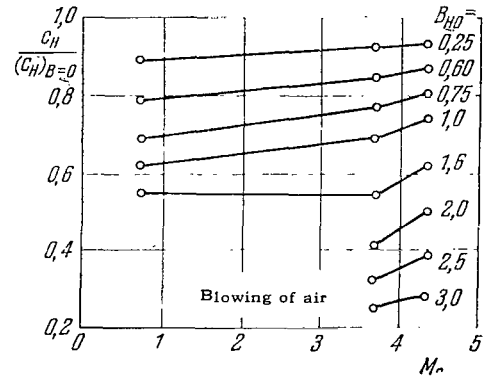

Figure 86.

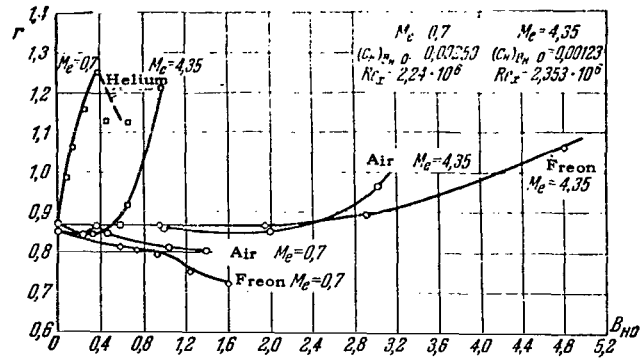

Figure 87.

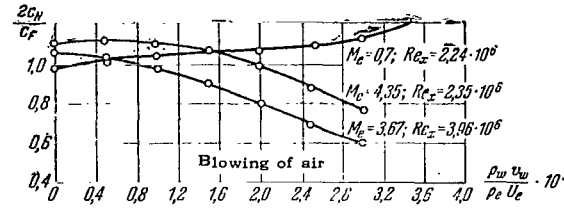

Figure 88.

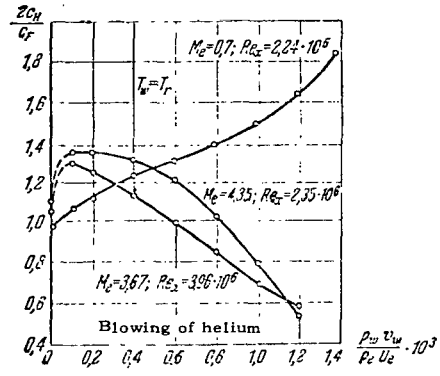

Figure 89.

Figure 87 shows the dependence of the recovery coefficient r on the blowing parameter at Mach numbers from 0.7 to 4.35. As can be seen from the Figure, for the Mach number of 0.7, the recovery coefficient decreases with increase of the blowing intensity during the injection of air and Freon, while in

the injection of helium, it first increases to a value of 1.25 and then decreases. At $M_e = 4.35$ the recovery coefficient initially decreases for all the gases injected, and then increases. Attention is drawn to the fact that the recovery coefficient exceeds unity.

Figures 88 and 89 show the dependence of the Reynolds analogy parameter $2c_H/c_F$ on the blowing of air and helium for various Mach numbers. The nature of the change of the Reynolds analogy parameter during the injection of helium at supersonic velocities should be noted. Initially, this parameter increases, /297
reaches a maximum equal to 1.35, and then decreases noticeably.

From a consideration of the experimental data of Pappas and Okuno it is obvious that the blowing of material into the boundary layer leads to a considerable change in the nature of the boundary layer; the change of such quantities as the recovery coefficient and Reynolds analogy parameter is quite different to the behavior of this quantity in the absence of blowing.

The experiments of Fogaroli and Saydah [142]. The paper of Fogaroli and /300
Saydah contains the results of an investigation in a hypersonic wind tunnel on the effects of air blowing on friction and heat transfer in the turbulent boundary layer on a porous cone at values of the Mach number on the cone of 5.3 and 8.1 and a range of blowing parameters $B_{h0} = \rho_w v_w / \rho_e U_e (c_h)_{B_h=0}$ from 0 to 20. The half-angle of the cone was 7.5°.

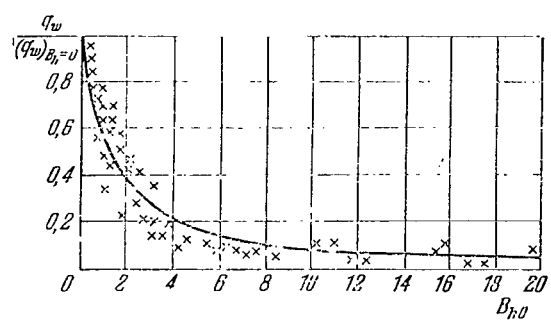

Figure 90.

Figure 90 shows the change in the ratio of the heat flux with blowing to the heat flux without blowing as a function of the blowing parameter for various values of the Mach number at the edge of the boundary layer. The data of other authors are also included (the points are not distinguished on the graph). The scatter of experimental points is quite large, so that it is difficult to say anything of the effect of the Mach number on the heat flux. On the same figure is shown a curve calculated from the following approximate formula:

$$\frac{q_w}{(q_w)_{B_h=0}} = \left[\left(\frac{1}{2}B_h\right)^2 + 1\right]^{1/2} - \frac{1}{2}B_h. \qquad (5.10)$$

The experimental data of other authors. Figure 91, taken from the paper by Nash * gives a composite graph of the data of various authors on drag measurements in the presence of blowing (v* is the dynamic velocity). On the same figure is shown the curve calculated from the formula /301

$$\frac{\tau_w}{(\tau_w)_{B=0}} = \exp\left[-6{,}94\left(\frac{\rho_w v_w}{\rho_e U_e}\right)\sqrt{\frac{\rho_w}{\rho_e}\frac{2}{(c_f)_{B=0}}}\times \left(1+\sqrt{\frac{(\tau_w)_{B=0}}{\tau_w}}\right)\right]. \qquad (5.11)$$

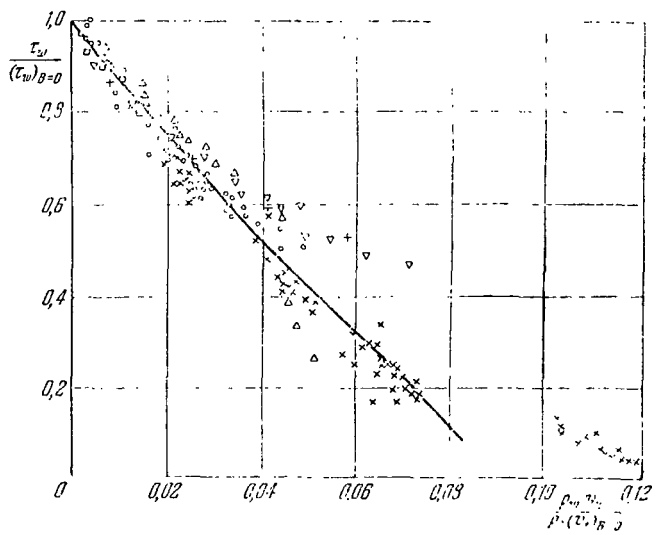

Figure 91.

Equation (5.11) was obtained by Nash as a result of generalizing Turcotte's formula [144], which was obtained for incompressible fluids.

From a consideration of the results given above from experimental investigations on the blowing of various materials into turbulent boundary layers the following conclusions can be reached: /302

The injection of material into the boundary layer decreases friction and heat transfer on the surface. The greatest effect occurs with the blowing of light gases.

*Figure 91 and equation (5.11) are taken from the review paper [143].

The boundary layer velocity profiles are deformed during blowing, becoming less blunt as the blowing intensity is increased. Very powerful blowing points of inflection appear on the velocity profiles, which then resemble jet profiles.

The injection of various gases into the boundary layer can have a very large effect on the recovery coefficient and Reynolds analogy parameter.

The Mach number at the outer edge of the boundary layer has an appreciable effect on drag $c_F/(c_F)_{B=0}$. This effect is larger the more intensive the blowing.

Most of the experimental data indicate that there is no effect or only a feeble effect of the Mach number on heat transfer $c_H/(c_H)_{B_H=0}$, $c_h/(c_h)_{B_h=0}$.

In conclusion, it should be noted that all the data considered above were obtained in experiments with nonreacting gas mixtures.

Up to the present, the number of investigations of turbulent boundary layers with injection of chemically reacting gases is very limited [121, 145].

30. The boundary conditions at the wall and at the outer edge of the boundary layer in the presence of mass transfer between a surface and the gas The heat flux at the wall

The formal boundary conditions for the longitudinal velocity component, concentration and total enthalpy in the presence of mass transfer between the surface and gas can be written in the form /303

$$\left.\begin{aligned} u = 0,\ c_i = c_{iw},\ H = h_w \quad &\text{at} \quad y = 0; \\ u = U_e,\ c_i = c_{ie},\ H = H_e \quad &\text{at} \quad y \to \infty. \end{aligned}\right\} \tag{5.12}$$

The boundary condition for the normal velocity component on a permeable wall is

$$v = v_w \quad \text{at} \quad y = 0 \tag{5.13}$$

in contrast to the condition v = 0 at y = 0 on an impermeable wall. The surface of the plate is usually regarded as semipermeable, i.e., permeable to the material being injected and impermeable to the gases wetting the surface.

The expressions for the enthalpy on the wall and at the outer edge of the boundary layer have the forms

$$h_w = \sum_i c_{iw} h_{iw}, \qquad h_{iw} = \int_0^{T_w} c_{pi}\, dT + h_i^0, \tag{5.14}$$

$$H_e = h_e + \frac{u^2}{2}, \quad h_e = \sum_i c_{ie} h_{ie}, \quad h_{ie} = \int_0^{T_e} c_{pi} dT + h_i^0. \tag{5.15}$$

The concentrations of the components at the outer edge of the boundary layer c_{ie} are usually assumed to be known from the solution of the outer stream. In most cases it is assumed that the outer stream is in a state of thermochemical equilibrium, i.e., $c_{ie} = c_{ie}^{(e)}$. Thus, the boundary conditions at the outer edge of the boundary layer are usually completely defined. As regards the conditions at the wall for the concentration c_{iw} and the velocity v_w, it will be seen subsequently that these conditions are interdependent. The value of v_w can in principle be given if blowing through a porous wall is being considered. In this case, the concentration at the wall c_{iw} can be determined from additional conditions during the solution of the problem.

In the case of flow along a subliming wall the normal velocity component v_w cannot be given a priori, but must, like the concentration on the surface, c_{iw}, be determined from additional conditions during the solution of the problem (in the case of equilibrium sublimation one of these additional conditions is expressed by the Clausius-Clapeyron equation, which relates the concentration of the sublimate to the temperature and pressure on the wall). /304

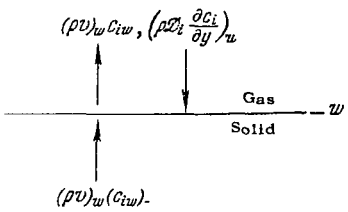

Figure 92.

In order to establish the additional relationships relating the flux of material injected into the boundary layer through a porous wall (or formed as a result of sublimation) to the concentration of the components at the wall, the conditions for the conservation of the i^{th} component at the gas-solid interface are set up (Fig. 92). From the figure it can be seen that the i^{th} component is transferred from the gas to the wall by means of diffusion. The mass flux of the i^{th} component transferred in this way is obviously equal to $\left(\rho \mathcal{D}_i \frac{\partial c_i}{\partial y}\right)_w$ ($\mathcal{D}_i$ is the effective diffusion coefficient (1.58); only mass diffusion is taken into account here). At the same time the i^{th} component is transferred from the surface into the boundary layer of the stream by the mass flux $(\rho v)_w$ injected through the wall. The quantity of the i^{th} component transferred in this way is obviously equal to $(\rho v)_w c_{iw}$. At the same time, if the i^{th} component occurs in the mixture injected into the boundary layer through the porous wall (or during sublimation) and the concentration of this component within the wall is equal to $(c_{iw})_-$, the quantity of the i^{th} component supplied to the boundary layer by blowing will be $(\rho v)_w (c_{iw})_-$. If a chemical reaction occurs at the wall as a result of

which a quantity g_{iw} of the i^{th} component is formed (or consumed) (g_{iw} is the mass rate of formation of the i^{th} component per unit area), the equation for the conservation of the i^{th} component can clearly be written in the following form, bearing in mind the transfer processes mentioned above:

$$g_{iw} = -\rho_w \mathcal{D}_{iw}\left(\frac{\partial c_i}{\partial y}\right)_w + \rho_w v_w [c_{iw} - (c_{iw})_-]. \tag{5.16}$$

By substituting into the left-hand part of equation (5.16) the expression for g_{iw} (equation (4.35)), it is found that /305

$$\rho_w \mathcal{D}_{iw}\left(\frac{\partial c_i}{\partial y}\right)_w - \rho_w v_w [c_{iw} - (c_{iw})_-] = k_{wi}[(\rho c_i)_w^{n_i} - K_w (\rho c_j)_w^{n_j}]. \tag{5.17}$$

For components not occurring in the mixture being injected into the boundary layer, the quantity $(c_{iw})_-$ has to be taken to be zero. If a single component is injected, $(c_{iw})_- = 1$. It is obvious that within the wall the condition $\sum_i (c_{iw})_- = 1$ is always satisfied for an injected mixture.

In the absence of chemical reactions ($g_{iw} = 0$), the condition (5.16) becomes

$$\rho_w v_w [c_{iw} - (c_{iw})_-] - \rho_w \mathcal{D}_{iw}\left(\frac{\partial c_i}{\partial y}\right)_w = 0. \tag{5.18}$$

When a single component is supplied through the wall ($(c_{iw})_- = 1$), equation (5.18) can be written in the form

$$\rho_w v_w = \rho_w v_w c_{iw} - \rho_w \mathcal{D}_{iw}\left(\frac{\partial c_i}{\partial y}\right)_w. \tag{5.19}$$

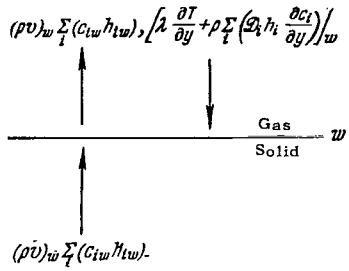
$(\rho v)_w \sum_i (c_{iw} h_{iw}), \left[\lambda \frac{\partial T}{\partial y} + \rho \sum_i \left(\mathcal{D}_i h_i \frac{\partial c_i}{\partial y}\right)\right]_w$
Gas
Solid
w
$(\rho v)_w \sum_i (c_{iw} h_{iw})_-$

Figure 93.

Let us now proceed to a consideration of the heat balance at the gas-solid interface (Fig. 93). Heat is supplied to the solid surface by means of heat conduction and mass diffusion:

$$q_w = \lambda_w \left(\frac{\partial T}{\partial y}\right)_w + \sum_i \rho_w \mathcal{D}_{iw} h_{iw} \left(\frac{\partial c_i}{\partial y}\right)_w;$$

Heat is transferred from the wall into the boundary layer by means of the stream of material injected into the boundary layer: $(\rho_w v_w) \sum_1 c_{iw} h_{iw}$; however, the heat flux directed to the interface on the solid side reduces to $\rho_w v_w \sum_1 (c_{iw} h_{iw})_-$ (the temperature gradient in the solid is assumed to be zero). Hence, the heat flux causing heating of the wall (within the wall) is /306

$$q_s = \lambda_w \left(\frac{\partial T}{\partial y}\right)_w + \sum_i \rho_w \mathcal{D}_{iw} h_{iw} \left(\frac{\partial c_i}{\partial y}\right)_w - \rho_w v_w \sum_i [c_{iw} h_{iw} - (c_{iw} h_{iw})_-]. \quad (5.20)$$

Making use of the expression for the heat flux from the gas to the wall, equation (4.147), equation (5.20) can be transformed to

$$q_s = \frac{\mu_w}{\mathrm{Pr}} \left[\left(\frac{\partial h}{\partial y}\right)_w + \sum_i (\mathrm{Le}_i - 1) h_{iw} \left(\frac{\partial c_i}{\partial y}\right)_w\right] - \rho_w v_w \sum_i [c_{iw} h_{iw} - (c_{iw} h_{iw})_-]. \quad (5.21)$$

For a subliming component it is possible to write the equation

$$(h_{iw})_- = h_{iw} - h_{iL}, \quad (5.22)$$

where h_{iL} is the heat of sublimation of the i^{th} component. By substituting (5.22) into (5.20), it is found that

$$q_s = \lambda_w \left(\frac{\partial T}{\partial y}\right)_w + \sum_i \rho_w \mathcal{D}_{iw} h_{iw} \left(\frac{\partial c_i}{\partial y}\right)_w - \rho_w v_w \sum_i h_{iw} [c_{iw} - (c_{iw})_-] - \rho_w v_w h_L, \quad (5.23)$$

where

$$h_L = \sum_i (c_{iw})_- h_{iL} \quad (5.24)$$

is the overall heat of sublimation.

By expressing the diffusion flux of the i^{th} component $\rho_w \mathcal{D}_{iw} (\partial c_i/\partial y)_w$ by means of equation (5.18), the following expression for the heat flux, which is very important in practical applications, can be obtained: /307

$$q_w = \lambda_w \left(\frac{\partial T}{\partial y}\right)_w - \sum_i g_{iw} h_{iw} - (\rho_w v_w) h_L. \qquad (5.25)$$

In conclusion, it is to be noted that the analysis carried out here for a subliming surface can be easily generalized to the case of evaporation at a gas-liquid interface. It is only necessary to replace the heat of sublimation h_L by the heat of vaporization h_v.

The conditions (5.16 - (5.19) obtained in this section represent the conditions linking the mass flux injected into the boundary layer (or formed as a result of sublimation) with the concentrations of the components at the wall. Thus, all the boundary conditions at the wall are now completely defined.

31. Velocity profiles and drag on a flat plate during injection of material into the boundary layer

In the general case, the expression for the velocity profile in the turbulent core based on von Kármán's formula (2.69) and the shear stress distribution in the boundary layer (5.3) has the form of equation (5.5). In order to determine the integration constant C_6 in equation (5.5) the same assumptions are made as were used in Section 12: it is assumed that the derivative $d\eta/d\varphi$ at the edge of the laminar sublayer on the side of the turbulent core has the same value as in an incompressible fluid in the absence of blowing; i.e., $(d\eta/d\varphi)_{\eta_L+0} = 1/f = \varkappa\alpha$. In other words, it is assumed that $(d\eta/d\varphi)_{\eta_L+0}$ is independent of compressibility, heat transfer and the injection of material. The turbulence constants $\varkappa$ and α are assumed to have the same values as in incompressible fluids ($\varkappa = 0.4$, $\alpha = 12$). From a consideration of the slopes of the velocity profiles during blowing (Figs. 77 and 78), it is obvious that the assumption made concerning the value of the derivative at the interface between the laminar sublayer and turbulent core will not lead to appreciable errors in the calculations.

Using the assumptions outlined above, the following expression can be obtained for the velocity profile in the turbulent core: /308

$$\eta = \eta_0 + \frac{\zeta}{f} \int_{\bar{u}_2}^{\bar{u}} \exp\left[\varkappa\zeta \int_{\bar{u}_2}^{\bar{u}} \left(\frac{\frac{\rho}{\rho_w}}{1 + B\bar{u}}\right)^{1/2} d\bar{u}\right] d\bar{u}. \qquad (5.26)$$

The slope of the velocity profile in the turbulent core is obviously given by

$$\frac{d\eta}{d\varphi} = \frac{1}{f}\exp\left[\varkappa\zeta\int_{\bar{u}_l}^{\bar{u}}\left(\frac{\frac{\rho}{\rho_w}}{1+B\bar{u}}\right)^{1/2}d\bar{u}\right]. \qquad (5.27)$$

Here $\bar{u}_L$ is the dimensionless velocity at the edge of the laminar sublayer (the problem of determining $\bar{u}_L$ will be considered below).

In the case of the flow along a plate of a stream with constant density and blowing into the boundary layer of a material of the same composition as the approaching stream ($\rho = \text{const} = \rho_e$), the expression for the velocity profile (5.26) assumes the following form after the integrals are evaluated:

$$\eta = \eta_l - \alpha\sqrt{1+B_*\varphi_l} + \alpha\sqrt{1+B_*\varphi}\exp\left[\frac{2\varkappa}{B_*}\left(\sqrt{1+B_*\varphi}-\sqrt{1+B_*\varphi_l}\right)\right]. \qquad (5.28)$$

Here

$$B_* = \frac{B}{\zeta} = \frac{\nu_w}{\nu_*}, \qquad \varphi_l = \frac{u_l}{\nu_*} = \bar{u}_l\zeta. \qquad (5.29)$$

In order to determine the velocity profile in the laminar sublayer, equation (3.106) is used after first simplifying it by making the assumption of a constant viscosity in the sublayer ($\mu = \text{const} = \mu_w$). By substituting equation (5.3) into equation (3.106) and carrying out the integration, the following expression is obtained for the velocity profile in the laminar sublayer:

$$\varphi = \frac{1}{B_*}[\exp(B_*\eta) - 1]. \qquad (5.30)$$

At small blowing intensities, the exponential can be expanded in series and all the terms except the first two can be discarded, giving /309

$$\varphi = \eta\left(1+\frac{1}{2}B_*\eta\right). \qquad (5.31)$$

In the absence of blowing, equations (5.30) and (5.31) reduce to the expression obtained earlier (equation (3.30)) for the linear velocity profile.

Velocity profiles in the laminar sublayer calculated from equation (5.30) are shown in Fig. 94. The velocity profile for an incompressible fluid in the absence of blowing is also shown. At first sight, the way in which the velocity profile in the laminar sublayer changes in Fig. 94 appears paradoxial, since here the velocity profile becomes fuller as the blowing parameter increases, which contradicts the experimental data given earlier (Figs. 77 and 78). However, this paradoxical nature is only apparent, since Figs. 77 and 78 deal with

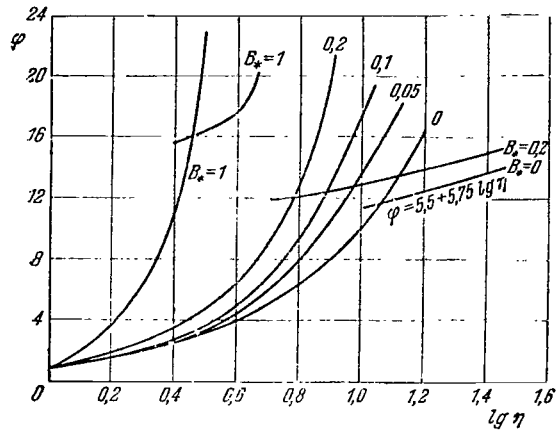

Figure 94.

the actual velocity u/U_e, while Fig. 94 gives the velocity profile in terms of the universal coordinate $\varphi = u/v^*$.

The problem of the thickness of the laminar sublayer and the velocity at its outer edge adjoining the turbulent core remains very unclear at present in the presence of blowing. The small number of experimental data available makes it possible to conclude that there is a decrease in the relative thickness of the laminar sublayer as the intensity of blowing increases. Unfortunately there are no quantitative data based on reliable experimental results. /310

The expression (5.30) for the velocity profile in the laminar sublayer, which is based on the shear stress distribution law (5.3), is in good agreement with the existing experimental data in the laminar sublayer (Fig. 76), and can obviously be regarded as quite reliable. Thus, if the thickness of the laminar sublayer η_L can be determined by any means, φ_L can then be determined from equation (5.30), so that

$$\bar{u}_L = \varphi_L / \zeta$$

For determining the thickness of the laminar sublayer, Van Driest [146] has used a condition analogous to the condition (3.102), except that the shear stress at the edge of the sublayer is taken to be the determining factor rather than the shear stress at the wall, as in equation (3.102). By analogy with equation (3.102) this condition can be written as

$$\delta_2 = \alpha \frac{\nu_w}{\sqrt{\frac{\tau}{\rho_w}}}. \qquad (5.32)$$

The combined use of equations (5.32), (5.3) and (5.30) lead to the following expression for the thickness of the laminar sublayer

$$\eta_l \exp\left(\frac{1}{2} B_* \eta_l\right) = \alpha. \tag{5.33}$$

In the absence of flowing ($B_* = 0$), equation (5.33) reduces to the condition $\eta_L = \alpha$ which was used earlier (Chapters III, IV).

The results of calculating η_L and φ_L from equations (5.33) and (5.30) are shown in Fig. 95. /311

In addition to the velocity profiles in the laminar sublayer obtained from equation (5.30), Fig. 94 also shows the velocity profiles in the turbulent core obtained from equation (5.28) for three values of the blowing parameter, $B_* = 0$, 0.2 and 1. The boundary of the laminar sublayer was determined from equation (5.33) in each case.

Let us now consider the calculation of drag on a flat plate in the presence of blowing. It is not difficult to see that with the assumptions made in the present chapter ($C_6 = 1/\text{f}$), the expression for the momentum loss thickness (5.7) becomes

$$\delta^{**} = \frac{\zeta^2 \mu_w}{\rho_e U_e^2} \int_0^1 \frac{\rho}{\rho_w} \bar{u}(1-\bar{u}) \exp\left[\varkappa\zeta \int_0^{\bar{u}} \left(\frac{\frac{\rho}{\rho_w}}{1+B\bar{u}}\right)^{1/2} d\bar{u}\right] d\bar{u}. \tag{5.34}$$

Here, as previously in Section 12 of Chapter III, it is assumed in the calculation of δ^{**} that the derivative $\dot{\eta}$ is given over the entire boundary layer by equation (5.27), which was obtained for the turbulent core. In this case, the zone of the laminar sublayer is as it were omitted, and the inner edge of the turbulent core is correspondingly extended to the wall ($\bar{u}_L \to 0$). As shown in Chapter III, such an assumption is applicable for flows close to an impermeable wall, and it will be all the more applicable in the presence of blowing, since blowing decreases the relative thickness of the laminar sublayer.

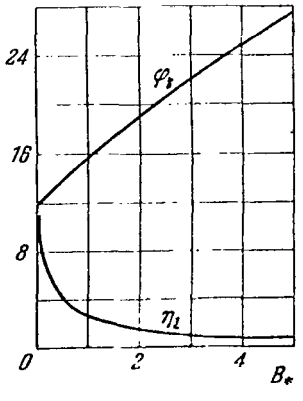

Figure 95.

In order to evaluate the integral in the right-hand part of equation (5.34), the asymptotic expansion (3.39) can be used. As a result of this evaluation, it is found to a first approximation /312

$$\delta^{**} = \frac{\mu_w (1 + B)}{f\varkappa^2 \rho_e U_e} \exp\left[\varkappa\zeta \int_0^1 \left(\frac{\frac{\rho}{\rho_w}}{1 + B\bar{u}}\right)^{1/2} d\bar{u}\right]. \tag{5.35}$$

Further, by substituting equation (5.35) into the integral momentum relationship (5.8) and following the procedure indicated in Section 12, the following system of equations is obtained, which make it possible to determine the local friction coefficient on a flat plate:

$$\left.\begin{aligned} &\frac{c_f}{c_{f0}} = \left(\frac{FK}{2N}\right)^2, \qquad K = \int_0^1 \left(\frac{\frac{\rho}{\rho_e}}{1 + B\bar{u}}\right)^{1/2} d\bar{u}, \\ &F = 0{,}242 c_{f0}^{-1/2}, \qquad G = \lg\left(\frac{\mu_e}{\mu_w}\right), \\ &N + \lg N = \lg\frac{FK}{2} + \frac{1}{2}(F + G). \end{aligned}\right\} \tag{5.36}$$

Here c_{f0} is the friction coefficient on a plate in an incompressible fluid in the absence of blowing, given either by von Kármán's formula (3.59) or by equation (3.80). The relationships given in Chapter I can be used for calculating the viscosity of the gas mixture at the wall. The same methods can be used to help in calculating the viscosity of the gas mixture. The calculation of the function N can be accomplished without difficulty from the last of equations (5.36) by using tables of logarithms to base ten, since the right-hand part of (5.36) is known. In order to determine the function K (see the second of equations (5.36)), it is necessary to determine the dependence of the gas (gas mixture) density in the boundary layer on the velocity. The form of this dependence is determined from the flow conditions in the boundary layer (the presence or absence of chemical reactions), and by the assumptions used in establishing the relationship between the velocity, concentration and temperature (for instance, the assumptions as to the magnitudes of the Prandtl and Schmidt numbers).

If the Reynolds number in the first of equations (5.36) tends to infinity ($Re_x \to \infty$), the following limiting formula is obtained for the ratio c_f/c_{f0} using a similar approach to that used in considering flow along an impermeable plate in Section 12: /313

$$\frac{c_f}{c_{f0}} = K^2. \tag{5.37}$$

Equation (5.37) makes it possible to determine the limiting value of the flow coefficient $c_m = \rho_w v_w / \rho_e U_e$ at which friction at the wall becomes equal to

zero. Remembering that by definition $B = 2c_m/c_f$, equation (5.37) can be rewritten with the use of the second of equations (5.36) as

$$1 = \left[\int_0^1 \sqrt{\frac{\frac{\rho}{\rho_e}}{\frac{c_f}{c_{f0}} + \frac{2c_m}{c_{f0}}\bar{u}}}\, d\bar{u} \right]^2. \tag{5.38}$$

If $c_f/c_{f0} = 0$ is substituted in the right-hand part of equation (5.38), an expression is obtained for the limiting value of the flow coefficient:

$$(c_m)_{\lim} = \frac{c_{f0}}{2} \left[\int_0^1 \sqrt{\frac{\frac{\rho}{\rho_e}}{\bar{u}}}\, d\bar{u} \right]^2. \tag{5.39}$$

When a gas of the same density as the gas in the approaching stream is injected into the boundary layer (ρ = const = ρ_e), equation (5.39) yields a limiting value $(c_m)_{\lim} = 2c_{f0}$.

Let us now consider further some special cases of flow close to a flat plate in the presence of mass injection into the boundary layer.

32. The boundary layer on a flat plate in the presence of blowing at Prandtl and Schmidt numbers equal to unity [147]

The flow of a gas of homogeneous composition along a flat plate will be considered. The gas injected through the porous wall into the boundary layer will also be regarded as homogeneous, but with different physico-chemical properties to the gas of the main flow. In addition, it will be assumed that the injected material is inert with respect to the gas of the main flow, i.e., there are no chemical reactions, and the mixture in the boundary layer can be regarded as a binary mixture. It will also be assumed that the specific heat capacities of both the components are constant, i.e., are independent of temperature, and the Schmidt and Prandtl numbers are taken equal to unity. /314

With these assumptions the boundary layer equations (4.85) - (4.87) assume the form:

$$\left.\begin{aligned} \rho u \frac{\partial u}{\partial x} + \rho v \frac{\partial u}{\partial y} &= \frac{\partial}{\partial y}\left[(\mu + \varepsilon)\frac{\partial u}{\partial y}\right], \\ \rho u \frac{\partial H}{\partial x} + \rho v \frac{\partial H}{\partial y} &= \frac{\partial}{\partial y}\left[(\mu + \varepsilon)\frac{\partial H}{\partial y}\right], \\ \rho u \frac{\partial c_2}{\partial x} + \rho v \frac{\partial c_2}{\partial y} &= \frac{\partial}{\partial y}\left[(\mu + \varepsilon)\frac{\partial c_2}{\partial y}\right]. \end{aligned}\right\} \tag{5.40}$$

The boundary conditions for the system of equations (5.40) can be written as

$$\left.\begin{array}{l} u = 0, \quad v = v_w, \quad H = H_w, \; c_2 = c_{2w} \quad \text{at} \quad y = 0; \\ u = U_e, \; H = H_e, \quad c_2 = 0 \qquad\qquad \text{at} \quad y \to \infty. \end{array}\right\} \tag{5.41}$$

Here and below the subscript 2 indicates parameters referring to the injected material, and the subscript 1 those of the main approaching stream.

Since the mixture in the boundary layer is binary, there is no need for a conservation equation for the first component ($c_1 = 1 - c_2$). The condition for the concentration c_2 at the outer edge of the boundary layer indicates that there is none of the injected material in the external stream.

For a mixture of two gases, the equation of state (1.86) assumes the form

$$p = \rho \frac{R}{M} T, \tag{5.42}$$

where

$$M = \frac{M_1 M_2}{M_1 c_2 + M_2 (1 - c_2)} \tag{5.43}$$

is the molecular weight of the binary mixture.

From the system of equations (5.40) and the boundary conditions (5.41) it follows that the velocity, total enthalpy, and concentration fields are similar: /315

$$\frac{u}{U_e} = \frac{H - H_w}{H_e - H_w} = \frac{c_{2w} - c_2}{c_{2w}}. \tag{5.44}$$

The following obvious relationships are obtained from (5.44):

$$H = H_w + (H_e - H_w)\,\bar{u}, \tag{5.45}$$

$$c_2 = c_{2w}(1 - \bar{u}) \tag{5.46}$$

From the definition of the total enthalpy it follows that

$$\begin{aligned} H &= c_p T + \frac{u^2}{2}; \\ c_p &= c_2 c_{p2} + (1 - c_2) c_{p1} = c_{p1} + (c_{p2} - c_{p1}) c_2. \end{aligned} \tag{5.47}$$

Bearing in mind that

$$H_w = c_{pw} T_w = [c_{2w} c_{p2} + (1 - c_{2w}) c_{p1}] T_w, \tag{5.48}$$

$$H_e = c_{pe} T_e + \frac{U_e^2}{2} = c_{p1} T_e + \frac{U_e^2}{2}, \tag{5.49}$$

the following equation giving the relationship between the temperature and velocity is obtained from (5.45) by using (5.47) - (5.49):

$$\frac{T}{T_w} = [1 - \omega\bar{u} - \beta\bar{u}^2 - \theta(1-\bar{u})][1-\theta(1-\bar{u})]^{-1}. \tag{5.50}$$

Here

$$\left.\begin{aligned} \omega &= 1 - \left(1 + \frac{\gamma-1}{2} M_e^2\right)\frac{T_e}{T_w}; \quad & M_e^2 &= \frac{U_e^2}{(\gamma-1)c_{p1}T_e}; \\ \beta &= \frac{\gamma-1}{2} M_e^2 \frac{T_e}{T_w}; & \theta &= c_{2w}\left(1 - \frac{c_{p2}}{c_{p1}}\right). \end{aligned}\right\} \tag{5.51}$$

In the absence of material injection into the boundary layer ($c_{2w} = 0$) or during the injection of a gas with the same specific heat capacity as that of the gas in the main stream ($c_{p2} = c_{p1}$), equation (5.50) reduces to Crocco's integral (3.47).

Further, by using the equation of state (5.42) and equations (5.43) and (5.50) an expression is obtained for the density in the boundary layer /316

$$\frac{\rho}{\rho_w} = \frac{[1-\delta][1-\theta(1-\bar{u})]}{[1-\delta(1-\bar{u})][1-\omega\bar{u}-\beta\bar{u}^2-\theta(1-\bar{u})]}, \tag{5.52}$$

where

$$\delta = c_{2w}\left(1 - \frac{M_1}{M_2}\right). \tag{5.53}$$

It follows from (5.52) that besides the Mach number M_e at the outer edge of the boundary layer and the temperature factor T_w/T_e, there is third important parameter which governs the density distribution in the boundary layer; this is the concentration of the injected material at the wall c_{2w}.

In order to find a solution in closed form, it is necessary to establish a relationship between the blowing parameter B, given by equation (5.2), and the concentration c_{2w}. This relationship can be obtained from (5.19), which expresses the condition for conservation of the injected material at the wall. Bearing in mind the assumption that the Schmidt number is equal to unity ($Sc = \mu_w/\rho_w\mathcal{D}_{ijw}$), equation (5.19) can be reduced to the form

$$\rho_w v_w = \rho_w v_w c_{2w} - \tau_w\left(\frac{dc_2}{du}\right)_w. \tag{5.54}$$

By making use of (5.46), the required relationship between the blowing parameter B and the concentration of the injected material at the wall can be found from equation (5.54):

$$c_{2w} = \frac{B}{1+B}, \tag{5.55}$$

$$B = \frac{c_{2w}}{1-c_{2w}}. \tag{5.56}$$

It follows from equation (5.55) that the concentration of the injected material at the wall is always less than unity for any finite value of the parameter B, and assumes the following limiting values: $c_{2w} \to 0$ when $B \to 0$; $c_{2w} \to 1$ when $B \to \infty$.

By using equation (5.55), c_{2w} in equation (5.52) can be replaced by B, and making some simple rearrangements, it is found that /317

$$\frac{\rho}{\rho_e} = (1-\omega-\beta)\left\{1+B\left[1-\left(1-\frac{c_{p2}}{c_{p1}}\right)(1-\bar{u})\right]\right\} \times \left\{1+B\left[1-\left(1-\frac{M_1}{M_2}\right)(1-\bar{u})\right]\right\}^{-1} \times \left\{1-\omega\bar{u}-\beta\bar{u}^2-\frac{B}{1+B}\left(1-\frac{c_{p2}}{c_{p1}}\right)(1-\bar{u})\right\}^{-1}. \tag{5.57}$$

When the gas is moving with a small velocity ($\beta = 0$) and there is no heat transfer between the gas and wall ($\omega = 0$) equation (5.57) becomes:

$$\frac{\rho}{\rho_e} = \frac{1+B}{1+B\left[1-\left(1-\frac{M_1}{M_2}\right)(1-\bar{u})\right]}. \tag{5.58}$$

The function K which governs drag and which in the general case is given by the second of equations (5.36) reduces to the following form when $\omega = \beta = 0$:

$$K = \frac{2}{B}\sqrt{\frac{1+B}{\frac{M_1}{M_2}-1}}\left[\operatorname{arctg}\sqrt{\frac{M_1}{M_2}-1} - \operatorname{arctg}\sqrt{\frac{\frac{M_1}{M_2}-1}{B\frac{M_1}{M_2}+1}}\right] \tag{5.59}$$

when $M_1 > M_2$

and

$$K = \frac{2}{B}\sqrt{\frac{1+B}{1-\frac{M_1}{M_2}}}\left[\operatorname{arth}\sqrt{1-\frac{M_1}{M_2}} - \operatorname{arth}\sqrt{\frac{1-\frac{M_1}{M_2}}{1+B\frac{M_1}{M_2}}}\right] \tag{5.60}$$

when $M_1 < M_2$.

If the injected gas has the same molecular weight as the gas in the main stream ($M_1 = M_2$), and $\omega = \beta = 0$, the equation for K becomes

$$K = \frac{2}{B}(\sqrt{1+B} - 1). \tag{5.61}$$

In the general case, the density is given by equation (5.57), and the integral in the expression for K (5.36) must be determined numerically or graphically. /318

In carrying out calculations of the friction coefficient the blowing parameter B must be specified. Once the friction coefficient c_f is determined, by using the system (5.36), it is possible to find the relative flow rate of the injected gas from the relationship

$$\frac{\rho_w v_w}{\rho_e U_e} = \frac{1}{2} B c_f \tag{5.62}$$

Thus, calculations for various values of the blowing parameter B make it possible to establish a relationship between the drag and the flow rate of the material injected, i.e., to determine the relationship $c_f = c_f(\rho_w v_w/\rho_e U_e)$ for the given flow conditions.

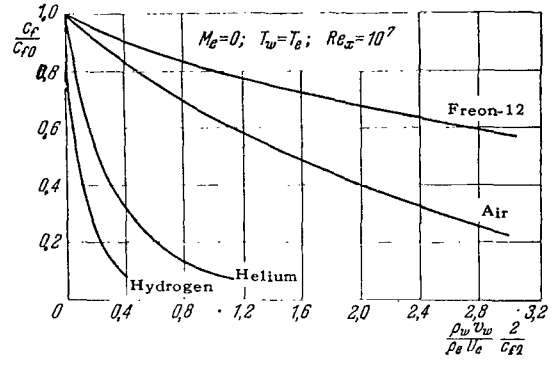

Figure 96.

Figure 96 shows graphs of the friction coefficients as functions of the blowing parameter during the injection of various gases (Freon-12, air, helium and hydrogen) into an air boundary layer. The calculations were carried out for the conditions $M_e = 0$, $T_W/T_e = 1$, $Re_x = 10^7$.

Figure 97 indicates the effect of the ratio of molecular weights on the blowing parameter at a fixed value of the friction coefficient. It can be seen from the figure that on changing from injection of a heavy gas to injection of a light gas causes a considerable decrease in the value of the blowing parameter. /319

Figure 98 shows the dependence of drag on the relative flow rate of the injected gas for the conditions $M_e = 3$, $Re_x = 4 \cdot 10^6$, $T_w/T_e = 1.1$. The upper curve was obtained for injection of air into air, and the lower for injection of helium into air.

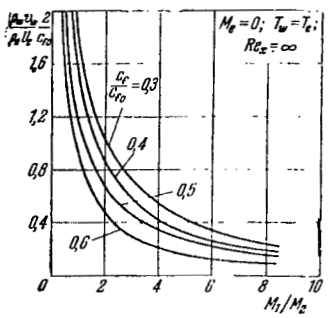

Figure 97.

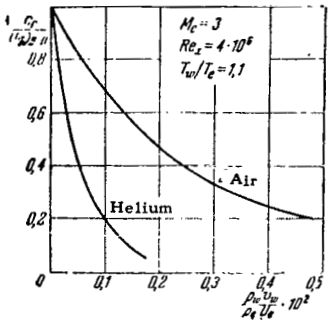

Figure 98.

This method of calculating drag on a porous plate can be generalized relatively easily to the case of sublimation of material from a surface along which a high-temperature gas flows [148]. It is known that if the temperature of the surface is lower than the triple-point temperature on the phase diagram, then during the flow of a gas mixture along the solid with a partial vapor pressure of the component of the solid in the approaching stream smaller than the saturated vapor pressure at the temperature of the surface, the solid will evaporate (sublime) without forming a liquid phase. The transfer mechanisms of various quantities (momentum, heat and material) in the boundary layer during the injection of material through a porous wall and during sublimation are similar. The only difference lies in the boundary conditions. While the concentration of the injected material can be varied at will during porous injection, during sublimation the concentration of the material being formed at the wall depends on the heat of sublimation and the surface temperature. /320

The concentration of subliming material at the wall c_{2w} is expressed in terms of the partial vapor pressure p_2 by the equation

$$c_{2w} = \frac{M_2}{M_w} \frac{p_2}{p_e}, \qquad (5.63)$$

where M_w is the molecular weight of the mixture at the wall (see equation (5.43)).

During equilibrium sublimation, the partial pressure of the sublimate at the wall p_2 is equal to the partial pressure of the saturated vapor p_2^* at the temperature T_w, which is expressed by the Clausius-Clapeyron equation [149]:

$$\ln p_2^* = b - \frac{h_L M_2}{RT_w}, \qquad (5.64)$$

where b is an experimental constant, h_L is the latent heat of sublimation. By replacing the molecular weight M_w in equation (5.63) by its value from equation (5.43) and making use of equation (5.64), an expression is obtained for the concentration of the sublimate at the wall in terms of the wall temperature and the boiling temperature $T_K(p_e)$:

$$c_{2w} = \left\{1 + \frac{M_1}{M_2}\left[\exp\frac{h_L M_2}{R}\left(\frac{1}{T_w} - \frac{1}{T_K}\right) - 1\right]\right\}^{-1}. \qquad (5.65)$$

When the wall temperature is equal to the boiling temperature ($T_w = T_K$), the concentration of the subliming material at the wall becomes equal to unity, which corresponds to the boiling regime, when the supply and concentration of vapor are not interrelated by the boundary diffusion condition.

Once the concentration of the sublimate at the wall (c_{2w}) is known, it is a simple matter to determine the value of the blowing parameter B, which is related to c_{2w} by equation (5.56). If this equation is used, the following expression is obtained for the blowing parameter during sublimation of material at the surface: /321

$$B = \frac{M_e}{M_1}\left\{\exp\frac{h_L M_2}{R}\left(\frac{1}{T_w} - \frac{1}{T_K}\right) - 1\right\}^{-1}. \qquad (5.66)$$

Thus, the method of calculating drag on a porous plate is completely applicable for calculating equilibrium sublimation situations, except that the blowing parameter B cannot be specified arbitrarily, but must satisfy equation (5.66).

33. Heat and mass transfer in the boundary layer on a flat plate in the presence of blowing at Prandtl and Schmidt numbers other than unity

Flow in a turbulent boundary layer on a flat plate in the presence of blowing at Prandtl and Schmidt numbers other than unity will be considered in this Section, in contrast to the previous Section where Pr = Sc = 1. The need for this study arises from the fact that during injection of gases with different physical properties to those of the gases in the main stream into the boundary layer, and in particular, during the injection of light gases, such as hydrogen and helium, the Prandtl and Schmidt numbers can differ appreciably from unity. For example, the Schmidt number of a gas mixture of hydrogen and air evaluated for the conditions T = 273°K and p = 1 atm can vary from 0.2 to 1.7, depending on the concentrations of the components. The Schmidt number for a mixture of helium and air can also take values from 0.2 to 1.7, while the Prandtl number for the same

mixture varies from 0.5 to 1.1 depending on the concentrations of the components (see Fig. 99, in which the mass concentration of helium is plotted along the abscissa).

As noted briefly in previous sections, the divergence of the Prandtl and Schmidt numbers from unity in the laminar sublayer usually has no very appreciable effect in calculating drag, but may be very important in heat and mass transfer between the gas and wall.

/322

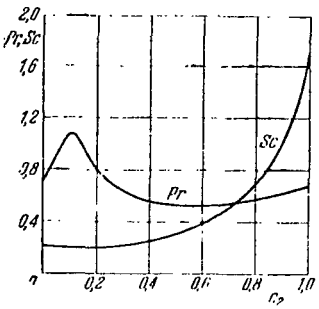

Figure 99.

In order to simplify the analysis, it will be assumed that the Prandtl and Schmidt numbers are constant across the cross section of the laminar sublayer and are equal to their values at the wall. Apart from this, the analysis will be similar to that given in the previous section (chemical reactions are assumed absent, the specific heat capacities of the components are constant, and the mixture is binary).

In order to establish an approximate relationship between the velocity, total enthalpy and concentration profiles, use is made of the turbulent boundary layer equations (4.97) - (4.100) in terms of Crocco variables, which are simplified by the assumption of local similarity $\frac{\partial H}{\partial \xi} = \frac{\partial c_i}{\partial \xi} = 0$. In this case the equations expressing the conservation of the injected component and the conservation of energy in the laminar sublayer, (4.98) and (4.97) become

$$\tau \frac{d^2 c_2}{du^2} = (\mathrm{Sc} - 1) \frac{\partial \tau}{\partial u} \frac{dc_i}{du}, \tag{5.67}$$

$$\frac{\partial \tau}{\partial u} \frac{dH}{du} = \frac{\partial q}{\partial u}. \tag{5.68}$$

Here

$$q = \frac{\tau}{\mathrm{Pr}} \left[\frac{dH}{du} + (\mathrm{Pr} - 1) u + (\mathrm{Le} - 1)(c_{p2} - c_{p1}) T \frac{dc_2}{du} \right]. \tag{5.69}$$

The quantity q is termed the generalized heat flux.

In the turbulent core the same equations are written in the form

$$\frac{d^2 H}{du^2} = 0, \tag{5.70}$$

$$\frac{d^2 c_2}{du^2} = 0. \tag{5.71}$$

The boundary conditions for equations (5.67) - (5.70) are

$$\left.\begin{array}{lll} \text{at } u=0 & H=H_w, & c_2=c_{2w}; \\ \text{at } u=U_e & H=H_e, & c_2=0. \end{array}\right\} \tag{5.72}$$

The problem of determining heat transfer in this case reduces, as usual, to determining the drag coefficient and establishing the relationship between drag and heat transfer. /323

Relationship of the profiles of concentration and total enthalpy to the velocity profile in the laminar sublayer. If equation (5.3) is used for the shear stress distribution in the boundary layer, equation (5.67) can be reduced to

$$\frac{c_2''}{c_2'} = \frac{(\mathrm{Sc}-1)\,B}{1+B\bar{u}}. \tag{5.73}$$

Here the primes denote differentiation with respect to the dimensionless velocity $\bar{u} = u/U_e$.

By integrating equation (5.73) once and determining the integration constant from condition (5.19), which in the present case ($\mathrm{Sc} \neq 1$) assumes the form

$$\left(\frac{dc_2}{d\bar{u}}\right)_w = -B\,\mathrm{Sc}\,(1-c_{2w}), \tag{5.74}$$

it is found that

$$c_2' = -B\mathrm{Sc}\,(1-c_{2w})\;(1+B\bar{u})^{\mathrm{Sc}-1}. \tag{5.75}$$

Integration of (5.75) using the second of the boundary conditions (5.72) leads to the following relationship obtained to interrelate the concentration and velocity profiles in the laminar sublayer:

$$c_2 = 1-(1-c_{2w})(1+B\bar{u})^{\mathrm{Sc}}. \tag{5.76}$$

It should be noted that equation (5.76) can still not be used, since the relationship between the blowing parameter B and the concentration at the wall c_{2w}.

We can now turn to the energy equation (5.68). By introducing the dimensionless quantities

$$\bar{H} = \frac{H}{h_e}; \quad \bar{\tau} = \frac{\tau}{\tau_w}; \quad \bar{q} = \frac{qU_e}{h_e\tau_w}; \quad \bar{u} = \frac{u}{U_e}, \tag{5.77}$$

this equation can be reduced to the form:

$$\frac{d\bar{\tau}}{d\bar{u}}\frac{d\bar{H}}{d\bar{u}} = \frac{d\bar{q}}{d\bar{u}}, \tag{5.78}$$

where

/324

$$\bar{q} = \frac{\bar{\tau}}{\mathrm{Pr}}\left[\frac{d\bar{H}}{d\bar{u}} + (\mathrm{Pr}-1)\frac{U_e^2}{h_e}\bar{u} + (\mathrm{Le}-1)(c_{p2}-c_{p1})c_p^{-1}\left(\bar{H} - \frac{U_e^2}{2h_e}\bar{u}^2\right)\frac{dc_2}{d\bar{u}}\right]. \tag{5.79}$$

In contrast to (5.69), the temperature T in equation (5.79) is expressed in terms of the total enthalpy and velocity according to the equation

$$T = \left(H - \frac{u^2}{2}\right)c_p^{-1}. \tag{5.80}$$

If equation (5.3) is used, and equation (5.78) is integrated, determining the integration constant from the condition at the wall, it is found that

$$\bar{q} = \bar{q}_w + B(\bar{H} - \bar{h}_w). \tag{5.81}$$

Here

$$\left.\begin{aligned} \bar{q}_w &= \frac{q_w U_e}{h_e \tau_w} = \frac{2c_h}{c_f}(\bar{H}_r - \bar{h}_w), \\ c_h &= \frac{q_w}{\rho_e U_e (H_r - h_w)}, \quad c_f = \frac{2\tau_w}{\rho_e U_e^2}, \end{aligned}\right\} \tag{5.82}$$

q_w is the heat flux from the gas to the wall, defined by equation (4.147); H_r is the equilibrium enthalpy of a thermally insulated wall, or the recovery enthalpy (the definitions of these quantities will be given later).

The expression for $\bar{q}$ from equation (5.79) is substituted into relationship (5.81); after some simple rearrangements it is found that

$$\frac{d\bar{H}}{d\bar{u}} + (\mathrm{Pr}-1)\frac{U_e^2}{h_e}\bar{u} + (\mathrm{Le}-1)(c_{p2}-c_{p1})c_p^{-1}\left(\bar{H} - \frac{U_e^2}{2h_e}\bar{u}^2\right)\frac{dc_2}{d\bar{u}} - \frac{B\,\mathrm{Pr}}{1+B\bar{u}}\bar{H} = \frac{\mathrm{Pr}}{1+B\bar{u}}(\bar{q}_w - B\bar{h}_w). \tag{5.83}$$

Equation (5.35) represents a linear, first-order equation with variable coefficients which can be integrated by quadrature. However, to obtain the final result

in a simpler form, we can confine our attention to the approximate determination of the total enthalpy distribution in the laminar sublayer, in which $\bar{H}$ is sought in the form of a power series with respect to the longitudinal velocity $\bar{u}$. Remembering that $\bar{u} < 1$, only three terms need be retained. In this case, /325

$$\bar{H} = \frac{H}{h_e} = a_0 + a_1\bar{u} + a_2\bar{u}^2. \tag{5.84}$$

By using the condition at the wall, $H = h_w$ when $u = 0$, it is found that $a_0 = h_w/h_e = \bar{h}_w$. By next differentiating equation (5.84) with respect to $\underline{u}$ and assuming that $\underline{u} = 0$, it is found that

$$a_1 = \left(\frac{d\bar{H}}{d\bar{u}}\right)_w, \qquad a_2 = \frac{1}{2}\left(\frac{d^2H}{d\bar{u}^2}\right)_w. \tag{5.85}$$

The coefficient a_1 is found from equation (5.83) when $\underline{u} = 0$:

$$a_1 = \left(\frac{d\bar{H}}{d\bar{u}}\right)_w = \mathrm{Pr}\,\bar{q}_w + B\Lambda\bar{h}_w. \tag{5.86}$$

Here

$$\Lambda = \frac{(c_{p2} - c_{p1})(1 - c_{2w})\,\mathrm{Sc}\,(\mathrm{Le} - 1)}{c_{p1} + (c_{p2} - c_{p1})\,c_{2w}}. \tag{5.87}$$

The expression for the coefficient a_2 is obtained by differentiating equation (5.83) with respect to $\underline{u}$ and then assuming $\underline{u} = 0$. It is found ultimately that

$$\left(\frac{d^2\bar{H}}{d\bar{u}^2}\right)_w = \mathrm{Pr}(\Lambda + \mathrm{Pr} - 1)B\bar{q}_w + (1 - \mathrm{Pr})(\gamma - 1)M_e^2 + B^2\bar{h}_w\Lambda[\Lambda + \Lambda(\mathrm{Le} - 1)^{-1} + \mathrm{Sc} - 1 + \mathrm{Pr}];$$
$$(\gamma - 1)M_e^2 = \frac{U_e^2}{h_e}. \tag{5.88}$$

By substituting the values of the coefficients a_0, a_1 and a_2 into (5.84), a relationship is obtained interrelating the velocity profile and the total enthalpy profile in the laminar sublayer /326

$$\bar{H} = \frac{H}{h_e} = \bar{h}_w + (\mathrm{Pr}\,\bar{q}_w + B\Lambda\bar{h}_w)\bar{u} + \{\mathrm{Pr}(\Lambda + \mathrm{Pr} - 1)B\bar{q}_w + (1 - \mathrm{Pr})(\gamma - 1)M_e^2 + B^2\bar{h}_w\Lambda[\Lambda + \Lambda(\mathrm{Le} - 1)^{-1} + \mathrm{Sc} - 1 + \mathrm{Pr}]\}\frac{\bar{u}^2}{2}. \tag{5.89}$$

Dependence of the profiles of concentration and total enthalpy on the velocity profiles in the turbulent core. In order to establish the relationship between the concentration and velocity profiles, equation (5.71) is integrated once:

$$\frac{dc_2}{d\bar{u}} = C. \tag{5.90}$$

The integration constant C is determined from the equality of the diffusion fluxes of the injected material on either side of the edge of the laminar sublayer:

$$\frac{1}{Sc}\left(\frac{dc_2}{d\bar{u}}\right)_{\bar{u}_l-0} = \left(\frac{dc_2}{d\bar{u}}\right)_{\bar{u}_l+0}. \tag{5.91}$$

Making use of equations (5.91) and (5.75) and integrating equation (5.90), a relationship is obtained between the concentration and velocity in the turbulent core:

$$c_2 = B(1 - c_{2w})(1 + B\bar{u})^{Sc-1}(1 - \bar{u}). \tag{5.92}$$

By equating the concentrations obtained from equations (5.92) and (5.76) at the edge of the laminar sublayer, an equation relating the concentration at the wall c_{2w} to the blowing parameter B is obtained

$$c_{2w} = 1 - (1 + B)^{-1}(1 + B\bar{u}_l)^{1-Sc}. \tag{5.93}$$

It should be noted that at Schmidt numbers equal to unity, equation (5.93) reduces to equation (5.55) of the previous section. Using (5.93), equation (5.92) is brought to the form

$$c_2 = \frac{B}{1 + B}(1 - \bar{u}). \tag{5.94}$$

The relationship between the total enthalpy and the velocity in the turbulent core was established similarly. By integrating equation (5.70) once, it is found that /327

$$\frac{d\bar{H}}{d\bar{u}} = \text{const} = \frac{\bar{q}}{\bar{\tau}}. \tag{5.95}$$

The integration constant in equation (5.95) is determined from the condition that the generalized heat flux on both sides of the edge of the laminar sublayer should be equal. By using this condition and the relationship (5.8) it is found that

$$\frac{d\bar{H}}{d\bar{u}} = \frac{1}{1 + B\bar{u}_l}[\bar{q}_w + B(\bar{H}_l - \bar{h}_w)]. \tag{5.96}$$

By integrating equation (5.96) and determining the integration constant from the condition at the outer edge of the boundary layer, the following relationship between the total enthalpy and velocity in the turbulent core is obtained:

$$\bar{H} = \bar{H}_e - [1 + B\bar{u}_t]^{-1}[\bar{q}_w + B(\bar{H}_t - \bar{h}_w)](1 - \bar{u}). \qquad (5.97)$$

It is not difficult to see that in the absence of blowing (B = 0) equation (5.97) reduces to equation (4.150) of the previous Chapter.

Determination of the recovery enthalpy H_r and the Reynolds analogy parameter $2c_h/c_f$. By putting $\bar{u} = \bar{u}_L$ in equation (5.97), it is found that

$$\bar{H}_t = (1 + B\bar{u}_t)(1 + B)^{-1}\bar{H}_e - (1 - \bar{u}_t)(1 + B)^{-1}(\bar{q}_w - B\bar{h}_w). \qquad (5.98)$$

By equating the values of $\bar{H}_L$ given by equations (5.98) and (5.89) at the edge of the laminar sublayer, it is found that

$$\begin{aligned} &\bar{h}_w[1 + B\Lambda\bar{u}_t - B(1 - \bar{u}_t)(1 + B)^{-1} + \\ &\quad + B^2\Lambda[\Lambda + \Lambda(\mathrm{Le} - 1)^{-1} + \mathrm{Sc} + \mathrm{Pr} - 1]\frac{\bar{u}_t^2}{2}] + \\ &+ \bar{q}_w\left[\mathrm{Pr}\,\bar{u}_t + (1 - \bar{u}_t)(1 + B)^{-1} + \mathrm{Pr}(\Lambda + \mathrm{Pr} - 1)B\frac{\bar{u}_t^2}{2}\right] = \\ &\quad (1 + B\bar{u}_t)(1 + B)^{-1}\bar{H}_e - (1 - \mathrm{Pr})\frac{\gamma - 1}{2}M_e^2\bar{u}_t^2. \end{aligned} \qquad (5.99)$$

When there is no heat transfer between the gas and the wall ($\bar{q}_w = 0$, $\bar{h}_w = \bar{H}_r$), the following expression for the recovery enthalpy is easily obtained from equation (5.99): /328

$$\begin{aligned} H_r = &\{h_e\left(1 + \mathrm{Pr}^{1/3}\frac{\gamma - 1}{2}M_e^2\right) - H_e(1 + B)^{-1}(1 - \bar{u}_t)B\} \times \\ &\times\left\{1 + B\Lambda\bar{u}_t - B(1 - \bar{u}_t)(1 + B)^{-1} + \right. \\ &\left. + B^2\Lambda[\Lambda + \Lambda(\mathrm{Le} - 1)^{-1} + \mathrm{Sc} + \mathrm{Pr} - 1]\frac{\bar{u}_t^2}{2}\right\}^{-1}. \end{aligned} \qquad (5.100)$$

The approximate relationship (3.150) has been used in obtaining this result.

By substituting equation (5.82) into equation (5.99) and solving the resulting expression for the Reynolds analogy parameter, it is found that

$$\begin{aligned} \frac{2c_h}{c_f} = &\{1 + \mathrm{Pr}^{1/3}\frac{\gamma - 1}{2}M_e^2 - \bar{H}_e B\frac{1 - \bar{u}_t}{1 + B} - \\ &- \bar{h}_w\left[1 + B\Lambda\bar{u}_t - B\frac{1 - \bar{u}_t}{1 + B} + B^2\Lambda[\Lambda + \Lambda(\mathrm{Le} - 1)^{-1} + \right. \\ &\left. + \mathrm{Sc} + \mathrm{Pr} - 1]\frac{\bar{u}_t^2}{2}\right]\left\{[\bar{H}_r - \bar{h}_w]\left[\mathrm{Pr}^{1/3} - \right.\right. \\ &\left.\left. - \frac{1 - \bar{u}_t}{1 + B}B + \mathrm{Pr}(\Lambda + \mathrm{Pr} - 1)B\frac{\bar{u}_t^2}{2}\right]\right\}^{-1}. \end{aligned} \qquad (5.101)$$

In this case, the approximate relationship (3.159) has been used.

In the absence of blowing (B = 0), equations (5.100) and (5.101) reduce to their analogs obtained in Chapter III.

It can also be seen from equations (5.100) and (5.101) that when the Prandtl and Schmidt numbers are equal to unity, $H_r = H_e$ and $2c_h/c_f = 1$ regardless of blowing.

The temperature and density distributions in the boundary layer. Once the distributions of total enthalpy $\bar{H}$ and concentration are known from equations (5.80) and (5.47), the temperature distribution in the boundary layer can be found as

$$\frac{T}{T_e} = \frac{1}{1+\left(\frac{c_{p2}}{c_{p1}}-1\right)c_2}\left(\bar{H} - \frac{\gamma-1}{2}M_e^2\bar{u}^2\right). \tag{5.102}$$

In the laminar sublayer the values of $\bar{H}$ and c_2 are given by equations (5.89) and (5.76), and in the turbulent core by equations (5.97) and (5.94). /329

Using the condition that the pressure is constant across the boundary layer, the equation of state (5.42) and equations (5.43) and (5.102), the following density distribution is obtained in the boundary layer:

$$\frac{\rho}{\rho_e} = \frac{1+\left(\frac{c_{p2}}{c_{p1}}-1\right)c_2}{1+\left(\frac{M_1}{M_2}-1\right)c_2}\left(\bar{H} - \frac{\gamma-1}{2}M_e^2\bar{u}^2\right)^{-1}. \tag{5.103}$$

Equation (5.36) can then be used for calculating drag from the known dependence of density on velocity. It should be noted that the concentration of the injected material at the wall c_{2w} is determined in terms of the blowing parameter B according to equation (5.93).

The calculation sequence. As starting data, the following must be given: the Mach number at the edge of the boundary layer M_e, the Reynolds number $Re_x = U_e x/\nu_e$, the wall temperature T_w, and the temperature at the outer edge of the boundary layer T_e. In addition, it is necessary to be given the molecular weights and specific heat capacities of the injected gas and the gas wetting the surface of the plate.

For the given value of the blowing parameter B, the local friction coefficient in the presence of blowing c_f and the friction parameter ζ, related to c_f by equation (3.8), are determined by the method given in Section 32, i.e., for Prandtl and Schmidt numbers equal to unity. Then from the known values of B and ζ, the parameter B_* is determined (see equation (5.29)). The thickness of

the laminar sublayer η_L and the velocity at the edge of the laminar sublayer $\bar{u}_L$ are evaluated from equations (5.33) and (5.30). Then, knowing the Schmidt number as the parameter, the dependence of c_{2w} on B (Fig. 100 a) is determined from equation (5.93). From the known mixture composition at the wall (c_{w2}) and the conditions at the wall (T_w, p), the actual Schmidt number at the wall is determined (Sc_w)* (Fig. 100 b). From the data of Figs. 100 a and 100 b (see arrows on Figures) it is possible to find the dependence of Sc_w on the blowing parameter, which is given in Fig. 100 c. After the relationship between B and Sc_w is found, equation (5.93) is used to determine the actual concentration of the material being injected at the wall, c_{2w}. Analogously, it is possible to determine the value of the Prandtl numbers, but in many cases the real need for this does not occur, since the Prandtl number has a much more feeble dependence on composition than the Schmidt number and can be taken as constant. The Lewis number ($Le_w = Pr_w/Sc_w$) can then be determined from the known values of Pr and Sc. The subsequent sequence of calculations is: the function A (from equation (5.87)), the recovery enthalpy H_r (from equation (5.100)), the Reynolds analogy parameter (from equation (5.101)), the heat flux $\bar{q}_w$ (from equation (5.82)), the enthalpy and concentration in the laminar sublayer (from equations (5.89) and (5.76)) and in the turbulent core (from equations (5.97) and (5.94)), the temperature and density in the boundary layer (from equations (5.102) and (5.103)), and drag (from equation (5.36)), are determined.

/330

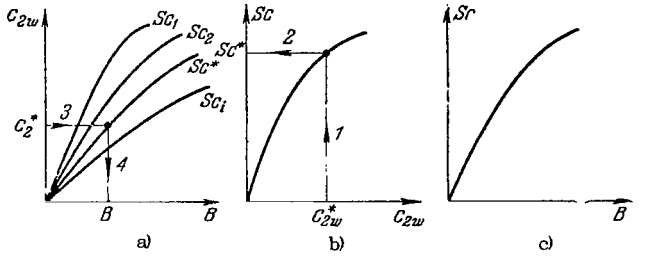

Figure 100.

The heat flux from the gas to the wall is calculated from the relationship

$$q_w = \frac{\bar{q}_w h_e \tau_w}{U_e}. \qquad (5.104)$$

*Methods for calculating diffusivities and viscosities of gas mixtures were considered in Chapter I, where advice and assistance on their calculation was given (see for instance the monograph by Bretshnayder [8]).

In the present case, the flux of heat used for heating the solid (inside the solid) is obtained from equation (5.21): /331

$$q_s = \frac{q_w - B\tau_w [h_w - (h_2)_-]}{U_e}. \qquad (5.105)$$

Figure 101 shows the dependence of the ratio $c_f/(c_f)_{B=0}$ on the flow rate of the injected gas (hydrogen) which was obtained for Pr = Sc = 1 (solid curve) and for Pr = 0.7, Sc = Sc_w) (dashed curve). By comparing the two curves it can be seen that deviations of the Prandtl and Schmidt numbers from unity have only a small effect on the drag coefficient. Because of this, there is no need to evaluate higher order approximations (for c_f, H_r, $2c_h/c_f$). This makes it possible to say that with a sufficiently high degree of accuracy for practical purposes, the drag coefficient in the presence of blowing can be calculated in many cases using methods based upon the assumptions that the Prandtl and Schmidt numbers are equal to unity (Section 32).

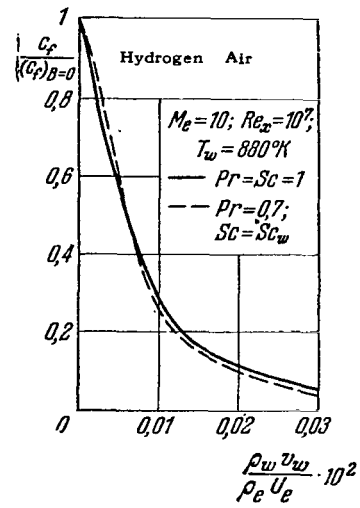

Figure 101.

When the parameters characterizing heat and mass transfer between the gas and wall ($2c_h/c_f$, H_r) are being calculated, however, it is necessary to take into account any deviations of the Prandtl and Schmidt numbers from unity.

REFERENCES

1. Hirschfelder, J. O., C. F. Curtiss and R. B. Bird. Molecular Theory of Gases and Liquids, New York, Wiley (London, Chapman and Hall), 1954; Russian translation: Moscow, 1961.
2. Chapman, S., and T. G. Cowling. The Mathematical Theory of Nonuniform Gases, Cambridge Univ. Press, 1952; Russian translation: Moscow, 1960.
3. Kogan, M. N. Dinamika Razrezhennogo Gaza (The dynamics of rarefied gases), "Nauka", Moscow, 1967.
4. Tirskiy, G. A. An analysis of the chemical composition of laminar multicomponent boundary layers on the surface of a burning plate, Kosmicheskiye Issledovaniya, 2, No. 4, pp. 570-594, (1964).
5. Tirskiy, G. A. The determination of effective diffusivities in a laminar boundary layer, Doklad. Akad. Nauk SSSR, 155, No. 6, pp. 1278-1282 (1963).
6. Loytsyanskiy, L. G. Mekhanika Zhidkostey i Gaza (Mechanics of liquids and gases), "Nauka", Moscow, 1970.
7. Golubev, I. F. Vyazkost' Gazov i Gazovykh Smesey (The viscosities of gases and gas mixtures), Fizmatgiz, Moscow, 1959.
8. Bretshnayder, St. Svoystva Gazov i Zhidkostey (The properties of gases and liquids), "Khimiya", Moscow-Leningrad, 1966.
9. Hansen, F. Approximations for the Thermodynamic and Transport Properties of High-temperature Air, NASA TR, R-50 (1959).
10. Reynolds, O. On the dynamical theory of incompressible viscous fluids and the determination of the criterion, Phil. Trans. Roy. Soc., London, 186, (1894); Russian translation in "Problemy Turbulentnosti", ONTI, Moscow, pp. 185-227, 1936.
11. Monin, A.S. and A.M. Yaglom. Statisticheskaya Gidromekhanika (Statistical Hydromechanics), Part 1, "Nauka", Moscow, 1965.
12. Van Driest, E.R. Turbulent boundary layer in compressible fluids, J. Aero. Sci., 18, No. 3, 145-160 (1951); Russian translation: Sb. "Mekhanika", No. 1, 1952.
13. Loysyanskiy, L. G. Laminarnyi Pogranichnyi Sloi (The Laminar Boundary Layer), Fizmatgiz, Moscow, p. 335, 1962.
14. Loysyanskiy, L. G. The hypothesis of localness in turbulent motion in the presence of viscosity, Prikl. Matem. i Mekh., 22, No. 5 (1958).
15. Shlikhting, G. (H. Schlichting). Teoriya Pogranichnogo Sloya (Boundary layer Theory), "Nauka", Moscow, 1969.
16. Klebanoff, P.S. Characteristics of turbulence in a boundary layer with zero pressure gradient, NACA Rep. No. 1247, 1135-1153 (1955).
17. Loysyanskiy, L. G. Mekhanika Zhidkosti i Gaza (Mechanics of Liquids and Gases), Gostekhizdat, Moscow, 1957.
18. Spalding, D.B. and Chi, S.W. The drag of a compressible turbulent boundary layer on a smooth flat plate with and without heat transfer, J. Fluid Mech., 18, Part 1, 117-143 (1964); Russian translation: Mekhanika, No. 6, (88), IL., 1964.
19. Frankl', F.I. and V.V. Voyshel'. Friction in a turbulent boundary layer around a plate in a plane-parallel flow of a compressible gas at large velocities, Tr. TsAGI, No. 321 (1937).
20. Sovremennoe Sostoyanie Gidroaérodinamiki Vyazkoy Zhidkosti (Modern Developments in Fluid Dynamics), ed. S. Goldstein, Vol. 2, I.L., Moscow, 1948.

21. Wilson, R. E. Turbulent boundary layer characteristics at supersonic speed-theory and experiment, Journ. Aero. Sci., 17, No. 9, 585-595 (1950).
22. Van Driest, E. R. The turbulent boundary layer with variable Prandtl number, in "50 Jahre Grenzschichtforschung", Braunschweig, 1955: Russian translation: Problema Pogranichnogo Sloya i Voprosy Teploperedachi, Energoizdat, Moscow-Leningrad, 1960.
23. Ievlev, V. M. Some problems in the hydrodynamic theory of heat transfer in gas flows, Doklad. Akad. Nauk, SSSR, 86, No. 1, 1952.
24. Ginzburg, I. P. and A. A. Shemetz. The turbulent boundary layer of a plate in a compressible fluid, Uchenye zapiski LGU, No. 280, ser. Matem., No. 35 (1960).
25. Kalikhman, L. E. The turbulent boundary layer on a flat plate along which a gas flows, Doklad. Akad. Nauk, SSSR, 106, No. 1 (1956).
26. Kutateladze, S. S. and A. I. Leont'yev. Turbulentnyy pogranichnyy sloy szhimaemogo gaza (The turbulent boundary layer in a compressible gas), Sib. Otd. Akad. Nauk SSSR, Novosibirsk, 1962.
27. Loytsyanskiy, L. G. and Yu. V. Lapin. The application of von Kármán's method to the calculation of turbulent boundary layers on a plate in a gas stream, Tr. Leningr. Politekhn. In-ta im. M. I. Kalinin, No. 217, Mashgiz, Moscow-Leningrad, 1961.
28. Zysina-Molozhen, L. M. and I. N. Soskova. An investigation of heat transfer and drag during the turbulent flow of a compressible gas, Teplomassoperenos, 1, "Energiya", Minsk, 1968.
29. Persch, J. A theoretical investigation of turbulent boundary layer flow with heat transfer at supersonic and hypersonic speeds. Proc. Fourth Midwestern Conference on Fluid Mechanics, Lafayette, 8-9, 1955.
30. Avduyevskiy, V. S. Methods for calculating three dimensional turbulent boundary layers in compressible gases, Izv. Akad. Nauk SSSR, Otd. Tekhn. Nauk, Mekh. i Mashinstroenie, No. 4, 1962.
31. von Kârmân, T. Problems of drag in compressible fluids, in Collection "Gazovaya Dinamika" (Gas dynamics), GONTI, p. 58-59, 1939.
32. Tucker, M. Approximation calculation of turbulent boundary layer development in compressible flow, NACA TN, No. 2337, 1951.
33. Rubesin, M. W. and H. A. Johnson. Critical review of skin-friction and heat-transfer solution of the laminar boundary layer of a flat plate, Trans. A. S. M. E., 71, No. 4, 1949.
34. Young, G. B. W. and E. Jassen. The compressible boundary layer, Journ. Aero. Sci., 19, No. 4, 1952.
35. Chapman, D. R. and R. M. Kestor. Measurements of turbulent skin friction on cylinders in axial flow at subsonic and supersonic velocities, Journ. Aero. Sci., 20, No. 7, 441-449, 1953.
36. Coles, D. Measurements of turbulent friction on a smooth flat plate in supersonic flow, Journ. Aero. Sci., 21, No. 7, 433-449, 1954.
37. Korkegi, R. M. Transition studies and skin-friction measurements on an insulated flat plate at a Mach number of 5.8, Journ. Aero. Sci., 23, No. 2, 97-108, 1956.
38. Matting, F. W., Chapman, D. R., Nyholm, J. R. and A. G. Thomas. Turbulent skin friction at high Mach numbers and Reynolds numbers in air and helium, NASA TR No. 82, 1961

39. Moore, D. R. and J. Harkness. Experimental investigations of the compressible turbulent boundary layer at very high Reynolds numbers, AIAA Journal, 3, No. 4, 1965; Russian translation: Raketn. Tekhn. i Kosmonavt., No. 4, 1965.
40. Lobb, R. K., Winkler, E. M. and J. Persch. Experimental investigations of turbulent boundary layers in hypersonic flow, Journ. Aero. Sci., 22, No. 1, 1-10, 1955; Russian translation: Vopr. Raketn. Tekhn., No. 5, I. L., 1955.
41. Hill, F. K. Boundary layer measurement in hypersonic flow, Journ. Aero. Sci., 23, No. 9, 35-42 (1956); Russian translation: Vopr. Raketn. Tekhn., No. 1, I. L., 1957.
42. Hill, F. K. Turbulent boundary layer measurements at Mach numbers from 8 to 10, Physics of Fluids, 2, No. 6, 1959.
43. Sommer, S. C. and B. J. Short. Free-flight measurements of skin friction of turbulent boundary layers with high rates of heat transfer at high supersonic speeds, Journ. Aero. Sci., 23, No. 6 (1956); Russian translation: Vopr. Raketn. Tekhn., No. 4, I. L., 1957.
44. Winkler, E. M. Investigation of flat plate hypersonic turbulent boundary layers with heat transfer, ARC Paper, No. 856-59, 1959.
45. Kozlov, L. V. An experimental study of skin friction on a flat plate in a supersonic stream in the presence of heat transfer, Izv. Akad. Nauk SSSR, Otd. Tekh. Nauk, Mekh. i Mash., No. 2, 1963.
46. Nikuradse, J. Gesetzmässigkeiten der turbulenten Strömung in glatten Rohren, VDI Forschungsheft 356 (1932); Russian translation: "Problemy Turbulentnosti", ONTI, Moscow, 1936.
47. Monaghan, R. The measurement of heat transfer and skin friction at supersonic speeds. ARC CP Nos. 139, 140, 1959.
48. Loytsyanskiy, L. G. and Yu. V. Lapin. Application of von Kármán's method to the calculation of the turbulent boundary layer on a plate in gas stream. Tr. Leningr. Politekhn. In-ta im. M. I. Kalinin, No. 217, Mashgiz, Moscow-Leningrad, 1961.
49. Kheiz, U. D. and R. F. Probstin. Teoriya Giperzvukovykh Techeniy (Theory of Hypersonic Flow), I. L., Moscow, 1962.
50. Staff, A. K. Equations, Tables and Charts for Compressible Flow, NACA Rep. No. 1135, 1953.
51. Teplomassoobmen i Trenie v Turbylentnom Pogranichnom Sloe (Heat and Mass Transfer and Friction in Turbulent Boundary Layers), ed. S. S. Kutateladze, Sib. Otd., Akad. Nauk SSSR, Novosibirsk, 1964.
52. Kutateladze, S. S. and A. I. Leont'ev. Turbulentnyy Pogranichnyy Sloy Szhimaemogo Gaza (Turbulent Boundary Layers in Compressible Gases), Sib. Otd., Akad. Nauk SSSR, Novosibirsk, 1962.
53. Lipmann, H. W. and C. Dhavan. NACA TN No. 1117, 1952.
54. Pappas, C. C. Measurement of heat transfer in the turbulent boundary layer on a flat plate in supersonic flow and comparison with skin friction results, NACA TN No. 3222, 1954.
55. Hill, F. K. Turbulent boundary layer measurements at Mach numbers from 8 to 10, The Physics of Fluids, 2, No. 6, 658-680, 1959.
56. Czarnecki, K. R. and W. J. Monta. Effects on compressibility and heat transfer of the laminar sublayer at the turbulent boundary layer, NASA TN D-1998, 1964.
57. Loytsyanskiy, L. G. A semi-empirical theory for the interaction of processes of molecular and molar transport in the turbulent motions of fluids, Tr.

Vsesoyuznogo S'ezda po Teor. i Prikl. Mekhanike, 27. i - 3.ii. 1960, Akad. Nauk SSSR, Moscow-Leningrad, 1962.
58. Shirokov, M.F. Zhurn. Tekhn. Fiziki, III, No. 12 (1936); Fizicheskie Osnovy Gazodinamiki (Physical Fundamentals of Gasdynamics), Fizmatgiz, Moscow, 1958.
59. Van Driest, E.R. Convective Heat Transfer in Gases, in "Turbulent Flow and Heat Transfer", ed. Lin' Tszya-Tszyao, I.L., Moscow, 1963.
60. Sovremennoe Sostoyanie Aérodinamiki Bol'shikh Skorostey (Modern developments on High-Speed Aerodynamics), ed. L. Howarth, Vol. 2, I.L., Moscow, 1956.
61. Crocco, L. Boundary layer of gases along a flat plate, Rend. Mat. Univ. Roma, 12, 1941.
62. Kaye, J. Survey of friction coefficients, recovery factors and heat transfer coefficients for supersonic flow, Journ. Aero. Sci., 21, No. 2, 117-129, 1954.
63. Shoulberg, R.H., Hill, J.A.F. and M.A. Rivas. An experimental determination of flat plate recovery factors for Mach numbers between 1.9 and 3.14, Journ. Aero. Sci., 21, No. 11, 763-771, 1954.
64. Tendeland, T. Effects of Mach numbers and wall-temperature ratio on turbulent heat transfer at Mach numbers from 3.0 to 5, NASA TR No. 16, 1959.
65. Adcock, J.B., Peterson, J.B. and D.T. McRee. Experimental investigation of a turbulent boundary layer of Mach 6, high Reynolds numbers and zero heat transfer, NASA TN D-2907, 1965.
66. Kozlov, L.V. The relationship between aerodynamic heating and surface friction, Izv. Akad. Nauk SSSR, Mekh. i Mash., No. 4, 1963.
67. Van Driest, E.R. Turbulent boundary layer on a cone in a supersonic flow at zero angle of attack, Journ. Aero. Sci., 19, No. 1, 55-57, 1952.
68. Seiff, A. Examination of the existing data on the heat transfer of turbulent boundary layers, NACA TN No. 3284, 1954.
69. Bradfield, W.S. Conical turbulent boundary layer experiments and a correlation with flat plate data, Trans. A.S.M.E., Journ. of Heat Transfer, Ser. C, May, 22-28, 1960.
70. Rotta, I.K. Turbulentnyy pogranichnyy sloy v neszhimaemoy zhidkosti (Turbulent boundary layers in incompressible fluids), "Sudostr.", Leningrad, 1967.
71. Kalikhman, L.E. Turbulentnyy pogranichnyy sloy na krivolineynoy poverkhnosti obtekaemoy gazom (Turbulent boundary layers on curvilinear surfaces along which a gas flows), Oborongiz, Moscow, 1956.
72. Kutateladze, S.S. and A.I. Leont'ev. Turbulentnyy pogranichnyy sloy szhimaemogo gaza (Turbulent boundary layers in compressible gases), Sib. Otd. Akad. Nauk SSSR, Novosibirsk, 1962.
73. McLafferty, G.H. and R.S. Barber. The effect of adverse pressure gradients on the characteristics of turbulent boundary layers in supersonic streams, Journ. Aero-Space Sci., 29, No. 1, 1962.
74. Sasman, P.K. and R.J. Cresci. Compressible turbulent boundary layer with pressure gradient and heat transfer, AIAA Journ., 4, No. 1, 1966; Russian translation: Raketn. Tekhn. i Kosmonavt., No. 1, 1966.
75. Eckert, E.R.G. Engineering relations for friction and heat transfer to surfaces in high velocity flow, Journ. Aero. Sci., 22, 585-586, 1955.
76. Ievlev, V.M. Some problems in the hydrodynamic theory of heat transfer in the flow of incompressible fluids, Doklad. Akad. Nauk SSSR, 86, No. 6, 1952.

77. Schultz-Grunow, F. Entstehung von Langswirbeln in Grenzschichten, ZAMM 38, 85-95, 1958.
78. Hama, F.K. Boundary layer characteristics for smooth and rough surfaces, Trans. Soc. Naval Architects and Marine Engrs, 62, 333-358, 1954.
79. Fedyevskiy, K. K., and Ginevskiy, A. S. A method for calculating turbulent boundary layers in the presence of a longitudinal pressure gradient, Zhurnal Tekhn. Fiz., 27, No. 2, 309-326, 1957.
80. Lapin, Yu. V. The turbulent boundary layer in a gas stream in the presence of heat transfer and Prandtl numbers different to unity, Tr. Leningrad. Politekhn. In-ta im. M.I. Kalinina, No. 217, Mashgiz, Moscow-Leningrad, 1961.
81. Stetson, K.F. Boundary layer transition on blunt bodies with highly cooled boundary layers, Journ. Aero-Space Sci., 27, No. 2, 81-92, 1960.
82. Ting-Yi Li, Geiger, R.E. Stagnation point of a blunt body in hypersonic flow, Journ. Aero. Sci., 24, No. 1, 25-33, 1957.
83. Korobkin, I. and K. Gruenewald. Investigation of local laminar heat transfer on a hemisphere for supersonic Mach numbers at low rates of heat flux, Journ. Aero. Sci., 24, No. 3, 188-194, 1957.
84. Chernyy, G.G. Techeniya gaza s bol'shoy sverkhzvukovoy skorost'yu (Gas flows at high supersonic velocities), Fizmatgiz, Moscow, 1959.
85. Sibulkin, M. Estimation of turbulent heat transfer of the sonis point of a bluntnosed body, Jet Prop., 28, No. 8, 548-554, 1958; Russian translation: Vopr. Raketn. Tekhn., No. 3, I.L., 1959.
86. Van Driest, E.R. The problem of aerodynamic heating, Aeron. Engng. Rev., 15, No. 10, 1956.
87. Arthur, P.D. and J.C. Williams. Maximum turbulent boundary layer heating rates on a hemispherical nose, A.R.S. Journal, 30, No. 2, 207-208, 1960.
88. Avduyevskiy, V.S., Danilov, Yu.I. Koshkin, V.K., Kutyrin, I.N., Mikhailova, M.M., Mikheyev, Yu.S., and O.S. Sergel'. Osnovy teploperedachi v aviatsionnoy i raketnoy tekhnike (Fundamentals of heat transfer in aviation and rocket technology), Oborongiz, Moscow, 1960.
89. Zel'dovich, Ya.B. and Yu.P. Rayzer, Fizika udarnykh voln i vysokotemperaturnykh gidrodinamicheskikh yavleniy (The physics of shock waves and high-temperature hydrodynamic phenomena), Fizmatgiz, Moscow, 1963.
90. Stupochenko, Ye. V., I. P. Stakhanov, Ye. V. Samuylov, A. S. Pleshanov, I. B. Rozhdestvenskiy. Termodinamicheskiye svoystva vozdukha v intervale temperatur ot 1000 do 12000°K i intervale davleniy ot 0.001 do 1000 atm (Thermodynamic properties of air at temperatures from 1000 to 12000°K and pressures from 0.001 to 1000 atm), in "Fizicheskaya Gazodinamika" (Gas Dynamics), Akad. Nauk SSSR, Moscow, 1959.
91. Predvoditelev, A. S., et al., Tablitsy termodinamicheskikh funktsiy vozdukha (dlya temperatur ot 200 do 6000°K i davleniy ot 0.00001 do 100 atm) (Tables of thermodynamic functions of air for temperatures from 200 to 6000°K and pressures from 0.00001 to 100 atm), Akad. Nauk SSSR, Moscow, 1962.
92. Dorrance, W. H. Giperzvukovyye techeniya vyazkogo gaza (Hypersonic flows of viscous gases), "Mir," Moscow, 1966.
93. Penner, S. S. Chemistry problems in jet propulsion, Aeronautical sciences and controlled flight, 1, Pergamon Press, London, 1957.
94. Lighthill, M. J. Dynamics of the dissociating gas, Part 1, Equilibrium flow, Journal of Fluid Mech., 2, No. 1, 1-32 (1957); Russian translation: Vopr. Raketn. Tekhn., Nos. 5, 6, IL, 1957.

95. Godnev, I. V. Vychisleniye termodinamicheskikh funktsiy po molekulyarnym dannym (Calculation of thermodynamic functions from molecular data), Gostekhizdat, Moscow, 1956.
96. Glesston, S. (Glasstone) Teoreticheskaya khimiya (Theoretical chemistry), IL, Moscow, 1950.
97. Kondrat'yev, V. N. Kinetika khimicheskikh gazovykh reaktsiy (The kinetics of chemical gas reactions), Akad. Nauk SSSR, Moscow, 1958.
98. Zakhar'yevskiy, M. S. Kinetika khimicheskikh reaktsiy (The kinetics of chemical reactions), Izd. Leningrad. Gos Univ. im. Zhdanova, 1959.
99. Glesston, S., K. Leydler and G. Eyring (Glasstone, Laidler and Eyring) Teoriya absolyutnykh skorostey reaktsiy (The theory of absolute reaction rates), IL, Moscow, 1948.
100. Rosner, D. Convective diffusion as an intruder in kinetic studies of surface catalyzed reactions. A.I.A.A. Journal, 2, No. 4, (1964); Russian translation: Raketn. Tekhn. i Kosmonavt., No. 4, 1964.
101. Gurney, J. P. General formulation of surface catalytic reactions, A.I.A.A. Journ., 4, No. 7, (1966); Russian translation: Raketn. Tekhn. i Kosmonavt., No. 7, 1966.
102. Rey, K. Khimicheskaya kinetika vozdukha pri vysokoy temperatur (Chemical kinetics of air at high temperatures), in "Issledovaniye giperzvukovykh techeniy" (Study of hypersonic flows), "Mir," Moscow, 1964.
103. Chung, P. M. Chemical reacting nonequilibrium boundary layer, Advances in Heat Transfer, ed. Hartnett, J. P., Irvine, T. F., 2, Academic Press, New York, 1965.
104. Hansen, F. Approximation for the thermodynamic and transport properties of high temperature air, NASA, T.R., No. 50 (1959).
105. Glass, I. I. and A. Takano Nonequilibrium expansion of dissociated oxygen and ionized argon around a corner. Progress Aero. Sci., 6, Pergamon Press, Oxford, 1965.
106. Stupochenko, Ye. V., S. A. Losev, and A. I. Osipov. Relaksatsionnyye protsessy v udarnykh volnakh (Relaxation processes in shock waves), "Nauka," Moscow, 1965.
107. Coulard, R. J. On catalytic recombination rates in hypersonic stagnation heat transfer, Jet Propul., 28, No. 11, 737-745 (1958); Russian translation: Vopr. Raketn. Tekhn., No. 5, IL, 1959.
108. Lapin, Yu. V. Turbulentnyy pogranichnyy sloy na kataliticheskoy poverkhnosti v neravnovesno dissotsiiruyushchem gaze (Turbulent boundary layers on a catalytic surface in a nonequilibrium dissociating gas), M. Zh. G., No. 3, (1967).
109. Lapin, Yu. V. The turbulent boundary layer in a dissociating gas. Zh. Tekhn. Fiz., 32, No. 4, 473-479 (1962).
110. Lapin, Yu. V. Vliyaniye kataliticheskoy rekombinatsii na teploperedachu v zamorozhennom turbulentnom pogranichnom sloye (The effect of catalytic recombination on heat transfer in a frozen turbulent boundary layer), Tr. Leningr. Politekhn. Inst. im. M. I. Kalinina, No. 248, "Mashinostroyeniye," Moscow-Leningrad (1965).
111. Dorrance, W. H. Hypersonic flows of viscous gases, Russian translation: "Mir," Moscow, 1966.
112. Lapin, Yu. V. and G. P. Sergeyev. Vliyaniye dissotsiatsii na treniye i teploobmen v turbulentnom pogranichnom sloye (The effect of dissociation on friction and heat transfer in a turbulent boundary layer), Tr. Leningr.

Politekhn. Inst. im. M. I. Kalinina, No. 230, "Mashinostroyeniye," Moscow-Leningrad (1964).
113. Dorrance, W. H. Dissociation effects upon compressible turbulent boundary layer skin friction and heat transfer, A. R. S. Journal, 31, No. 1 (1961); Russian translation: Vopr. Raketn. Tekhn., No. 12, IL, 1961.
114. Rose, P. H., R. F. Probstein, and Mc. C. Adams. Turbulent heat transfer through a highly cooled, partially dissociated boundary layer, Journ. Aero-Space Sci., 25, No. 12, 751-760 (1958); Russian translation: Mekhanika, No. 4 (56), IL, 1959.
115. Kosterin, S. I. and Yu. A. Koshmarov. Turbulent boundary layer on a flat plate in a stream of dissociating gas, International J. Heat and Mass Transfer, 6, 46-49, Pergamon Press, (1960).
116. Ginzburg, I. P. The turbulent boundary layer in a compressible fluid (mixture of gases), Vestn. Leningrad. Univ., No. 1, 75-88, (1961).
117. Kulgein, N. G. Heat transfer from a nonequilibrium turbulent boundary layer to catalytic surface, AIAA Journ., 3, No. 2 (1965); Russian translation: Raketn. Tekhn. i Kosmonavt., No. 2, 1965.
118. Plastics - the most sturdy materials at very high temperatures (review), Vopr. Raketn. Tekh., No. 4, IL, (1960).
Plastics in rocket technology (review), Vopr. Raketn. Tekh., Nos. 7, 8, IL, 1961.
119. Tirskiy, G. A. Analysis of the composition of a laminar boundary layer on the surface of a hot plate, Kosmicheskiye Issledovaniya, 2, No. 4 (1964).
120. Avdueyvskiy, V. S., Yu. I. Danilov, et al. Osnovy teploperedachi v aviatsionnoy i raketnoy tekhnike (Fundamentals of heat transfer in the aviation and rocket technologies), Oborongiz, Moscow, 1960.
121. Wooldridge, C. E. and R. J. Muzzy. Boundary layer turbulence measurements with mass addition and combustion, AIAA Journ., 4, No. 11 (1966); Russian translation: Raketn. Tekhn. i Kosmonavt., No. 11, 1966.
122. Spalding, D. B., D. M. Auslander, and T. R. Sundarom. The calculation of heat and mass transfer through the turbulent boundary layer on a flat plate at high Mach numbers, with and without chemical reaction, in "Supersonic Flow, Chemical Processes and Radiative Transfer", Oxford, pp. 211-276, 1964.
123. Dorrance, W. H. and F. J. Dore. The effect of mass transfer on the compressible turbulent boundary layer skin friction and heat transfer, Journ. Aero. Sci., 21, No. 6, 404-410 (1954).
124. Dorrance, W. H. The effect of mass transfer on the compressible turbulent boundary layer skin friction and heat transfer - an addendum, Journ. Aero. Sci., 23, No. 3, 283-284 (1956).
125. Motulevich, V. P. Heat transfer and friction on a plate in a gas stream during the formation of a turbulent boundary layer with supply of a foreign material through pores, Inzh.-Fiz. Zh., 3, No. 8, (1960).
126. Motulevich, V. P. Sublimation of a plate into a gas stream with the formation of a turbulent boundary layer, in "Fizicheskaya gazodinamika, teploobmen i termodinamika gaziv vysokikh temperatur" ("Physical gasdynamics, heat transfer and the thermodynamics of gases at high temperatures"), Akad. Nauk SSSR, Moscow, 1962.

127. Motulevich, V. P. Turbulent heat and mass transfer on a plate during porous blowing and suction of various gases, Inzh.-Fiz. Zhurn., 6, No. 4, (1963).
128. Kalikhman, L. Ye. The turbulent boundary layer of an incompressible fluid on a porous wall, Zhurn. Tekhn. Fiz., 25, No. 11, (1955).
129. Ginzburg, I. P., G. V. Kocheryzhenkov, and N. I. Mordvinova. The turbulent boundary layer on a permeable plate, Vest. Leningr. Gos. Un-ta 13, ser. Matem., Mekh., i Astron., No. 3 (1964).
130. Kutateladze, S. S. and A. I. Leont'yev. Turbulentnyy pogranichnyy sloy szhimayemogo gaza (The turbulent boundary layer of a compressible gas), Sib. Otd., Akad. Nauk SSSR, 1962.
131. Teplo, massoobmen i treniye v turbulentnom pogranichnom sloye (Heat and mass transfer and friction in turbulent boundary layers), ed. S. S. Kutateladze, Sib. Otd., Akad. Nauk SSSR, 1964.
132. Denison, R. M. The turbulent boundary layer on chemically active ablating surface, Journ. Aero. Sci., 28, No. 6 (1961); Russian translation: Vopr. Raketn. Tekhn., No. 1, IL, 1962.
133. Sovershennyy, V. D. The turbulent boundary layer on a porous surface, Mekh. Zhidk. i Gaza, No. 3, (1966).
134. Mugalev, V. P. An approximate method of calculating friction and heat transfer during injection of air into a turbulent boundary layer, Tr. Mosk. Fiz.-Tekhn. In-ta, No. 5, (1960).
135. Loytsyanskiy, L. G. Mekhanika Zhidkosti i Gaza (Mechanics of Liquids and Gases), Gostekhizdat, Moscow, 1957.
136. Barnes, J. W. and H. H. Tang. Strong and weak interaction parameters for turbulent flow, AIAA Journal, 4, No. 10 (1966); Russian Translation: Raketn. Tekhn. i Kosmonavt. No. 10, 1966.
137. Mugalev, V. P. An experimental study of the turbulent boundary layer on a plate with blowing of air and carbon dioxide into a supersonic stream, Tr. Mosk. Fiz.-Tekhn. In-ta, Oborongiz, No. 4 (1959).
138. Mugalev, V. P. An experimental investigation of subsonic turbulent boundary layers on a plate with blowing, Izv. Vyssh. Uch. Zaved., Ser. Aviats. Tekhn., No. 3 (1959).
139. Mugalev, V. P. An investigation of heat transfer and the turbulent boundary layer characteristics on a porous surface, in "Teplo- i Massoperenos" (Heat and Mass Transfer) Vol. I, "Energiya", Moscow, 1968.
140. Pappas, C. C. and A. F. Okuno. The relation between skin friction and heat transfer for the compressible turbulent boundary layer with gas injection, NASA T. N. D-2857 (1965).
141. Mickley, H. S. and R. C. Davis. Momentum transfer for flow over a flat plate with blowing, NACA T. N. No. 4017 (1957).
142. Fogaroli, R. P. and A. R. Saydah. Turbulent heat transfer and skin friction measurements on a porous cone with air injection at high Mach number, AIAA Journ., 4, No. 6 (1966); Russian Translation: Raketnaya Tekhn. i Kosmonavt., No. 6 (1966).
143. Squire, L. C. Some notes on turbulent boundary layers with fluid injection at high supersonic speeds, ARC C. P. No. 740 (1964).
144. Turcotte, D. L. A sublayer theory for fluid injection into the compressible turbulent boundary layer, Journ. Aero-Space Sci., 27, No. 9 (1960).
145. Kulgein, N. G. Transport processes in a combustive turbulent boundary layer, Journ. Fluid Mech., 12, part 3, (1962).

146. Van Driest, E. R. On the aerodynamic heating of blunt bodies, Zeitschr. angew. Math. und Phys., 9, 5/6 (1958).
147. Lapin, Yu. V. Friction and heat transfer in a compressible turbulent boundary layer on a plate in the presence of mass injection, Zhurn. Tekhn. Fiz., 30, No. 8 (1960).
148. Lapin, Yu. V., Turbulent heat and mass transfer on a plate in the presence of sublimation and porous injection of various gases, Zhurn. Tekhn. Fiz., 34, No. 5 (1964).
149. Karapet'yants, M. Kh. Khimicheskaya Termodinamika (Chemical thermodynamics), Goskhimizdat, Moscow, 1953.

NOTATION

Latin symbols

A — see formula (3.173);
A_k — chemical symbols of reacting materials, Eq. (4.1);
a — velocity of sound;

$$B=\frac{\rho_w v_w}{\rho_e U_e}\frac{2}{c_f},\qquad B_0=\frac{\rho_w v_w}{\rho_e U_e}\frac{2}{(c_f)_{B=0}},$$

$$B_F=\frac{\rho_w v_w}{\rho_e U_e}\frac{2}{c_F},\qquad B_{F0}=\frac{\rho_w v_w}{\rho_e U_e}\frac{2}{(c_F)_{B=0}},$$

$$B_h=\frac{\rho_w v_w}{\rho_e U_e}\frac{1}{c_h},\qquad B_{h0}=\frac{\rho_w v_w}{\rho_e U_e}\frac{1}{(c_h)_{B_h=0}},$$

$$B_H=\frac{\rho_w v_w}{\rho_e U_e}\frac{1}{c_H},\qquad B_{H0}=\frac{\rho_w v_w}{\rho_e U_e}\frac{1}{(c_H)_{B_H=0}},$$

$$B_*=\frac{B}{\zeta}=\frac{v_w}{v_*}$$

} blowing parameters;

b — sighting distance, Eq. (1.16);
c_F — mean friction coefficient, Eq. (3.62);
c_H — mean heat transfer coefficient;
c_f — local friction coefficient, Eq. (2.85);
c_h — local heat transfer coefficient, Eq. (2.91);
c_i — mass concentration of i^{th} component, Eq. (1.29);
c_m — flow coefficient of injected material, Eq. (2.86);
C_r — recombination parameter, Eq. (4.137);
c_v — specific heat capacity at constant volume, Eq. (1.43);
c_p — specific heat capacity at constant pressure;
c_{pi} — specific heat capacity of i^{th} component at constant pressure;
c_{vi} — specific heat capacity of i^{th} component at constant volume;
D — energy of dissociation per unit mass of molecules, Eq. (4.46);
D_{ij} — diffusion coefficient of multicomponent mixture, Eq. (1.58);
$\mathcal{D}_{ij}$ — diffusion coefficient of binary mixture, Eq. (1.59);
$\mathcal{D}_i$ — effective diffusion coefficient, Eq. (1.58);
$\mathcal{D}_i^T$ — thermodiffusion coefficient;
$\mathcal{D}_T$ — coefficient of eddy diffusivity, Eq. (2.31);

Da — Damköhler number, Eq. (4.102);
d — sphere diameter;
E — internal energy of gas, Eq. (1.38);
E_0 — energy of gas at zero absolute temperature;
E_a — activation energy;
ΔE_0 — dissociation energy per mole of initial material, Eq. (4.22);
E_{aw} — energy of activation of reaction surface;
e_i — energy of internal degrees of freedom of particles of the i^{th} sort;
f_i — distribution function;
F — function given by Eqs. (3.77) and (3.92);
G — function defined by Eq. (3.78);
g_{ij} — see Eq. (1.16);
g_{iw} — mass rate of formation of i^{th} component per unit surface area;
g_i — statistical weight;
H — total enthalpy of mixture, Eq. (1.94);
$H^* = \delta^*/\delta^{**}$ — form parameter;
h — enthalpy of mixture, Eq. (1.100);
h_i — enthalpy of i^{th} component;
h_i^0 — heat of formation of i^{th} component under standard conditions;
H_r — recovery enthalpy;
h — Planck's constant;
h_{iL} — heat of sublimation of the i^{th} component;
j_i — mass flux density vector of i^{th} component, Eq. (1.10);
k — Boltzmann's constant;
k_T — thermodiffusion ratio, Eq. (1.61);
K_i — numerical rate of formation of particles of i^{th} sort per unit volume, Eq. (1.27);
K_n — see Eq. (4.7)
K_p — see Eq. (4.12)
K_x — see Eq. (4.15)
K_c — see Eq. (4.16)
} equilibrium constants;
k_{wi}, k_{wj} — rate constants for the forward and reverse surface reactions;
k', k'' — rate constants for forward and reverse reactions in gas phase;
K_w — equilibrium constant for surface reaction;
k_d — dissociation rate constant;
k_r — recombination rate constant;
I_{ij} — collision integral, Eq. (1.16);
$I(ii)$ — see Eq. (3.36);
L — characteristic length;
Le_i — effective Lewis number, Eq. (1.103);
Le — Lewis number for binary system, Eq. (1.105);
Le_t — turbulent Lewis number, Eq. (2.34);
l — turbulent mixing length;
M_i — molecular weight of i^{th} component;
M — molecular weight of mixture;
M_e — Mach number at outer edge of boundary layer;
m_i — mass of particles of i^{th} type;
n_i — numerical density of particles of the i^{th} sort, Eq. (1.1);
n — number of particles per unit volume, Eq. (1.7);
$[n_i] = n_i/N_A$ — number of moles of i^{th} component per unit volume;
n_i, n_j — orders of the forward and reverse surface reactions;
N_A — Avogadro's number;

N — see Eq. (3.82);
p — pressure of mixture, given by Eq. (1.8);
p_i — partial pressure of i^{th} component, Eq. (1.8);
p_d — characteristic pressure of ideally dissociating gas;
P — pressure tensor, Eqs. (1.12) and (1.64);
P_i — pressure tensor for i^{th} component, Eq. (1.11);
Pr — Prandtl number;
Pr_T — turbulent Prandtl number, Eq. (2.33);
Q_p — sum of states for gas at unit pressure;
Q — total sum of states; see also Eq. (3.181);
Q_c — sum of states for gas at unit concentration;
q_i — flux density vector for kinetic energy of i^{th} component, Eq. (1.13);
q — heat flux density vector, Eqs. (1.14) and (1.76);
q_w — heat flux from gas to wall, Eq. (2.88);
q_s — heat flux within solid, Eq. (5.20);
R — universal gas constant;
Re* — Reynolds number formed from the displacement thickness, Eq. (3.43);
Re** — Reynolds number formed from the momentum loss thickness, Eq. (3.17);
Re_x — Reynolds number formed from parameters at outer edge of the boundary layer, Eq. (3.18);
r — radius vector with projected lengths x, y, z;
r_w — transverse radius of curvature of body of revolution;
Sc_T — turbulent Schmidt number, Eq. (2.35);
Sc — Schmidt number for a binary mixture, Eq. (1.105);
Sc_i — effective Schmidt number, Eq. (1.103);
$\dot{S}$ — rate of deformation tensor, Eq. (1.67);
T — gas temperature, Eq. (1.8);
T_d — characteristic dissociation temperature;
T_r — characteristic rotary temperature and recovery temperature;
T_v — characteristic vibratory temperature;
t — time;
$\underline{v}_i$ — velocity of particles of i^{th} sort (components v_{ix}, v_{iy}, v_{iz});
$\underline{v}$ — mass-average velocity, Eq. (1.4);
$\overline{\underline{v}}_i$ — mass velocity of particles of i^{th} sort, Eq. (1.3);
$\overline{\underline{V}}_i$ — diffusion velocity of i^{th} component, Eqs. (1.6) and (1.53);
$\underline{V}_i$ — thermal velocity of particles of i^{th} sort, Eq. (1.5);
v_* — dynamic velocity, Eq. (3.8);
u — longitudinal velocity component;
w_i — mass rate of formation of i^{th} component, Eq. (1.30);
W — active section of catalytic surface;
x — component of the vector $\underline{r}$ on the x axis;
x_i — molar concentration;
X — catalytic particle.

Greek symbols:

α — universal turbulence constant, Eq. (3.102);
β — see Eqs. (3.48) and (3.49);
$\bar{\beta}$ — see Eq. (4.117);
γ = c_p/c_v;
γ_w — catalytic activity of wall, Eq. (4.61);
δ^* — displacement thickness, Eq. (2.77);
δ^{**} — momentum loss thickness, Eq. (2.76);
δ — boundary layer thickness, Eq. (5.53);
δ_u^{**} — energy loss thickness, Eq. (2.89);
ε — eddy viscosity, Eq. (2.30);
$\dot{\varepsilon}$ — unit tensor, Eq. (1.66);
ζ — friction parameter, Eq. (3.8);
η — universal coordinate, Eq. (3.8);
η_L — coordinate at edge of laminar sublayer;
$\varkappa$ — universal turbulence constant ($\varkappa = 0.4$), Eq. (2.69);
λ — molecular thermal conductivity;
λ_T — eddy thermal conductivity, Eq. (2.32);
λ_{eff} — effective thermal conductivity, Eq. (1.82);
λ_R — thermal conductivity taking mass transfer into account, Eq. (1.81);
μ — dynamic viscosity;
ν — kinematic viscosity;
ν_k', ν_k'' — stoichiometric coefficients of reaction, Eq. (4.1);
ξ — Crocco variable, Eq. (2.59);
ρ_i — partial density of ith component, Eq. (1.8);
ρ — gas density, Eq. (1.8);
ρ_d — characteristic density of partially excited dissociating gas, Eq. (4.50);
ρ_{dL} — characteristic density of ideally dissociating gas, Eq. (4.51);
σ — see Eq. (4.20);
τ — shear stress;
φ — universal coordinate, Eq. (3.8);
$\Phi(\hat{u})$ — see Eq. (3.34);
Ψ — flux density vector, Eq. (1.9);
ψ_i — summatory invariant, Eq. (1.21);
Ψ — see Eq. (3.25);
ω — see Eqs. (3.48) and (3.49);
Ω — see Eq. (3.196).

Subscripts

e — parameters at outer edge of boundary layer;
w — parameters at wall;
s — parameters at critical point;
∞ — parameters at infinity in approaching stream;
0 — parameters in incompressible fluid, or parameters in absence of blowing;

r — parameters in absence of heat transfer between gas and wall;
L — parameters at edge of laminar sublayer;
T — parameters in turbulent core;
t — parameters at point of transition of laminar to turbulent motion.

Superscripts

(e) — equilibrium flow;
(f) — frozen flow;
(ne) — nonequilibrium flow;
$\overline{}$ — overscore: in Chapter I, statistical averaging with respect to velocity, Eq. (1.2); in Chapter II, averaging with respect to time, Eq. (2.2); in Chapters III - V, dimensionless quantities.

AUTHOR INDEX

Avduyevskiy, V. S., 62, 135, 154, 225
Adams, McC., 216
Adcock, J. B., 127
Arthur, P. D., 153
Auslander, D. M., 229

Barber, R. S., 135
Barnes, J. W., 331
Bird, R. B., 2, 9, 14, 18, 21, 25
Bradfield, W. S., 133, 134
Bretsznajder, 23, 26, 264

Chung, P. M., 171
Chapman, D. R., 64, 67
Chapman, S., 2, 14
Chernyy, G. G., 149
Chi, S. W., 60, 63, 108
Coles, D., 66, 134
Cowling, T. G., 2, 14
Cresci, R. J., 135
Crocco, L., 124
Curtiss, C. F., 2, 9, 14, 18, 21, 25
Czarnecki, K. R., 106

Danilov, Yu. I., 154, 225
Davis, R. C., 235
Denison, R. M., 230
Dhawan, C., 101
Dore, F. J., 229
Dorrance, W. H., 158, 201, 213, 215, 229

Eckert, E. R. G., 136, 154
Eyring, H., 167, 168

Fedyayevskiy, K. K., 144
Fogaroli, R. P., 240
Frankel', F. I., 60

Geiger, R. E., 147
Ginevskiy, A. S., 144
Ginzburg, I. P., 143, 222, 230
Glass, I. I., 175
Glasstone, S., 167, 168
Godnev, I. V., 167
Goldstein, S., 92
Golubev, I. F., 23
Goulard, R. J., 179, 213
Gruenewald, K., 147
Gurney, J. P., 169

Hama, F. K., 139
Hansen, F., 25, 175
Harkness, J., 69
Heis, W. D., 81
Hill, F. K., 74, 101, 103, 108, 131
Hill, J. A. F., 124
Hirschfelder, J. O., 2, 9, 14, 18, 21, 25
Howarth, L., 123

Ievlev, V. M., 60, 136

Janssen, E., 62
Johnson, H. A., 229

Kalikhman, L. Ye., 60, 105, 135, 229
Karapet'yants, M. Kh., 256
Kármán, T. von, 62
Kaye, J., 156
Kester, R. M., 64
Klebanoff, P. S., 124
Kocheryzhenkov, G. V., 230
Kogan, M. N., 14
Kondrat'yev, V. N., 167
Korkegi, R. M., 16
Korobkin, I., 147
Koshkin, V. K., 154
Koshmarov, Yu. A., 222
Kosterin, S. I., 222
Kozlov, L. V., 77, 96, 131
Kulgein, N. G., 222, 241
Kutateladze, S. S., 61, 66, 98, 135, 230
Kutyrin, I. N., 154

Laidler, K., 167, 168
Lapin, Yu. V., 61, 81, 144, 205, 209, 214, 250, 256
Lees, L., 197
Leont'yev, A. I., 61, 63, 98, 135, 230
Li, Ting-Yi, 147
Lighthill, M. J., 159

Lin, C. C., 123
Lipmann, H. W., 101
Lobb, R. K., 71
Loytsyanskiy, L. G., vi, 20, 31, 46, 49,59, 61, 81, 104, 121, 230
Losev, S. A., 177

McLafferty, G. H., 135
McRee, D. T., 127
Matting, F. W., 67
Mickley, H. S., 235
Mikhaylova, M. M., 154
Mikheyev, Yu. S., 154
Monaghan, R., 80
Monin, A. S., 31
Monta, W. J., 106
Moor, D. R., 69
Mordvinova, N. I., 230
Motulevich, V. P., 229
Mugalev, V. P., 230-232, 234, 235
Muzzy, R. J., 227

Nikuradse, J., 80
Nyholm, J. R., 67

Okuno, A. F., 235, 240
Osipov, A. I., 177

Pappas, C. C., 101, 124, 235, 240
Penner, S. S., 159
Persch, J., 62, 71
Peterson, J. B., 127
Pleshanov, A. S., 72
Predvoditelev, A. S., 157
Probstein, R. F., 81, 216

Rayzer, Yu. P., 156
Ree, K., 170
Repik, E. U., 80
Reynolds, O., 31
Rivas, M. A., 124
Rose, P. H., 216
Rosner, D., 168
Rotta, I. K., 135
Rozhdestvenskiy, I. B., 167
Rubesin, M. W., 82, 124

Samuylov, E. V., 157
Sandarom, T. R., 229
Sasman, P. K., 135
Saydah, A. R., 240
Schlichting, H., 50
Schultz-Grunow, F., 139

Seiff, A., 130
Sergel', O. S., 154
Sergeyev, G. P., 214
Shemets, A. A., 60
Shirokov, M. F., 122
Short, B. J., 76
Shoulberg, R. H., 124
Sibulkin, M., 149, 154
Sovershennyy, V. D., 230
Sommer, S. C., 76
Soskova, I. N., 61, 107
Spalding, D. B., 60, 63, 108, 229
Squire, L. C., 241
Stakhanov, I. P., 157
Stetson, K. F., 146
Stupochenko, E. V., 157, 177

Takano, A., 175
Tang, H. H., 231
Tendeland, T., 125
Thomas, A. G., 67
Tirskiy, G. A., 8, 225
Tucker, M., 62
Turcotte, D. L., 241

Van Driest, E. R., 33, 78, 63, 105, 107, 118, 123, 129, 132, 134, 153-155, 248
Voyshel', V. V., 60

Williams, J. C., 153
Wilson, R. E., 60, 63
Winkler, E. M., 71, 77, 108
Wooldridge, C. E., 227

Yaglom, A. M., 31
Young, G. B., 62

Zakhar'yevskiy, M. S., 166, 167
Zel'dovich, Ya. B., 156
Zysina-Molozhen, L. M., 61, 107

* U. S. GOVERNMENT PRINTING OFFICE : 1972 735-025/1076

NATIONAL AERONAUTICS AND SPACE ADMISTRATION
WASHINGTON, D.C. 20546

OFFICIAL BUSINESS
PENALTY FOR PRIVATE USE $300

FIRST CLASS MAIL

POSTAGE AND FEES PAID
NATIONAL AERONAUTICS AND
SPACE ADMINISTRATION

U.S.MAIL

044 001 C1 U 12 720128 S00903DS
DEPT OF THE AIR FORCE
AF WEAPONS LAB (AFSC)
TECH LIBRARY/WLOL/
ATTN: E LOU BOWMAN, CHIEF
KIRTLAND AFB NM 87117

POSTMASTER: If Undeliverable (Section 158 Postal Manual) Do Not Return

"The aeronautical and space activities of the United States shall be conducted so as to contribute . . . to the expansion of human knowledge of phenomena in the atmosphere and space. The Administration shall provide for the widest practicable and appropriate dissemination of information concerning its activities and the results thereof."

— NATIONAL AERONAUTICS AND SPACE ACT OF 1958

NASA SCIENTIFIC AND TECHNICAL PUBLICATIONS

TECHNICAL REPORTS: Scientific and technical information considered important, complete, and a lasting contribution to existing knowledge.

TECHNICAL NOTES: Information less broad in scope but nevertheless of importance as a contribution to existing knowledge.

TECHNICAL MEMORANDUMS: Information receiving limited distribution because of preliminary data, security classification, or other reasons.

CONTRACTOR REPORTS: Scientific and technical information generated under a NASA contract or grant and considered an important contribution to existing knowledge.

TECHNICAL TRANSLATIONS: Information published in a foreign language considered to merit NASA distribution in English.

SPECIAL PUBLICATIONS: Information derived from or of value to NASA activities. Publications include conference proceedings, monographs, data compilations, handbooks, sourcebooks, and special bibliographies.

TECHNOLOGY UTILIZATION PUBLICATIONS: Information on technology used by NASA that may be of particular interest in commercial and other non-aerospace applications. Publications include Tech Briefs, Technology Utilization Reports and Technology Surveys.

Details on the availability of these publications may be obtained from:

SCIENTIFIC AND TECHNICAL INFORMATION OFFICE

NATIONAL AERONAUTICS AND SPACE ADMINISTRATION

Washington, D.C. 20546